Self-assembly in complex chemical systems

Li, Jianwei

Self-Assembly in Complex Chemical Systems

Jianwei Li

The work described in this thesis was executed at the Stratingh Institute for Chemistry, University of Groningen, The Netherlands.

The author of this thesis wishes to thank the University of Groningen for Ubbo Emmius Fellowship.

Cover design by Jianwei Li and Nan Xia.
Printed by Ipskamp Drukkers BV, Enschede, The Netherlands.

ISBN: 978-90-367-6872-6
eISBN: 978-90-367-6873-3

university of groningen

Self-Assembly in Complex Chemical Systems

PhD thesis

to obtain the degree of PhD at the
University of Groningen
on the authority of the
Rector Magnificus Prof. E. Sterken
and in accordance with
the decision by the College of Deans.

This thesis will be defended in public on

Friday 14 March 2014 at 14:30 hours

by

Jianwei Li

born on 8 September 1984
in Hubei, China

Supervisor
Prof. S. Otto

Assessment committee
Prof. D.A. Leigh
Prof. J.C.M. van Hest
Prof. S.R. Harutyunyan

To my family

Contents

Chapter 1

Self-Organization in Complex Chemical Systems

Life is dynamically self-organized. Understanding self-organization in complex chemical systems can help us uncover the mystery of the origin of life. Dynamic Combinatorial Chemistry (DCC) is a promising tool to create and study chemical complexity as it allows easy access to molecular networks. It is a subject of combinatorial chemistry where the library members intercovert continuously by exchanging building blocks with each other. Dynamic combinatorial libraries (DCLs) are powerful tools for discovering the unexpected and have given rise to many fascinating molecules, ranging from interlocked structures to self-replicators. Furthermore, dynamic combinatorial molecular networks can produce emergent properties at systems level, which provides exciting new opportunities in systems chemistry. New materials with unexpected properties also may emerge from the molecular networks through self-assembly of molecules in the network that thereby promote their own synthesis. In this chapter, we will analyze some literature examples of DCLs that are under thermodynamic control, leading to synthetic receptors and complex self-organized supramolecular architectures. Also reviewed are extensions of the principles of DCC to systems that are not at equilibrium. Examples include self-replication and self-synthesizing materials. Finally, the contents of this thesis are outlined.

Part of this chapter has been published:
J. Li, P. Nowak, S. Otto, *J. Am. Chem. Soc.* **2013**, *135*, 9222-9239.

1.1 Self-Organization and Supramolecular Interactions

Life is a highly complex system containing components such as membranes, nucleic acids and proteins. The self-organization in these entities is still a mystery for scientists.[1] Self-organization is a spontaneous process where some form of global order or coordination arises out of the local interactions between the components of an initially disordered system.[2] In chemical systems, there are two types of self-organization: static and dynamic self-assembly.[3] Static self-assembly involves formation of well-ordered equilibrium structures by building blocks. These structures are characterized by a global or local minimum of free energy. For example, molecular crystals and most folded proteins form by static self-assembly. The opposite, dynamic self-assembly, occurs when a system dissipates energy. In chemistry, these non-equilibrium conditions are rare, but may be obtained by a permanent feed of fresh reactants.

Supramolecular non-covalent interactions play an important role in self-organization processes.[4] The noncovalent interactions are interactions such as ion-pairing, hydrogen bonding, hydrophobic interactions, cation-π and π-π interactions. They are driving forces for self-organization in complex chemical systems. Molecular recognition selects the basic components. This selection process is usually under thermodynamic control. The selected components may grow through sequential and eventually hierarchical binding of multiple components in the correct relative arrangement. The growth may present cooperativity and kinetically controlled nonlinear behavior which will drive the system out of equilibrium.

1.2 Systems Chemistry

Since self-organization in complex systems is of such significance, defining a subject area that deals with complex chemical systems appears justified. Chemistry has focused for a long time on the synthesis and properties of pure molecules. Yet, with the analytical tools now at the disposal of the modern chemist, complex mixtures are becoming tractable. Such mixtures may exhibit unique new properties. Life is one of the most compelling and inspiring examples of what complex chemistry may give rise to. Yet life is only one manifestation of complexity in chemistry; many other functional systems may be synthesized that are only limited by the creativity of the chemist. The rapidly developing discipline of systems chemistry[5] studies complexity and emergence in chemical systems. It tries to uncover the

theory behind the system-level properties which are not simply the sum of the attributes of the individual components.

1.3 Dynamic Combinatorial Chemistry

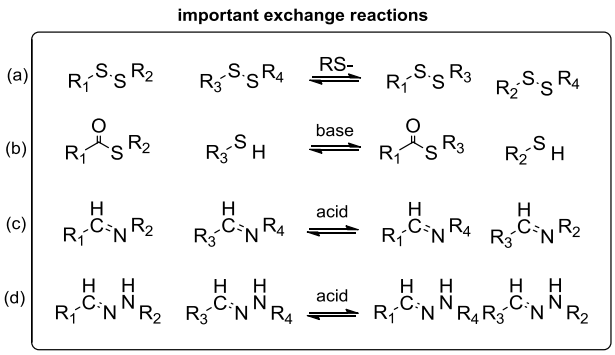

Scheme 1.1 Reversible reactions used for dynamic combinatorial chemistry to date: (a) disulfide exchange; (b) thioacetal exchange; (c) transimination; (d) hydrazone exchange. This scheme is modified from ref. 6b.

Dynamic combinatorial chemistry (DCC)[5a-c,6] is a promising tool to create and study chemical complexity as it allows easy access to molecular networks. It is a subset of combinatorial chemistry, where the library members interconvert continuously by exchanging building blocks with each other. The members of a dynamic combinatorial library (DCL) are formed in a combinatorial way by linking building blocks together through reversible chemical bonds. The distribution of all molecules in such a network is typically governed by thermodynamics. Changing supramolecular noncovalent interactions in the library by changing experiment conditions or adding specific template molecules may alter the stability of the library members and thereby alter the composition of the library. Alternatively, new self-organized supramolecular structures may be obtained through self-recognition of specific library members.

1.3.1 Exchange Reactions in DCC

There are many reversible reactions which can be used in DCC.[6b] The most important reactions are summarized here (Scheme 1.1). Only the disulfide exchange reaction is discussed here as it plays a very important role in much of the work described in this thesis.

Disulfide exchange is one of the most widely used reactions in DCC. As the thiol group is encountered in the amino acid cysteine, disulfide chemistry is common in biological systems. It takes place in aqueous solution at neutral or mildly basic conditions (pH 7 to 9) in the presence of air. There are usually two steps involved in the preparation of DCLs of disulfides (Scheme 1.2). The first step is the irreversible oxidation of the thiols to disulfides mediated by the oxygen present in the air. The disulfides exchange and equilibrate in the second step when there are catalytic amounts of thiolate in DCLs.

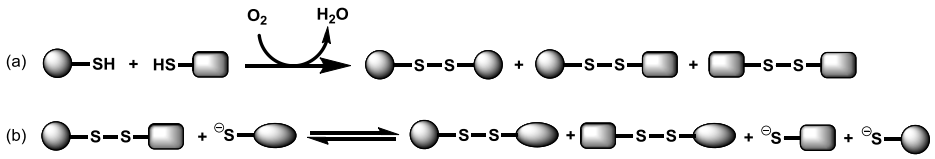

Scheme 1.2 Mechanism for disulfide exchange, (a) thiol oxidation and (b) disulfide exchange.

1.3.2 External Templating in DCLs

The most explored approach to changing the thermodynamically controlled product distribution of DCLs is through *external templating*; i.e. the addition of chemical templates that cannot take part in the reversible chemistry that connects the building blocks. Molecular recognition between the template and library species often leads to useful changes in the product distribution of DCLs (Scheme 1.3).[7] The library members which bind to the template will be amplified. This effect may be utilized for the discovery of synthetic receptors[8-10] and ligands for biomacromolecules,[11,12] in many cases leading to unexpected supramolecular structures such as cages,[13] rotaxanes[14] and catenanes[15]. Some particularly relevant examples will now be discussed.

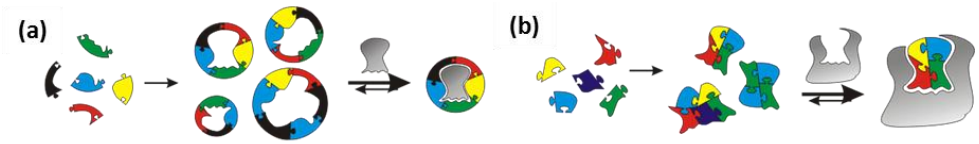

Scheme 1.3 Different ways of selecting specific member of a DCL on the basis of an external template: (a) selection of a host by a separately introduced guest; and (b) selection of a guest by a separately introduced host.

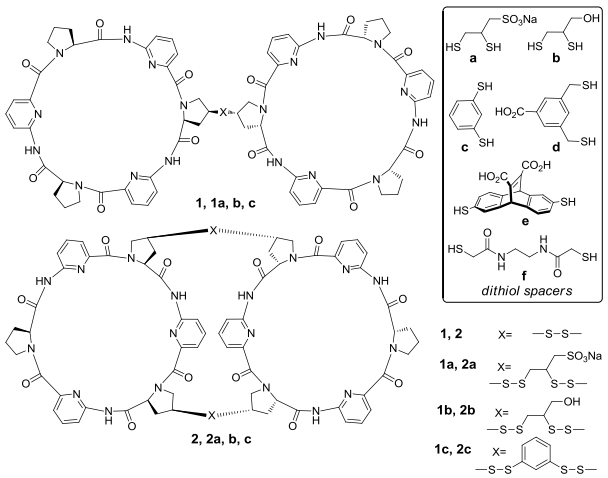

Figure 1.1 Building blocks and amplified receptors in cyclopeptide DCLs. This figure is modified from ref. 17, 18 and 20.

1.3.2.1 Exploring Synthetic Receptors

A compelling illustration of the power of DCC in the discovery of synthetic receptors involves one of the most challenging systems to recognize: anions in water.[16] This work also led to the discovery of a new mechanism for achieving high binding affinities in synthetic receptors: reinforced molecular recognition. In collaboration with the group of Kubik our group developed a highly efficient family of anion binders. In a first study[17] a library was prepared by dissolving **1** and **a-f** (Figure 1.1) in a 2:1 (v/v) mixture of acetonitrile and water. Exposing this DCL to KI or K_2SO_4 induced the amplification of three different receptors (**1a**, **1b** and **1c**). ITC measurements showed that **1c**, in particular, is an efficient receptor for both iodide ($K = 5.6 \times 10^4$ M^{-1}) and sulfate ($K = 6.7 \times 10^6$ M^{-1}). Further studies,[18] based on an X-ray crystal structure of the sulfate complex of **1b** and an analysis of the solvent dependence of complex stability, demonstrated that the high affinity exhibited by this system is a consequence of reinforced recognition.[19] The binding is not only due to the direct interactions between receptor and guest but also due to interactions within the receptor that do not directly involve the guest. Subsequent work targeted receptors in which the two cyclopeptide rings are connected via two linkers (**2**, **2a-c** in Figure 1.1).[20] Receptors **2b** and **2d** are both strongly amplified by KI, Na_2SeO_4 and Na_2SO_4. ITC measurement showed an exceptional affinity and selectivity for sulfate ions in aqueous solution (log K_a = 8.67 in 67 volume% acetonitrile in water); currently the world record for anion binding by a neutral receptor in aqueous solution.

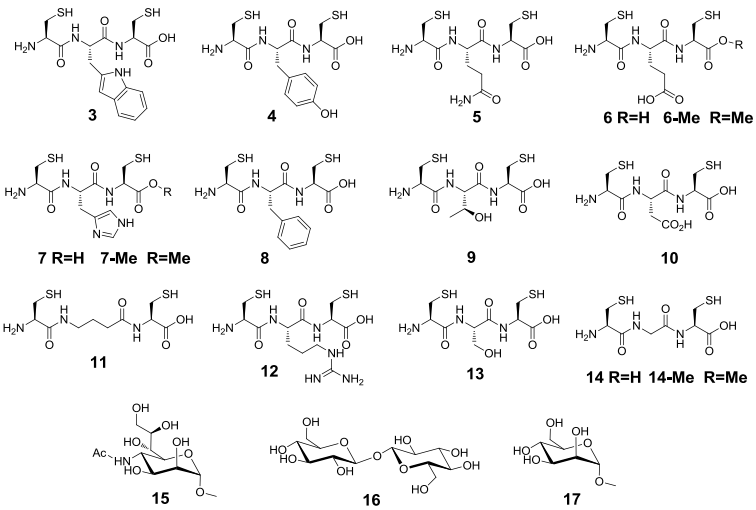

Figure 1.2 Tripeptide building blocks (**3**-**14**) and carbohydrate templates (**15**-**17**) for DCLs aimed at recognizing sugars in water. This figure is modified from ref. 21.

Another long-standing challenge in supramolecular chemistry is the recognition of sugars in water.[21] Ravoo and co-workers have used a dynamic combinatorial approach to identifying biomimetic carbohydrate receptors. They used disulfide exchange to prepare DCLs from a set of tripeptides under physiological conditions. The tripeptides contained N- and C-terminal Cys residues to mediate the disulfide exchange reaction. Arg, Asp, Glu, Gln, His, Ser, and Thr were selected as the second residues because of their potential hydrogen bonding interactions with carbohydrates; GABA (γ-aminobutyric acid), Phe, Trp, and Tyr provide hydrophobic and aromatic moieties; and Gly was introduced as an inert residue (Figure 1.2). In a DCL composed of three tripeptides (**6**-**Me**, **7**-**Me** and **8**-**Me**), the cyclic dimer His-His (**7**-**7**) was amplified by neurotransmitter NANA (**15**). HisHis and NANA formed a cooperative 1:2 complex (K_1 = 72.7 M^{-1}, K_2 = 7.76 $\times 10^3$ M^{-1}). In a DCL of six tripeptides (**3**-**8**), a selective 1:1 interaction of the cyclic dimer Tyr-Tyr (**4**-**4**) with trehalose (**16**) was found (K = 2.85 $\times 10^3$ M^{-1}), and in a DCL of five tripeptides (**9**-**13**), a selective 1:1 interaction of cyclic dimer Thr-Thr (**9**-**9**) with α-D-methylfucopyranoside (**17**) was identified (K = 4.0 $\times 10^3$ M^{-1}).

1.3.2.2 Exploring Ligands for Biomolecules

Creation of ligands that recognize biomacromolecules such as proteins and nucleic acids paves the way for applications as therapeutic agents, as well as diagnostic biosensors for rapid monitoring of imbalances and illnesses.[22] However, biomacromolecules are challenging templates to work with in dynamic combinatorial chemistry. Most reversible chemistries are best operated at millimolar concentrations. The limited solubility or availability of biomolecules then makes it difficult to use stoichiometric quantities of the biomolecule relative to the library members. Furthermore, the conditions for reversible chemistry need to be compatible with the stability of biomolecules that are often sensitive to pH, temperature, and chemical agents.[6f,6g] Nevertheless DCC has produced some promising results also in this area.

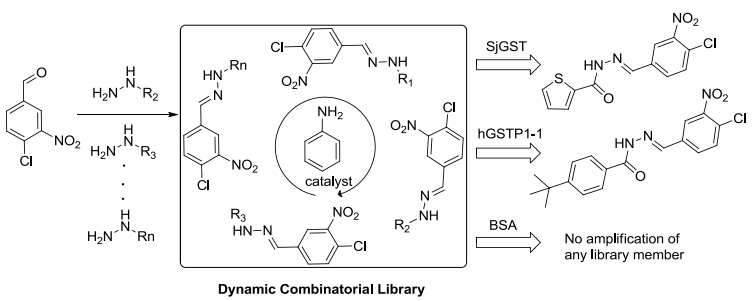

Figure 1.3 An aniline-catalysed acylhydrazone DCL and the influence of protein targets on its composition. This figure is modified from ref. 24.

In 2006, Greaney, Campopiano and coworkers reported the discovery of discovery of Glutathione S-Transferase (GST) inhibitors using DCC based on the reversible Michael addition.[23] The GSTs are potential drug targets in parasitic diseases such as malaria and schistosomiasis and for cancer therapy, where resistance to chemotherapeutic drugs has been directly correlated with the overexpression of GSTs in tumor cells. In a first study a DCLs was prepared from glutathione (GSH) and three other thiol-containing tripeptide analogues and the Michael acceptor ethacrynic acid (EA), a known inhibitor of the GST class. Addition of SjGST dramatically amplified the GS-EA Michael adduct. Subsequently a larger library was prepared using a single thiol GSH and 14 EA analogues, in order to identify to best hydrophobic acceptor for binding to the GST active site. Two new inhibitors for the GST enzyme were identified. Encouraged by these results, a new system using hydrazone chemistry for DCLs was developed.[24] Ordinarily, hydrazone exchange requires a pH lower

than 4.0, which it incompatible with most protein targets. However, following work by Dawson[25] they used aniline as a nucleophilic catalyst, which allowed for conducting reversible hydrazone chemistry at pH 6.2. In the library templated by hGST P1-1 or SjGST, two isoform-selective binders were amplified (Figure 1.3). Yet there is no amplification in the presence of bovine serum albumin, compared with the library without any templates. Conjugating a glutathione moiety to the aldehyde enhanced the solubility of the resulting library members, and led to the selection of compounds with significant binding ability. Interestingly, a catalytically inactive SjGST mutant selected the same library member as its active counterpart, confirming that the catalytic activity of the enzyme was not critical to the selection process. Subsequent binding studies confirmed that the selected compounds were indeed the most potent members of the library.

The above examples are from protein-directed libraries (further examples can be found in ref 11). Nucleic acids (DNA/RNA) are another class of important biomacromolecules whose recognition is fundamental to many biochemical processes related to transcription, regulation, and gene expression. Interestingly, they may exhibit a diversity of secondary structures due to their flexibility. These features make it both attractive and challenging to develop synthetic molecules capable of binding to nucleic acids. DNA and RNA have been successfully targeted with DCC systems in several studies.[12] Again, we only present some selected examples in more detail.

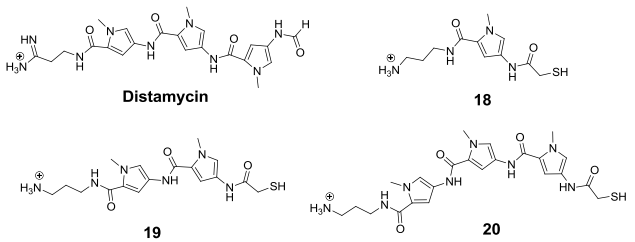

Figure 1.4 Structures of dithiol-functionalized polyamides designed to mimic distamycin. This figure is modified from ref. 26.

Distamycin-like polyamides can bind to the minor groove of double-stranded DNA with an affinity similar to naturally DNA-binding proteins in a sequence-specific manner. Based on this finding, Balasubramanian and coworkers designed three building blocks **18**, **19**, **20** in a dynamic combinatorial approach to screen for a good binder for duplex DNA (Figure 1.4).[26] Comparing the library distribution with and without duplex DNA, they found that the

disulfide dimers **19**-**20** and **20**-**20** were amplified. The binding between the selected compounds and DNA was confirmed by thermal melting studies.

Later, they used the same dynamic combinatorial strategy to explore binders for a quadruplex DNA.[27] They prepared two groups of libraries by mixing L1 and derivatives of p-benzylic thiols (G1) or neutral carbohydrate derivatives (G2). The DCL made from G1 was screened against two intramolecular quadruplex forming sequences (c-Kit21, c-Myc22) and a 22-mer duplex DNA for comparison. In the G1 library with quadruplex, the two guanidinium disulfides L1-29 and L1-30 were amplified. However, in the same library with duplex DNA, no amplification was observed. In the case of carbohydrate building blocks (G2), L1-31 was most strongly amplified by c-Kit21 and binds it with a Kd value of 9.1 ± 1.1 μM. This disulfide as well as the disulfide L1-32 bound to c-Myc22 with similar Kd values of 24.4 ± 4.8 μM and 21.1 ± 3.7 μM, respectively.

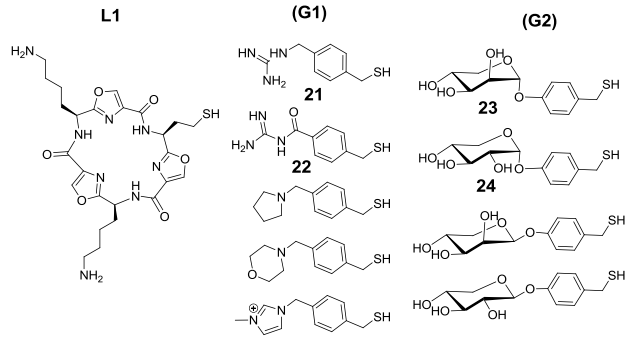

Figure 1.5 Structures of oxazole-based peptide macrocycle L1, cationic benzylic thiols (G1), and netral carbohydrate benzylic dithiols (G2). This figure is modified from ref. 27.

1.3.2.3 Template-Induced Self-Organization in DCLs

Metal coordination cages are an interesting and popular class of architectures in supramolecular chemistry. Nitschke's group has developed an extensive body of work combining reversible imine chemistry with metal-ligand coordination.[28] One particularly appealing recent example involves a capsule that is capable of structural reconstitution on receipt of a signal (the presence of perchlorate) to create a tight binding pocket for another anion (chloride).[29] The complex, barrel-like structure of the chloride receptor is templated by five perchlorate anions. Firstly, they set up a library of coordination complexes (**A**) by the reaction of p-toluidine, 6,6'-diformyl-3,3'-bipyridine (**L**) and $Co[N(SO_2CF_3)_2]_2 \cdot H2O$ in

acetonitrile. When they used $Co(SO_3CF_3)_2 \cdot 6H2O$ instead of the triflimide salt, tetrahedral product $Co_4\mathbf{L}_{68}^{+}$ (**B**) was obtained almost exclusively (Figure 1.6).

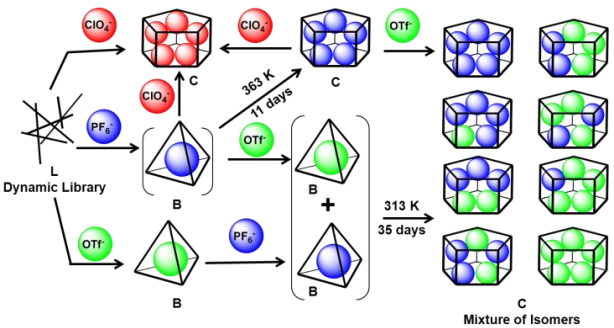

Figure 1.6 Chemical network showing the effects of sequential addition of anions. This figure is modified from ref. 29.

The ^{19}F NMR spectrum of the solution confirmed the encapsulation of a triflate ion (OTf^-) within **B**, suggesting that this anion acted as a template for the formation of the tetrahedral cage. Indeed, the addition of sodium triflate to **A** was found to template **B**·OTf^-, while the addition of lithium perchlorate to either **A** or cage **B** resulted in the transformation into a unique product: the $Co_{10}\mathbf{L}_{15}^{20+}$ pentagonal prism **C**. Mass spectrometric analysis of **C** reveals that a single chloride anion was bound, even though it was not added purposely. Interestingly, the authors did not succeed in removing the chloride anion, not even by the addition of silver perchlorate, which reveals the high affinity between chloride and **C**. The addition of KPF_6 to **A** initially yields **B**·PF_6. However, after heating this sample at 363 K for 11 days, they obtained a new product **C**·$(PF_6)_5$, which is isomorphous to **C**. These results reveal that one anion triggers a structural reorganization that allows the newly formed structure to function as a highly efficient binder of another anion. Such processes start to mirror how biological systems are able to manifest complex response to environment stimuli.

Very recently, Sanders and coworkers present the efficient formation of a donor-acceptor [3]catenane from a dynamic combinatorial library containing building block **24** and **25** in an aqueous NaNO3 (1 M) solution.[30] The synthesis yield was improved in the presence of spermine (0.5 mM) (Figure 1.7). The amplification of the [3]catenane by spermine highlights the importance of the assembly of large complex structures which can be controlled by small template molecules through a multitude of seemingly weak interactions in a highly competitive medium.

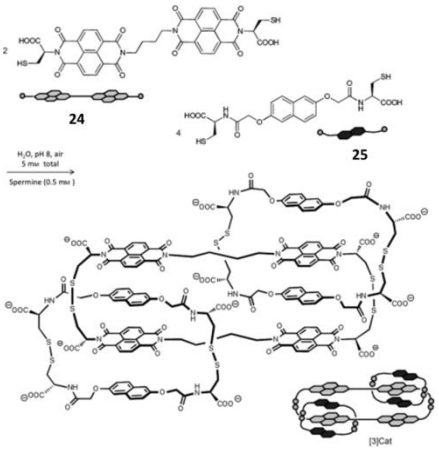

Figure 1.7 Synthesis of a [3]catenane in water, templated by the presence of spermine. This figure is modified from ref. 30.

1.3.3 Internal Templating in DCLs

Recently it has been demonstrated that DCLs may also show fascinating results as a consequence of *internal templating*, where molecular recognition takes place between or within library members. Such interactions may give rise to interlocked structures. If library species can bind intermolecularly to copies of themselves, this will lead to self-assembly, which provides the driving force to shift the equilibrium in favor of the very molecules that self-assemble.[31-34] Our group has coined the term self-synthesizing materials to describe the resulting structures.[31] Note that self-recognition of species in a DCL also constitutes a new mechanism for self-replication with implications for origin-of-life scenarios and potential for creating life de-novo. This is particularly true where the production of replicators is no longer governed by equilibrium thermodynamics but is under kinetic control.

1.3.3.1 Self-Organized Supramolecular Architectures in DCLs

The tendency of DCLs to easily yield thermodynamic products with high yields and selectivities is also reflected in libraries where the template molecule is also a part of the library (*internal templating*). Such self-templating behavor can be successfully exploited to create topological bonds. The reversibility of the reactions used to tie a catenane, rotaxane or knot is crucial for achieving high selectivity, since they provide an error-correction mechanism which allows for the conversion of any misassembled kinetic products to the thermodynamic ones. With this mechanism, the unlikely threading events necessary for the formation of the desired products are no longer an obstacle.

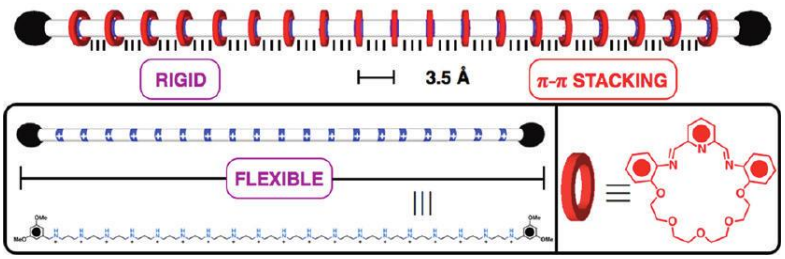

Figure 1.8 A rigid [20]-rotaxane formed 20 equivalents of a dynamic macrocycle cooperatively assembling around the flexible template rod. This figure is modified from ref. 35.

A remarkable efficiency of this principle has been recently employed by the Stoddart group to synthesize a series of oligorotaxanes (Figure 1.8)[35] based on their previous work on imine DCLs of simple rotaxanes stabilized by the ammonium – crown ether motif.[14a] Exceptional yields stemmed from the cooperative effect, caused by stacking interactions between the neighboring rings. It has been shown that a library containing an excess of rods had a highly non-statistical distribution, with a strong preference towards fully saturated oligorotaxanes; a clear indication of cooperativity. The cooperative behavior was absent in case when the library components were mismatched, i.e. the distance between the ammonium recognition groups was larger than the optimal 0.35 nm. Similarly, an imine clipping protocol has been found application in the thermodynamically controlled synthesis of [c2]-daisy chains in almost quantitative yields.[14b] Extension of this approach to polymeric and switchable daisy chains is the next challenge which can integrate motions of nanomachines to meso and macroscales.[14c]

Catenanes have also profited a lot in the recent years from the DCC approach. An approach was utilized by Sanders and coworkers, who focused mainly on aromatic and hydrophobic interactions between the library components made from naphthalene diimide (NDI) acceptor and naphthalene donor building blocks (Figure 1.9). This work has led to the discovery of donor-acceptor [2]-catenanes,[36] showing that unfavorable aromatic interactions can be often overcome by the hydrophobic effect, giving rise to unexpected structures.[37] Increased understanding of the delicate balance between various effects stabilizing interlocked structures and fine-tuning of the parameters of the building blocks (linker length, flexibility, chirality) has recently helped to develop DCLs rich in uncommon giant macrocycles and catenanes, with the possibility to control their distribution (Figure 1.9).[38]

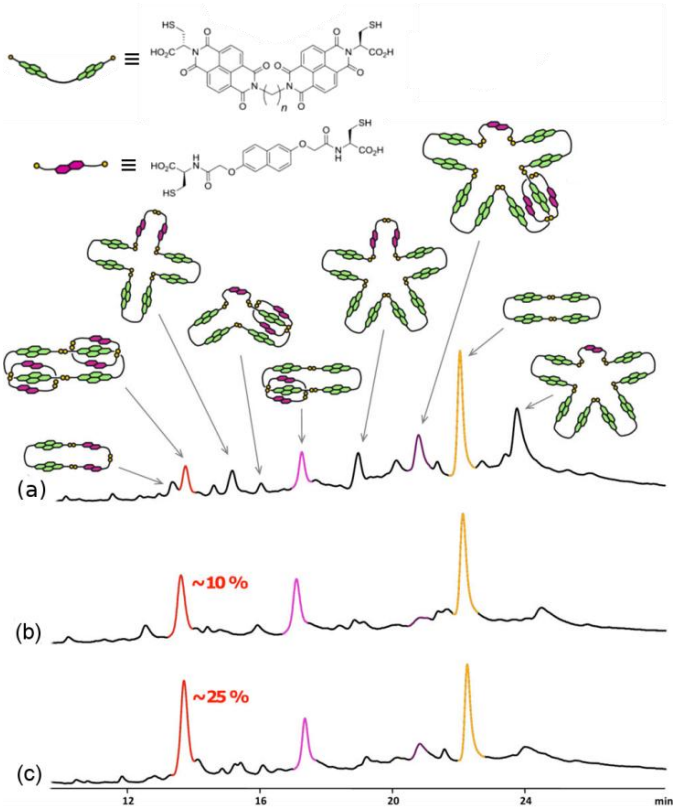

Figure 1.9 HPLC traces of DCLs formed by donor (purple) and acceptor (green) building blocks mixed in ratios: 1:1 (a), 2:1 (b) and 2:1 after stepwise addition of the donor (c). This figure is modified from ref. 38.

Mechanical bonds may also lead to the formation of molecules with more complex topologies which involve interweaving one or more long and flexible molecules. Error-correction mechanisms in DCLs based on self-recognizing motifs can lead to the formation of only the best-fitting knots with high selectivities. Chemists have been utilizing this strategy to create remarkable structures like Borromean rings,[39] Solomon links[40] and pentafoil knots.[41] In contrast to the structures obtained so far, a recent system containing a trefoil knot reported by Sanders and coworkers involved only purely organic building blocks.[42] The importance of the reversible character of the library is illustrated well by the kinetics of the system (Figure 1.10), where entropy favors formation of the kinetically controlled dimeric macrocycles, but the hydrophobic effect drives the library towards the

formation of the thermodynamically controlled trefoil knot later on.

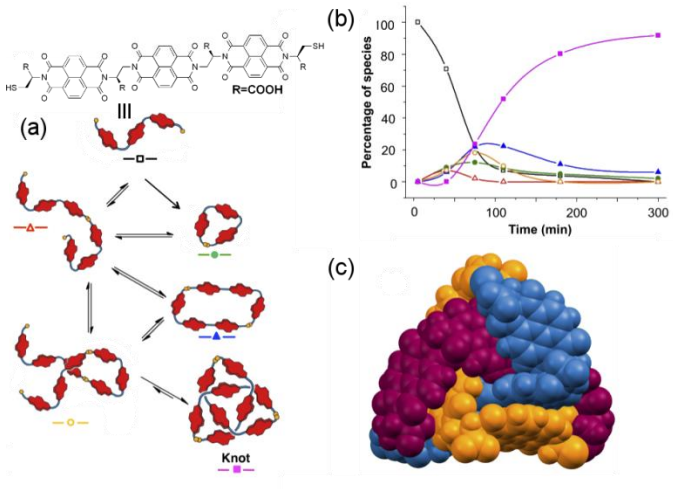

Figure 1.10 Chemical equilibria (a) and the kinetic profile (b) of the library forming the organic trefoil knot (c). The symbols on the plot correspond to the ones below each structure. This figure is modified from ref. 39.

1.3.3.2 Self-Replication in DCLs

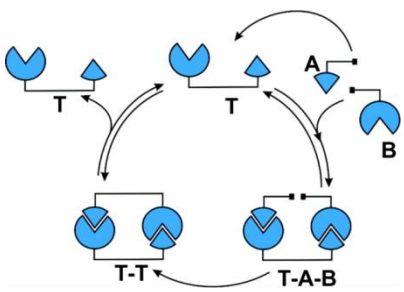

Scheme 1.4 Minimal self-replicating system. This scheme is modified from ref. 6a.

Self-replication is the basis of all living systems and has likely played a central role in the origin of life. While research on synthetic replicating systems has been gaining significance in the scientific community,[43] synthetic replicators still lack qualities which are essential to biological systems. Minimal self-replication systems (Scheme 1.4)[43, 44] typically consist of three components: two substrate molecules, **A** and **B**, and a template/product molecule **T**. In the mixture, the template molecule binds molecule **A** and **B** forming a ternary complex (**T**-**A**-**B**). Subsequently, a covalent bond can form between **A** and **B** giving rise to a duplex of the product **T**-**T**. This can dissociate to produce two molecules of **T** which will act as

templates in the next reaction cycles. The complex **T-T** may suppress the formation of ternary complex (**T-A-B**) and be a "dead-end" of the cycle. Most synthetic systems have a relatively poor replicating efficiency due to the incomplete dissociation of the duplex molecule **T-T**.[6a]

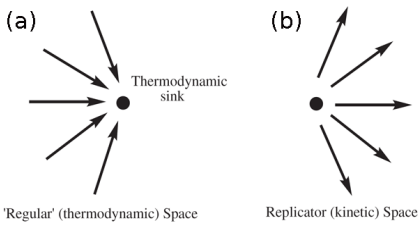

Figure 1.11 (a) Standard chemical systems are convergent in nature. (b) DKS systems are divergent and therefore able to evolve. This figure is modified from ref. 45.

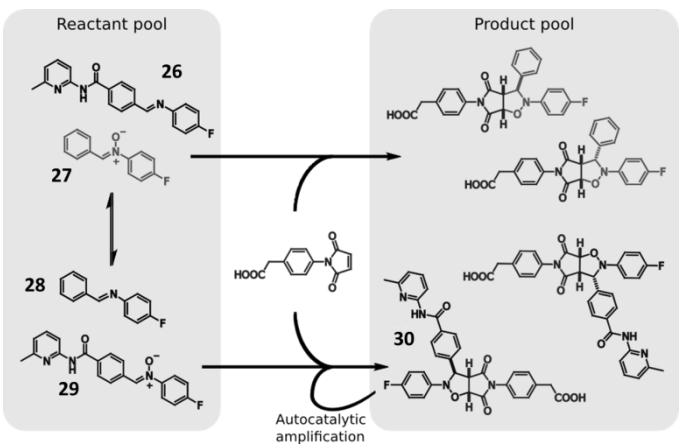

Figure 1.12 Only the molecule capable of self-replication (**30**) is selected in a system with equilibrating substrates (**26**-**29**). This figure is modified from ref. 46.

The majority of the replicators so far have been only studied from the replication point of view, which is already challenging enough. Thus, most replicators are the thermodynamic products; i.e. they are more stable than the building blocks (food molecules) used to make them. Furthermore, replication is usually irreversible. However, living organisms operate under far-from-equilibrium conditions, by constantly making copies of themselves and thus counteracting their continuous decay. If their replication rate is equal to or greater than their

decay, they exhibit dynamic kinetic stability (DKS).[45] In contrast to thermodynamically controlled systems, replicator networks subject to continuous growth and decay are divergent in nature, which enables them to evolve (Figure 1.11). Replication by synthetic systems that involve a reversible reaction would bring us a step closer to achieving DKS. Combining the principles of dynamic combinatorial chemistry with replicator chemistry appears to be a promising way forward.

The first DCL in which the selection process was determined by a replication reaction has been developed by the Sadownik and Philp.[46] The irreversible replication process consumed the food library member from the dynamic reagent pool, thus driving the reequilibration of the library and determining its fate (Figure 1.12). Autocatalytic properties have been also found in related imine libraries in which the replication reaction was actually imine formation, making the replication process itself reversible.[47]

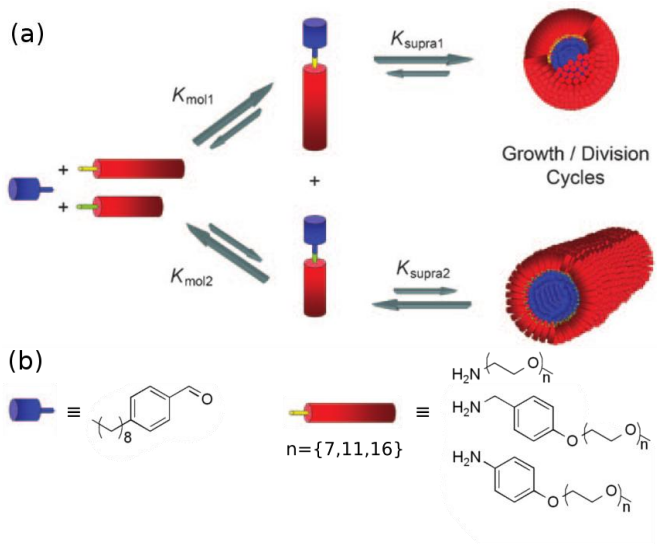

Figure 1.13 (a) A DCL composed of hydrophilic amines (red) and hydrophobic aldehydes (blue) reacting into imines. Autocatalytic growth of different micelles favors more efficient replicators. (b) Chemical structures of the aldehyde and amines. This figure is modified from ref. 48.

Imine formation has also been implemented to form a dynamic amphiphile capable of reversibly assembling into spherical micelles and cylindrical micelles.[48] Because the imines are stabilized while forming supramolecular assemblies, formation of micelles promotes further imine formation, leading to the growth of the aggregates. Bigger micelles become

unstable, leading, in turn, to their division (Figure 1.13). In such case, the replicating entity is not constituted by a single molecule, but by the entire micelle, a process referred to as autopoiesis.[49] Remarkably, small DCLs composed of different amine building blocks showed a pronounced preference towards incorporation of one of them into imines, therefore showing selection of the more efficient autopoeietic system.

A conceptually similar approach has been used to create a self-replicating network composed by dithiol-functionalized peptidic building blocks.[31] These building blocks first form a mixture of macrocycles, some of which then form fibers thanks to the propensity of peptide chains for β-sheet formation. When the fibers grow long enough, they become susceptible to shear stresses and break, duplicating the number of catalytically active fiber ends (Figure 1.14). Because macrocycles of various sizes can be formed in the library, different self-replicating fibers can, in principle, exist. Competition for food molecules between replicators leads to selection of one of them, where the nature of the selected macrocycle size may depend on the agitation method.

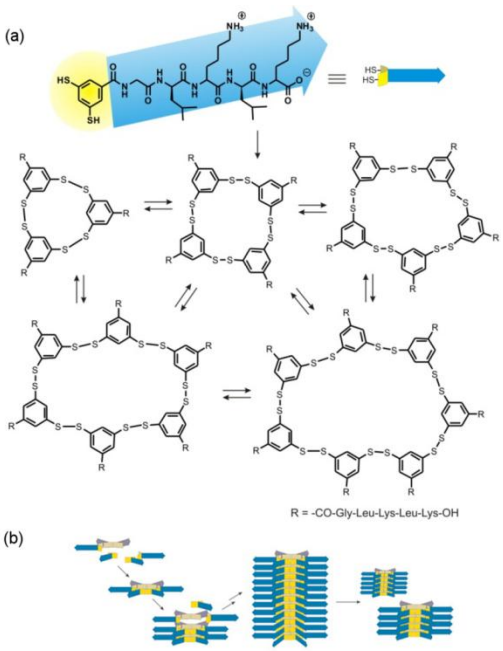

Figure 1.14 (a) A dithiol-functionalized peptide is oxidized into hexameric macrocycles which are able to stack and form fibres. (b) Mechanical breakage of the fibres duplicates the number of replicators. This figure is modified from ref. 31.

Replication facilitated by coiled-coiled peptide self-assembly of food molecules has been also employed by Ashkenasy and coworkers in order to form replicating binary networks under partial thermodynamic control.[50] The system was doubly responsive, in a way that the outcome of the replication could be influenced by both chemical and physical inputs (templates and light, respectively).

Watson-Crick DNA base pairing constitutes a reliable way of templated information transfer into a complementary strand, which in turn can be used for building cross-catalytic systems. In nature however, a polymerase enzyme is required to synthesize a complementary copy and the reaction itself is irreversible. In contrast, the DCC methodology has allowed for enzyme-free functionalization of an oligomer, based on nucleobase pairing.[51] Reversible thioester bond formation between thioester-functionalized nucleobases and oligocystein provides a possibility to keep the system at the thermodynamic equilibrium and influence its composition by introduction of an oligonucleotide template (Figure 1.15). In contrast to enzymatic DNA polymerization, this process is reversible, allowing for error correction and relatively high fidelity, compared to other enzyme-free polymerizations. While no autocatalytic processes have been investigated, this study constitutes an important step towards cross-replication of information rich polymers.

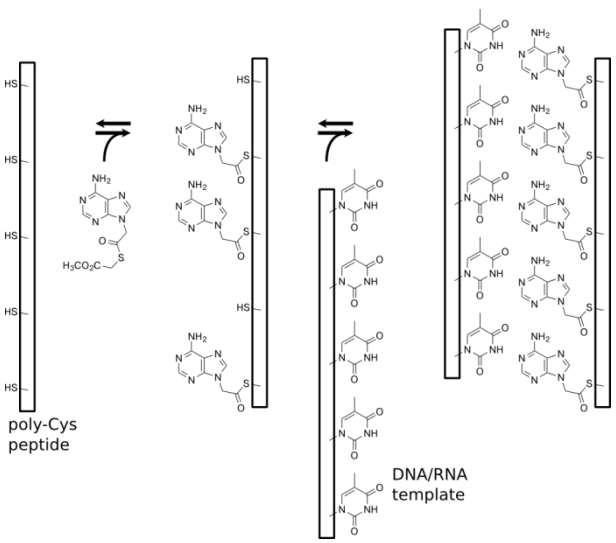

Figure 1.15 A statistical configuration of nucleobases on a polypeptide is efficiently templated to form a complementary strand. This figure is modified from ref. 50.

Another characteristic of self-replicators which appeals strongly to chemists is that they constitute a route to self-synthesizing materials. The above examples have shown that the self-organization in DCLs can drive the occurrence of self-replication. At the same time, the very molecule that assembles promotes its own synthesis driven by its assembly into supramolecular nanomaterials such as micelles, vesicles and fibers. Among these materials, nanostructured hydrogels are emerging as a promising group of materials for contemporary technologies.[52]

1.3.3.3 Hydrogels

Polymer gels have been known for centuries and have found application in many fields including food, medicine, materials science, cosmetics and pharmacology. However, this conventional type of gel has its inherent shortage of reversibility.[53] Many small molecule gelators could overcome this problem, since they are held together by noncovalent interactions, making them much easier for the body to degrade. They even can be injected directly to the specific position in the body for delivering a drug without covalently binding it.

In general, hydrogels are viscoelastic solid-like materials forming by entrapping and adhering water molecules in an elastic cross-linked 3D network.[54] The hydrogels of a low molecular weight compound are usually prepared by dispersing the gelators in water solution at a proper concentration. The dispersed organic molecules should then aggregate via noncovalent interactions. Highly ordered aggregation gives rise to crystals while a more disordered aggregation results in an amorphous precipitate. A gel can be produced by incooperating solvent molecules in networks entangled by fibers which are formed in 1D aggregation. The properties of the hydrogel depend on many factors, i.e. the concentration of the gelators, the noncovalent forces between the gelators, the pH and temperature of the solution. Under these different experimental conditions, hydrogel can change its properties and the gelation process can be reversibly controlled. DCLs are mixtures consisting of many library members, providing unexpected gelators forming hydrogels.

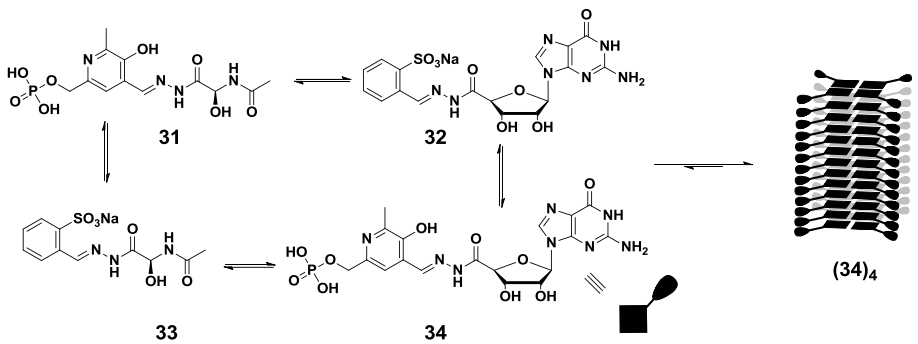

Figure 1.16 The gelation amplified the hydrazone formation. This figure was modified from ref. 55.

Lehn and coworkers have described the formation of a stable hydrogel in a hydrazine DCL.[55] The library was prepared by hydrazide-functionalized guanosine and serine building blocks and other two aldehyde building blocks. They will react in sodium acetate buffer (pH 6.0) and form a library of four interconverting hydrazones (**31**-**34**) (Figure 1.16). Hydrazone **32** was amplified in the mixture resulting from its self-assembly forming hydrogel.

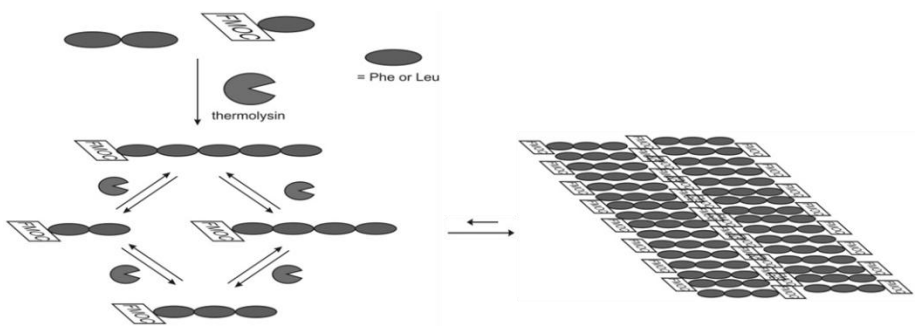

Figure 1.17 A mixture of a DCL was produced by thermolysin-mediated reversible amide bond formation. Self-assembly of the trimeric peptide into fibers shifts the equilibrium towards this product and also causes gelation of the solvent. This figure is modified from ref. 56.

Another example of gelation in a DCL is from Ulijn's group.[56] The DCL was constructed using reversible amide bond formation, mediated by thermolysin, which is an enzyme that can catalyze both amide bond hydrolysis and formation. They started a library with dipeptides and fluorenyl-protected amino acids (Figure 1.17). Due to the function of thermolysin, the library reached a thermodynamic equilibrium of a dynamic mixture of

peptides of different lengths. When phenylalanine or leucine was used as a building block, the corresponding trimeric peptides self-assembled into fibers shifting the equilibrium and amplifying itself. The fibers can entangle and subsequently form a hydrogel.

1.4 Conclusions and Contents of this Thesis

DCC has matured as a successful tool to construct and study complex systems. Self-organization in these dynamic molecular networks drives the evolution of DCLs, leading to discoveries of new phenomena and solutions to urging problems. However, there is still much room for further development. For example, most synthetic receptors are produced by one template. We can introduce more templates to construct more complex systems in which self-organization may help us to find more interesting behaviors in the libraries. There are only limited examples of self-replicating DCLs. We are just at the starting point of exploring self-synthesizing materials. Nanomaterials with unexpected properties and new functions could emerge from the complex DCL pools under the guidance of self-organization. It is these considerations that inspired much of the work described in this thesis the contents of which are summarized below.

In Chapter 2, we described a dynamic catenane system developed using DCC. An azobenzene derived dithiol building block forms a small DCL dominated by a [2]catenane, which may be converted into a family of [2] and [3] catenanes by adding cyclodextrin homologues as templates. Methods for extracting the equilibrium constants for the individual catenation steps are developed. The results reveal that the self-organized [3]catenanes form by positive (for β-CD) or negative (γ-CD) cooperativity. This quantitative assessment of equilibrium constants for catenantion is potentially applicable to any catenanes containing dynamic covalent bonds.

Encouraged by these results, we explored another naphthalene derived asymmetric dithiol building block in Chapter 3. It forms a DCL dominated by [2]catenane isomers. These [2]catenane isomers can be converted into four tetrameric macrocycles whose structures were identified by analyzing thiols fragments obtained by partially reducing the disulfide macrocycles. By introducing a phenyl ammonium salt, γ-CD or both of them as templates into the library, each of the four tetrameric isomers can be amplified selectively. Interestingly, one of the tetramers was neither amplified by the phenyl ammonium salt nor by γ-CD, but nearly quantitative amplification took place in the presence of both templates together. By

measuring binding constant of each step, we found that this unusual amplification was due to the cooperative formation of a self-organized Russian-Doll type complex.

In Chapter 4, we described the preparation of DCLs using the same building block as in the previous chapter, but this time we used an adamantane derived ammonium salt as the template. Upon changing the concentration of template, a nonlinear increase in amplification factor was found. This behavior is driven by the aggregation of one of the tetramer isomers. This isomer self-organized into nanosheets as evident from cryo-TEM analysis.

We investigated the self-replication in DCLs using an amphiphilic dithiol building block in Chapter 5. From the HPLC-MS analysis of the library, the tetramer of this building block was found to self-replicate. Mixing this building block with another dithiol building block produced a much more complex library. Seeding this library by the self-replicating tetramer promoted its own formation, providing evidence for autocatalysis. The self-replication process was driven by the self-organization of the tetramer into nanosheets that can fold to form vesicle-like compartments.

In Chapter 6, by designing a building block to contain the right ingredients a multi-responsive self-assembling hydrogel was obtained through a process of template-induced self-synthesis in a DCL. The system can be switched between gel and solution by light, redox reactions, pH, temperatures changes, mechanical energy and sequestration or addition of Mg (II) salt.

In Chapter 7, we describe how stacks of macrocycles self-organize into fibers using reversible disulfide-bond formation. These pre-organized macrocycles are then covalently captured by photoinitiated exchange of disulfide bonds, inducing the formation of hydrogels. This strategy allows access to structures beyond the thermodynamic minima traditionally targeted by DCC.

Finally, Chapter 8 provides an overview of the thesis emphasizing the contribution of DCC to systems chemistry and particular to self-organization in complex chemical systems. Potential directions for future research are discussed.

1.5 Acknowledgements

Piotr Nowak is greatly acknowledged for the help with preparing the section on self-replication.

1.6 References

[1] Kauffman, S. A. *The Origins of Order, Self-Organization and Selection in Evolution*, Oxford University, New York, **1993**.

[2] Boissonade, J. in *Origins of Life: Self-Organization and/or Biological Evolution?* **2009**, 23-26.

[3] (a) Whitesides, G. M.; Grzybowski, B. *Science* **2009**, *29*, 2418-2481.

[4] (a) Lehn, J.-M. *Proc. Natl. Acad. Sci. U. S. A.* **2002**, *99*, 4763-4768; (b) Lehn, J.-M. *Angew. Chem. Int. Ed.* **2013**, *52*, 2836-2850.

[5] (a) Ludlow, R. F.; Otto, S. *Chem. Soc. Rev.* **2008**, *37*, 101-108; (b) Peyralans, J. J.-P.; Otto, S. *Curr. Opin. Chem. Biol.* **2009**, *13*, 705-713; (c) Hunt, R. A. R.; Otto, S. *Chem. Comm.* **2011**, *47*, 847-858; (d) Newth, D.; Finnigan, J. *Aust. J. Chem.* **2006**, *59*, 841-848; (e) Szostak, J. W. *Nature* **2009**, *459*, 171-172; (f) Whitesides, G. M.; Ismagilov R. F. *Science* **1999**, *284*, 89-92; (g) Nitschke, J. R. *Nature* **2009**, *462*, 736-738; (h) Stankiewicz, J.; Eckardt, L. H. *Angew. Chem. Int. Ed.* **2006**, *45*, 342-344.

[6] (a) Otto, S. *Acc. Chem. Res.* **2012**, *45*, 2200-2210; (b) Corbett, P. T.; Leclaire, J.; Vial, L.; West, K. R.; Wietor, J.-L.; Sanders, J. K. M.; Otto, S. *Chem. Rev.* **2006**, *106*, 3652-3711; (c) Cougnon, F. B. L.; Sanders, J. K. M. *Acc. Chem. Res.* **2012**, *45*, 2211-2221; (d) Lehn, J.-M. *Top. Curr. Chem.* **2011**, *322*, 1-32; (e) Lehn, J.-M. *Chem. Soc. Rev.* **2007**, *36*, 151-160; (f) Miller, B. L. *Dynamic Combinatorial Chemistry in Drug Discovery, Bioorganic Chemistry, and Materials Science*, Wiley, Hoboken, NJ, **2012**; (g) Reek, J. N. H.; Otto, S. *Dynamic Combinatorial Chemistry*, Wiley-VCH, Weinheim, **2010**.

[7] Otto, S.; Furlan, R. L. E.; Sanders, J. K. M. *Science* **2002**, *297*, 590-593.

[8] Literatures of anion receptors: (a) Custelcean, R. *Top. Curr. Chem.* **2012**, *322*, 193-216; (b) Bru, M.; Alfonso, I.; Burguete, M. I.; Luis, S. V. *Angew. Chem. Int. Ed.* **2006**, *45*, 6155-6159; (c) Bru, M.; Alfonso, I.; Bolte, M.; Burguete, M. I.; Luis, S. V. *Chem. Commun.* **2011**, *47*, 283-285; (d) Beeren, S. R.; Sanders, J. K. M. *Chem. Sci.* **2011**, *2*, 1560-1567; (e) Vilar, R. *Struct. Bond.* **2008**, *129*, 175-206.

[9] Literatures of cation receptors: (a) Besenius, P.; Cormack, P. A. G.; Ludlow, R. F.; Otto, S.; Sherrington, D. C. *Chem. Commun.* **2008**, 2809-2811; (b) Saggiomo, V.; Lüning, U. *Chem. Commun.* **2009**, 3711-3713; (c) Saggiomo, V.; Lüning, U. *Tetrahedron Lett.* **2009**, *50*, 4663-4665; (d) Xu, X. N.; Wang, L.; Wang, G. T.; Lin, J. B.; Li, G. Y.; Jiang, X. K.; Li, Z. T. *Chem. Eur. J.* **2009**, *15*, 5763-5774; (e) Ceborska, M.; Tarnowska, A.; Ziach, K.; Jurczak, J. *Tetrahedron* **2010**, *66*, 9532-9537; (f) Klein, J. M.; Saggiomo, V.; Reck, L.; McPartlin, M.; Pantoş, G. D.; Lüning, U.; Sanders, J. K. M. *Chem. Commun.* **2011**, *47*, 3371-3373; (g) Klein, J. M.; Clegg, J. K.; Saggiomo, V.; Reck, L.; Lüning, U.; Sanders, J. K. M. *Dalton Trans.* **2012**, *41*, 3780-3786; (h) Klein, J. M.; Saggiomo, V.; Reck, L.; Lüning, U.; Sanders, J. K. M. *Org. Biomol. Chem.* **2012**, *10*, 60-66.

[10] Literatures of receptors for neutral molecules: (a) Vial, L.; Ludlow, R. F.; Leclaire, J.; Perez-Fernandez, R.; Otto, S. *J. Am. Chem. Soc.* **2006**, *128*, 10253-10257; (b) Hamieh, S; Ludlow, R. F.; Perraud, O.; West, K. R.; Mattia,

E.; Otto, S. *Org. Lett.* **2012**, *14*, 5404-5407; (c) Chung, M. K.; Severin, K.; Lee, S. J.; Waters, M. L.; Gagne, M. R. *Chem. Sci.* **2011**, *2*, 744-747.

[11] Literatures of protein-directed DCLs: (a) Nour, H. F.; Islam, T.; Fernández-Lahore, M.; Kuhnert, N. *Rapid Commun. Mass spectrum.* **2012**, *26*, 2865-2876; (b) Demetriades, M.; Leung, I. K. H.; Chowdhury, R.; Chan, M. C.; McDonough, M. A.; Yeoh, K. K.; Tian, Y. M.; Claridge, T. D. W.; Ratcliffe, P. J.; Woon, E. C. Y.; Schofield, C. J. *Angew. Chem. Int. Ed.* **2012**, *51*, 6672-6675; (c) Woon, E. C. Y.; Demetriades, M.; Bagg, E. A. L.; Aik, W.; Krylova, S. M.; Ma, J. H. Y.; Chan, M.; Walport, L. J.; Wegman, D. W.; Dack, K. N.; McDonough, M. A.; Krylov, S. N.; Schofield, C. J. *J. Med. Chem.* **2012**, *55*, 2173-2184; (d) Ingerman, L. A.; Cuellar, M. E.; Waters, M. L. *Chem. Commun.* **2010**, *46*, 1839-1841; (e) Nasra, G.; Petita, E.; Supuranb, C. T.; Winumc, J.-Y.; Barboiu, M. *Bioorg. Medicinal Chem. Lett.* **2009**, *19*, 6014-6017; (f) Cancilla, M. T.; He, M. M.; Viswanathan, N.; Simmons, Robert L.; Taylor, M.; Fung, A. D.; Cao, K.; Erlanson, D. A. *Bioorg. Medicinal Chem. Lett.* **2008**, *18*, 3978-3981; (g) Valade, A.; Urban, D.; Beau, J.-M. *ChemBioChem* **2006**, *7*, 1023-1027.

[12] Literatures of nucleic acid-directed DCLs: (a) Leal, N. A.; Sukeda, M.; Benner, S. A. *Nucl. Acids Res.* **2006**, *34*, 4702-4710; (b) McNaughton, B. R.; Gareiss, P. C.; Miller, B. L. *J. Am. Chem. Soc.* **2007**, *129*, 11306-11307; (c) Valade, A.; Urban, D.; Beau, J. M. *J. Comb. Chem.* **2007**, *9*, 1-4; (d) Scott, D. E.; Dawes, G. J.; Ando, M.; Abell, C.; Ciulli, A. *ChemBioChem* **2009**, *10*, 2772-2779; (e) Azema, L.; Bathany, K.; Rayner, B. *ChemBioChem* **2010**, *11*, 2513-2516; (f) Lopez-Senin, P.; Gomez-Pinto, I.; Grandas, A.; Marchan, V. *Chem. Eur. J.* **2011**, *17*, 1946-1953.

[13] (a) West, K.; Bake, K.; Otto, S. *Org. Lett.* **2005**, *7*, 2615-2618; (b) Ajami, D.; Rebek, J. *Angew. Chem. Int. Ed.* **2007**, *46*, 9283-9286; (c) Kerckhoffs, J. M. C. A.; Mateos-Timoneda, M. A.; Reinhoudt, D. N.; Crego-Calama, M. *Chem. Eur. J.* **2007**, *13*, 2377-2385; (d) Christinat, N.; Scopelliti, R.; Severin, K. *Angew. Chem. Int. Ed.* **2008**, *47*, 1848-1852; (e) Takahagi, H.; Fujibe, S.; Iwasawa, N. *Chem. Eur. J.* **2009**, *15* , 13327-13330; (f) Dreos, R.; Randaccio, L.; Siega, P.; Tavagnacco, C.; Zangrando, E. *Inorg. Chim. Acta* **2010**, *363*, 2113-2124; (g) Ziach, K.; Ceborska, M.; Jurczak, J. *Tetrahedron Lett.* **2011**, *52*, 4452-4455; (h) Stefankiewicz, A. R.; Sambrook, M. R.; Sanders, J. K. M. *Chem. Sci.* **2012**, *3*, 2326-2329.

[14] (a) Haussmann, P. C.; Khan, S. I.; Stoddart, J. F. *J. Org. Chem.* **2007**, *72*, 6708–6713; (b) Bozdemir, O. A.; Barin, G.; Belowich, M. E.; Basuray, A. N.; Beuerle, F.; Stoddart, J. F. *Chem. Commun.* **2012**, *48*, 10401–10403; (c) Du, G.; Moulin, E.; Jouault, N.; Buhler, E.; Giuseppone, N. *Angew. Chem. Int. Ed.* **2012**, *51*, 12504–12508.

[15] Lam, T. S. R.; Belenguer, A.; Roberts, S. L.; Naumann, C.; Jarrosson, T.; Otto, S.; Sanders, J. K. M. *Science* **2005**, *308*, 667-669.

[16] Kubik, S. *Chem. Soc. Rev.* **2010**, *39*, 3648-3663.

[17] Otto, S.; Kubik, S. *J. Am. Chem. Soc.* **2003**, *125*, 7804-7805.

[18] Rodriguez-Docampo, Z.; Pascu, S. I.; Kubik, S.; Otto, S. *J. Am. Soc. Chem.* **2006**, *128*, 11206-11210.

[19] Otto, S. *Dalton Trans.* **2006**, 2861-2864.

[20] Rodriguez-Docampo, Z.; Eugenieva-Ilieva, E.; Reyheller, C.; Belenguer, A. M.; Kubik, S.; Otto, S. *Chem. Commun.* **2011**, *47*, 9798-9800.

[21] (a) Davis, A. P.; Wareham, R. S. *Angew. Chem. Int. Ed.* **1999**, *38*, 2978-2996; (b) Striegler, S. Curr. *Org. Chem.* **2003**, *7*, 81-102; (c) Barwell, N. P.; Crump, M. P.; Davis, A. P. *Angew. Chem. Int. Ed.* **2009**, *48*, 1775-1779; (d) Ferrand, Y.; Crump, M. P.; Davis, A. P. *Science* **2007**, *318*, 619-622.

[22] Verma, A.; Rotello, V. M. *Chem. Commun.* **2005**, 303-312.

[23] Shi, B. L.; Stevenson, R.; Campopiano, D. J.; Greaney, M. F. *J. Am. Chem. Soc.* **2006**, *128*, 8459-8467.

[24] (a) Bhat, V. T.; Caniard, A. M.; Luksch, T.; Brenk, R.; Campopiano, D. J.; Greaney, M. F. *Nat. Chem.* **2010**, *2*, 490-497; (b) Miller, B. L. *Nat. Chem.* **2010**, *2*, 433-434.

[25] (a) Dirksen, A.; Dirksen, S.; Hackeng, T. M.; Dawson, P. E. *J. Am. Chem. Soc.* **2006**, *128*, 15602-15603; (b) Dirksen, A.; Dawson, P. E. *Bioconjugate Chem.* **2008**, *19*, 2543-2548.

[26] Ladame, S.; Whitney, A.; Balasubramanian, S. *Angew. Chem. Int. Ed.* **2005**, *44*, 5736-5739.

[27] Bugaut, A.; Jantos, K.; Wietor, J. L.; Rodriguez, R.; Sanders, J. K. M.; Balasubramanian, S. *Angew. Chem. Int. Ed.* **2008**, *47*, 2677-2680.

[28] Nitschke, J. R. *Acc. Chem. Res.* **2007**, *40*, 103-112.

[29] Riddell, I. A.; Smulders, M. M. J.; Clegg, J. K.; Hristova, Y. R.; Breiner, B.; Thoburn, J. D.; Nitschke, J. R. *Nat. Chem.* **2012**, *4*, 751-756.

[30] Cougnon, F. B. L.; Jenkins, N. a; Pantoş, G. D.; Sanders, J. K. M. *Angew. Chem. Int. Ed.* **2012**, *51*, 1443–1447.

[31] Carnall, J. M. A.; Waudby, C. A.; Belenguer, A. M.; Stuart, M. C. A.; Peyralans, J. J.-P.; Otto, S. *Science* **2010**, *327*, 1502-1506.

[32] Moulin, E.; Giuseppone, N. *Top. Curr. Chem.* **2012**, *322*, 87-105.

[33] Moulin, E.; Cormos, G.; Giuseppone, N. *Chem. Soc. Rev.* **2012**, *41*, 1031-1049.

[34] Giuseppone, N. *Acc. Chem. Res.* **2012**, *45*, 2178-2188.

[35] (a) Belowich, M. E.; Valente, C.; Stoddart, J. F. *Angew. Chem. Int. Ed.* **2010**, *49*, 7208–7212; (b) Belowich, M. E.; Valente, C.; Smaldone, R. A.; Friedman, D. C.; Thiel, J.; Cronin, L.; Stoddart, J. F. *J. Am. Chem. Soc.* **2012**, *134*, 5243–5261.

[36] Au-Yeung, H. Y.; Pantoş, G. D.; Sanders, J. K. M. *Proc. Natl. Acad. Sci. U. S. A.* **2009**, *106*, 10466–10470.

[37] (a) Cougnon, F. B. L.; Au-Yeung, H. Y.; Pantoş, G. D.; Sanders, J. K. M. *J. Am. Chem. Soc.* **2011**, *133*, 3198–3207; (b) Au-Yeung, H. Y.; Pantoş, G. D.; Sanders, J. K. M. *J. Org. Chem.* **2011**, *76*, 1257–1268.

[38] Cougnon, F. B. L.; Ponnuswamy, N.; Jenkins, N. A.; Pantoş, G. D.; Sanders, J. K. M. *J. Am. Chem. Soc.* **2012**, *134*, 19129–19135.

[39] Chichak, K. S.; Cantrill, S. J.; Pease, A. R.; Chiu, S.-H.; Cave, G. W. V; Atwood, J. L.; Stoddart, J. F. *Science* **2004**, *304*, 1308–1312.

[40] Pentecost, C. D.; Chichak, K. S.; Peters, A. J.; Cave, G. W. V; Cantrill, S. J.; Stoddart, J. F. *Angew. Chem. Int.*

Ed. **2007**, *46*, 218–222.

[41] Ayme, J.-F.; Beves, J. E.; Leigh, D. A.; McBurney, R. T.; Rissanen, K.; Schultz, D. *Nat. Chem.* **2012**, *4*, 15–20.

[42] Ponnuswamy, N.; Cougnon, F. B. L.; Clough, J. M.; Pantoş, G. D.; Sanders, J. K. M. *Science* **2012**, *338*, 783–785.

[43] Patzke, V.; von Kiedrowski, G. *ARKIVOC* **2007**, 293–310.

[44] (a) Paul, N.; Joyce, G. F. *Curr. Opin. Chem. Biol.* **2004**, *8*, 634-639; (b) Robertson, A.; Sinclair, A. J.; Philp, D. *Chem. Soc. Rev.* **2000**, *29*, 141-152.

[45] Pross, A. *J. Syst. Chem.* **2011**, *2*, 1.

[46] Sadownik, J. W.; Philp, D. *Angew. Chem. Int. Ed.* **2008**, *47*, 9965–9970.

[47] del Amo, V.; Slawin, A. M. Z.; Philp, D. *Org. Lett.* **2008**, *10*, 4589–4592.

[48] Nguyen, R.; Allouche, L.; Buhler, E.; Giuseppone, N. *Angew. Chem. Int. Ed.* **2009**, *48*, 1093–1096.

[49] Stano, P.; Luisi, P. L. *Chem. Commun.* **2010**, *46*, 3639–3653.

[50] Dadon, Z.; Samiappan, M.; Wagner, N.; Ashkenasy, G. *Chem. Commun.* **2012**, *48*, 1419–1421.

[51] Ura, Y.; Beierle, J. M.; Leman, L. J.; Orgel, L. E.; Ghadiri, M. R. *Science* **2009**, *325*, 73–77.

[52] (a) Vlierberghe, S. V.; Dubruel, P.; Schacht, E. *Biomacromolecules* **2011**, *12*, 1387-1408; (b) Peppas, N. A.; Hilt, J. Z.; Khademhosseini, A.; Langer, R. *Adv. Mater.* **2006**, *18*, 1345-1360; (c) Fisher, O. Z.; Khademhosseini, A.; Langer, R.; Peppas, N. A. *Acc. Chem. Res.* **2010**, *43*, 419-428; (d) Hirano, Y.; Mooney, D. J. *Adv. Mater.* **2004**, *16*, 17-25.

[53] Estroff, L. A.; Hamilton, A. D. *Chem. Rev.* **2004**, *104*, 1201-1217.

[54] (a) Nayak, S.; Lyon, L. A. *Angew. Chem. Int. Ed.* **2005**, *44*, 7686-7708; (b) Sangeetha, N. M.; Maitra, U. *Chem. Sov. Rev.* **2005**, *34*, 821-836.

[55] Sreenivasachary, N.; Lehn, J.-M. *Proc. Natl. Acad. Sci. U. S. A.* **2005**, *102*, 5938-5943.

[56] Williams, R. J.; Smith, A. M.; Collins, R.; Hodson, N.; Das, A. K.; Ulijn, R. V. *Nature Nanotechn.* **2009**, *4*, 19-24.

Chapter 2

Quantitative Assessment of Cooperativity in Dynamic Combinatorial Catenanes

In Chapter 1 we have summarized the recent literatures on DCC which shows that it is a versatile tool for making dynamic catenanes. However, hardly any examples have been reported where the equilibrium constants for the formation of catenanes were determined. Since the synthesis of catenanes from DCL is governed by thermodynamics, when the final equilibrium is reached, their extent of formation in the library reflect the strength of the noncovalent interactions that drive catenation. By fitting the concentrations of the various species that can be directly quantified to an equilibrium model, we should be able to assess the equilibrium constant for catenation. In this Chapter, we synthesized an azobenzene derived dithiol building block which forms a small dynamic combinatorial library dominated by a [2]catenane. This [2]catenane may be converted into a family of [2] and [3] catenanes by adding cyclodextrin homologues as templates. Methods for extracting the equilibrium constants for the individual catenation steps are developed. The results reveal that the [3]catenanes form by positive (for β-CD) or negative (for γ-CD) cooperativity.

J. Li, P. Nowak, S. Otto *manuscript in preparation.*

2.1 Introduction

Catenanes represent an important class of mechanically interlocked molecules and are popular motifs for the construction of molecular machines.[1] Catenane synthesis is increasingly performed using reversible chemistry, that ensures that catenane production occurs under thermodynamic control, allowing for error-correction which enhances the yield of the catenation step.[2] Dynamic combinatorial chemistry[3] is a particularly powerful tool for the discovery and synthesis of new catenanes.[4] This has been already discussed in Chapter 1. In the case of applying this strategy for exploring new catenanes, the noncovalent interactions lead to catenation and shift the equilibrium of the mixture towards the formation of the catenanes. The production of catenanes relies in nearly all cases on noncovalent interactions that drive the self-assembly of the components prior to the ring-closing reaction that produces the catenane.

Given the importance of these noncovalent interactions in catenation, methods that allow the direct quantitative assessment of their strength are desirable. Insight into interaction energies is essential for applications that involve the movement of catenane rings with respect to each other.[5] Furthermore, knowing the formation energy of self-assembled catenanes from DCLs helps us have a better understanding of the emergence of supramolecular architectures from complex chemical systems. Finally, for the synthesis of catenanes containing three or more rings, catenane synthesis may exhibit positive or negative cooperativity.[6]

A general method for the quantitative analysis of cooperativity in the formation of higher catenanes has not yet been described. This may stem from the fact that the most common methods for determining binding interactions in supramolecular chemistry (NMR, UV or ITC titrations) cannot be used to determine binding interactions in catenanes as the mechanical bond between the rings in a catenane do not allow for typical titration experiments.

We now show that a global analysis of product distributions obtained for reversible catenation reactions performed at different concentrations allows the quantification of binding interactions within the catenanes, even when the concentration of some of the components involved in catenation cannot be directly quantified. We demonstrate the use of this methodology for two different [3]-catenane systems: one which exhibits positive

cooperativity and one where catenation is negatively cooperative. This methodology should be applicable to any thermodynamically controlled catenation reaction.

We have analyzed the binding strength and cooperativity in a series of new catenanes that we discovered through the use of dynamic combinatorial chemistry.[3] These are based on the well-established interaction between cyclodextrins and azobenzene.[7] As the amounts of cyclodextrins in the libraries changed, the concentration distribution of catenanes varied. We reasoned that the different distribution of products is related to their formation constants[8] which can be obtained by the computer program DCLFit. The data show different cooperativity in the library templated by β-cyclodextrin (β-CD) compared to γ-cyclodextrin (γ-CD). Finally, the responsiveness of the [3]-catenanes was revealed by introducing another guest molecule into this system.

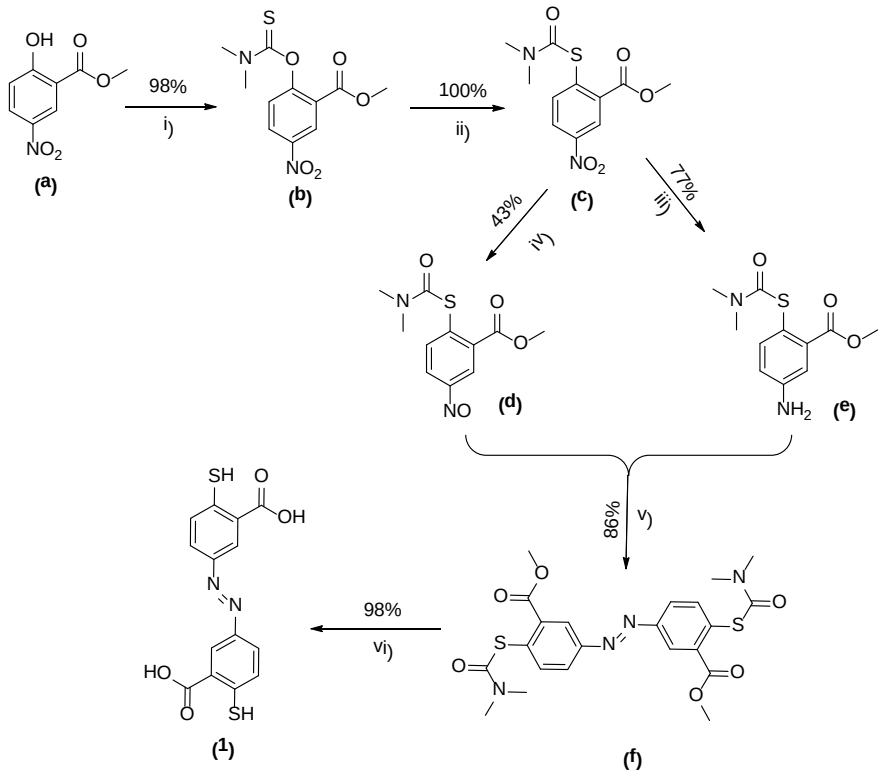

Scheme 2.1. Building block synthesis. i) Me_2N-C(S)-Cl, DABCO, 0°C→RT, DMF; ii) 150°C, 20 min; iii) Zn, acetic acid, 120°C, 45 min; iv) 2-methoxyethanol, water, NH_4Cl, Zn, $FeCl_3$, 5h; v) acetic acid, RT, overnight; vi) 1.75 M KOH in diethyleneglycol, 30 min, 110°C.

2.2 Results and Discussion

2.2.1 Design and Synthesis of Building Block

Building block **1**, which was used for the preparation of the DCLs, is an azobenzene-derived compound. It contains two thiol groups which can be oxidized to form a small DCL of macrocyclic disulfides. The building block also features two carboxylic acid groups for water solubility.

The structure and synthesis route of building block **1** are shown in Scheme 2.1. Generally, its synthesis is straightforward and the yield of each step is relatively high, except for the synthesis of intermediate **d**. The crucial point of this step is that when powdered zinc was added, the solution should be stirred extremely vigorously to mix all reactants well, otherwise the synthesis may fail. Also the last step requires some special attention. Because the final product can be oxidized easily in the air, it should be dried by lyophilisation.

2.2.2 DCL Preparation and Analysis of Components

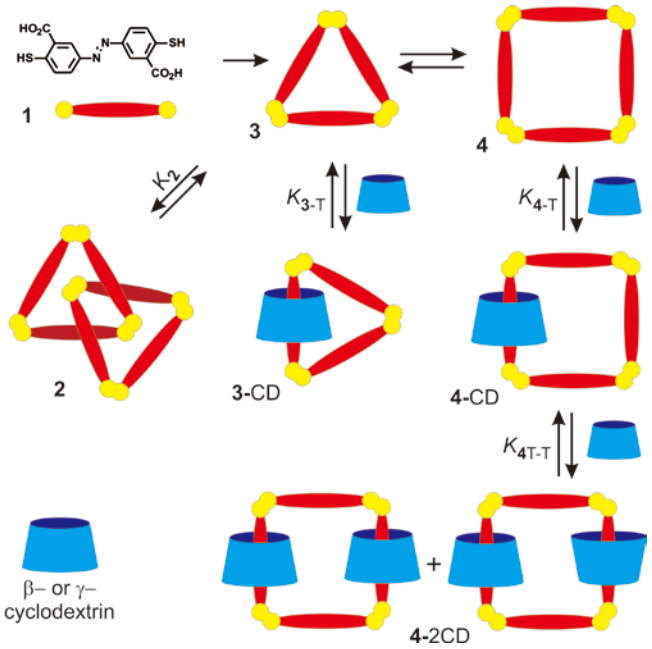

Scheme 2.2. DCLs of building block **1** in the presence of β-CD or γ-CD.

We first prepared a dynamic combinatorial library (DCL) from azobenzene derived dithiol **1** (Scheme 2.2). Stirring this compound in aqueous solution in the presence of oxygen from the air gave rise to a small dynamic combinatorial library of disulfides. Disulfide exchange in these systems takes place through reaction between the disulfides and residual thiolate anion[9] and the equilibrium distribution is reached after 4 days. The resulting mixture was analyzed by HPLC-MS (Figure 2.1) which revealed that the mass of the dominant peak is 1994.3, corresponding to six units of **1**. MS-MS analysis of this peak (Figure 2.1a) showed the trimer of **1** as the only fragmentation product, suggesting that this compound is [2]catenane **2** made from two interlocked timers of **1**. Cyclic trimer **3** and tetramer **4** were also detected as minor constituents of the small dynamic combinatorial library.

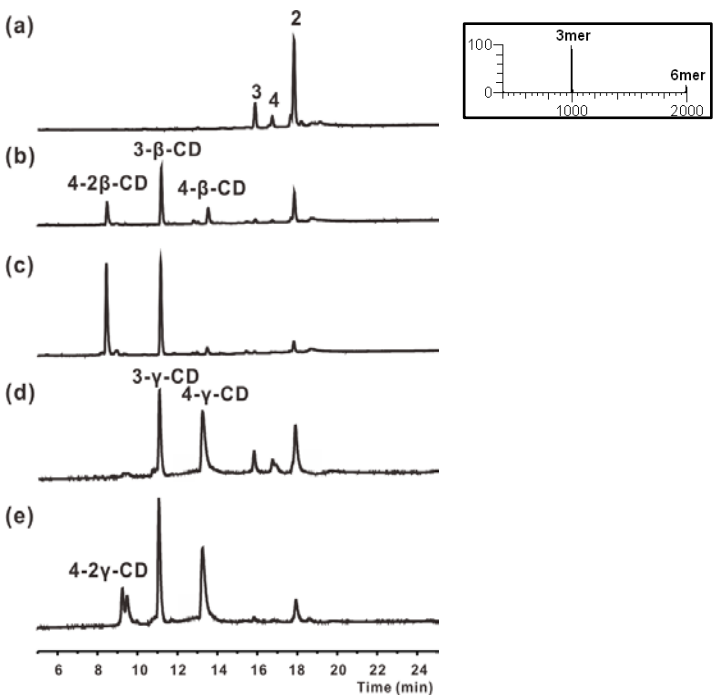

Figure 2.1. HPLC-MS analysis of a DCL made from 2.0 mM building block **1** in aqueous borate buffer (50 mM, pH 8.2) (a) without β-CD; (b) with 0.25 eq. β-CD; (c) 1.0 eq. β-CD; (d) with 0.25 eq. γ-CD and (e) 1.0 eq. γ-CD. The inset shows MS-MS fragmentation spectrum of [2]catenane **2.**

We then prepared the same DCL, but this time added 0.25 equivalents (with respect to **1**) of one of the cyclodextrin (CD) homologues (α-CD, β-CD or γ-CD), respectively, as a template. Upon addition of α-CD the library composition remained unchanged, but in the

presence of β-CD or γ-CD new peaks appeared in the HPLC chromatograms. Upon addition of β-CD three new peaks appeared, as shown in Figure 2.1b. MS analysis (see experimental section) revealed that these correspond to isomeric [3]catenanes **4**-2β-CD consisting of one tetrameric macrocycle interlocked with two β-CDs, and [2]catenanes **3**-β-CD and **4**-β-CD, consisting of one trimeric or one tetrameric macrocycle, respectively, interlocked with one β-CD.[10] Further support for the formation of catenanes comes from a control experiment: upon addition of β-CD to a non-dynamic (i.e. fully oxidised) library, containing trimer, tetramer and catenane **2**, we did not detect any of the peaks in the HPLC corresponding to the CD-containing catenanes. This experiment excludes that the peaks in the HPLC chromatograms correspond to inclusion complexes. When γ-CD was used as a template instead of β-CD, analogous [2]- and [3]catenanes were obtained, but in different ratios (Figure 2.1d). Formation of the γ-CD [3]catenanes was less favourable than for β-CD, suggesting differences in the cooperativity of catenation between the two CD homologues. When the amount of cyclodextrin was increased to one equivalent compared to building block **1**, α-CD still did not amplify any species. However, for the libraries in the presence of β-CD or γ-CD, the concentration of the [3]catenanes increased at the expense of the other catenanes (Figure 2.1c,e).

We have isolated the two [3]catenanes **4**-2β-CD as a mixture of isomers and [2]catenane **3**-β-CD using preparative HPLC. The ^{1}H-NMR spectrum of **4**-2β-CD (Figure 2.2) showed broad peaks of the azobenzene units, whereas the [2]catenane **3**-β-CD (Figure 2.3) gave sharp signals, in which all three azobenzene units were indistinguishable.[11] Given the asymmetric shape of cyclodextrins a reduction in symmetry of the azobenzene units may be expected. Stoddart[10b] has observed such desymmetrization in cyclodextrin catenanes with two chemically different stations to which the cyclodextrin can bind, but not in an analogous catenane with two degenerate stations. As catenane **3**-β-CD contains three degenerate stations the fact that no desymmetrization is detected is therefore not unexpected. These results suggest that the [3]catenanes **4**-2β-CD have slower rotation kinetics, presumably because the motions of the two β-CD rings are coupled. This notion was supported by inspection of CPK models, which revealed that it is sterically not feasible to have two cyclodextrin rings occupy adjacent azobenzene stations in catenanes **4**-2β-CD, hence the cyclodextrin rings cannot change stations independently.

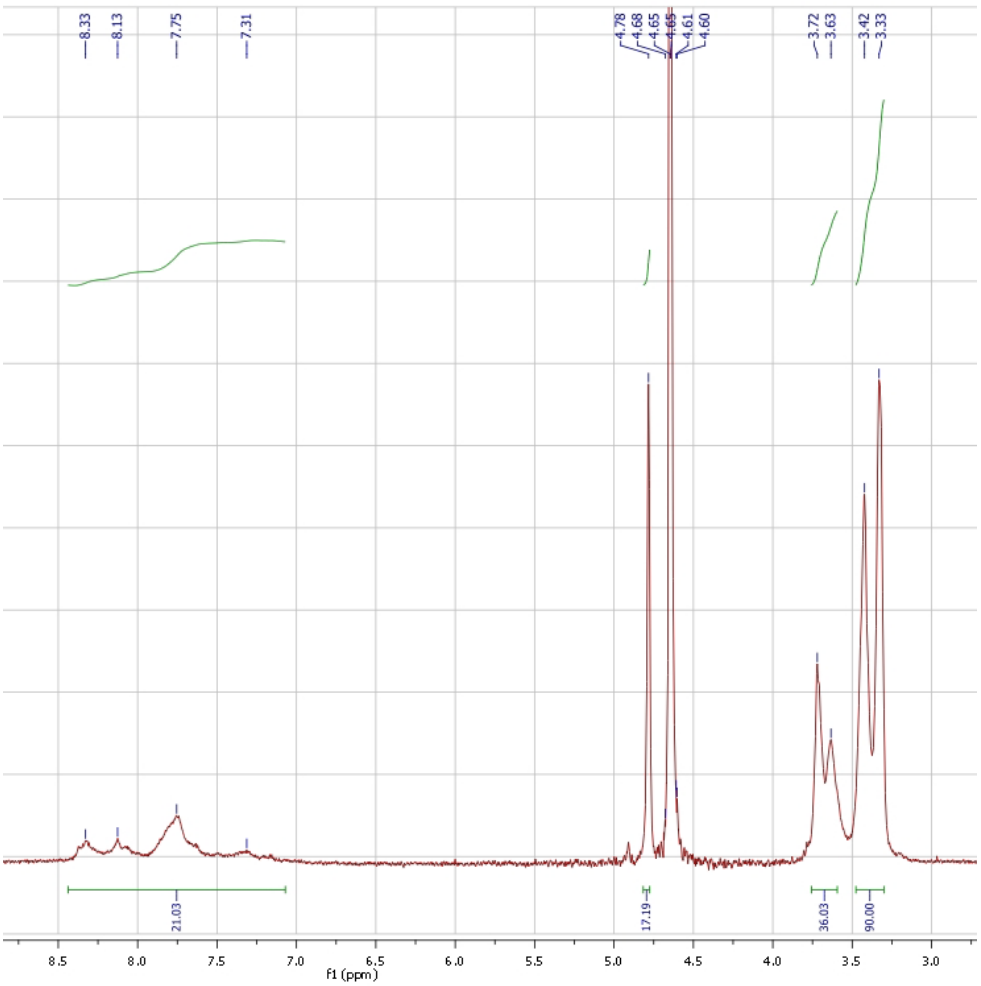

Figure 2.2 ^{1}H NMR of [3]catenanes **4**-2β-CD (0.3 mM) in D_2O (pD 8.3)**.**

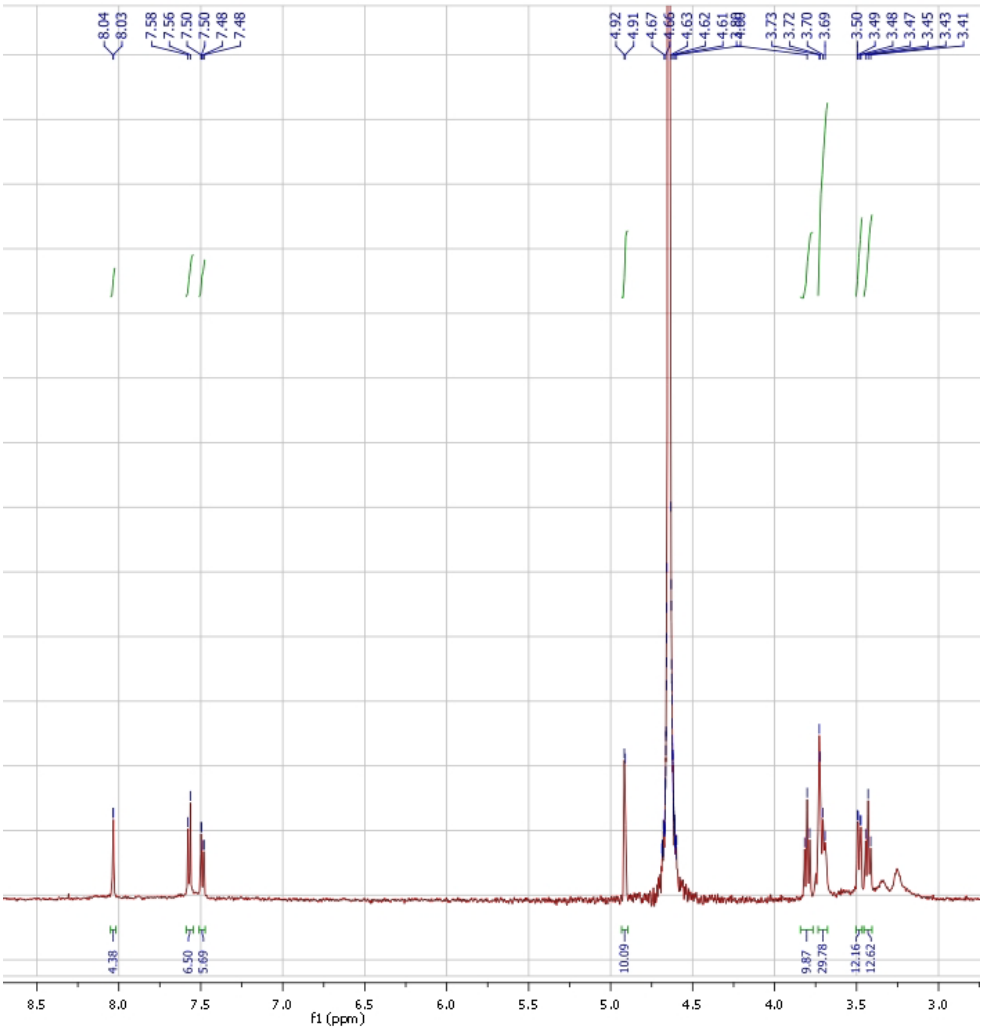

Figure 2.3 ^{1}H NMR of [2]catenane **3**-β-CD (0.5 mM) in D_2O (pD 8.3).

2.2.3 Determination of Equilibrium Constants of Catenanes

Establishing the equilibrium constant for catenation for **2** is trivial. The catenane and the macrocycle from which it is constituted appear as separate peaks on the HPLC trace and the concentration of both species can be quantified.[12] This then directly gives the equilibrium constant from equation 2.1:

$$K_2 = [\text{catenane } \mathbf{2}]/[\text{trimer } \mathbf{3}]^2 \qquad \text{[equation 2.1]}$$

The equilibrium constant for catenation obtained for this system is $logK_2 = 3.63 \pm 0.18$

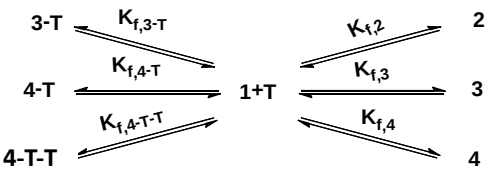

Scheme 2.3. Model used to fit the library distributions obtained for different concentrations of cyclodextrin template T.

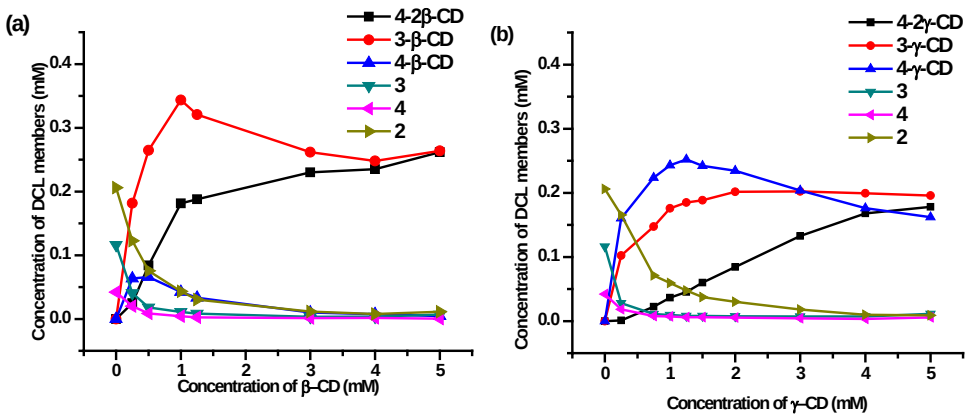

Figure 2.4 Product distribution in the DCL made from building block **1** (2.0 mM) as a function of the concentration of (a) β-CD and (b) γ-CD template.

Having established the nature of the main species in the DCL in the presence of the cyclodextrin homologues, we proceeded with the determination of the binding affinities. Note that, since cyclodextrins do not have a chromophore, the concentration of free cyclodextrin is not directly measurable in the present system. Thus we cannot use equation 2.1 and we needed to resort to an approach that relies on fitting the concentrations of the various species that can be directly quantified to an equilibrium model that explicitly includes the catenanes and the corresponding non-catenated macrocycles. The model is shown in Scheme 2.3. The only specific equilibrium constants that are fitted include those that relate library members to their appropriate building blocks (termed formation constants: K_f). The building block represents a common reference state through which the relative stabilities of all the species in the mixture may be compared. Note that these equilibria do not represent realistic reaction pathways, since disulfide reduction does not occur under the conditions of our experiments. In other types of DCLs, such as those based on imines,

building blocks are in equilibrium with library members and the corresponding formation constants do have a physical meaning; in most disulfide libraries, only disulfides are in equilibrium with each other. The conversion of thiol building blocks into disulfides is effectively irreversible. Therefore the values of the equilibrium constants that relate library members to their building blocks have no physical meaning.[13] Nevertheless the differences between these values can be used to assess the other equilibria in the system. For example, the equilibrium constant ($K_{4\text{-}T}$) for [2]catenane formation from **4** and **T** equals to $K_{f,\mathbf{4}\text{-}\mathbf{T}}/K_{f,\mathbf{4}}$. This methodology has previously been validated in disulfide DCLs of host-guest systems.[12]

In order to obtain accurate estimates of the equilibrium constants in the system, it is necessary to accumulate a data set containing a number of different DCLs under a range of experimental conditions (i.e. the same concentration of building block and different cyclodextrin concentrations). Thus two series of eight DCLs were set up, with concentrations of building block **1** (2.0 mM) and concentrations of β-CD or γ-CD in the range of 0 and 5 mM (Figure 2.4). When all the libraries were fully oxidized, the concentrations of DCL members in the DCLs with or without β-CD or γ-CD were determined by analytical HPLC.

Table 2.1. Peak area (mAU × sec.) of species in libraries with different concentration of β-CD

[β-CD] (M)	Area of **4**-2β-CD	Area of **3**-β-CD	Area of **4**-β-CD	Area of **3**	Area of **4**	Area of **2**	Total Peak Area
0	0	0	0	8.03E+02	2.77E+02	2.03E+03	3.11E+03
2.50E-04	1.62E+02	8.96E+02	4.17E+02	2.01E+02	1.32E+02	1.21E+03	3.02E+03
5.00E-04	5.51E+02	1.30E+03	4.32E+02	8.80E+01	5.60E+01	7.45E+02	3.18E+03
1.00E-03	9.93E+02	1.60E+03	2.25E+02	5.40E+01	2.30E+01	4.21E+02	3.31E+03
1.25E-03	1.08E+03	1.57E+03	2.18E+02	4.10E+01	1.60E+01	3.00E+02	3.22E+03
3.00E-03	1.51E+03	1.29E+03	1.44E+02	1.60E+01	9.00E+00	1.13E+02	3.09E+03
4.00E-03	1.64E+03	1.27E+03	5.00E+01	1.80E+01	1.00E+01	7.60E+01	3.06E+03
5.00E-03	1.72E+03	1.30E+03	3.10E+01	3.40E+01	3.00E+00	1.10E+02	3.20E+03
Average Value of Peak Area							3.15E+03

Table 2.2. Peak area (mAU × sec.) of species in libraries with different concentration of γ-CD

[γ-CD] (M)	Area of **4**-2γ-CD	Area of **3**-γ-CD	Area of **4**-γ-CD	Area of **3**	Area of **4**	Area of **2**	Total Peak Area
0	0	0	0	8.71E+02	2.35E+02	1.94E+03	3.05E+03
2.50E-04	6.00E+00	4.94E+02	1.03E+03	1.36E+02	1.19E+02	1.60E+03	3.39E+03
7.50E-04	1.44E+02	7.13E+02	1.44E+03	5.30E+01	5.00E+01	6.89E+02	3.09E+03
1.00E-03	2.36E+02	8.52E+02	1.57E+03	4.60E+01	4.60E+01	5.75E+02	3.32E+03
1.25E-03	2.92E+02	8.95E+02	1.63E+03	3.90E+01	3.90E+01	4.63E+02	3.36E+03
1.50E-03	3.88E+02	9.12E+02	1.56E+03	3.90E+01	3.80E+01	3.61E+02	3.30E+03
2.00E-03	5.44E+02	9.76E+02	1.51E+03	3.70E+01	3.40E+01	2.92E+02	3.40E+03
3.00E-03	8.57E+02	9.79E+02	1.32E+03	3.50E+01	2.70E+01	1.76E+02	3.39E+03
4.00E-03	1.08E+03	9.65E+02	1.14E+03	3.50E+01	2.10E+01	9.60E+01	3.34E+03
5.00E-03	1.15E+03	9.47E+02	1.05E+03	5.50E+01	3.60E+01	8.60E+01	3.29E+03
Average Value of Peak Area							3.29E+03

We recorded the UV spectra of each catenane library member. The normalized UV spectra of the catenanes are essentially identical (Figure 2.5). From HPLC analysis using UV detection at 254 nm, we found that the total HPLC peak area is similar and independent of the library composition. The peak area of each library species is listed below in Table 2.1 and Table 2.2. These data demonstrate that the various members have similar molar absorbtivities per unit of building block **1**.

$$[\text{library member}] = \frac{\text{peak area of library member}}{\text{average total peak area} \times \text{number of units of } \mathbf{1}} \times 2\ \text{mM} \qquad \text{[equation 2.2]}$$

We calculated the concentration of each library species using the equation 2.2.

The concentrations of all the library members are listed in Table 2.3 and 2.4.

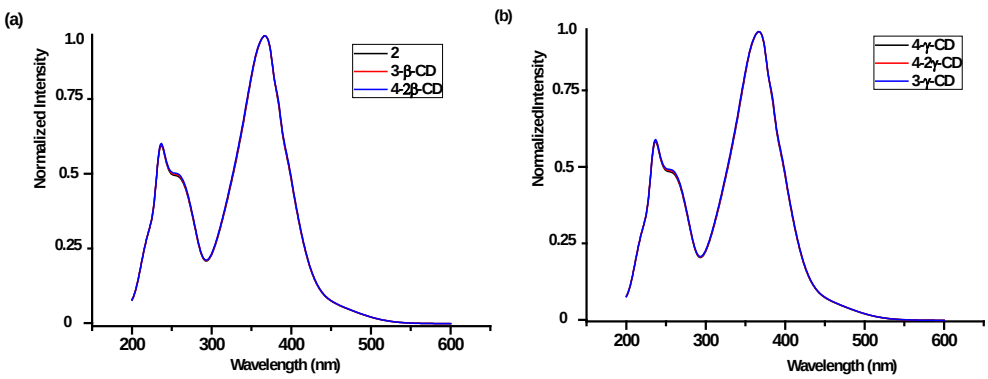

Figure 2.5 Normalized UV spectra (highest absorbance = 1) of (a) catenane **2** and cantenanes formed from β-CD and (b) γ-CD. The fact that the UV spectra in each graph overlap indicates that catenation does not influence the UV spectra of the macrocycles involved.

Table 2.3. Concentration (M) of species in libraries with different concentration of β-CD

[β-CD]	[**4**-2β-CD]obs	[**3**-β-CD]obs	[**4**-β-CD]obs	[**3**]obs	[**4**]obs	[**2**]obs
0	0	0	0	1.63E-04	4.21E-05	2.06E-04
2.50E-04	2.46E-05	1.82E-04	6.34E-05	4.07E-05	2.01E-05	1.23E-04
5.00E-04	8.39E-05	2.65E-04	6.58E-05	1.79E-05	8.51E-06	7.56E-05
1.00E-03	1.51E-04	3.24E-04	3.42E-05	1.10E-05	3.48E-06	4.27E-05
1.25E-03	1.64E-04	3.18E-04	3.32E-05	8.30E-06	2.39E-06	3.04E-05
3.00E-03	2.30E-04	2.62E-04	2.20E-05	3.30E-06	1.44E-06	1.15E-05
4.00E-03	2.49E-04	2.58E-04	7.60E-06	3.58E-06	1.52E-06	7.66E-06
5.00E-03	2.62E-04	2.64E-04	4.65E-06	6.98E-06	5.32E-07	1.12E-05

Table 2.4. Concentration (M) of species in libraries with different concentration of γ-CD

[γ-CD]	[**4**-2γ-CD]obs	[**3**-γ-CD]obs	[**4**-γ-CD]obs	[**3**]obs	[**4**]obs	[**2**]obs
0	0	0	0	1.80E-04	3.64E-05	2.00E-04
2.50E-04	1.00E-06	1.02E-04	1.60E-04	2.81E-05	1.84E-05	1.65E-04
7.50E-04	2.23E-05	1.47E-04	2.24E-04	1.10E-05	7.80E-06	7.11E-05
1.00E-03	3.66E-05	1.76E-04	2.43E-04	9.54E-06	7.08E-06	5.94E-05
1.25E-03	4.53E-05	1.85E-04	2.52E-04	8.02E-06	6.08E-06	4.77E-05
1.50E-03	6.01E-05	1.88E-04	2.42E-04	8.00E-06	5.93E-06	3.73E-05
2.00E-03	8.43E-05	2.02E-04	2.34E-04	7.54E-06	5.31E-06	3.02E-05
3.00E-03	1.33E-04	2.02E-04	2.04E-04	7.18E-06	4.20E-06	1.82E-05
4.00E-03	1.68E-04	1.99E-04	1.76E-04	7.17E-06	3.33E-06	9.86E-06
5.00E-03	1.78E-04	1.96E-04	1.62E-04	1.14E-05	5.64E-06	8.89E-06

Fitting the corresponding dataset to the model in Scheme 2.2 may be performed with the help of established multivariate analysis algorithms, which iterate and adjust the values of the equilibrium constant until the error between fitted and observed data is minimal. We have previously implemented these in our DCLFit software.[12] As with any multivariate analysis, it is important to ensure that the fitting converges on an error value that corresponds to the global minimum, rather than a local minimum. Thus, we ran the fitting procedure starting from 500 different estimates of initial equilibrium constants and found the same minimum error 496 times, each time giving closely comparable values for the equilibrium constants. The comparisons between fitted concentration profiles and observed profiles are shown in Figure 2.6.

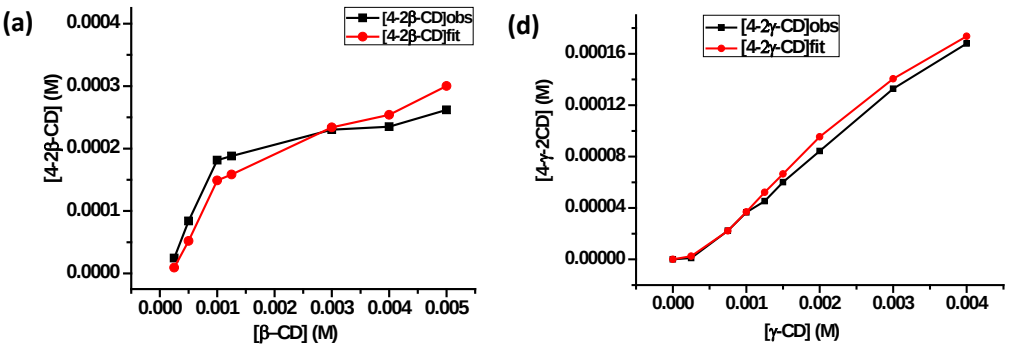

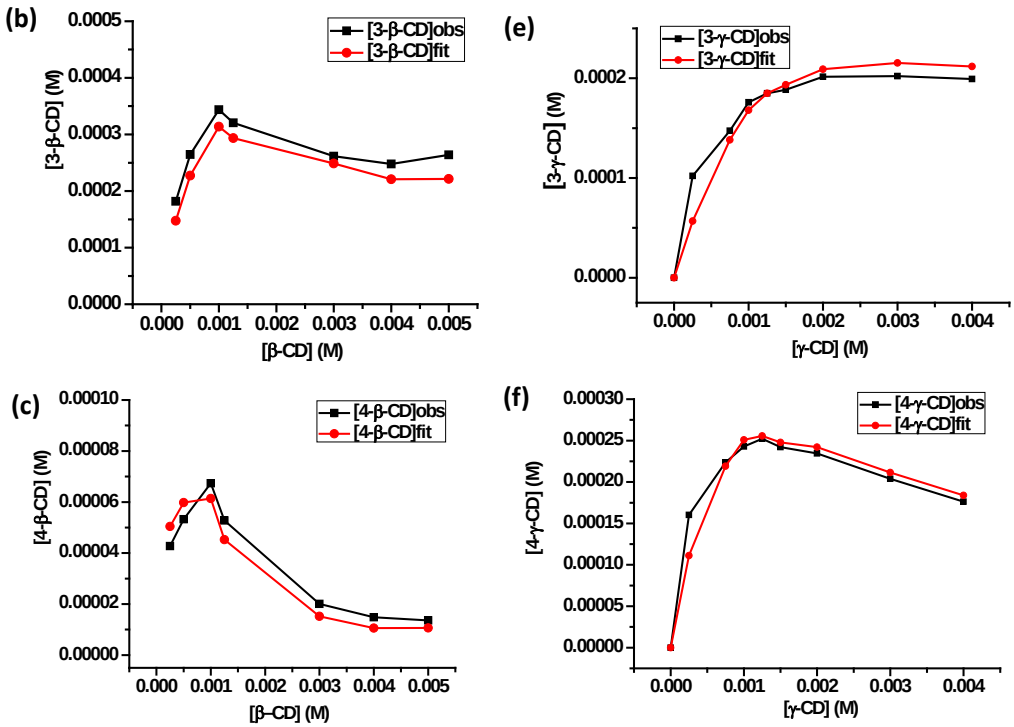

Figure 2.6 Observed and fitted concentrations of (a) **4**-2β-CD; (b) **3**-β-CD; (c) **4**-β-CD as a function of the concentration of the β-CD template; (d) **4**-2γ-CD; (e) **3**-γ-CD; (f) **4**-γ-CD as a function of the concentration of the γ-CD template.

Table 2.5 Equilibrium Constants for Catenane Formation

T	$logK_1$	$logK_{3\text{-}T}$	$logK_{4\text{-}T}$	$logK_{4\text{-}T\text{-}T}$	$logK_{4T\text{-}T}$[a]
β-CD	3.16±0.15	3.88±0.12	3.65±0.13	7.70±0.25	4.05±0.22
corrected[b]	3.16±0.15	3.41±0.12	3.05±0.12	7.70±0.25	4.05±0.22
γ-CD	2.45±0.08	4.19±0.08	4.71±0.12	7.17±0.16	2.46±0.11
corrected[b]	2.45±0.08	3.71±0.08	4.13±0.08	7.17±0.16	2.46±0.11

[a] $K_{4T\text{-}T}$ refers to the equilibrium constant for the formation of this [3]catenane from [2]catenane **4**-T. [b] Equilibrium constants to which a statistical correction has been applied to account for the number accessible azobenzene sites. No statistical correction was applied for the formation of the [3]catenanes, since the [2]catenanes have only a single accessible cyclodextrin binding site.

The equilibrium constants of binding of T (β-CD/γ-CD) within [2]catenane **3**-T (**3**-β-CD/**3**-γ-CD), [2]catenane **4**-T (**4**-β-CD/4-γ-CD) and [3]catenanes **4**-T-T (**4**-2β-CDs/**4**-2γ-CDs) are shown in Table 2.5. Note that the latter equilibrium constant refers to the formation of the "termolecular" catenane from one tetrameric macrocycle and two T molecules. The value of $K_{\mathbf{4}T\text{-}T}$ (for the formation of **4**T-T from **4**T and one unit of T) can be estimated from $logK_{\mathbf{4}T\text{-}T} = logK_{\mathbf{4}\text{-}T\text{-}T} - logK_{\mathbf{4}\text{-}T}$. Errors are based on two repeats of the entire experiment (including two independently generated sets of DCLs). The entire analysis was repeated twice for two separately prepared sets of DCLs, and the equilibrium constants for catenane formation are shown in Table 2.5.

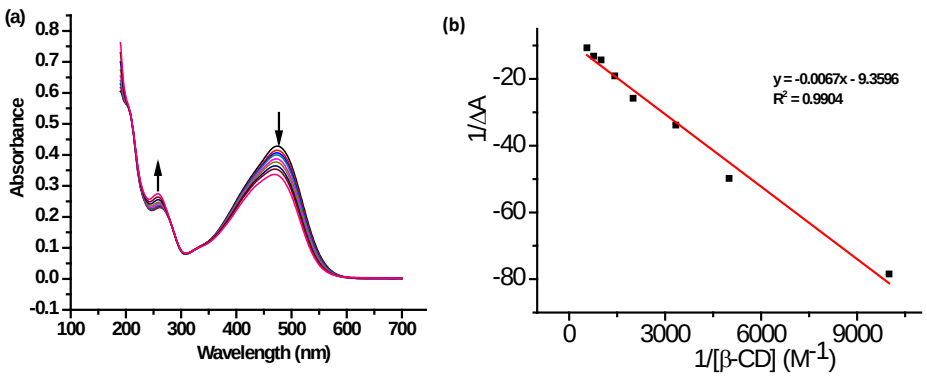

Figure 2.7 (a) Changes in UV absorbance upon the addition of β-CD. The concentration of building block **1** is 2.5×10^{-5} M and the β-CD concentration ranges from 0 to 18 mM ; (b) Hildebrand-Benesi plot of the data of Figure 2.7 (a) at 475 nm.

We also measured the equilibrium constant between building block **1** and β-CD and γ-CD by UV titration. The concentration of building block **1** was kept at 2.5×10^{-5} M. Upon the addition of β-CD, the absorbance at 475 nm decreased, accompanied by an increasing absorbance at 255 nm (Figure 2.7a). We assumed that the binding between building block **1** and β-CD is 1:1 and applied our data to the modified Hildebrand-Benesi equation[13]:

$$\frac{1}{\Delta A} = \frac{1}{K_a \Delta\varepsilon [H][G]} + \frac{1}{\Delta\varepsilon [H]} \qquad \text{[equation 2.3]}$$

[H] and [G] present the concentration of buiding block **1** (host) and β-CD (guest) respectively. K_a stands for the affinity constant between building block **1** and β-CD. ΔA presents the difference of UV absorbance after and before the addition of β-CD. Δε, represents the difference of the molar extinction coefficient between the host and host-guest

complex at the wavelength of 475 nm, and is estimated to be 4.27×10^{3} M^{-1} cm^{-1}. The affinity constant was calculated using the equation:

$$K_a = \frac{1}{k\Delta\varepsilon[H]} \qquad \text{[equation 2.4]}$$

Where *k* is the slope of the line plot in Figure 2.7b.

The equilibrium constant for binding between building block **1** and γ-CD was determined as the same way as that for binding of **1** to β-CD (Figure 2.8). These equilibrium constants are also included in Table 2.5. In order to compare the values for binding of the CDs to building block **1** and the various catenation equilibria, we corrected the catenation equilibrium constants for the number of azobenzene binding sites. The corrected binding constants of $K_{\mathbf{3}\text{-T}}$ and $K_{\mathbf{4}\text{-T}}$ are calculated from $K_{\mathbf{3}\text{-T,corr}} = K_{\mathbf{3}\text{-T}}/3$ and $K_{\mathbf{4}\text{-T,corr}} = K_{\mathbf{4}\text{-T}}/4$ because there are three and four binding sites in [2]catenanes **3**-T and **4**-T, respectively. The thus corrected equilibrium constants for binding β-CD within [2]catenanes **3**-β-CD and **4**-β-CD are similar to binding of β-CD to monomer **1** (see Table 2.5). However, the equilibrium constant for incorporating the second β-CD to yield the [3]catenanes is an order of magnitude larger, indicating that the formation of **4**-2β-CD exhibits strong positive cooperativity.

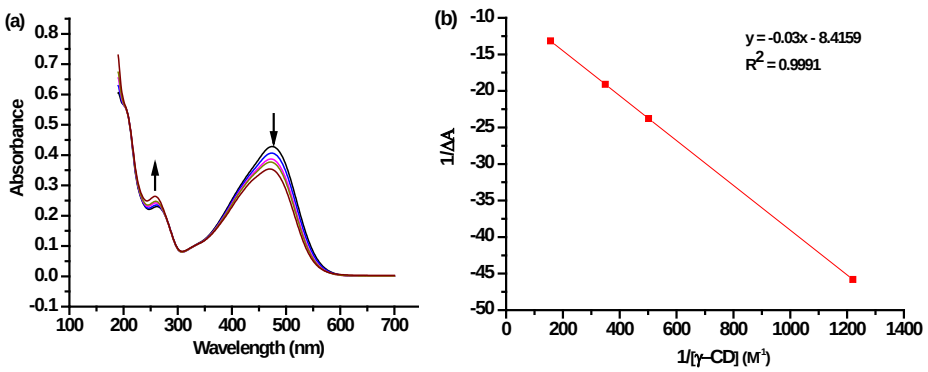

Figure 2.8 (a) Changes in UV absorbance upon the addition of γ-CD; The concentration of building block **1** is 2.5×10^{-5} M and the γ-CD concentration ranges from 0 to 62 mM ; (b) Hildebrand-Benesi plot of the data of Figure 2.8a at 475 nm.

Repeating the same analysis for γ-CD reveals a very different behaviour. The binding affinity between **1** and γ-CD is weaker than the one between **1** and β-CD. Yet, the catenation of the first γ-CD is somewhat more favourable than the corresponding process for β-CD,

especially for the tetramer. However, the incorporation of the second γ-CD to yield [3]catenane **4**-2γ-CD is two orders of magnitude weaker than the binding of the first γ-CD, hence [3]catenation with this cyclodextrin homologue shows strong negative cooperativity.

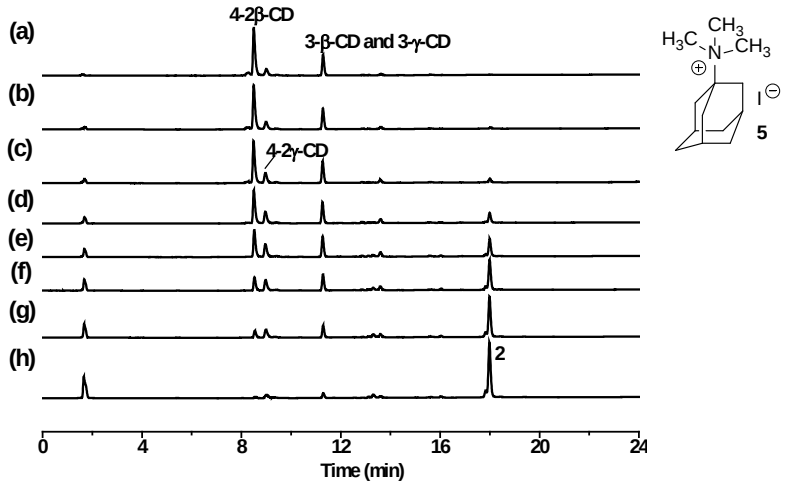

Figure 2.9 HPLC-MS analysis of DCL made from 2 mM building block **1**, α-CD, β-CD and γ-CD (2.0 mM each) in aqueous borate buffer (50 mM, pH 8.2) (a) without adamantaneammonium iodide (**5**); (b) 0.50 mM; (c) 1.0 mM; (d) 1.5 mM; (e) 2.0 Mm; (f) 4.0 Mm; (g) 8.0 mM and (h) 16 mM **5.**

It is interesting to note how the concentration of the two [2]catenanes depend on cyclodextrin concentration (Figure 2.4). At low cyclodextrin concentrations the catenated tetramer 4-γ-CD dominates, while at higher concentrations the catenated trimer 3-γ-CD is present at higher concentrations, despite the fact that 4-γ-CD exhibits the highest binding affinity (Table 2.5). This behavior is a consequence of the system maximizing global binding energy. At high cyclodextrin concentrations, when building block **1** is limiting, it is possible to harvest more binding energy by making more copies of a relatively weakly binding catenane. At lower cyclodextrin concentrations, when the cyclodextrin is limiting, the system will preferentially catenate the macrocycle that has the highest affinity. Similar systems effects have been observed previously in a dynamic combinatorial host-guest system.[14]

The quantitative data in Table 2.5 predicts that [3]catenanes based on β-CD are more stable than those based on γ-CD. This prediction was verified in a competition experiment in which both cyclodextrins were added together (alongside α-CD) to the same DCL. HPLC analysis confirmed that [3]catenanes **4**-2β-CD dominate the mixture (Figure 2.9a).

Interestingly, while a small amount of **4**-2β-CD was observed, no mixed catenane **4**-β-CD-γ-CD could be detected, indicating that the catenanes are self-sorting.

2.2.4 Investigating the Responsiveness of the Catenanes

The responsiveness of this system was investigated by introducing adamantane derivative **5**, known to bind β-CD (log*K* =3.99±0.02) and to a lesser degree to γ-CD (log *K*=3.50±0.06).[15] DCLs were analysed at increasing concentration of guest **5**. When the amount of **5** was increased to 1.5 mM, the concentration of the catenanes made from β-CD decreased while the quantity of [3]catenanes **4**-2γ-CD increased slightly. Guest **5** acts as a competitive binder for β-CD allowing more γ-CD to catenate the azobenzene macrocycles. Upon further increasing the concentration of **5**, the concentration of species catenated by both β-CD and γ-CD decreased liberating the azobenzene moieties for incorporation into catenane **2** (Figure 2.9). These results show that it is possible to switch between different catenanes by addition of a competitive guest molecule.

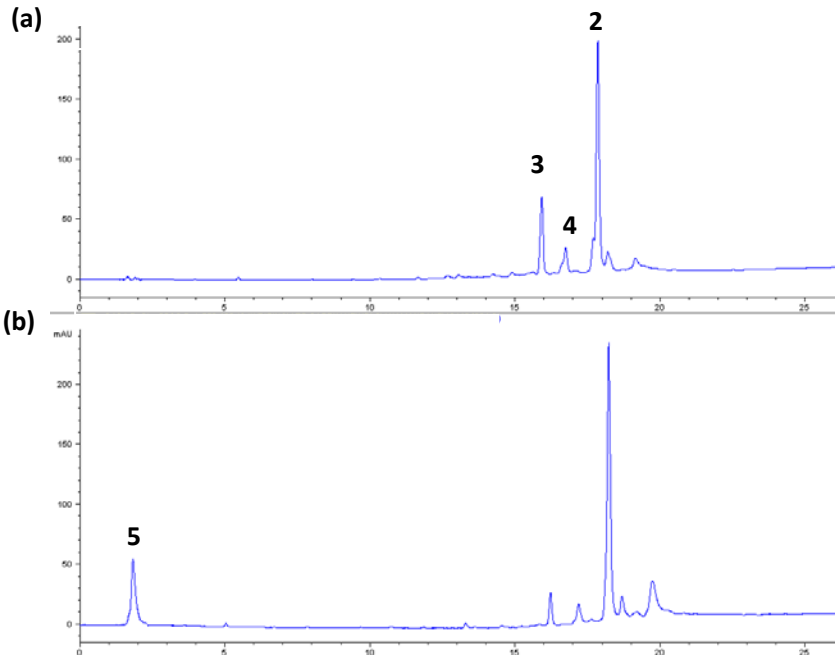

Figure 2.10 HPLC analysis of the DCL made from 2.0 mM building block **1** in aqueous borate buffer (50 mM, pH 8.2) (a) without guest **5**; (b) with 2.0 eq. guest **5**.

Comparing Figure 2.1a with Figure 2.9h, we found that catenane **2** may be amplified by guest **5**. We then performed a separate experiment by analyzing the library prepared from building block **1** without and with guest **5** using HPLC. The results are shown in Figure 2.10, validating the assumption that catenane **2** can be amplified by guest **5**.

2.3 Conclusions

In conclusion, we have shown that the addition of cyclodextrin converts catenane **2** into a family of new cyclodextrin catenanes. We also developed the methodology for extracting the equilibrium constants for the formation of these catenanes from their constituent rings. Such quantitative analysis revealed a considerable difference in cooperativity in [3]catenane formation: strong positive cooperativity was observed with β-CD, while γ-CD derived [3]catenanes exhibited strong negative cooperativity. The quantification of catenation equilibria provides useful insight into the binding interactions underlying the catenation process and is potentially applicable to any catenanes containing dynamic covalent bonds.

2.4 Experimental Section

2.4.1 Materials

All chemicals, unless otherwise stated, were purchased from Sigma-Aldrich and used as received. HPLC or LC-MS grade solvents were obtained from BIOSOLVE. All solvents used in synthesis were distilled prior to use and anhydrous solvents were distilled from a drying agent under a nitrogen atmosphere.

Procedures of Synthesizing Building Block (1)

Synthesis of methyl 2-((dimethylcarbamothioyl)oxy)-5-nitrobenzoate (b):

Methyl 2-hydroxy-5-nitrobenzoate (**a**) (2.00 g, 10.0 mmol) was dissolved in anhydrous DMF (20.0 mL) at room temperature under a nitrogen atmosphere. Dimethylthiocarbamoyl chloride (1.85 g, 15.0 mmol) was added, followed by gradual addition of DABCO (1.68 g, 15.0 mmol), turning the solution orange. The reaction mixture was stirred for 24 hours, until TLC analysis indicated complete consumption of starting materials. A mixture of brine and water (400 mL, 50:50 composition) was added, causing a large amount of precipitate to form. After a further 10 minutes of stirring, the precipitate was filtered, washed with distilled water, and dried, yielding a white solid (2.80 g, 98%). ^{1}H NMR (400 MHz, $CDCl_3$) δ ppm 8.84 (d, *J*

= 2.82 Hz, 1H), 8.39 (dd, *J* = 8.87, 2.83 Hz, 1H), 7.29 (d, *J* = 8.87 Hz, 1H), 3.89 (s, 3H), 3.45 (br s, 3H), 3.41 (br s, 3H). ^{13}C NMR (100 MHz, $CDCl_3$) δ (ppm): 186.0, 162.8, 158.0, 145.0, 128.0, 127.1, 126.4, 125.3, 52.7, 43.4, 39.1. ESI-HRMS $[M+H]^+$ found: 285.0552 (expected: 285.0540).

Synthesis of methyl 2-((dimethylcarbamoyl)thio)-5-nitrobenzoate (c):

Methyl 2-((dimethylcarbamothioyl)oxy)-5-nitrobenzoate (**b**) (0.500 g, 2.00 mmol) was heated in a flask at 150 °C for 20 minutes, forming a brown liquid. The reaction mixture was cooled down to room temperature and solidified. The solid was ground to give a yellow power (0.500 g, 100%). ^{1}H NMR (400 MHz, $CDCl_3$) δ ppm 8.53 (d, *J* = 2.1 Hz, 1H), 7.91 (d, *J* = 8.4 Hz, 1H), 7.81 (d, *J* = 8.4 Hz, 1H), 3.97 (s, 4H), 3.11 (br s, 6H). ^{13}C NMR (100 MHz, $CDCl_3$) δ (ppm): 165.1, 164.2, 147.1, 139.0, 137.4, 135.0, 125.4, 125.2, 53.6, 52.4, 37.2. ESI-HRMS: $(M+H)^+$ found: 285.0552 (expected: 285.0540).

Synthesis of methyl 2-((dimethylcarbamoyl)thio)-5-nitrosobenzoate (d)[16]:

Methyl 2-((dimethylcarbamoyl)thio)-5-nitrobenzoate (**c**) (11.4 g, 80.0 mmol) was dissolved in methoxyethanol (400 mL) and a solution of NH_4Cl (6.79 g, 127 mmol) in H_2O (100 mL) was added. The reaction mixture was warmed to 30°C and finely powdered zinc (20.38 g, 312 mmol) was added in portions over a period of 30 minutes maintaining the temperature between 30-35°C while stirring vigorously. The mixture was allowed to react at 35°C for 2 hours and then filtered and washed with methoxyethanol. The filtrate was added to a solution of $FeCl_3$ (25.2 g, 155.4 mmol) in H_2O (300 mL) and ethanol (120 mL) over the course of 90 minutes while the temperature was kept at -5°C. After 1 hour, the mixture was poured into water (800 mL) and the yellow precipitate collected and purified by silica column chromatography (hexane/ethyl acetate 3/1) yielding **d** as a light green solid (43%). ^{1}H NMR (400 MHz, $CDCl_3$) δ ppm 8.71 (d, *J* = 2.57 Hz, 1H), 8.26 (dd, *J* = 8.66, 2.59 Hz, 1H), 7.83 (d, *J* = 8.65 Hz, 1H), 3.93 (s, 3H), 3.14 (br s, 3H), 3.03 (br s, 3H). ^{13}C NMR (100 MHz, $CDCl_3$) δ (ppm): 189.1, 174.6, 152.1, 138.4, 136.7, 135.3, 124.8, 125.1, 53.2, 51.9, 36.7. ESI-HRMS: $(M+H)^+$ found: 268.0474 (expected: 268.0481).

Synthesis of methyl 5-amino-2-((dimethylcarbamoyl)thio)benzoate (e):

Methyl 2-((dimethylcarbamoyl)thio)-5-nitrobenzoate (**c**) (5.00 g, 35.0 mmol) was dissolved in acetic acid (200 mL), and heated to 120°C under a nitrogen atmosphere. Zinc powder (50.0 g) was added in portions, and the reaction was left to stir under reflux for 45 minutes. The reaction mixture was filtered and washed with acetic acid, diluted with water (150 ml), and the product extracted into dichloromethane (5 × 50 mL). The organic layer was then washed with sodium hydroxide (10%, aqueous solution) until the aqueous layer remained

basic, then washed once more with water. The organic layer was dried with Na_2SO_4, filtered, and concentrated in *vacuo*, to yield a yellow viscous oil. Diethyl ether (5.00 mL) was added, causing a white solid to precipitate overnight. The crude product was recrystallized by dissolving in a minimum amount of dichloromethane, followed by addition of diethyl ether, and evaporating at room temperature, yielding a white solid (3.50 g, 77%). ^{1}H NMR (400 MHz, $CDCl_3$) δ ppm 7.33 (d, *J* = 8.34 Hz, 1H), 7.17 (d, *J* = 2.68 Hz, 1H), 6.77 (dd, *J* = 8.34, 2.70 Hz, 1H), 3.84 (s, 3H), 3.04 (s, 6H). ^{13}C NMR (100 MHz, $CDCl_3$) δ (ppm): 167.7, 167.3, 147.8, 139.2, 136.5, 117.6, 116.7, 115.9, 52.1, 37.0. ESI-HRMS: $(M+H)^+$ found: 255.0798 (expected: 255.0798).

Synthesis of (E)-dimethyl 5,5'-(diazene-1,2-diyl)bis(2-((dimethylcarbamoyl)thio) benzoate) (f):

Methyl 2-((dimethylcarbamoyl)thio)-5-nitrosobenzoate (**d**) (2.68 g, 10.0 mmol) and methyl 5-amino-2-((dimethylcarbamoyl)thio)benzoate (**e**) (2.54 g, 10.0 mmol) were mixed in acetic acid (40 ml) and stirred at room temperature overnight in the dark. An orange percipitate formed and was collected by filtration as final product, yielding 4.33 g, 86%. ^{1}H NMR (400 MHz, $CDCl_3$) δ ppm 8.45 (d, *J* = 2.2 Hz, 2H), 8.03 (dd, *J* = 8.4, 2.2 Hz, 2H), 7.79 (d, *J* = 8.3 Hz, 2H), 3.94 (s, 6H), 3.10 (s, 12H). ^{13}C NMR (100 MHz, $CDCl_3$) δ (ppm): 166.4, 165.5, 151.7, 139.2, 137.8, 135.3, 133.7, 125.9, 125.1, 52.5, 37.1. ESI-HRMS: $(M+H)^+$ found: 505.1141 (expected: 505.1137).

Synthesis of (E)-5,5'-(diazene-1,2-diyl)bis(2-mercaptobenzoic acid) (1):

Under a nitrogen atmosphere, (E)-dimethyl 5,5'-(diazene-1,2-diyl)bis(2-((dimethyl carbamoyl)thio)benzoate) (**f**) (0.5 g, 1 mmol) was suspended in a 1.75 M solution (10.0 mL) of KOH in diethyleneglycol that had been purged with nitrogen for 2 hours. The solution was heated at 110°C for 30 minutes. After the solution had cooled down to room temperature, 80 mL of purged water was added followed by rapid addition of 10% HCl (6.00 mL). The precipitate was fitered quickly to avoid oxidation, washed extensively with purged water and dried under vacuum overnight to give an orange building block **1** (0.32g, 98%). ^{1}H NMR (400 MHz, $(CH_3)_2CO$) δ ppm 8.68 (d, *J* = 2.2 Hz, 2H), 7.99 (dd, *J* = 8.5, 2.3 Hz, 2H), 7.72 (d, *J* = 8.5 Hz, 2H), 4.17-4.12 (m, 2H). ^{13}C NMR could not be recorded due to poor solubility and limited stability. ESI-HRMS: $(M-H)^-$ found: 333.0005 (expected: 333.0004).

2.4.2 General Methods

Analytical HPLC Analysis

Analytic HPLC was carried out on Hewlett Packard 1050 or 1100 systems coupled to UV detectors and the data were processed using HP Chemstation software. Separations were

performed on a reversed phase Zorbax C8 column (4.6 x 150 mm, 5 μm particle size, Agilent). Except where otherwise stated, the chromatography was carried out at 45 °C and using UV detection at 254 nm. We recorded the UV spectrum of all the catenanes. They showed the same absorbance (Figure 2.5). The following LC analysis method was used:
Solvent A: Water (0.1% v/v formic acid); Solvent B: Acetonitrile (0.1% v/v formic acid)
Flow rate: 1.0 mL/min

Time (min)	B%
0	5
30	95

LC-MS Analysis

An Accela High Speed LC system (ThermoFisher Scientifics, Courtaboeuf, France) was coupled to a LTQ-Fleet Ion Trap Mass Spectrometer. Water was obtained from a MilliQ Gradient system and LC-MS-grade acetonitrile was bought from BIOSOLVE.
Analysis of samples was performed using a reversed-phase HPLC column (Zorbax C8, 4.6 x 150 mm, 5 μm, Agilent) at 45 °C with an injection volume of 4 μL. All UV traces were obtained by monitoring at 254 nm. The LC-MS analysis method is the same as the HPLC method described above.

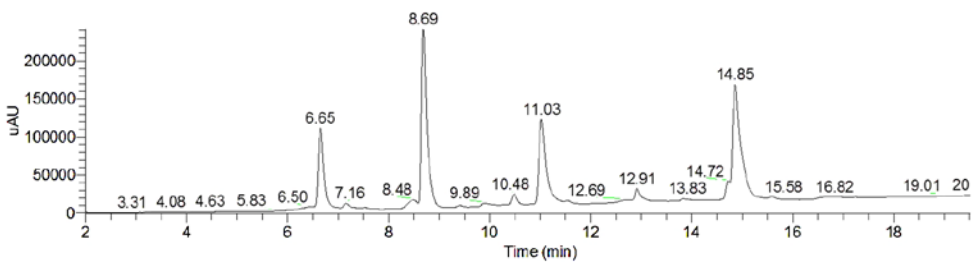

Figure 2.11 HPLC analysis of the fully oxidized library made from building blocks **1** (2.0 mM) and β-CD (0.5 mM) in a 0.5 mL borate buffer (50 mM, pH 8.3).

Mass spectra were recorded in positive ion mode. The electrospray voltage was set to 4.20 kV, and the capillary voltage was set to 25.0 V; the sheath and auxiliary gas flows (both nitrogen) were 5.00 L/min and 5.00 L/min, respectively, and the drying gas temperature was 320 °C.

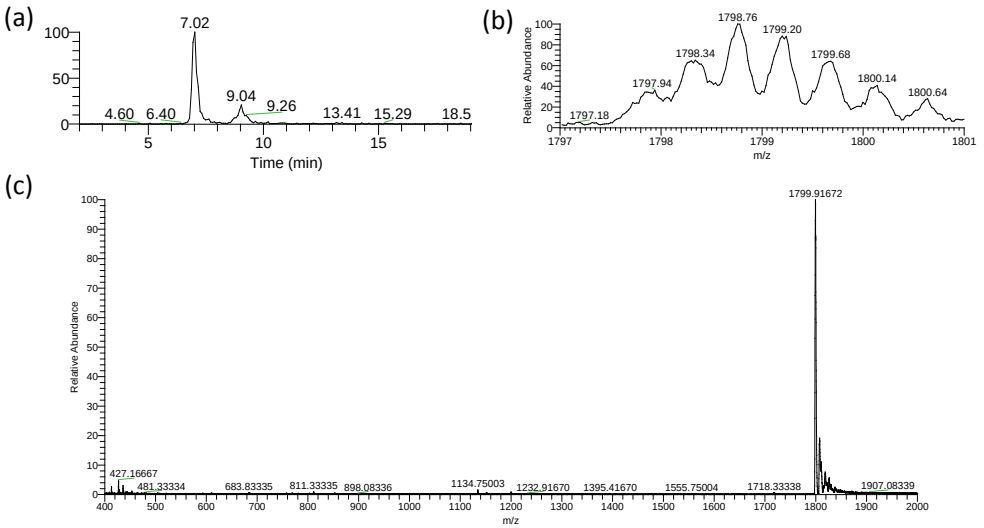

Figure 2.12 (a) Extracted ion chromatogram of m/z = 1799.50 - 1800.50 corresponding to **4**-2β-CD; (b) isotopic profile of the peak observed at 1799; (c) ESI-MS spectrum of the HPLC peak at 6.65 min. Expected m/z for [**4**-2β-CD+2H]$^{2+}$=1799.8453.

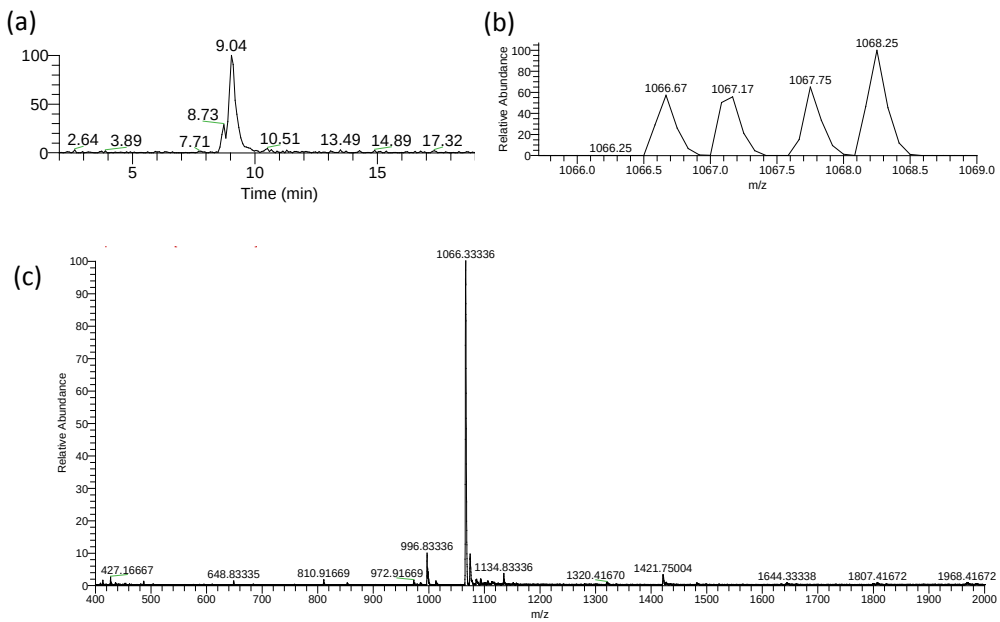

Figure 2.13 (a) Extracted ion chromatogram of m/z = 1065.50 - 1066.50 corresponding to of **3**-β-CD; (b) isotopic profile of the peak observed at 1066.00; (c) ESI-MS spectrum of the HPLC peak at 8.69 min. Expected m/z for [**3**-β-CD+2H]$^{2+}$=1066.5814.

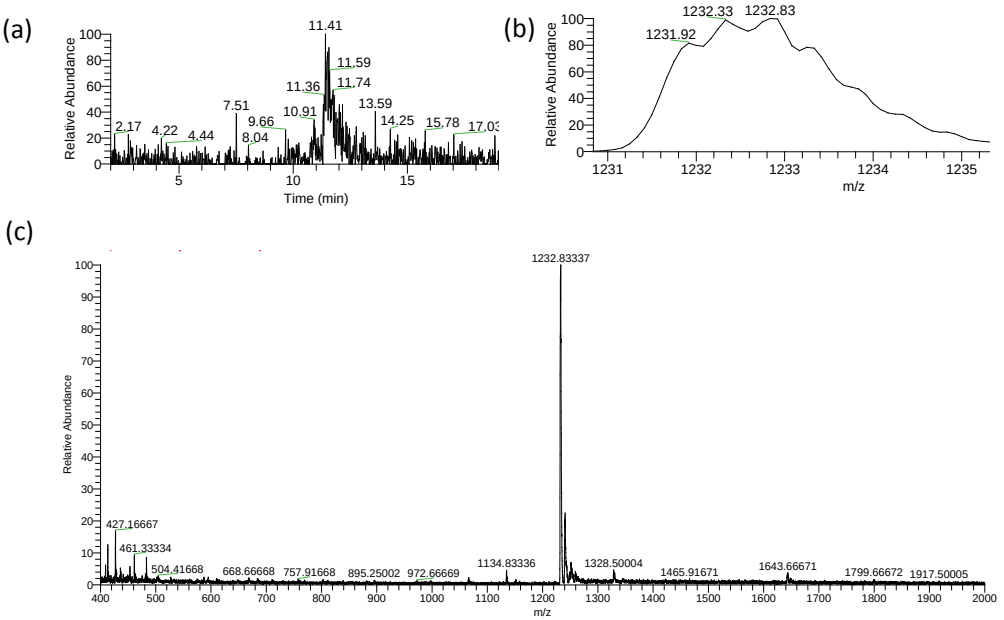

Figure 2.14 (a) Extracted ion chromatogram of m/z= 1232.00 - 1233.00 corresponding to **4**-β-CD; (b) isotopic profile of the peak observed at 1232.83; (c) ESI-MS spectrum of the HPLC peak at 11.03 min. Expected m/z for [**4**-β-CD+2H]$^{2+}$=1232.8132.

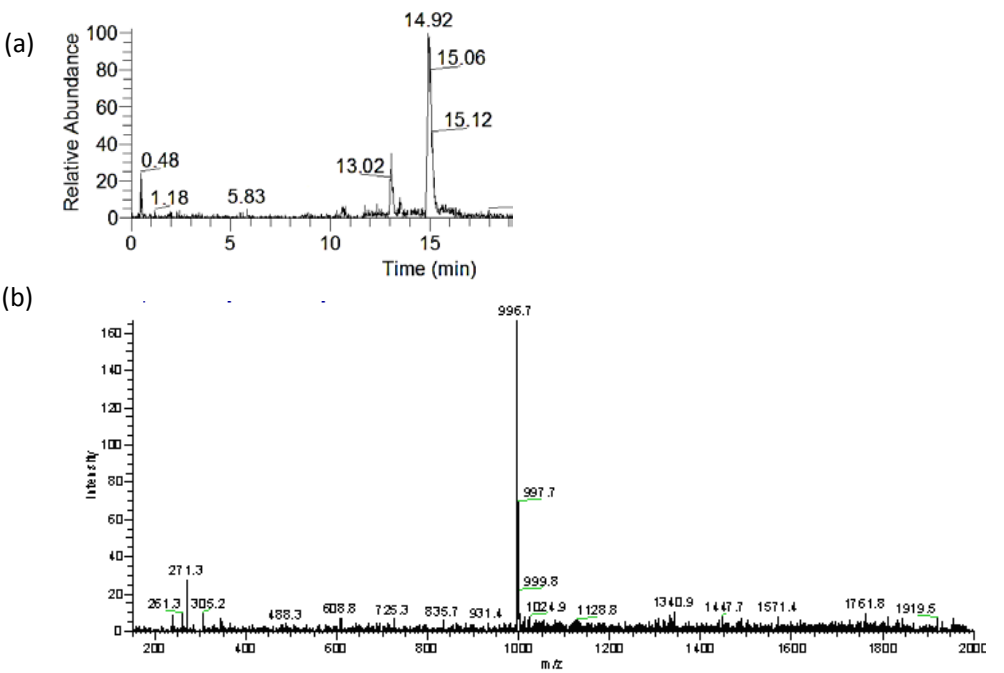

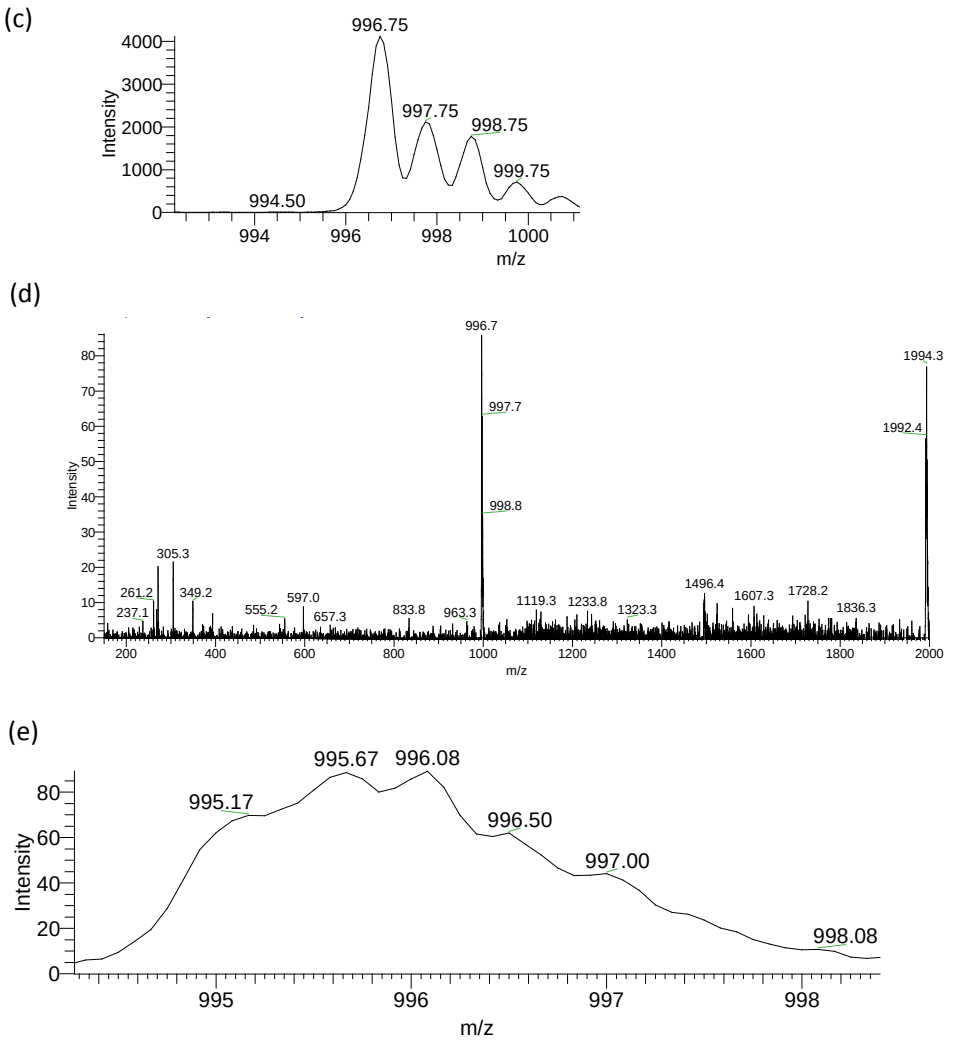

Figure 2.15 (a) Extracted ion chromatogram of m/z= 996.50 - 997.50 corresponding to singly charge **2** and doubly charge **3**. Two peaks corresponding to HPLC peaks at 12.91 min and 14.85 min were found; (b) ESI-MS spectrum of the HPLC peak at 12.91 min. and (c) isotopic profile of the peak observed at 996.75 in (b). Expected m/z for $[\mathbf{3}+H]^{+}$=996.91. The mass of the HPLC peak at 12.91 min corresponds to that of **3. (d)** ESI-MS spectrum of the HPLC peak at 14.85 min and (e) isotopic profile of the peak observed at 996.75 in (d). Expected m/z for $[\mathbf{2}+H]^{2+}$=996.91.

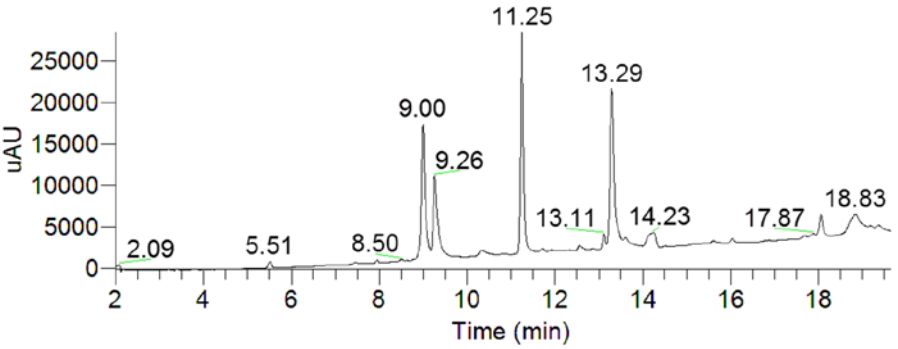

Figure 2.16 HPLC analysis of the fully oxidized library made from building blocks **1** (2.0 mM) and γ-CD (4 mM) in a 0.5 mL borate buffer (50 mM, pH 8.3).

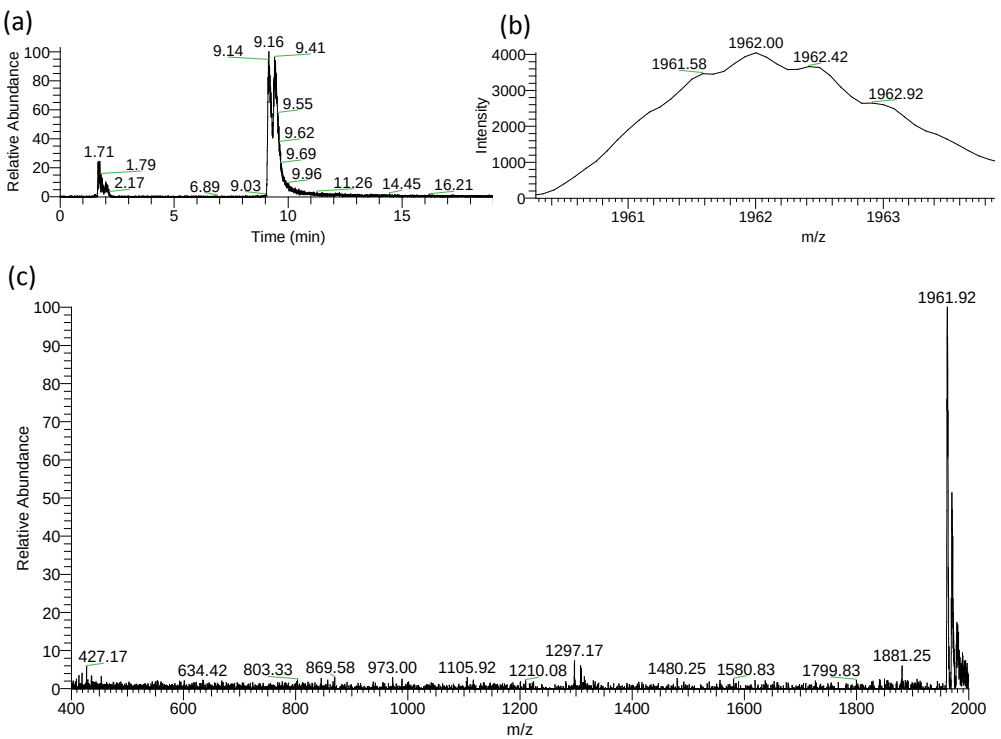

Figure 2.17 (a) Extracted ion chromatogram of m/z = 1961.50 - 1962.50 corresponding to **4**-2γ-CD; (b) isotopic profile of the peak observed at 1961.92; (c) ESI-MS spectrum of the HPLC peak at 9.00 min and 9.26 min. Expected m/z for $[\mathbf{4}\text{-}2\gamma\text{-CD}+2H]^{2+}$=1962.04.

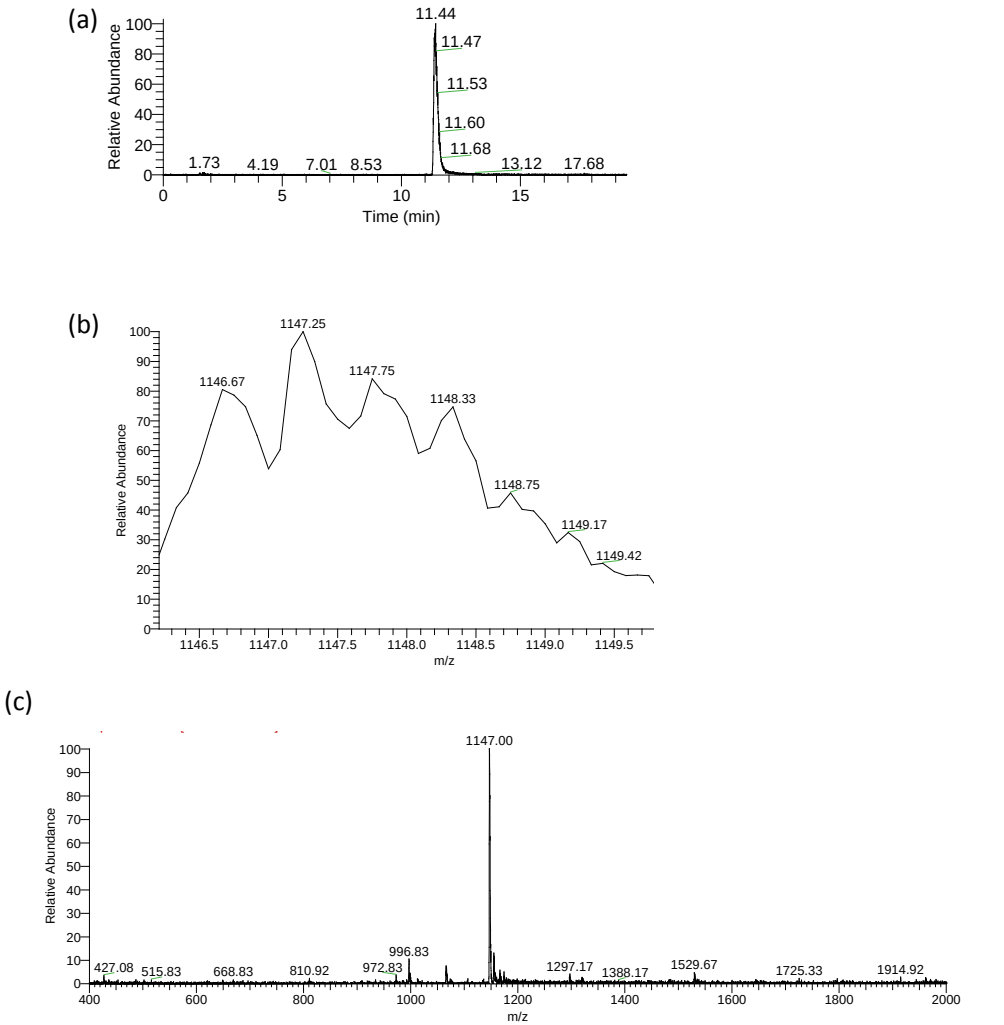

Figure 2.18 (a) Extracted ion chromatogram of m/z = 1146.50 - 1147.50 corresponding to **3**-γ-CD. (b) isotopic profile of the peak observed at 1147.00; (c) ESI-MS spectrum of the HPLC peak at 11.25 min. Expected m/z for $[\mathbf{3}\text{-}\gamma\text{-CD}+2H]^{2+}$=1147.13.

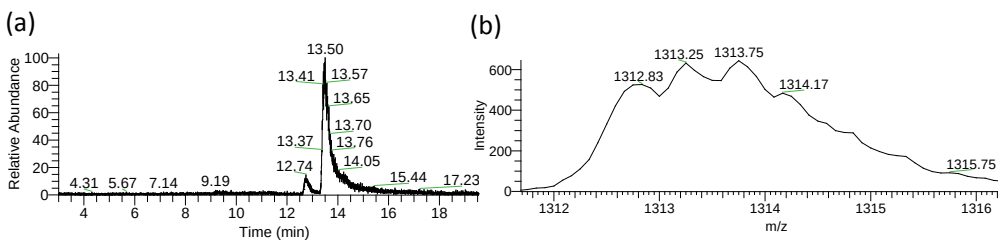

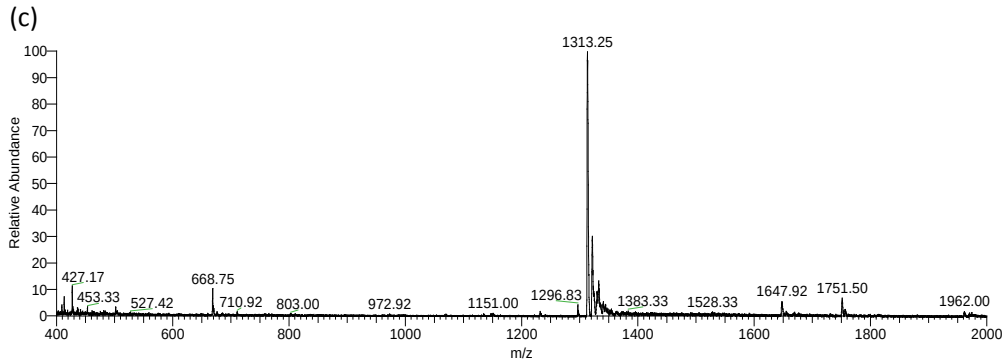

Figure 2.19 (a) Extracted ion chromatogram of m/z = 1312.80 - 1313.80 corresponding to **4**-γ-CD; (b) isotopic profile of the peak observed at 1313.25; (c) ESI-MS spectrum of the HPLC peak at 13.29 min. Expected m/z for $[\mathbf{4}\text{-}\gamma\text{-CD}+2H]^{2+}$=1313.30.

UV-vis Titration

UV-vis measurements were performed on a Varian Cary Bio UV-visible spectrophotometer. A quartz cuvette with 1 cm path length was used for the measurements. The absorption spectra were recorded from 200 nm to 650 nm.

2.5 References

[1] (a) Sauvage, J. P.; Dietrich-Buchecher, C. O. *Molecular Catenanes, Rotaxanes and Knots*, Wiley-VCH, Weinheim, **1999**. (b) Nepogodiev, S. A.; Stoddart, J. F. *Chem. Rev.* **1998**, *98*, 1959-1976. (c) Wenz, G.; Han, B. H.; Muller, A. *Chem. Rev.* **2006**, *106*, 782-817. (d) Terao, J. *Polym. Chem.* **2011**, *11*, 2444-2452. (e) Gavina, P.; Tatay, S. *Curr. Org. Synth.* **2010**, *7*, 24-43. (f) Armspach, D.; Ashton, P. R.; Moore, C. P.; Spencer, N.; Stoddart, J. F.; Wear, T. J.; Williams, D. J. *Angew. Chem. Int. Ed. Engl.* **1993**, *32*, 854-858.

[2] (a) Lehn, J. M. *Chem. Soc. Rev.* **2007**, *36*, 151-160. (b) Ayme, J. F.; Beves, J. E.; Campbell, C. J.; Leigh, D. A. *Chem. Soc. Rev.* **2013**, *42*, 1700-1712. (c) Forgan, R. S.; Sauvage, J. P.; Stoddart, J. F. *Chem. Rev.* **2011**, *111*, 5434-5464. (d) Qu, D.; Tian, H. *Chem. Sci.* **2011**, *2*, 1011-1015. (e) Langton, M. J.; Matichak, J. D.; Thompson, A. L.; Anderson, H. L. *Chem. Sci*. **2011**, *2*, 1897-1901.

[3] (a) Li, J.; Nowak, P.; Otto, S. *J. Am. Chem. Soc.* **2013**, 135, 9222-9239. (b) Otto, S. *Acc. Chem. Res.* **2012**, *45*, 2200-2210. (c) Cougnon, F. B. L.; Sanders, J. K. M. *Acc. Chem. Res.* **2012**, *45*, 2211-2221. (d) Hunt, R. A. R.; Otto, S. *Chem. Comm*. **2011**, *47*, 847-858. (e) Lehn, J.-M. *Top. Curr. Chem.* **2011**, *322*, 1-32. (f) Miller, B. L. *Dynamic Combinatorial Chemistry in Drug Discovery, Bioorganic Chemistry, and Materials Science*, Wiley,

Hoboken, NJ, **2010**. (g) Reek, J. N. H.; Otto, S. *Dynamic Combinatorial Chemistry*, Wiley-VCH, Weinheim, **2010**. (h) Lehn, J.-M. *Chem. Soc. Rev.* **2007**, *36*, 151-160. (i) Corbett, P. T.; Leclaire, J.; Vial, L.; West, K. R.; Wietor, J.-L.; Sanders, J. K. M.; Otto, S. *Chem. Rev.* **2006**, *106*, 3652-3711.

[4] (a) Chung, M. K.; Lee, S. J.; Waters, M. L.; Gagne, M. R. *J. Am. Chem. Soc.* **2012**, *134*, 11430-11443. (b) Chung, M. K.; Lee, S. J.; Waters, M. L.; Gagne, M. R. *J. Am. Chem. Soc.* **2012**, *134*, 11415-11429. (c) Cougnon, F. B. L.; Yeung, H. Y. A.; Pantos, G. D.; Sanders, J. K. M. *J. Am. Chem. Soc.* **2011**, *133*, 3198-3207. (d) West, K. R.; Ludlow, R. F.; Besenius, P.; Corbett, P. T.; Cormack, P. A. G.; Sherrington, D. C.; Otto, S. *J. Am. Chem. Soc.* **2008**, *130*, 10834-10835. (e) Lam, T. S. R.; Belenguer, A.; Robert, S. L.; Naumann, C.; Jarrosson, T.; Otto, S.; Sanders, J. K. M. *Science* **2005**, *308*, 667-669. (f) Au-Yeung, H. Y.; Pantos, G. D.; Sanders, J. K. M. *Proc. Natl. Acad. Sci. USA*, **2009**, *106*, 10466-10470. (g) Au-Yeung, H. Y.; Pantos, G. D.; Sanders, J. K. M. *J. Am. Chem. Soc.* **2009**, *131*, 16030-16032. (h) Au-Yeung, H. Y.; Pantos, G. D.; Sanders, J. K. M. *Angew. Chem. Int. Ed.* **2010**, *49*, 5331-5334.

[5] (a) Hernandez, J. V.; Kay, E. R.; Leigh, D. A. *Science* **2004**, *306*, 1532-1537. (b) Leigh, D. A.; Wong, J. K. Y.; Dehez, F.; Zerbetto, F. *Nature*, **2003**, *424*, 174-179. (c) Evans, N. H.; Serpell, C. J.; Beer, P. D. *Angew. Chem. Int. Ed.* **2011**, *50*, 2507-2510. (d) Fahrenbach, A. C.; Barnes, J. C.; Li, H.; Benitez, D.; Basuray, A. N.; Fang, L.; Sue, C. H.; Barin, G.; Dey, S. K.; Goddard III, W. A.; Stoddart, J. F. *Proc. Natl. Acad. Sci. USA* **2011**, *108*, 20416-20421.

[6] For general reviews about cooperativity see: (a) Ercolani, G. *J. Am. Chem. Soc.* **2003**, *125*, 16097-16103. (b) Badjic, J. D.; Nelson, A.; Cantrill, S. J.; Turnbull, W. B.; Stoddart, J. F. *Acc. Chem. Res.* **2005**, *38*, 723-732. (c) Hunter, C. A.; Anderson, H. L. *Angew. Chem. Int. Ed.* **2009**, *48*, 7488-7499.

[7] (a) Harada, A. *Acc. Chem. Res.* **2001**, *34*, 456-464. (b) Tamesue, S.; Takashima, Y.; Yamaguchi, H.; Shinkai, S.; Harada, A. *Angew. Chem. Int. Ed.* **2010**, *49*, 7461-7464. (c) Wang, Y.; Ma, N.; Wang, Z.; Zhang, X. *Angew. Chem. Int. Ed.* **2007**, *46*, 2823-2826. (d) Rotzler, J.; Mayor, M. *Chem. Soc. Rev.* **2012**, *42*, 44-46.

[8] Formation constants are the formal equilibrium constants that quantify the (in the case of disulfide chemistry fictitious) equilibrium between building blocks and library members.

[9] Otto, S.; Furlan, R. L. E.; Sanders, J. K. M. *J. Am. Chem. Soc.* **2000**, *122*, 12063-12064.

[10] Compared to the large number of examples of cyclodextrin-based rotaxanes, there are surprisingly few reports of cyclodextrin-based catenanes: See: (a) Luttinghaus, A.; Cramer, F.; Prinzbach, H.; Henglein, F. M. *Liebigs Ann. Chem.* **1958**, *613*, 185-198. (b) Armspach, D.; Ashton, P. R.; Moore, C. P.; Spencer, N.; Stoddart, J. F.; Wear, T. J.; Williams, D. J. *Angew. Chem. Int. Ed. Engl.* **1993**, *32*, 854-858. (c) Kuhnert, N.; Tang, B. *Tetrahedron Lett.* **2006**, *47*, 2985-2988. (d) Lim, C. W.; Sakamoto, S.; Yamaguchi, K.; Hong, J. *Org. Lett.* **2004**, *6*, 1079-1082.

[11] Per unit of building block, the total peak area in the HPLC trace was independent of the ratio between the different species in the library, indicating that the various library members have similar molar absorbtivities. More details are provided in Figure 2.5 and the related paragraph.

[12] Ludlow, R. F.; Liu, J.; Li, H.; Roberts, S. L.; Sanders, J. K. M.; Otto, S. *Angew. Chem. Int. Ed.* **2007**, *46*, 5762-5764.

[13] (a) Benesi, H. A.; Hildebrand, J. H. *J. Am. Chem. Soc.* **1949**, *71*, 2703-2707. (b) Kuntz, I. D.; Gasparro, F. P.; Johnston, M. D.; Taylor, R. P. *J. Am. Chem. Soc.* **1968**, *90*, 4778-4781.

[14] Corbett, P. T.; Sanders, J. K. M.; Otto, S. *J. Am. Chem. Soc.* **2005**, *127*, 9390-9392.

[15] Rekharsky, M. V.; Inoue, Y. *Chem. Rev.* **1998**, *98*, 1875-1917.

[16] Nishioka, H.; Liang, X.; Asanuma, H. *Chem. Eur. J.* **2010**, *16*, 2054.

Chapter 3

Cooperative Formation of a "Russian Doll" by Simultaneous Casting and Molding in a Dynamic Combinatorial Library

In Chapter 2 we made dynamic combinatorial catenanes by threading an azobenzene-derived dithiol building block through β- or γ- cyclodextrins. This made us wonder what would happen when we would use dithiol building blocks which are not long enough to get through the cyclodextrin homologues. Will the building blocks form macrocycles inside the cavity of cyclodextrins? Triggered by these questions, in this Chapter, we used a naphthalene dithiol building block with a shorter distance between the two thiol groups. Unlike the azobenzene building block, it is unsymmetrical. It produces isomers of tetrameric macrocycles. In the library without any template, these tetramer isomers interlock forming [2]catenane isomers. Upon the addition of γ-cyclodextrin, two tetramer isomers were casted and amplified inside the cavity of γ-cyclodextrin. It is known that hydrophobic ammonium salts can bind inside the tetramer isomers. We subsequently introduced a benzene-derived ammonium salt as a template in the library made from the naphthalene dithiol building block, resulting in the amplification (now through molding) of another tetramer isomer. These results showed that γ-cyclodextrin can cast a receptor while the benzene-derived ammonium salt can mold a receptor. Can casting and molding occur simultaneously? We decided to add the two templates together in a single library. Surprisingly, another isomer that was not amplified in any of the previous libraries was formed in nearly quantitative yield in the presence of both templates together. This unusual amplification was due to a ternary complexation between the tetramer isomer and the two templates. By evaluating the binding constant of each step of the complexation, we found that this complex exhibited positive cooperativity and self-assembled into a "Russian doll"-like supramolecular architecture.

J. Li, P. Nowak, H. Fanlo-Virgos, S. Otto *manuscript in preparation.*

3.1 Introduction

Cooperative binding effects are ubiquitous in biological systems. Cooperativity is well known as thermodynamically driving the formation of many biomolecular complexes, including, for example, oxygen binding to hemoglobin.[1] To obtain cooperativity in synthetic chemical systems, we need to develop systems that involve the assembly of three weakly binding molecules into stable complexes. The simplest of these are ternary complexes which form in two steps: the first step involves the formation of a two-molecule complex that contains a high-affinity binding site for a third molecule. In case of positive cooperativity, the final ternary complex is highly stable, even if all the binary interactions between any two components are weak. Thus, cooperativity is an emergent property revealing itself only at systems level.[2]

In Chapter 1, we have already discussed that Dynamic Combinatorial Chemistry (DCC)[3a-3c,4] has emerged as a powerful tool to investigate complex chemical systems at systems level. The DCL members exchange building blocks with each other, allowing a rich diversity of molecules to be generated. Even a library starting with only 8 building blocks could produce over 9000 library species, provided the building blocks have at least two groups that can participate in reversible covalent bond formation.[5] In such a large library, there may be many isomeric species which are formed by the same ingredients in different combinatorial ways. There is a certain parallel with nature in which diversity and complexity also derives from combining a limited number of building blocks in a combinatorial way.

Several examples have been shown in Chapter 1 that demonstrate that molecular recognition is a driving force for exploring synthetic receptors and ligands for biomolecules.[6] The receptors typically form around the template molecules. Such template-driven formation of receptors in DCLs is called substrate assisted molding (Scheme 3.1a).[4g,7] Similar to this approach, receptor assisted casting is another way of thermodynamic templating. Unlike molding, the library species are amplified inside a cavity of the template (Scheme 3.1b).[4g,7] With the help of receptor assisted casting, useful information about the structure of the receptor site of a biological macromolecule may be obtained. To the best of our knowledge, no examples of simultaneously applying these two strategies to a single library are reported. Combining them simultaneously in one library may induce different outcomes. One approach to achieve this is adding multiple template molecules to one library. The templates and the amplified receptors may assemble into multi-component complexes.

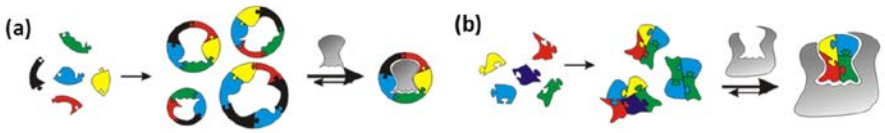

Scheme 3.1. (a) Molding of a receptor and (b) casting of a substrate in DCLs.

Among the complexes consisting of multi components, double-inclusion complexes, reminiscent of Russian Dolls, are fascinating supramolecular architectures. This type of complexes is usually formed by two host molecules and a metal ion.[8] A typical example was reported by Raston and coworkers.[8f] The "Russian doll" is readily formed by combining sodium *p*-sulfonatocalix[4]arene with 18-crown-6 that is able to bind a sodium cation. The structure of the "Russian doll" is shown in Figure 3.1a.

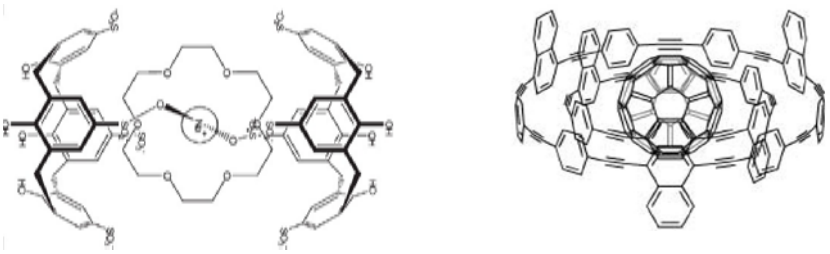

Figure 3.1 "Russian doll" structure consisting of (a) *p*-sulfonatocalix[4]arene with 18-crown-6 and sodium ion; (b) carbon nanorings and a C_{60} core.

Raymond and coworkers reported a similar type of complex.[8e] They first prepared a tetrahedral cluster by the coordination between organic ligands and Ga^{III} metal ions. Subsequently they found that the complex of [12]crown-4 and Li^+ was included in the tetrahedral cluster forming a "Russian doll" supramolecular architecture. Such double-inclusion complexes also can be composed of three organic molecules but these are rare examples.[9] One interesting example was reported by Oda and coworkers in 2004. They successfully obtained a "Russian doll" type supramolecular structure based on carbon nanorings and a C_{60} core in nonpolar organic solvents. Its structure is shown in Figure 3.1b.

In 2008, our group discovered that a series of spontaneously assembled [2]-catenane isomers was produced in quantitative yield upon oxidizing naphthalene dithiol building block **1** (Scheme 3.2).[10] The [2]-catenanes could be converted to tetrameric macrocycles upon addition of an adamantane-derived guest. Due to the asymmetry of the building block **1**, four possible tetramer isomers can be produced, which have different arrangements of the carboxylate groups on the macrocycles.

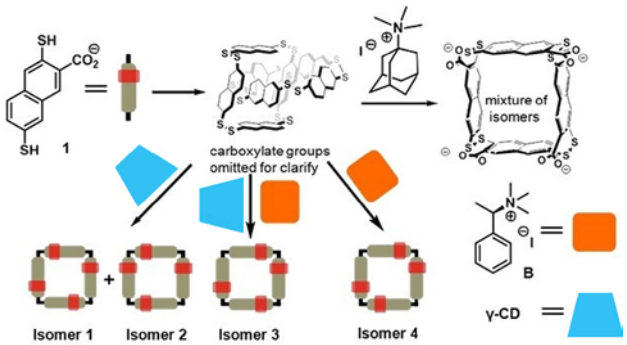

Scheme 3.2. DCLs of building block **1** without or with different templates.

Here we report that four of these isomers may be selectively amplified by using different templates. An isomer, which was not amplified by any single template could be produced in nearly quantitative yield by the combined action of two templates. This unusual amplification resulted from the formation of a self-assembled "Russian doll"-like complex, exhibiting positive cooperativity.

3.2 Results and Discussion

3.2.1 DCL Preparation and Library Behavior

We first prepared a library by dissolving only building block **1** (2.0 mM) in borate buffer (50 mM, pH 8.2) in a capped vial. After 7 days stirring, the library was fully oxidized. HPLC-MS analysis of the library showed a quantitative yield of [2]-catenanes formed by the interlocking of two tetrameric macrocycles (Figure 3.2a), as observed previously.[10] When we prepared a same library, but this time added benzene-derived guest **B** (8 mM), a dominant HPLC peak appeared. It corresponds to a tetramer isomer, isomer **4** (Figure 3.2b). The amplification of tetramer isomers is presumably associated with two factors: i) hydrophobic and π-π interactions between the phenyl ring of **B** and the hydrophobic cavity of the tetramer isomers and ii) the positive charge of **B** interacting electrostatically with the negatively charged carboxylate groups of the tetramer isomers. Similar templating effects have been observed in our previous studies.[10] As discussed in the introduction of this chapter, such template-driven formation of receptors in DCLs is called substrate assisted molding.[4g,7]

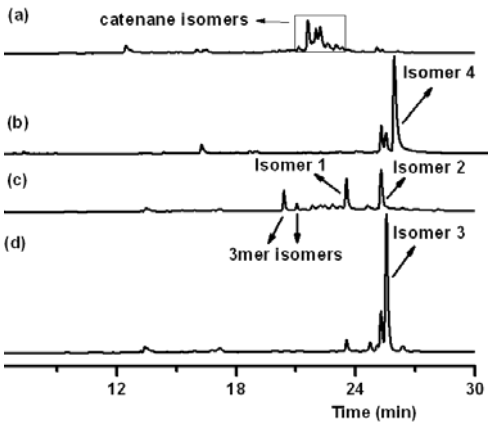

Figure 3.2 HPLC-MS analysis of DCLs made from 2.0 mM building block **1** in aqueous borate buffer (50 mM, pH 8.2) (a) without any template; with template (b) **B** (8.0 mM); (c) γ-CD (8.0 mM); (d) **B** (4.0 mM) and γ-CD (8.0 mM).

Cyclodextrine derivatives are frequently used for the development of artificial enzymes. The interaction between γ-cyclodextrin (γ-CD) and naphthalene units is well known.[11] Driven by hydrophobic interactions, one γ-CD can bind two naphthalene units inside its cavity. We decided to use γ-CD as a template for a new library by mixing it (8.0 mM) with building block **1** (2.0 mM) in borate buffer (50 mM, pH 8.2) in the hope that γ-CD could induce the casting of specific library members. After analyzing the composition of the resulting DCL by HPLC-MS, we found that the tetramer isomers **1** and **2** were strongly amplified alongside two trimer isomers (Figure 3.2c).

The above experiments show the amplification of three tetramer isomers independently using the strategy of molding and casting. These results induced us to apply these two templates (**B** and γ-CD) together in the same library to probe whether the molding and casting strategies can work simultaneously. We prepared a library made from building block **1** (2.o mM) and the two templates **B** (4.0 mM) and γ-CD (8.0 mM) in borate buffer (50 mM, pH 8.2). Surprisingly, analysis by HPLC-MS revealed that tetramer isomer **3**, which was not amplified before, was formed nearly quantitatively in the library containing the two templates together (Figure 3.2d).

3.2.2 Russian Doll Formation by Simultaneous Molding and Casting

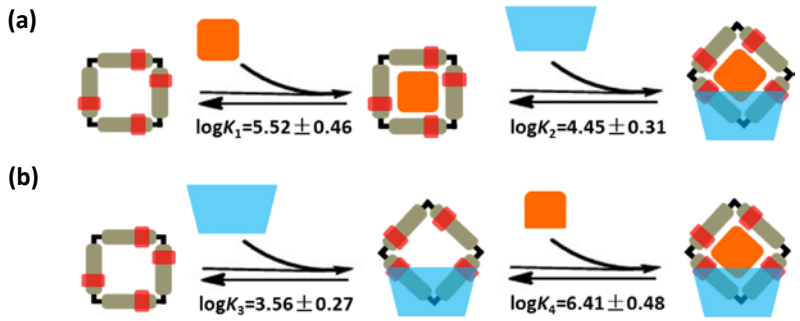

Scheme 3.3. Two procedures for UV titration of isomer **3** with template **B** and γ-CD. (a) Isomer **3** may be titrated with template **B** first to a saturated state and titrated by γ-CD subsequently. (b) Alternatively, the titration may be in reverse order, by changing the sequence of addition of template **B** and γ-CD.

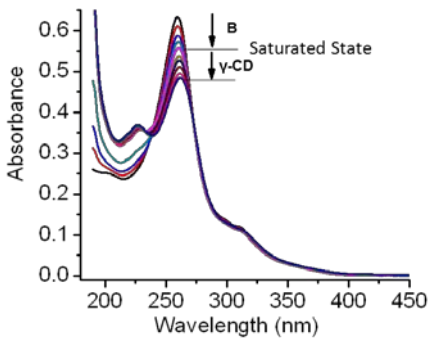

Figure 3.3. Change in UV absorbance changes of isomer **3** (4.5×10^{-6} M) in a borate buffer (50 mM, pH 8.2) when titrated by template **B** first and γ-CD subsequently.

The unusual amplification of tetramer isomer **3** appears to be driven by the formation of a complex involving the two template molecules together. To obtain further insight into the complexation, we evaluated the binding constants among the three components by UV-Vis titration. Isomer **3** may be titrated with template **B** first to a saturated state and titrated by γ-CD subsequently (Scheme 3.3a). We first purified tetramer isomer **3** using preparative HPLC. Isomer **3** (4.5×10^{-6} M in borate buffer 50 mM, pH 8.2) was then titrated with template **B**, inducing a decrease of the intensity of the UV peak at 260 nm (Figure 3.3). When binding was saturated, γ-CD was added until the UV absorbance at 260 nm remained unchanged.

The binding constant of each step was estimated. We firstly assumed that the binding between isomer **3** and **B** has a 1:1 stoichiometry and fitted our data to the modified Hildebrand-Benesi equation[12] 3.1:

$$\frac{1}{\Delta A} = \frac{1}{K_a \Delta\varepsilon[H][G]} + \frac{1}{\Delta\varepsilon[H]} \quad \text{..... Equation 3.1}$$

[H] and [G] present the concentration of isomer **3** (host) and **B** (guest) respectively. K_a stands for the affinity constant between isomer **3** and **B**. ΔA presents the difference of UV absorbance after and before the addition of **B**. Δε, represents the difference of the molar extinction coefficient between the host and host-guest complex at the wavelength of 260 nm, and is estimated to be 2.24×10^4 M^{-1} cm^{-1} based on the UV spectra of the tetramer and that of the host-guest mixture when binding is saturated. The affinity constant was calculated using the equation:

$$K_a = \frac{1}{k\Delta\varepsilon[H]}$$

Where *k* is the slope of the line in Figure 3.4 (b).

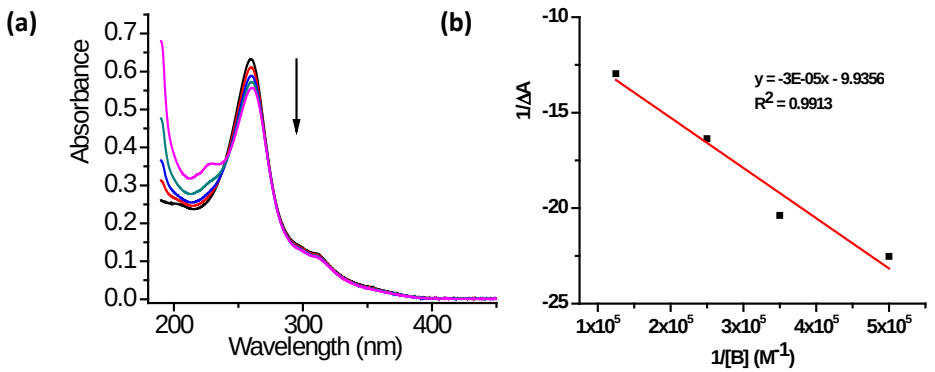

Figure 3.4 (a) Change in UV absorbance upon the addition of **B** to isomer **3**. The concentration of isomer **3** is 4.5×10^{-6} M and the concentration of **B** ranges from 0 to 8.0×10^{-6} M; (b) Hildebrand-Benesi (1:1 stoichiometry) plot of the data of Figure 3.4a at 260 nm.

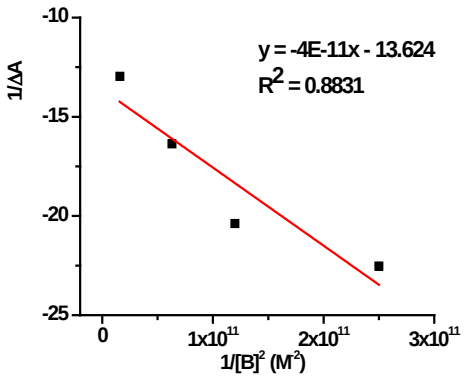

Figure 3.5. Hildebrand-Benesi (1:2 stoichiometry) plot of the data of Figure 3.4a at 260 nm.

If the binding between isomer **3** and **B** was assumed to have a 1:2 stoichiometry, the data should fit to the modified Hildebrand-Benesi equation 3.2:

$$\frac{1}{\Delta A} = \frac{1}{K_a \Delta\varepsilon [H][G]^2} + \frac{1}{\Delta\varepsilon [H]} \quad \text{..... Equation 3.2}$$

However, these data did not fit well for this stoichiometry (Figure 3.5). These results suggest that isomer **3** binds template **B** with a 1:1 stoichiometry. The binding constant (K_1) is shown in Scheme 3.3.

After isomer **3** was titrated with **B** to the extent that binding was saturated, it was titrated with γ-CD (Figure 3.6). The binding constant for this step was evaluated in a similar way as that for the first step using Equation 3.1.

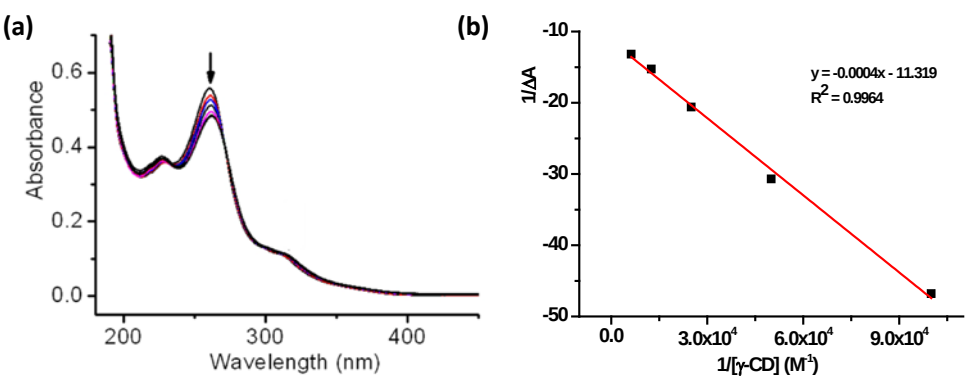

Figure 3.6 (a) Change in UV absorbance upon the addition of γ-CD to a solution containing isomer **3** (4.5×10^{-6} M) and **B** (8.0×10^{-6} M). The concentration of γ-CD ranges from 0 to 0.16 mM ; (b) Hildebrand-Benesi (1:1 stoichiometry) plot of the data of Figure 3.6a at 260 nm.

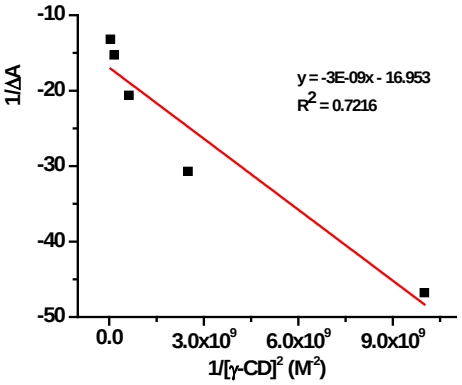

Figure 3.7 Hildebrand-Benesi (1:2 stoichiometry) plot of the data of Figure 3.6a at 260 nm.

We also analyzed our data using the 1:2 stoichiometry Hildebrand-Benesi equation (Equation 3.2, Figure 3.7) but this resulted in a very poor fit. The alternative scenario in which one γ-CD will bind two molecules of isomer **3** is highly unlikely because the volume of one γ-CD is too small to include four naphthalene moieties together. For this reason, we did not discuss this mode of binding. Thus, the binding between γ-CD and the complex consisting of isomer **3** and **B** is likely to have a 1:1 stoichiometry and the binding constant (K_2) is shown in Scheme 3.3. These results suggest that the binding stoichiometry of the termolecular complex is 1:1:1.

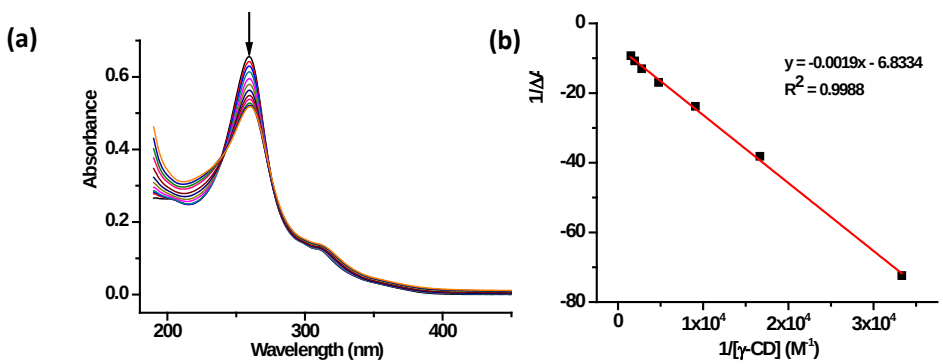

Figure 3.8 (a) Change in UV absorbance upon the addition of γ-CD to isomer **3**. The concentration of isomer **3** is 4.5×10^{-6} M and the concentration of γ-CD ranges from 0 to 0.66 mM; (b) Hildebrand-Benesi (1:1 stoichiometry) plot of the data of Figure 3.8a at 260 nm.

Alternatively, the titration may be performed in reversed order, by changing the sequence of addition of template **B** and γ-CD (Scheme 3.2b). Isomer **3** was first titrated with γ-CD and

then with template **B**. We determined the binding constant between isomer **3** and γ-CD using the same method as that described above. The UV-vis spectral changes (Figure 3.8a) and the Hildebrand-Benesi plots are shown in Figure 3.8b and Figure 3.9. The binding constant (K_3) between isomer **3** and γ-CD is shown in Scheme 3.3.

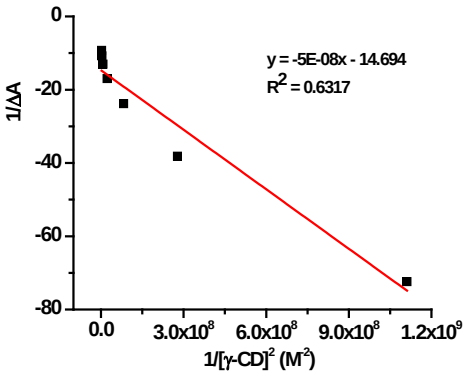

Figure 3.9 Hildebrand-Benesi (1:2 stoichiometry) plot of the data of Figure 3.8a at 260 nm.

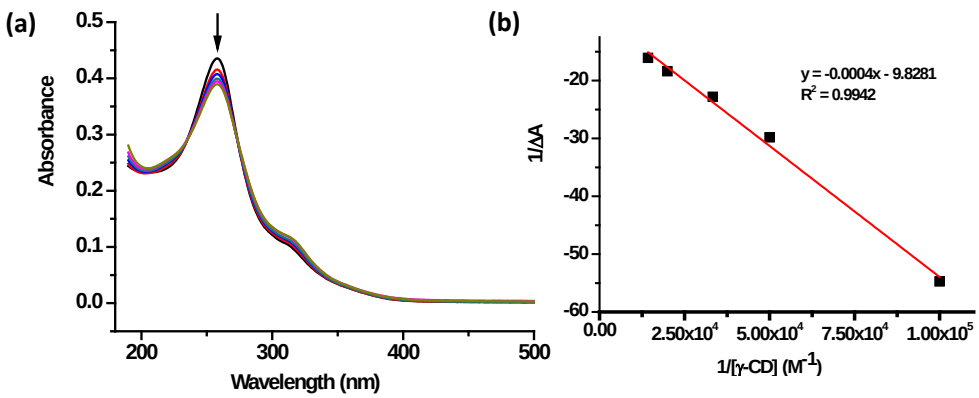

Figure 3.10 (a) Change in UV absorbance upon the addition of γ-CD to isomer **1**. The concentration of isomer **1** is 4.0×10^{-6} M and the concentration of γ-CD ranges from 0 to 0.07 mM; (b) Hildebrand-Benesi (1:1 stoichiometry) plot of the data of Figure 3.10a at 260 nm.

When template **B** was titrated to the saturated solution of isomer **3** and γ-CD, the UV-vis absorbance changed linearly with added **B**, until binding was saturated at approximately one equivalent. This behavior indicates that the stoichiometry is 1:1, but also that the binding constant is too high to be determined accurately using UV-vis titration. However, since $K_1K_2=K_3K_4$, and we know the values of K_1, K_2 and K_3, we can calculate the value of K_4. The

result is shown in Scheme 3.3. Comparing the binding constant of each step, we found that K_2 is larger than K_3, indicating that B binds better in the presence of γ-CD. These results clearly demonstrate that the ternary complex was formed with positive cooperativity.

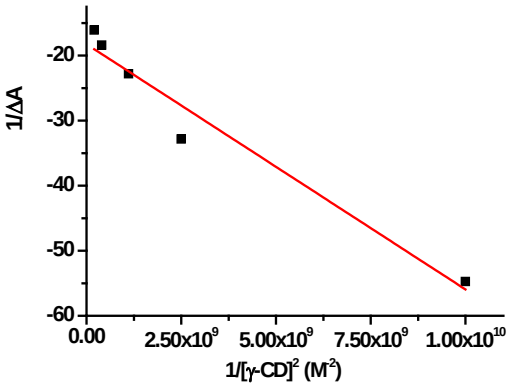

Figure 3.11 Hildebrand-Benesi (1:2 stoichiometry) plot of the data of Figure 3.10a at 260 nm.

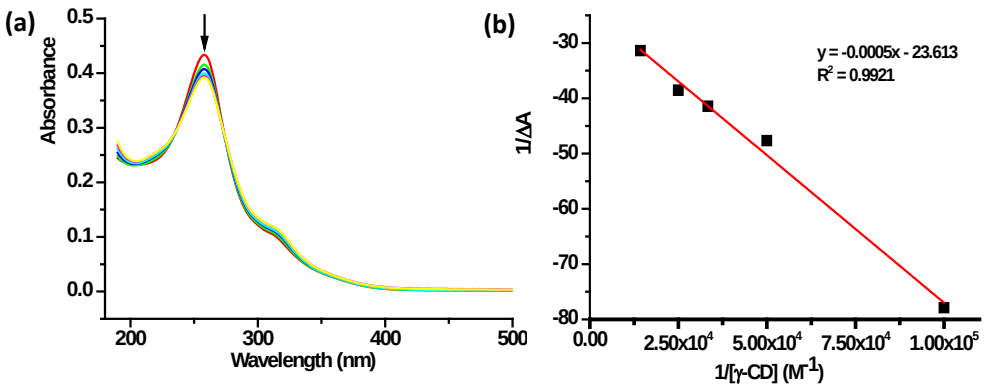

Figure 3.12 (a) Change in UV absorbance upon the addition of γ-CD to isomer **2**. The concentration of isomer **2** is 4.0×10^{-6} M and the concentration of γ-CD ranges from 0 to 0.05 mM; (b) Hildebrand-Benesi (1:1 stoichiometry) plot of the data of Figure 3.12a at 260 nm.

Considering that isomer **1** and isomer **2** were amplified by γ-CD, we also decided to perform UV-vis titrations of these two isomers with γ-CD respectively. The intensity of UV peak at 260 nm decreased when γ-CD was added to the solution of isomer **1** (Figure 3.10a). This behavior is similar to the spectral changes that were observed when γ-CD was added to a solution of isomer **3**. γ-CD was added until the UV absorbance at 260 nm remained unchanged. We then evaluated the binding constant between isomer **1** and γ-CD using Equation 3.1 (Figure 3.10b). We also fitted our data to the 1:2 stoichiometry Hildebrand-Benesi equation (Equation 3.2, Figure 3.11) and they did not fit well. Thus, the

binding between γ-CD and isomer **1** most likely has a 1:1 stoichiometry and a binding constant ($\log K_{1\text{-}\gamma\text{-}CD}$) of 4.39 ± 0.17.

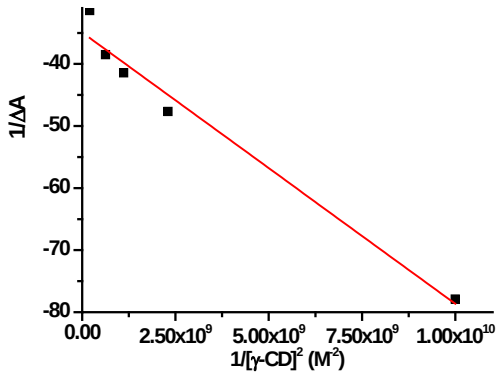

Figure 3.13 Hildebrand-Benesi (1:2 stoichiometry) plot of the data of Figure 3.12a at 260 nm.

We performed similar titration experiments for isomer **2**. The UV-vis spectral changes (Figure 3.12a) and the Hildebrand-Benesi plots (Figure 3.12b and Figure 3.13) are shown above. Isomer **2** showed similar binding behavior with γ-CD as isomer **1**. The binding stoichiometry between isomer **2** and γ-CD is 1:1 and their binding constant ($\log K_{2\text{-}\gamma\text{-}CD}$) is 4.67 ± 0.18.

The equilibrium constant for binding of isomer **1** to γ-CD is similar to that of binding of isomer **2**, but much larger than that for binding of isomer **3** to γ-CD. This is the reason why isomer **1** and isomer **2** were amplified to comparable extents in the library prepared from building block **1** and γ-CD. However, when **B** was added as a second template, isomer **3** was amplified in almost quantitative yield as a result of the cooperative complexation with the two templates.

3.2.3 Elucidating the Structure of Tetramer Isomers

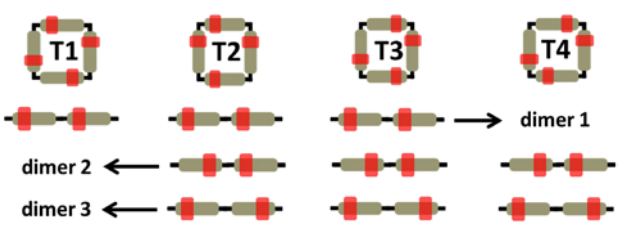

Scheme 3.5. Structures of the four isomers and their corresponding dimer fragments.

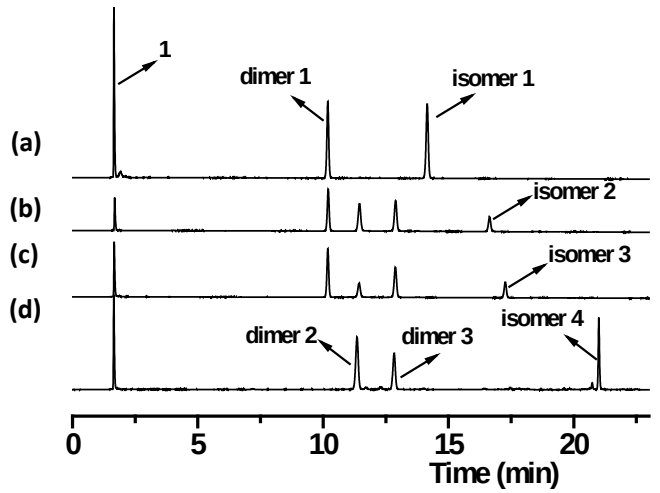

Figure 3.14. HPLC-MS analysis of the product distribution obtained upon partial reduction of (a) isomer **1**, (b) isomer **2**, (c) isomer **3** and (d) isomer **4,** through the addition of 0.3 equivalents of dithiothreitol per disulfide linkage.

From the analysis by LC-MS, the structures of the four isomers cannot be determined. Since they can be amplified selectively in good yields, it was possible to purify them by preparative HPLC. We then attempted to assign the isomers by NMR. Unfortunately, the ^{1}H NMR spectra showed very broad singals and could not be interpreted. Since the four isomers are held together by disulfide bonds, we decided to partially reduce these isomers and analyze the resulting fragments by HPLC-MS, which may give us insights into their structures. When 30% of the disulfide bonds of each isomer were reduced by dithiothreitol, HPLC-MS analysis revealed that different numbers of isomeric dimers were produced from different isomers. The isomer **1** and isomer **4** produced only one and two dimers respectively (Figure 3.14a and 3.14d) and isomer **2** and isomer **3** both gave rise to three dimers (Figure 3.14b and 3.14c). We analyzed the structures of the four tetramer isomers (T1, T2, T3 and T4) and listed all the possible structures of dimers in Scheme 3.5. Comparing the numbers of dimer isomers that each tetramer isomer can produce with the numbers of dimers isomers detected by HPLC-MS, we can deduce the structures of isomer **1** and isomer **4** (Scheme 3.1). The structure of T1 is corresponding to isomer **1** and the structure of T4 is corresponding to isomer **4**. However, T2 and T3 can both produce three dimer isomers (Scheme 3.5), which makes it difficult to unambiguously assign their structures. If we look further into the concentration relationship of dimer isomers produced by the structure T2 and T3, we can obtain additional clues to the assignment of the structures of isomer **2** and isomer **3**. Partial

reduction of the tetramer isomer T2 should produce the same concentration of dimer **2** and dimer **3**. For tetramer isomer T3, the concentration of dimer **1** should be equal to the sum of the concentrations of dimer **2** and dimer **3**. The HPLC-MS data in Figure 3.14 suggests that T2 corresponds to isomer **2** and T3 corresponds to isomer **3**.

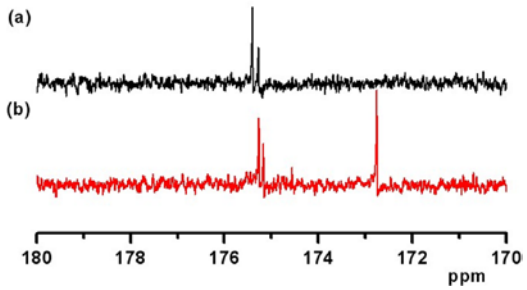

Figure 3.15. ^{13}C NMR spectra of (a) isomer **2** (1.0 mM) and (b) isomer 3 (1.0 mM) in D_2O (pD 8.2).

Considering that T3 has no symmetry elements, while T2 has a plane of symmetry, another way to elucidate the structures of isomers **2** and **3** is using ^{13}C NMR. The asymmetric structure of T3 should show four separate carbon signals of each of the four carboxylic acid groups while the symmetric T3 should show only two carbon signals for the carboxylic acid groups (Scheme 3.5). This was indeed observed from the ^{13}C NMR spectra of isomer **2** and isomer **3** (Figure 3.15). Therefore, the structures of each of the four isomers could be established using these two methods and the results are summarized in Scheme 3.1.

3.2.4 Investigating the Structure of the Russian-Doll Like Complex

We proceeded to investigate the mode of assembly of isomer **3**, template **B** and γ-CD by ^1H NMR experiments. By mixing isomer **3** with guest **B**, the chemical shifts of the aromatic protons of guest **B** shift downfield and split into two peaks, indicating that the benzene ring of the guest binds into the hydrophobic cavity of isomer **3**, consistent with our previous results[8] (Figure 3.16). Upon the subsequent addition of 4.0 equivalents γ-CD to the mixture, the largely overlapping proton signals between 8.1 ppm to 8.25 ppm of isomer **3** shifted downfield and became separated, which clearly demonstrated the binding between γ-CD and the complex consisting of isomer **3** and guest **B** (Figure 3.17). However, upon addition of γ-CD to a solution of guest **B**, no changes in chemical shifts were observed. These results clearly indicated that the isomer **3** binds the guest **B** and γ-CD together. These three molecules most likely self-assemble into a "Russian doll"-like complex. Its energy-minimized model is shown in Figure 3.18.

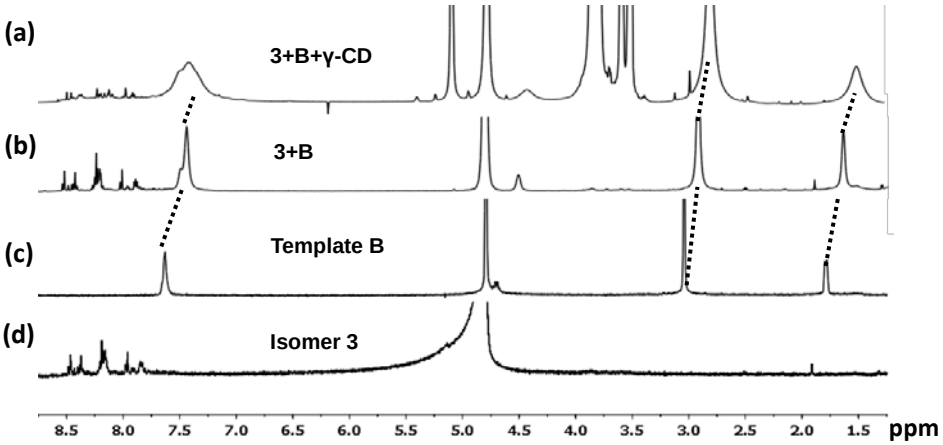

Figure 3.16. ^{1}H NMR spectra of (a) a mixture of isomer **3** (0.5 mM), template **B** (4.0 mM) and γ-CD (4.0 mM); (b) a mixture of isomer **3** (0.5 mM) and template **B** (4.0 mM); (c) template **B** (4.0 mM) and (d) isomer **3** (0.5 mM).

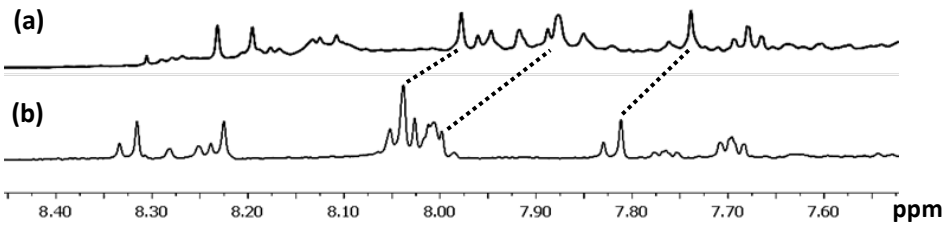

Figure 3.17. ^{1}H NMR spectra of (a) mixture of isomer **3** (0.5 mM), template **B** (4.0 mM) and γ-CD (4.0 mM); (b) mixture of isomer **3** (0.5 mM) and template **B** (4.0 mM).

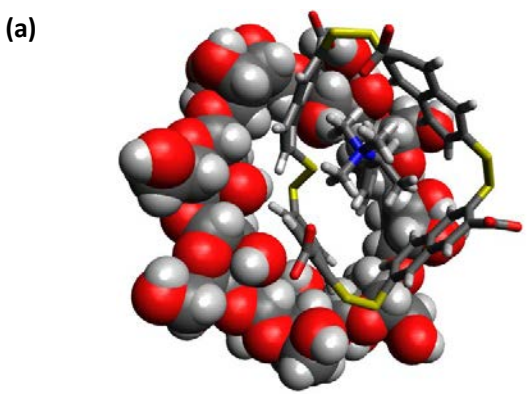

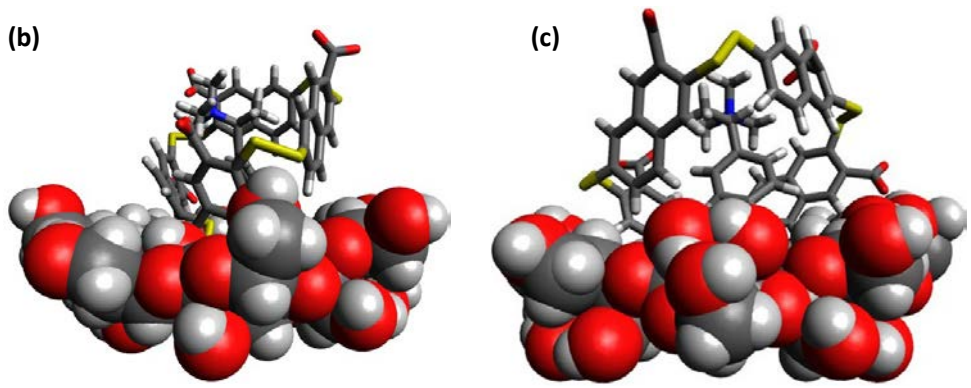

Figure 3.18 (a) Top view, (b) front view and (c) side view of the energy-minimized structure of the "Russian doll" complex consisting of isomer **3**, γ-CD and template **B** in water at pH 8.2. Carbon atoms are shown in grey, hydrogen in white, oxygen in red and sulfur in yellow.

3.3 Conclusion

In conclusion, we have shown that all four isomers of the tetramer macrocycles formed from building block **1** can be selectively amplified by different templates or a combination of templates from dynamic mixtures. The isomer with the lowest symmetry was only amplified through the positive cooperative self-assembly of two templates, which is the first example of simultaneous casting and molding of a library member. This approach represents a new strategy towards molecules capable of binding two different partners. In this case, binding shows allosteric cooperativity. Binding of the first partner enhances affinity for the second partner by approximately an order of magnitude. This particular isomer was amplified quantitatively. However, we still do not know why this effect is specific for this particular isomer. This question may be answered by obtaining the crystal structures of complexes of isomers and guest molecules. Unfortunately, attempts to crystallize the Russian doll complex has until now been unsuccessful.

3.4 Experimental Section

3.4.1 Materials

The source of all chemicals, unless otherwise stated, was the same as in Chapter 2. Building block **1** was prepared as reported previously.[10]

3.4.2 General Methods

Analytical HPLC

Analytical HPLC was carried out on Hewlett Packard 1050 or 1100 systems coupled to UV detectors and the data were processed using HP Chemstation software. Separations were performed on a reversed phase Zorbax C8 column (4.6 x 150 mm, 5 µm particle size, Agilent). Except where otherwise stated, the chromatography was carried out at 45 °C using UV detection at 260 nm. The HPLC method is the one used for LC-MS, described below.

LC-MS analysis

An Accela High Speed LC system (ThermoFisher Scientifics, Courtaboeuf, France) was coupled to a LTQ-Fleet Ion-Trap Mass Spectrometer. Water was obtained from a MilliQ Gradient system and LC-MS-grade acetonitrile was bought from BIOSOLVE.

Analysis of samples was performed using a reversed-phase HPLC column (Zorbax C8, 4.6 × 150 mm, 5 µm, Agilent) at 45 °C with an injection volume of 5.0 µL. All UV traces were obtained by monitoring at 260 nm. The following LC method was used for the analysis of libraries:

Solvent A: water (0.1% v/v formic acid); Solvent B: acetonitrile (0.1% v/v formic acid)
Flow rate: 1.0 mL/min

Time (min)	%B
0	20
5	20
30	90
35	90

The following LC method was used for the analysis of the 30% reduced isomers:
Solvent A: water (0.1% v/v formic acid); Solvent B: acetonitrile (0.1% v/v formic acid)
Flow rate: 1.0 mL/min

Time (min)	%B
0	40
35	95

Mass spectra of all the library species were recorded in negative ion mode. The electrospray voltage was set to 4.5 kV, the capillary voltage was set to 2.0 V; the sheath and auxiliary gas flows (both nitrogen) were 5.0 L/min and 3.0 L/min, respectively, and the drying gas temperature was 320 °C.

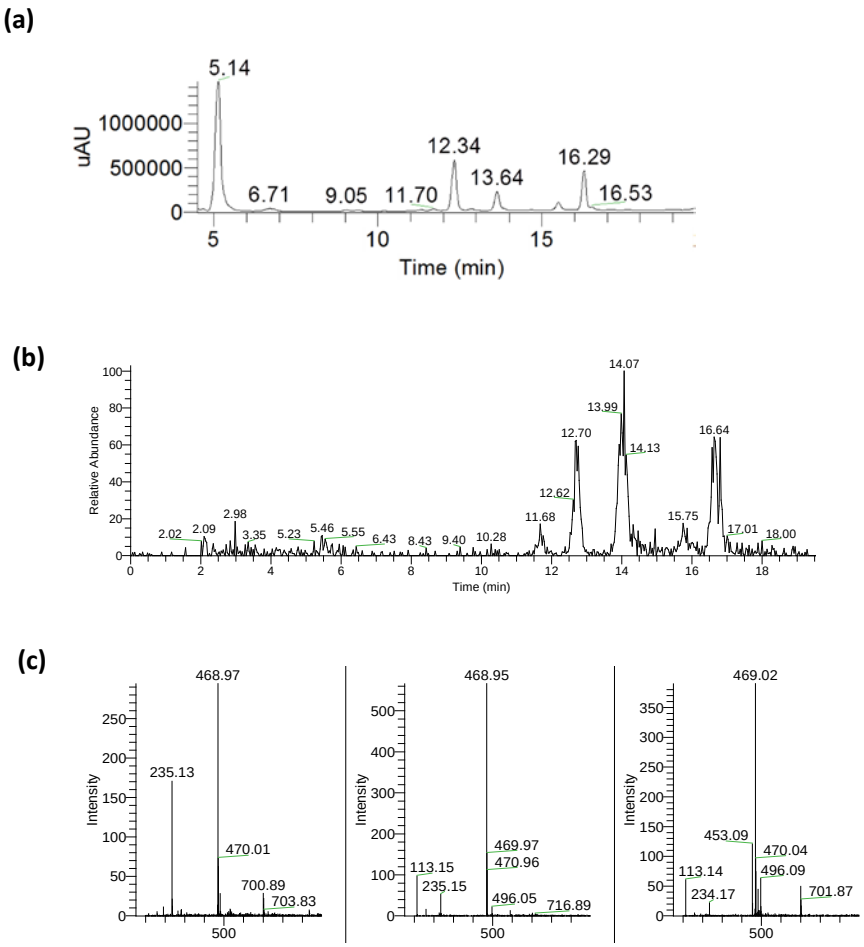

Figure 3.18. (a) UV trace of the HPLC analysis of fragments of isomer **2** obtained through the addition of 0.3 equivalents of dithiothreitol per disulfide linkage; (b) Extracted ion chromatogram of mass between 468.5 and 469.5 corresponding to linear dimers of building block **1**; (c) ESI-MS spectrum of linear dimer of building block **1** corresponding to the HPLC peaks at 12.34 min (left), 13.64 min (middle) and 16.29 min (right) Expected m/z for [**M**-H]$^-$=468.98.

UV-vis Titration

UV-vis measurements were performed on a Varian Cary Bio UV-visible spectrophotometer. A quartz cuvette with 1 cm path length was used for the measurements. The absorption spectra were recorded from 200 nm to 650 nm.

Molecular Modeling

The energy-minimized model of the "Russian doll" complex was simulated computationally using the AMBER force field as implemented in MacroModel version 8.0018 (Schrodinger Inc, Porland Oregon) and a continuum water model.[13] The MCMM method[14] was used to perform the conformational analysis. The lowest energy conformation of the "Russian doll" complex was found in 5000 steps.

3.5 Acknowledgements

We thank Hugo Fanlo Virgos for supplying the naphthalene dithiol building block. We gratefully acknowledge Piotr Nowak for performing the molecular modeling.

3.6 References

[1] Williamson, J. R. *Nat. Chem. Biol.* **2008**, *8*, 458-465.

[2] (a) Whitty, A. *Nat. Chem. Biol.* **2008**, *8*, 435-439. (b) Badjic, J. D.; Nelson, A.; Cantrill, S. J.; Turnbull, W. B.; Stoddart, J. F. *Acc. Chem. Res.* **2005**, *38*, 723-732.

[3] (a) Li, J.; Nowak, P.; Otto, S. *J. Am. Chem. Soc.* **2013**, *135*, 9222-9239. (b) Hunt, R. A. R.; Otto, S. *Chem. Comm.* **2011**, *47*, 847-858. (c) Peyralans, J. J.-P.; Otto, S. *Curr. Opin. Chem. Biol.* **2009**, *13*, 705-713; (d) Nitschke, J. R. *Nature* **2009**, *462*, 736-738. (e) Ludlow, R. F.; Otto, S. *Chem. Soc. Rev.* **2008**, *37*, 101-108. (f) Stankiewicz, J.; Eckardt, L. H. *Angew. Chem., Int. Ed.* **2006**, *45*, 342-344. (g) Newth, D.; Finnigan, J. *Aust. J. Chem.* **2006**, *59*, 841-848. (h) Whitesides, G. M.; Ismagilov R. F. *Science* **1999**, *284*, 89-92.

[4] (a) Otto, S. *Acc. Chem. Res.* **2012**, *45*, 2200-2210. (b) Cougnon, F. B. L.; Sanders, J. K. M. *Acc. Chem. Res.* **2012**, *45*, 2211-2221. (c) Lehn, J.-M. *Top. Curr. Chem.* **2011**, *322*, 1-32. (d) Miller, B. L. *Dynamic Combinatorial Chemistry in Drug Discovery, Bioorganic Chemistry, and Materials Science*, Wiley, Hoboken, NJ, **2010**. (e) Reek, J. N. H.; Otto, S. *Dynamic Combinatorial Chemistry*, Wiley-VCH, Weinheim, **2010**. (f) Lehn, J.-M. *Chem. Soc. Rev.* **2007**, *36*, 151-160. (g) Corbett, P. T.; Leclaire, J.; Vial, L.; West, K. R.; Wietor, J.-L.; Sanders, J. K. M.; Otto, S. *Chem. Rev.* **2006**, *106*, 3652-3711.

[5](a) Ludlow, R. F.; Otto, S. *J. Am. Chem. Soc.* **2010**, *132*, 5984-5986. (b) Ludlow, R. F.; Otto, S. *J. Am. Chem. Soc.* **2008**, *130*, 12218-12219.

[6] (a) James, L. I.; Beaver, J. E.; Rice, N. W.; Waters, M. J. *J. Am. Chem. Soc.* **2013**, *135*, 6450-6455. (b) Hamieh, S;

Ludlow, R. F.; Perraud, O.; West, K. R.; Mattia, E.; Otto, S. *Org. Lett.* **2012**, *14*, 5404-5407. (c) Beeren, S. R.; Sanders, J. K. M. *Chem. Sci.* **2011**, *2*, 1560-1567. (d) Beeren, S. R.; Sanders, J. K. M. *J. Am. Chem. Soc.* **2011**, *133*, 3804-3807. (e) Rauschenberg, M.; Bomke, S.; Karst, U.; Ravoo, B. J. *Angew. Chem. Int. Ed.* **2010**, *49*, 7340-7345. (f) Saggiomo, V.; Lüning, U. *Chem. Commun.* **2009**, 3711-3713. (g) Scott, D. E.; Dawes, G. J.; Ando, M.; Abell, C.; Ciulli, A. *ChemBioChem* **2009**, *10*, 2772-2779. (h) Bugaut, A.; Jantos, K.; Wietor, J. L.; Rodriguez, R.; Sanders, J. K. M.; Balasubramanian, S. *Angew. Chem. Int. Ed.* **2008**, *47*, 2677-2680. (i) Gareiss, P. C.; Sobczak, K.; McNaughton, B. R.; Palde, P. B.; Thornton, C. A.; Miller, B. L. *J. Am. Chem. Soc.* **2008**, *130*, 16254-16261. (j) Vial, L.; Ludlow, R. F.; Leclaire, J.; Perez-Fernandez, R.; Otto, S. *J. Am. Chem. Soc.* **2006**, *128*, 10253-10257. (k) Shi, B. L.; Stevenson, R.; Campopiano, D. J.; Greaney, M. F. *J. Am. Chem. Soc.* **2006**, *128*, 8459-8467.

[7] (a) Lehn, J.-M. *Proc. Natl. Acad. Sci. USA* **2002**, *99*, 4763-4768. (b) Lehn, J.-M.; Eliseev, A. V. *Science* **2001**, *291*, 2331-2332. (c) Huc, I.; Lehn, J.-M. *Proc. Natl. Acad. Sci. USA* **1997**, *94*, 2106-2110.

[8] (a) Moorthy, J. N.; Natarajan, P. *Chem. Eur. J.* **2010**, *16*, 7796-7802. (b) Dalgarno, S. J.; Fisher, J.; Raston, C. L. *Chem. Eur. J.* **2006**, *12*, 2772-2777. (c) Dalgarno, S. J.; Atwood, J. L.; Raston, C. L. *Chem. Commun.* **2006**, 4567-4574. (d) Hof, F.; Craig, S. L.; Nuckolls, C.; Rebek, Jr., J. *Angew. Chem. Int. Ed.* **2002**, *41*, 1488-1508. (e) Parac, T. N.; Scherer, M.; Raymond, K. N. *Angew. Chem. Int. Ed.* **2000**, *39*, 1239-1242. (f) Drljaca, A.; Hardie, M. J.; Raston, C. L.; Spiccia, L. *Chem. Eur. J.* **1999**, *5*, 2295-2299.

[9] (a) Shivanyuk, A. *J. Am. Chem. Soc.* **2007**, *129*, 14196-14199. (b) Kawase, T.; Tanaka, K.; Shiono, N.; Seirai, Y.; Oda, M. *Angew. Chem. Int. Ed.* **2004**, *43*, 1722-1724.

[10] West, K. R.; Ludlow, R. F.; Corbett, P. T.; Besenius, P.; Mansfeld, F. M.; Cormack, P. A. G.; Sherrington, D. C.; Goodman, J. M.; Stuart, M. C. A.; Otto, S. *J. Am. Chem. Soc.* **2008**, *130*, 10834–10835.

[11] (a) Luo, L.; Liao, G.; Wu, X.; Lei, L.; Tung, C.; Wu, L. *J. Org. Chem.* **2009**, *74*, 3506-3515. (b) Nakamura, A.; Inoue, Y. *J. Am. Chem. Soc.* **2003**, *125*, 966-972. (c) Toyoda, T.; Matsumura, S.; Mihara, H.; Ueno, A. *Macromol. Rapid Commun.* **2000**, *21*, 485-488. (d) Tan, W.; Ishikura, T.; Maruta, A.; Yamamoto, T.; Matsui, Y. *Bull. Chem. Soc. Jpn.* **1998**, *71*, 2323-2329.

[12] (a) Benesi, H. A.; Hildebrand, J. H. *J. Am. Chem. Soc.* **1949**, *71*, 2703-2707. (b) Kuntz, I. D.; Gasparro, F. P.; Johnston, M. D.; Taylor, R. P. *J. Am. Chem. Soc.* **1968**, *90*, 4778-4781.

[13] Still, W. C.; Tempczyk, A.; Hawley, R. C. *J. Am. Chem. Soc.* **1990**, *112*, 6127-6129.

[14] Chang, G.; Guida, W. C.; Stil, W. C. *J. Am. Chem. Soc.* **1989**, *111*, 4379-4386.

Chapter 4

Emergence of a Self-Replicator from a Dynamic Combinatorial Library Assisted by a Template Molecule

From previous work by our group we know that the four tetramer isomers described in Chapter 3 can also be amplified by an adamantane-derived template molecule. By gradually increasing the amount of the adamantane template, we found that three of the four tetramer isomers were amplified strongly while one of them was only amplified slightly in a library prepared in the presence of a small amount of template. Interestingly, in a new library in which the amount of template was increased by only 30%, the tetramer isomer that was only slightly amplified before was suddenly amplified 400%. In this chapter, we will explain why this sudden increase occurred.

J. Li, S. Otto *manuscript in preparation.*

4.1 Introduction

Self-replication (reproduction) is often considered as the hallmark of living systems. Self-replicating molecules are likely to have played an important role in the origin of life.[1] These molecules synthesize themselves auto-catalytically, promoting their own formation. To create de-novo life, one key step is the emergence of self-replicators from complex mixtures, a process that is still not well understood.

In DCLs it is known that, in most cases, addition of chemical templates which can bind to the library species will stabilize these compounds and shift the equilibrium to those library members. However, in some particular cases, without adding any template molecules, if one of the library species can bind to copies of itself, this species will self-assemble and the equilibrium will be shifted, promoting its own formation.[2,3] In this way, the self-assembly of this species may drive its self-replication. In many cases self-assembly requires that the concentration of the assembling molecule is above the critical concentration.[4] In a DCL, if the concentration of a library species cannot reach this threshold, self-replication would not happen. Addition of a template molecule into the DCL may amplify the concentration of this library member and help it to get over this barrier.

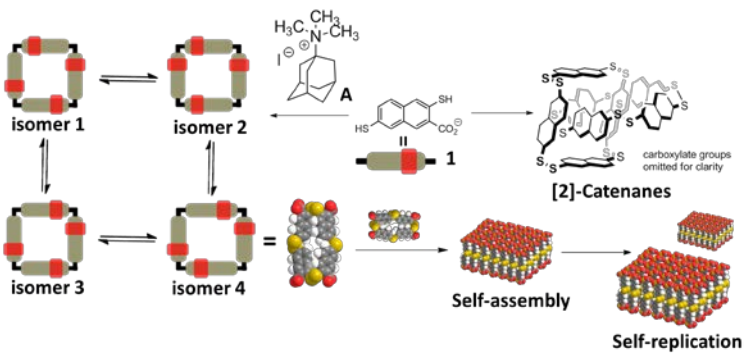

Scheme 4.1 Emergence of a self-replicator from a DCL assisted by an adamantane-derived template.

In Chapter 3 we have shown that a DCL prepared from a naphthalene dithiol building block **1** (Scheme 4.1), will spontaneously produce [2]-catenanes in quantitative yield. From our previous results,[5] we know that upon the addition of an adamantane-derived template molecule **A**, these catenanes can be converted into four tetrameric isomers. Using the same DCC here, we report the first example of a self-replicator emerging from a dynamic isomeric mixture with the assistance of a template molecule. Driven by molecular recognition with the

template, four isomers were all amplified in the DCL. When the concentration of one isomer reached a critical concentration, aggregation then took place and this isomer was amplified autocatalytically.

4.2 Results and Discussion

4.2.1 DCL Preparation and Library Behavior

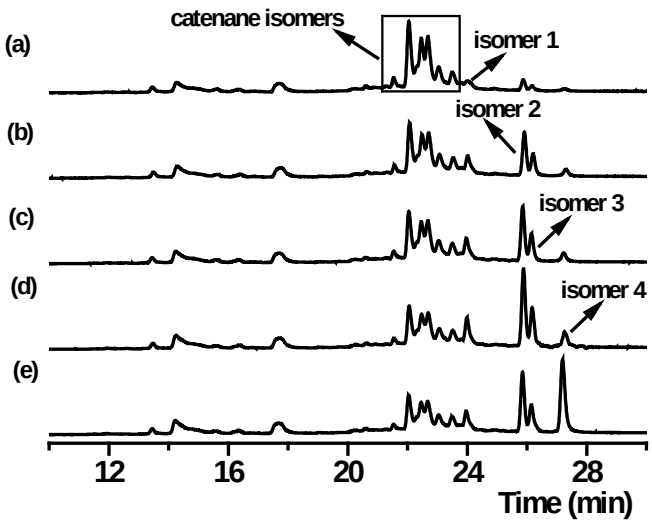

Figure 4.1 HPLC-MS analysis of DCLs made from 2.0 mM building block **1** in aqueous borate buffer (50 mM, pH 8.2) (a) without any template; with template **A** at a concentration of (b) 0.05 mM; (c) 0.067 mM; (d) 0.1 mM and (e) 0.13 mM.

We first prepared a group of libraries from building block **1** (2.0 mM) with different amounts of adamantane-derived template **A** (0 mM, 0.050 mM, 0.067 mM, 0.10 mM and 0.13 mM) in borate buffer (50 mM, pH 8.2). These libraries were stirred in capped vials in the presence of air. Disulfide exchange in these systems takes place through reaction between the disulfides and residual thiolate anions. After 2 days, all the thiolate anions were fully oxidized and the disulfide exchange stopped. The resulting mixture was then analyzed by HPLC-MS (Figure 4.1). In the library prepared without template **A**, the main library species are tetramer-tetramer interlocked catenane isomers. When the library was prepared with template **A**, the catenane isomers converted to four tetramer isomers. Very distinctly, isomer **1**, isomer **2** and isomer **3** were amplified to a much larger extent than isomer **4**. For

example, when the library made from 0.05 mM template **A**, the amplification factors of isomer **1**, isomer **2** and isomer **3** are 3, 4.5 and 3, respectively, while the amplification factor of isomer **4** is very small only 1.2. Even if the concentration of A was increased to 0.10 mM, isomer **4** was still only slightly amplified, whereas the amplification of the other isomers kept increasing. However, when the library was made with only 30% more of **A** (0.13 mM), isomer **4** was amplified more than 400%, while the amplification of the other isomers were not much affected (Figure 4.2). This sudden increase in the amplification of isomer **4** is indicative of the aggregation of this compound that sets in beyond a certain critical concentration.

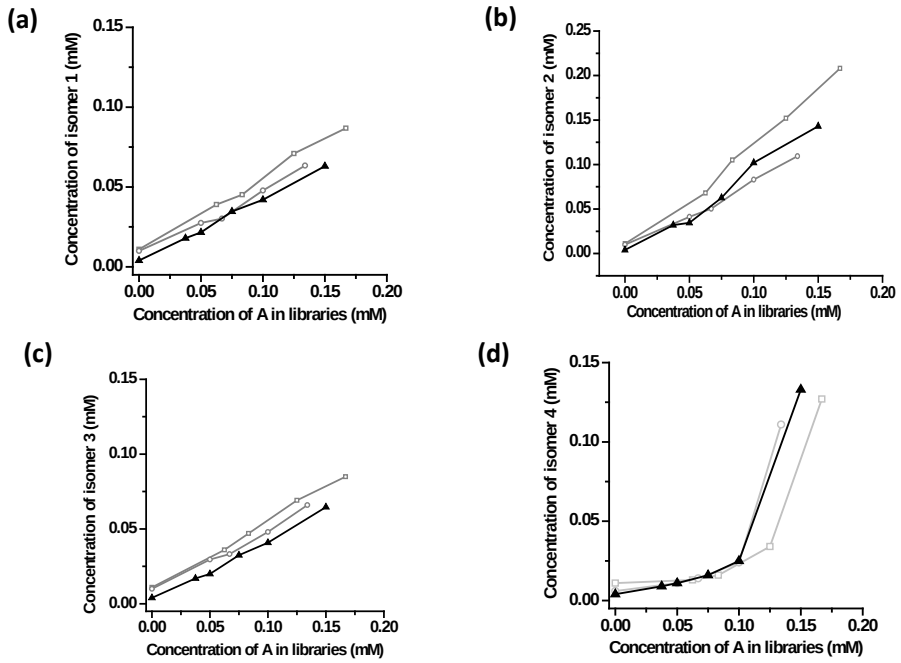

Figure 4.2. Relationship between the concentration of template **A** and the concentration of (a) isomer **1**, (b) isomer **2**, (c) isomer **3** and (d) isomer **4**. The black solid triangles stand for libraries made from 1.5 mM building block **1**. The grey empty circles stand for libraries made from 2.0 mM building block **1**. The grey empty squares stand for libraries made from 2.5 mM building block **1**.

We decided to prepare two more groups of libraries with different concentration of building block **1** and template **A**. One group was made from building block **1** (1.5 mM) without **A** and with **A** (0.038 mM, 0.050 mM, 0.075 mM, 0.10 mM and 0.15 mM) in borate buffer (50 mM, pH 8.2). The other group was made from building block **1** (2.5 mM) without

A and with **A** (0.063 mM, 0.083 mM, 0.13 mM and 0.17 mM) in borate buffer (50 mM, pH 8.2). We performed the same HPLC-MS analysis for all these libraries. The relationship between the concentration of template **A** in the libraries and the concentration of the four isomers was plotted in Figure 4.2, which reveals that a sudden increase of the amplification of isomer **4** occurred when its concentration exceeded approximately 0.03 mM (Figure 4.2d). However, we did not observe any sudden increase of the amplification of the other three isomers (Figure 4.2a-c). We reason that 0.03 mM probably is the critical concentration for aggregation of isomer **4**

4.2.2 Aggregation Investigation

(a)

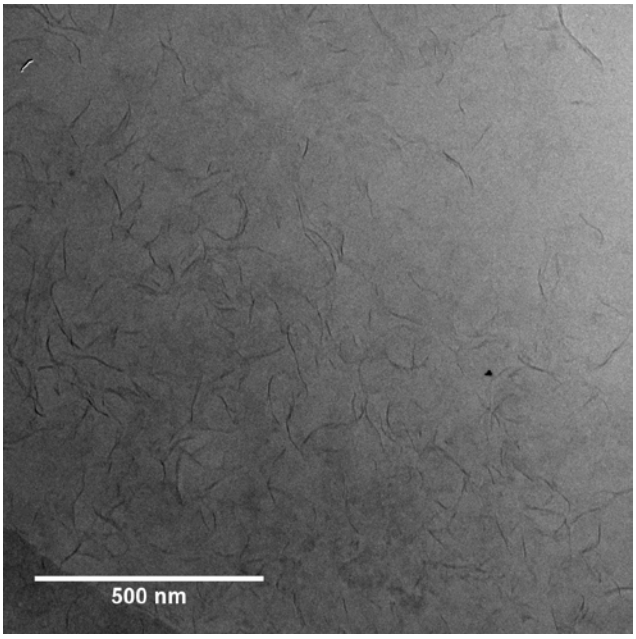

(b)

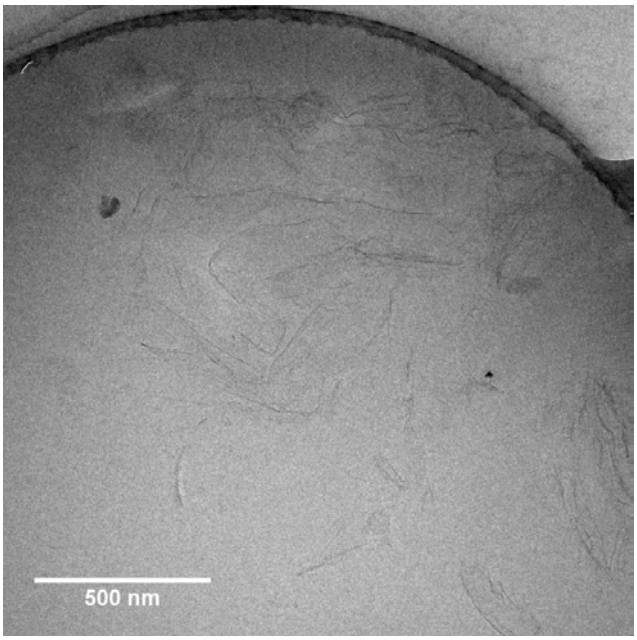

Figure 4.3. Cryo-TEM image of the sample of (a) the fully oxidized library prepared from building block 1 and template **A** (0.13 mM) and (b) a solution of only isomer **4** (0.040 mM) in borate buffer (50 mM, pH 8.2).

A direct way to assess whether aggregation is taking place is using cryo-TEM. We first investigated the aggregation in the fully oxidized library made from building block **1** (2.0 mM) and template **A** (0.10 mM) by cryo-TEM. No aggregates were observed. We then performed cryo-TEM for the sample made from 30% more amount of template **A** (0.13 mM) but the same concentration of building block **1**. Membrane-like nanosheets with a thickness around 1.8 nm (Figure 4.3a) were observed, suggesting that the sudden increase in the amplification of isomer **4** was associated with the formation of these self-assembled aggregates. Whereas the cryo-TEM was performed for the library containing template molecules, we wondered whether isomer **4** can also self-assemble in the absence of template. We purified isomer **4** by preparative HPLC and prepared two solutions of it in borate buffer (50 mM, pH 8.2). The concentration of one solution (0.020 mM) is below the critical concentration while the other (0.040 mM) is above the critical concentration. We performed cryo-TEM for these two samples, which showed dramatically different results. No aggregates were observed for the sample at the concentration of 0.020 mM, while the 0.040 mM sample showed nanosheets with a thickness of about 1.6 nm similar to those we observed for the library in the presence of template **A** (Figure 4.3b). These results revealed

that if the concentration of isomer **4** is above the critical concentration, it also can self-assemble into nanosheets even in the absence of template **A**.

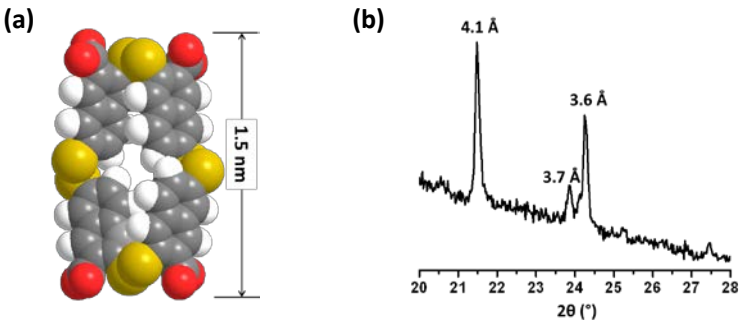

Figure 4.4. (a) Optimized structure (front view) of isomer **4** using the AMBER force field in water. The grey balls stand for carbon, the white balls stand for hydrogen, the red balls stand for oxygen and the yellow balls stand for sulfur. (b) Powder XRD of a dried nanosheet sample made from isomer **4** (0.5 mM) in aqueous solution (pH 8.2).

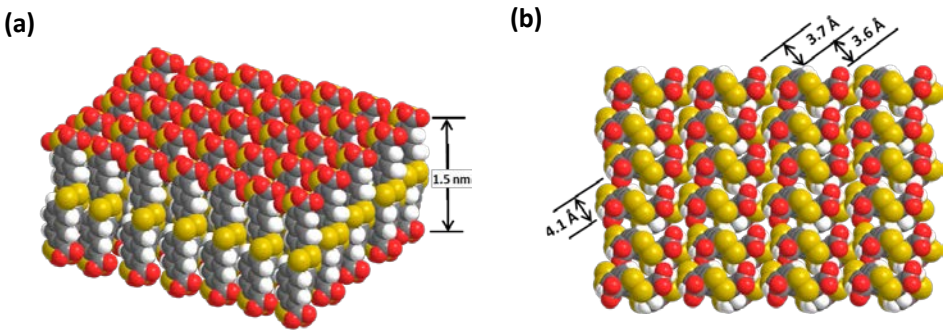

Figure 4.5. (a) Proposed aggregation mode of isomer **4** in aqueous solution (pH 8.2); (b) Top view of (a). The grey balls stand for carbon, the white balls stand for hydrogen, the red balls stand for oxygen and the yellow balls stand for sulfur.

We proceeded to investigate the aggregation mode of the nanosheets. We have already elucidated the structure of isomer **4** in Chapter 3. We determined the lowest-energy conformation using the AMBER force field[6] in water (Figure 4.4a). The distance between the two carboxylic acid groups is 1.5 nm which matches well with the thickness of the nanosheets. Furthermore, considering the hydrophobic naphthalene moiety of isomer **4**, we propose that the nanosheets assemble in a single layer driven by hydrophobic interactions (Figure 4.5). The hydrophobic interactions between the naphthalene moieties most likely give rise to the 4.1 Å and 3.6 Å peaks in the powder XRD (Figure 4.4b). The analysis of

powder XRD also showed a weak peak of a distance of 3.7 Å, which tentatively attribute to a tail-to-head intermolecular π-π interaction.

4.2.3 Self-Replication

The aggregation of a library species in a DCL may drive self-replication. In order to assess whether such behavior was occurring in our system, we decided to investigate the kinetic behavior of a new library prepared from building block **1** (2.0 mM) and template **A** (0.20 mM) in borate buffer (50 mM, pH 8.2). During the process of oxidation of the library, the library distribution was monitored every 43 minutes using HPLC until all the thiolate anions were fully oxidized (Figure 4.6). The kinetic of the growth of isomer **4** is sigmoidal and typical of a replicative process. In contrast, the other three isomers showed no sigmoidal growth.

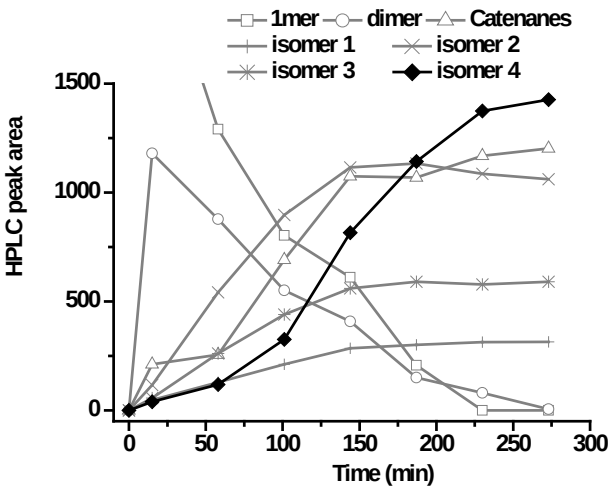

Figure 4.6. Kinetic study of the library made from building block **1** (2.0 mM) and template **A** (0.20 mM) in borate buffer (50 mM, pH 8.2).

This profile suggests that isomer **4** may be capable of promoting its own formation, but it is not a solid proof. A seeding experiment[7] is the most direct way to elucidate whether self-replication takes place. In this experiment, a molecule suspected of being self-replicator is added as a seed into the reaction mixture. If this molecule acts as a catalyst for its own formation, then the rate of formation of this compound will accelerate upon the addition of the seed.

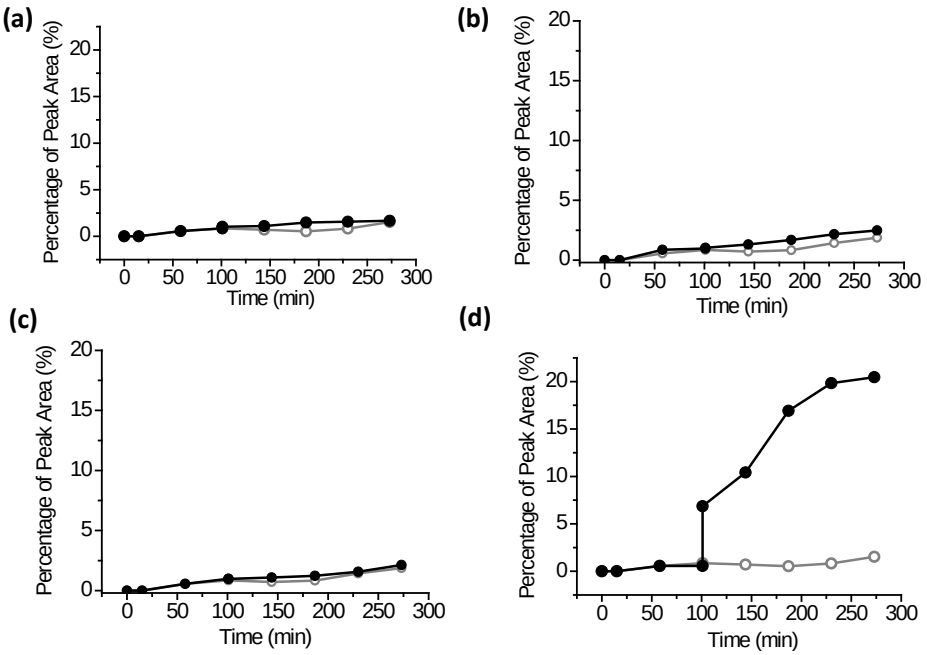

Figure 4.7. Kinetics of formation of (a) isomer **1**, (b) isomer **2**, (c) isomer **3** and (d) isomer **4** in a library (grey curve) made from building block **1** (2.0 mM) in borate buffer (50 mM, pH 8.2) and the same library but seeded (black curve) by 10% (mole) of isomer **4** (with respect to monomer) at t = 100 min.

In our case, purified isomer **4** was chosen as a seed molecule. We first prepared a new library by only dissolving building block **1** (2.0 mM) in borate buffer (50 mM, pH 8.2). The oxidation process was monitored by HPLC every 43 minutes until all the thiolate anions were fully oxidized. The kinetics of the growth of isomer **4** is shown in Figure 4.7. After full oxidation, only 2% of isomer **4** was produced. Afterwards, the same library was prepared, but 100 minutes after the preparation of the library, 10% (mole) of the purified isomer **4** (with respect to monomer) was added into the library, resulting in a concentration of isomer **4** that is above the critical aggregation concentration (0.03 mM). The concentration of all four isomers in the resulting library was monitored by HPLC (Figure 4.7). After full oxidation, compared with the library without seed, the seeded library produced 10 times more isomer **4**, which reveals that isomer **4** can be amplified by itself and that this process is autocatalytic. However, the kinetic profiles of other three isomers did not change significantly after the addition of isomer **4** as a seed.

To have further insight into the role of template **A** in the formation of aggregates of isomer **4**, we seeded the same library as in the previous seeding experiment, but this time with a mixture of 10% (mol) of isomer **4** (with respect to monomer) and **A** (0.10 mM). The library was seeded at the same time as before. The growth profiles are shown in Figure 4.8 and are similar to those obtained in the previous seeding experiment, but now isomer **4** accounted for 26% instead of 21% of the library material. The concentration of the other three isomers also increased somewhat. Their increase probably was caused by the addition of 0.10 mM **A**.

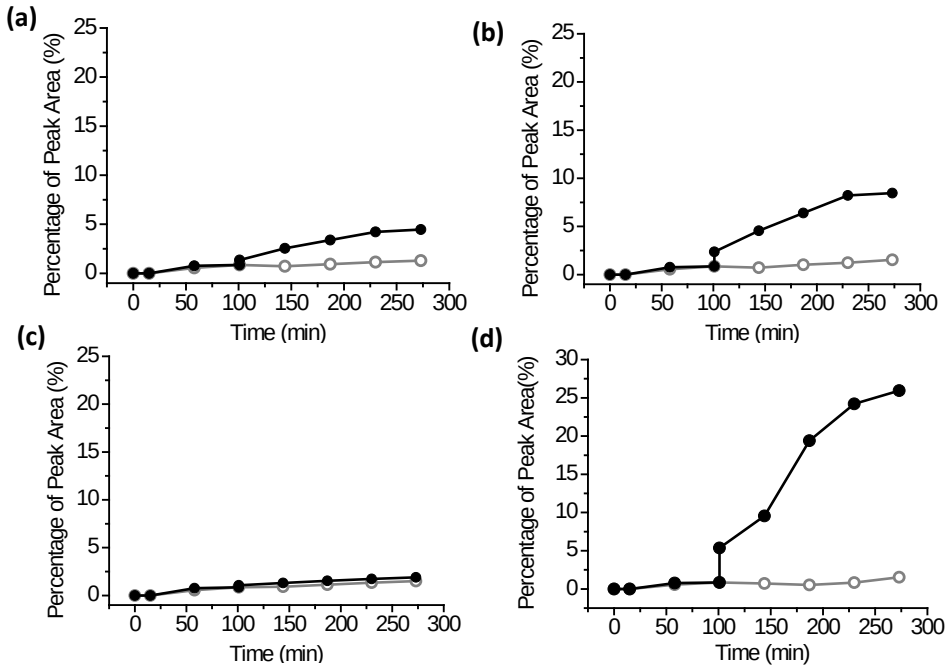

Figure 4.8. Kinetics of formation of (a) isomer **1**, (b) isomer **2**, (c) isomer **3** and (d) isomer **4** in a library (grey curve) made from building block **1** (2.0 mM) in borate buffer (50 mM, pH 8.2) and the same library but seeded (black curve) by a mixture of 10% (mole) of isomer **4** (with respect to monomer) and template **A** (0.10 mM).

Considering that the time at which template **A** was added to the library may have an influence on the self-assembly and growth of isomer **4**, we decided to perform another group of seeding experiments. We started a new library by mixing building block **1** (2.0 mM) and template **A** (0.10 mM) in borate buffer (50 mM, pH 8.2). The concentration of all isomers was again recorded every 43 minutes. The profiles are shown in Figure 4.9. Afterwards, the same library was prepared, but seeded with only 10% (mol) of isomer **4** (with respect to monomer) 100 minutes after the start of the experiment. The growth curve of isomer **4** is

very similar to the previous results (Figure 4.9d). The concentration of the other three isomers was not affected by seeding (Figure 4.9 a-c). These results reveal that, provided the concentration of isomer **4** is above the critical aggregation concentration, template **A** will not significantly affect the self-replication process.

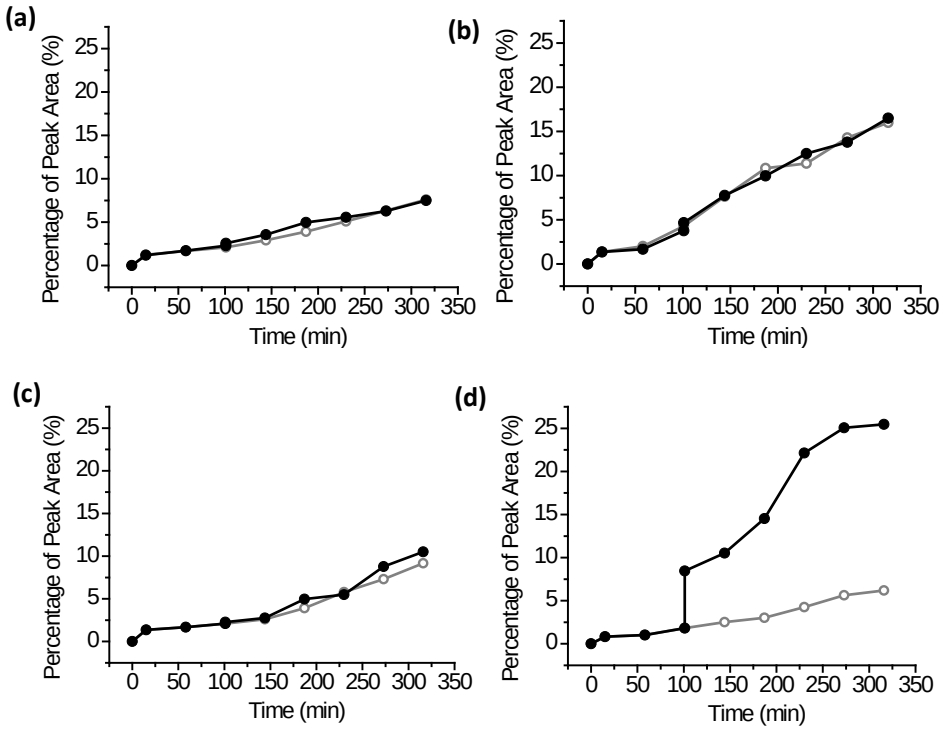

Figure 4.9. Kinetics of formation of (a) isomer **1**, (b) isomer **2**, (c) isomer **3** and (d) isomer **4** in a library (grey curve) made from building block **1** (2.0 mM) and template **A** (0.10 mM) in borate buffer (50 mM, pH 8.2) and the same library but seeded (black curve) by 10% (mole) of isomer **4** (with respect to monomer).

4.3 Conclusion

In conclusion, we have shown that naphthalene derived dithiol building block **1** can be oxidized and produce a series of [2]-catenanes. In the presence of adamantane-derived guest molecule **A**, the [2]-catenanes were converted into four tetramer isomers. When the concentration of one of these tetramers was amplified beyond a critical aggregation concentration, it self-assembled by binding to copies of itself, catalyzing its own formation. While the template is crucial for allowing the self-assembling tetramer to reach the critical

aggregation concentration, once this concentration has been exceeded, the template does not play a significant role in the replication process. This is the first example of the emergence of a self-replicator in a DCL assisted by a template molecule.

4.4 Experimental Section

4.4.1 Materials

All chemicals, unless otherwise stated, were the same as previous chapters. Building block **1** has prepared as reported previously.[5]

4.4.2 General Methods

Analytical HPLC

Analytical HPLC was carried out on Hewlett Packard 1050 or 1100 systems coupled to UV detectors and the data were processed using HP Chemstation software. Separations were performed on a reversed phase Zorbax C8 column (4.6 x 150 mm, 5 μm particle size, Agilent). Except where otherwise stated, the chromatography was carried out at 45 °C using UV detection at 260 nm. The HPLC method is the one used for LC-MS, described below.

LC-MS analysis

An Accela High Speed LC system (ThermoFisher Scientifics, Courtaboeuf, France) was coupled to a LTQ-Fleet Ion-Trap Mass Spectrometer. Water was obtained from a MilliQ Gradient system and LC-MS-grade acetonitrile was bought from BIOSOLVE.

Analysis of samples was performed using a reversed-phase HPLC column (Zorbax C8, 4.6 × 150 mm, 5 μm, Agilent) at 45 °C with an injection volume of 5.0 μL. All UV traces were obtained by monitoring at 260 nm. The following LC method was used for the analysis of libraries:

Solvent A: water (0.1% v/v formic acid); Solvent B: acetonitrile (0.1% v/v formic acid)
Flow rate: 1.0 mL/min

Time (min)	%B
0	20
5	20
30	90
35	90

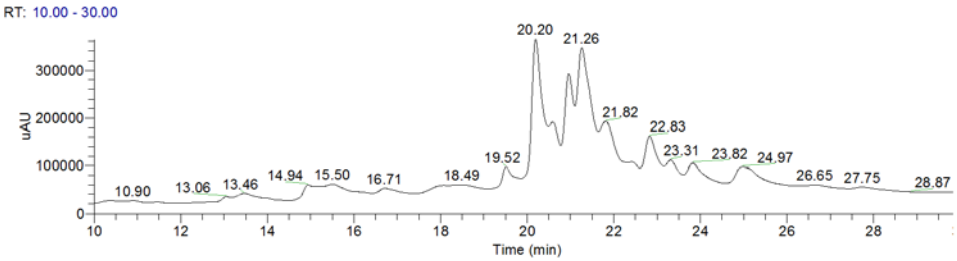

Figure 4.10. UV trace of the HPLC analysis of the library made from building block **1** (2.0 mM) and template **A** (0.05 mM) in borate buffer (50 mM, pH 8.2).

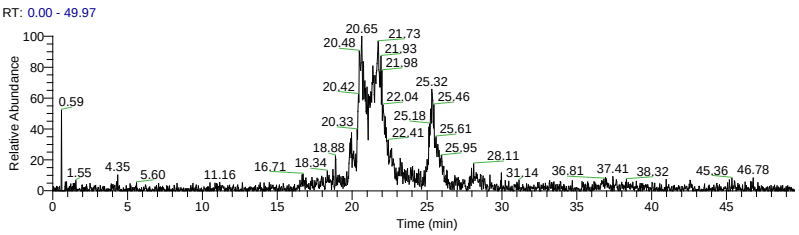

Figure 4.11. Extracted ion chromatogram of mass between 934.5 and 935.5, corresponding to isomeric [2]catenanes **1_4-1_4.**

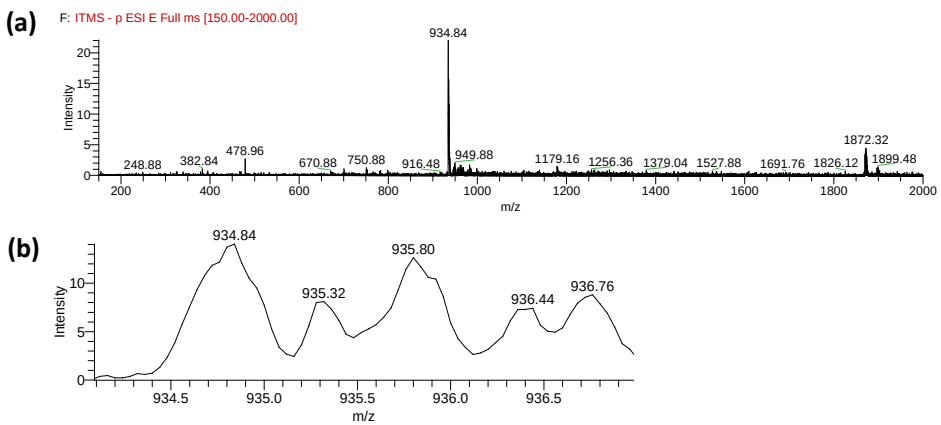

Figure 4.12. (a) ESI-MS spectrum of the HPLC peaks between 19.52 min and 21.26 min. Expected m/z for $[\mathbf{M}\text{-}2\mathrm{H}]^{2-}$= 934.78 corresponding to isomeric [2]catenanes **1_4-1_4**; (b) isotopic profile of the peak observed at 934.84.

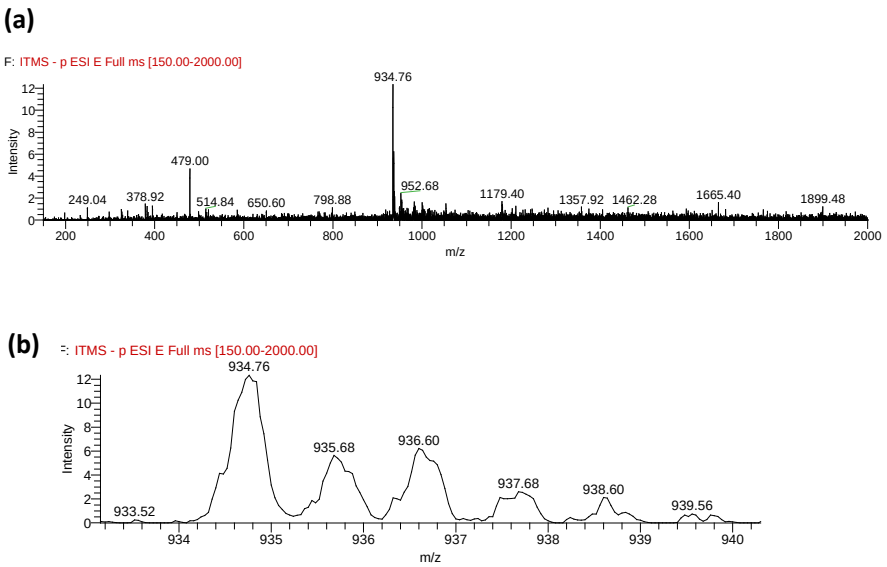

Figure 4.13. (a) ESI-MS spectrum of the HPLC peaks at 21.82 min, 22.83 min, 23.82 min and 24.97 min. Expected m/z for [**M**-H]$^-$= 934.78 corresponding to four tetramer isomers **1**$_4$; (b) isotopic profile of the peak observed at 934.76.

Cryo-TEM analysis

A 10 μL drop of library sample was placed on a Quantifoil 3.5/1 holey carbon coated grid. Blotting and vitrification in ethane was done in a Vitrobot (FEI, Eindhoven, The Netherlands). The grids were observed in a Philips CM120 cryo-electron microscope operating at 120 kV with a Gatan model 626 cryo-stage. Images were recorded under low-dose conditions with a slow-scan CCD camera.

Molecular Modeling

The stable structure of isomer **4** was simulated computationally using the AMBER force field[6] as implemented in MacroModel version 8.0018 (Schrodinger Inc, Porland Oregon) and a continuum water model[8]. MCMM method[9] was used to perform the conformational analysis. The lowest energy conformation of isomer **4** was found in 3000 steps. The most stable structure of isomer **4** was shown in Figure 4.4a and Figure 4.14.

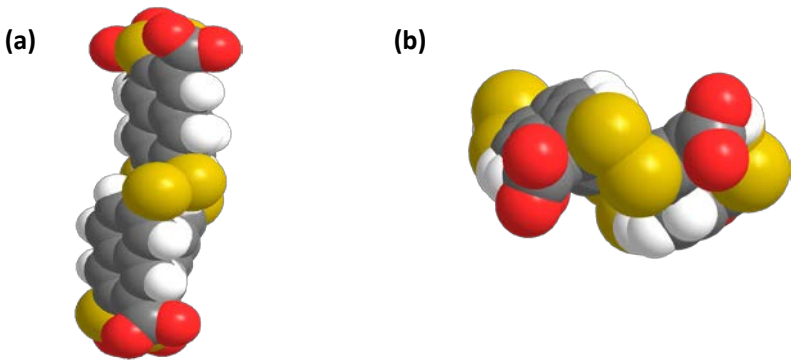

Figure 4.14. Optimized structure of isomer **4** from (a) side view and (b) top view obtained using the AMBER force field in water. The grey balls stand for carbon, white balls stand for hydrogen, red balls stand for oxygen and yellow balls stand for sulfur.

4.5 Acknowledgement

Hugo Fanlo Virgos is acknowledged for providing the naphthalene dithiol building block.

4.6 References

[1] (a) Szostak, J. W. *Nature*, **2009**, *459*, 171-172. (b) Joyce, G. F. *Nature* **2002**, *420*, 278-279. (c) Tjivikua, T.; Ballester, P.; Rebek, J., Jr. *J. Am. Chem. Soc.* **1990**, *112*, 1249-1250.

[2] (a) Li, J.; Nowak, P.; Otto, S. *J. Am. Chem. Soc.* **2013**, *135*, 9222-9239. (b) Hunt, R. A. R.; Otto, S. *Chem. Comm.* **2011**, *47*, 847-858. (c) Otto, S. *Acc. Chem. Res.* **2012**, *45*, 2200-2210. (d) Cougnon, F. B. L.; Sanders, J. K. M. *Acc. Chem. Res.* **2012**, *45*, 2211-2221. (e) Lehn, J.-M. *Top. Curr. Chem.* **2011**, *322*, 1-32. (f) Miller, B. L. *Dynamic Combinatorial Chemistry in Drug Discovery, Bioorganic Chemistry, and Materials Science*, Wiley, Hoboken, NJ, **2010**. (g) Reek, J. N. H.; Otto, S. *Dynamic Combinatorial Chemistry*, Wiley-VCH, Weinheim, **2010**. (h) Lehn, J.-M. *Chem. Soc. Rev.* **2007**, *36*, 151-160. (i) Corbett, P. T.; Leclaire, J.; Vial, L.; West, K. R.; Wietor, J.-L.; Sanders, J. K. M.; Otto, S. *Chem. Rev.* **2006**, *106*, 3652-3711.

[3] Carnall, J. M. A.; Waudby, C. A.; Belenguer, A. M.; Stuart, M. C. A.; Peyralans, J. J.-P.; Otto, S. *Science*, **2010**, *327*, 1502-1506.

[4] (a) Xu, H.; Dill, K. A. *J. Phys. Chem. B* **2005**, *109*, 23611-23617. (b) Southall, N. T.; Dill, K. A.; Haymet, J. *J. Phys. Chem. B* **2002**, *106*, 521-533. (c) Tanford, C. *The Hydrophobic Effect: Formation of Micelles and Biological Membranes*, Krieger, Malabar, FL, **1991**.

[5] West, K. R.; Ludlow, R. F.; Corbett, P. T.; Besenius, P.; Mansfeld, F. M.; Cormack, P. A. G.; Sherrington, D. C.; Goodman, J. M.; Stuart, M. C. A.; Otto, S. *J. Am. Chem. Soc.* **2008**, *130*, 10834–10835.

[6] (a) Weiner, S. J.; Kollman, P. A.; Case, D. A.; Singh, U. C.; Ghio. C.; Alagona, G.; Profeta, S.; Weiner, P. *J. Am. Chem. Soc.* **1984**, *106*, 765-784. (b) Weiner, S. J.; Kollman, P. A.; Nguyen, D. T.; Case, D. A. *J. Comp. Chem.* **1986**, *7*, 230-252

[7] Cairns-Smith, A. G. *Genetic Takeover and the Mineral Origins of Life*, Cambridge, England: Cambridge University Press, **1982**.

[8] Still, W. C.; Tempczyk, A.; Hawley, R. C. *J. Am. Chem. Soc.* **1990**, *112*, 6127-6129.

[9] Chang, G.; Guida, W. C.; Stil, W. C. *J. Am. Chem. Soc.* **1989**, *111*, 4379-4386.

Chapter 5

Spontaneous Emergence from a Dynamic Combinatorial Library of a Self-Replicating Molecule Capable of Forming Compartments

In Chapter 4, we discovered how a macrocycle can catalyze its own synthesis in a DCL. From previous work in our group we have known that self-assembly of a peptide derived disulfide macrocycle in a DCL can drive self-replication. In this chapter, we extend the concept of self-assembly driven self-replication to amphiphilic molecules. A dynamic combinatorial library was prepared from a neutral amphiphilic dithiol building block with a polyethyleneglycol tail. It can be linked together by disulfide bonds forming macrocycles with different sizes. From the kinetic analysis of the library, the tetramer was suspected to be a self-replicator. Mixing this building block with another dithiol building block produced a much more diverse library. Templating this library by the self-replicating tetramer promoted its own formation. This self-replication process was driven by the self-assembly of the tetramer. The self-assemblies were relatively irregular nanosheets some of which spontaneously folded to form compartments.

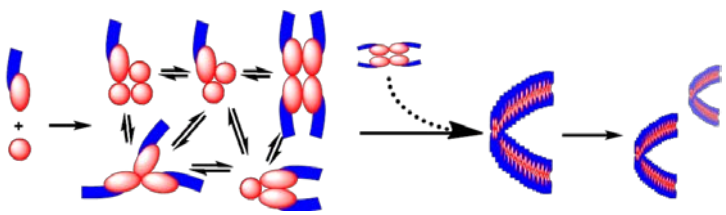

J. Li, W. Smit, G. M. Coll, M. Colomb-Delsuc, S. Otto *manuscript in preparation.*

5.1 Introduction

How life started still remains one of the most challenging questions that contemporary science faces. While defining life is surprisingly difficult, it is generally accepted the life requires the following key ingredients: *compartmentalization*[1], m*etabolism*[2] and *reproduction*[3]. Thus far, research in this area has proceeded along mostly separate lines in which chemical systems that model one or two of these three ingredients took centre stage.[4] However, bringing all these lines of research together in one system will help us have a much better understanding of the origin of life.

A sophisticated way to fabricate such a chemical system is investigating the emergence of compartments (compartmentalization) made from self-replicating molecules (reproduction) from a network of interconverting molecules (a primitive form of metabolism). Such network can be created by the Dynamic Combinatorial Chemistry[5] (DCC) approach. In Chapter 4, we have investigated that if one of the library species can bind to copies of itself, this species will self-assemble and the equilibrium will be shifted, amplifying its concentration. In this way, the self-assembling library members are essentially self-replicating.[6] When the self-assemblies are compartments, compartmentalization will be driven by self-replication in such a network.

Amphiphiles are common building blocks to construct membranes of biological organisms.[7] In an aqueous environment, the membranes are self-assembled by segregation of hydrophobic parts of amphiphiles from water.[8] The self-assembly can be controlled by the relative volume fractions of hydrophilic and hydrophobic parts. This balance is tunable in DCLs consisting of differently sized amphiphilic macrocycles.

Here, we designed and synthesized dithiol building block **1** containing a hydrophobic head and a hydrophilic tetraethylene glycol tail (Scheme 5.1). The hydrophobic heads can be linked together by disulfide bonds forming size tunable hydrophobic cores and the hydrophilic tails stay outside, keeping the macrocyclic molecules water soluble. Among these macrocycles, the tetramer was observed to amplify itself by aggregation into membrane-like sheets. The sheets may fold into compartments in solution. These compartments also emerged from a much more complex library with nine detected species made by mixing two building blocks **1** and **2**.

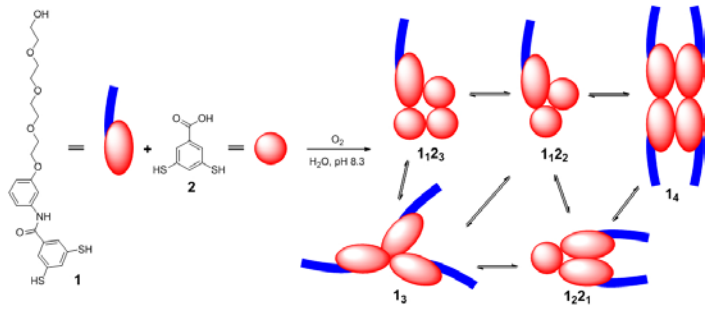

Scheme 5.1. The composition of a DCL made from building block **1** (1.0 mM) and **2** (0.3 mM) in borate buffer (50 mM, pH 8.3).

5.2 Results and Discussion

5.2.1 Building Block Synthesis

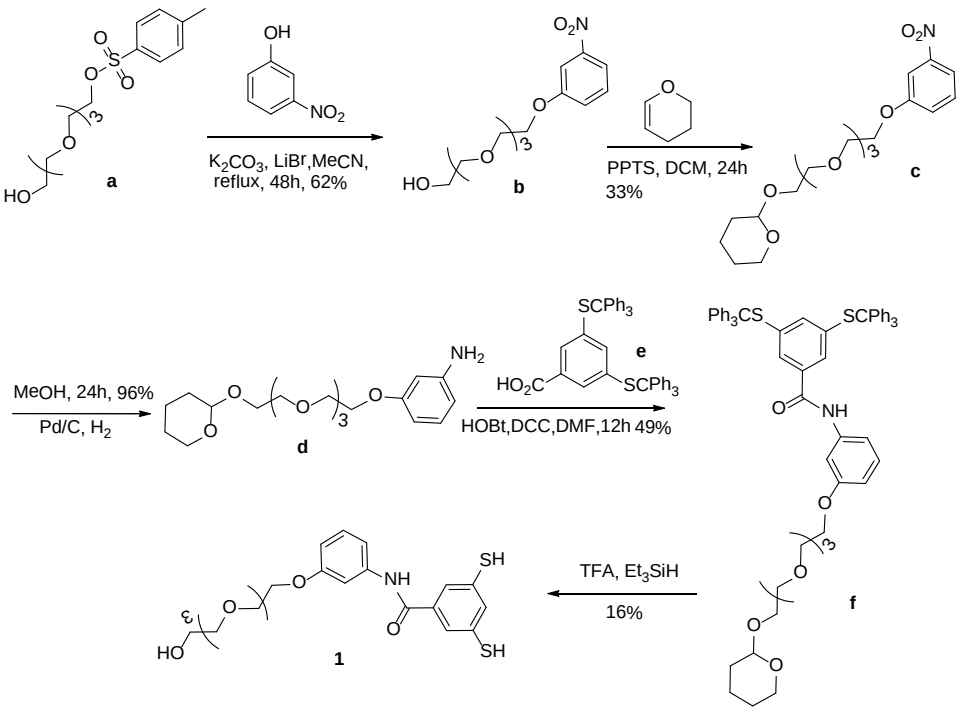

Scheme 5.2. Synthetic route to building block **1**

Building block **1** was produced following the synthetic route shown in Scheme 5.2. The yields of compound **c** and for the final step in the synthesis of building block **1** were quite low. Since starting materials of the reaction to compound **c** were found by TLC analysis to remain after the reaction, we increased the temperature to 40 °C and also increased the reaction time, but these conditions failed to improve the yield. For the reaction to building block **1**, the low yield is due to the instability of thiol compounds. They are oxidized readily in the air. Furthermore, the product has a relatively high polarity and therefore interacts strongly with the silica column, causing loss of material during chromatography.

5.2.2 DCL Preparation and Component Analysis

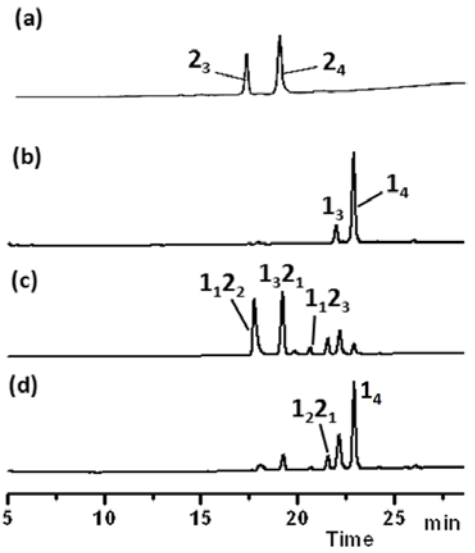

Figure 5.1. HPLC-MS analysis of the fully oxidized libraries made from (a) building block **2** (1.0 mM), (b) building block **1** (1.0 mM) and (c) building blocks **1** (1.0 mM) and **2** (0.3 mM) in a 0.5 mL borate buffer (50 mM, pH 8.3) and (d) the same library as (c) but with 25 (mol) % of $\mathbf{1}_4$ added after 4 days.

We first prepared a DCL only from building block **2** (1.0 mM) in 0.5 mL borate buffer (50 mM, pH 8.3). Building block **2** does not feature a hydrophilic chain, but contains a carboxylic acid group assisting water solublility. The library was left stirring in the presence of oxygen from the air. The thiols were oxidized to form disulfide bonds. Residual thiolate mediates the disulfide exchange reaction that enables equilibrium to be reached. After 2 days,

the library was fully oxidized. The final library composition was analyzed by HPLC-MS, showing comparable amounts of trimer $\mathbf{2_3}$ and tetramer $\mathbf{2_4}$ (Figure 5.1 a).

We then made a similar library from building block **1** (1.0 mM) in 0.5 mL borate buffer (50 mM, pH 8.3) monitoring the oxidation process by HPLC-MS. Unlike building block **2**, after 4 days oxidation, there is still 52% of monomer **1** left (Figure 5.2a). During these 4 days, some tetramer $\mathbf{1_4}$ was produced but only a small amount. However, after this period a sudden change in composition occurred and $\mathbf{1_4}$ became the dominant product, consuming the monomer **1** and dimers $\mathbf{1_2}$. Interestingly, the oxidation of **1** appears to accelerate once the formation of $\mathbf{1_4}$ becomes significant. After 10 days, all the thiols were oxidized and the distribution did not change any further. The library was dominated by $\mathbf{1_4}$ (Figure 5.1b and Figure 5.2a). The kinetic of the growth of $\mathbf{1_4}$ is distinctly sigmoidal, suggesting that this macrocycle may be able to promote its own formation (Figure 5.2a).

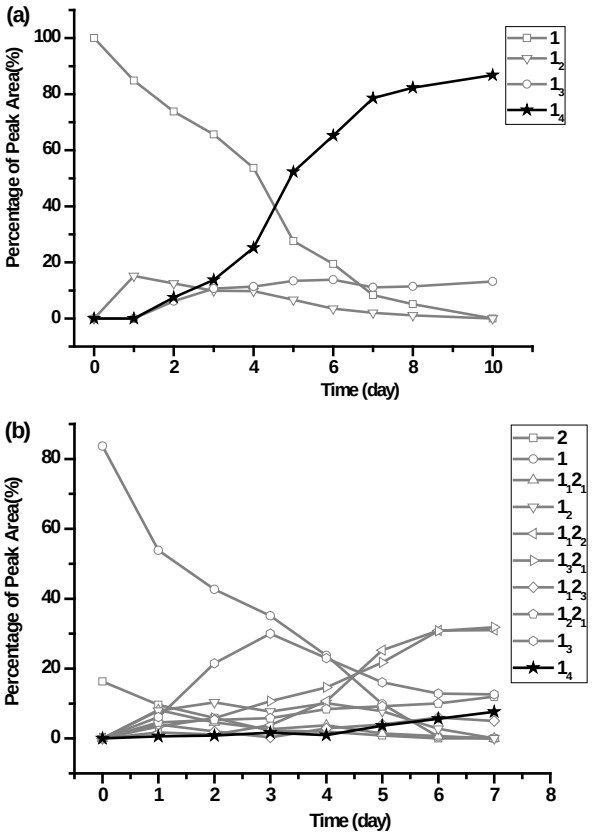

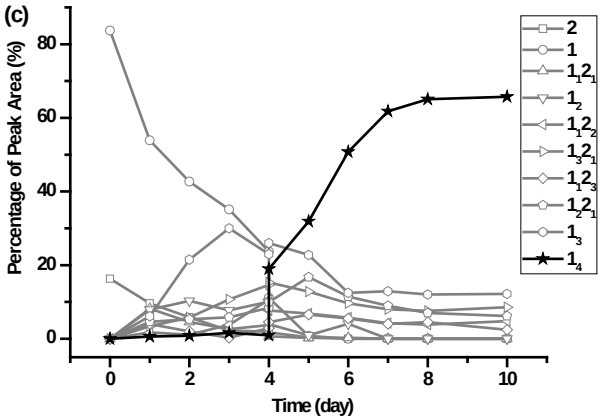

Figure 5.2. Kinetic study of the libraries made from (a) building block **1** (1.0 mM) and (b) building blocks **1** (1.0 mM) and **2** (0.3 mM) in borate buffer (50 mM, pH 8.3) and (c) the same library as (b) to which 25 (mol) % of the tetramer $\mathbf{1_4}$ was added after 4 days.

5.2.3 Self-Replication

We proceeded with investigating whether self-replication took place through a classical seeding experiment (for more details about seeding experiments, see Chapter 4). Upon mixing building block **1** (1.0 mM) and **2** (0.3 mM) together and allowing the mixture to oxidize, we identified ten library species by HPLC-MS (Figure 5.2b and experimental section). After full oxidation, only 7.5% of $\mathbf{1_4}$ was produced (Figure 5.2b). Afterwards, the same library was prepared, but four days after the start of the oxidation process it was seeded with 25% percent of a mixture of two libraries made by separately oxidizing **1** and **2**. The overall concentrations of the building blocks remained the same as that in the library without seeding. After full oxidation, the concentration of macrocycle $\mathbf{1_4}$ was increased to 65% (Figure 5.2c). These results clearly indicate that the tetrameric macrocycle $\mathbf{1_4}$ can be amplified by binding to copies of itself at the expense of other oligomers even in a fairly complex and competitive library and that this process is autocatalytic. To verify the importance of self-association through hydrophobic interactions, we repeated the DCL experiments in the presence of an organic cosolvent. We anticipated that the cosolvent would inhibit self-replication by preventing the aggregation of the hydrophobic phenyl rings. HPLC analysis of the fully oxidized library prepared by building block **1** (1.0 mM) in 90:10 (v/v) isopropanol/H_2O solution (pH 8.3) reveals the formation of comparable amounts of trimer $\mathbf{1_3}$ and tetramer $\mathbf{1_4}$, similar to the product distribution obtained for the DCL made from building

block **2** which cannot produce aggregated species (Figure 5.3). These results suggest that the amplification of $\mathbf{1_4}$ is driven by hydrophobic interactions between the non-polar parts of $\mathbf{1_4}$.

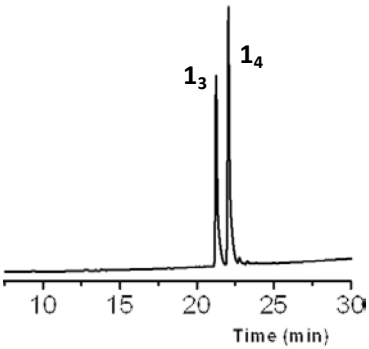

Figure 5.3. HPLC analysis of the fully oxidized library made from building block **1** (1.0 mM) in 90/10 (v/v) isopropanol/H2O solution (pH 8.3).

The aggregates formed by $\mathbf{1_4}$ were examined using fluorescence emission spectroscopy, with Nile Red (Figure 5.4a) as a hydrophobic probe.[9] Nile Red is a lipophilic stain. In water it will not fluoresce, however when in aqueous solution containing lipids, it can show intense fluorescence. It is widely applied to identify different aggregate morphologies formed by amphiphile mixtures. We found a distinctive emission peak at 660 nm in the sample containing $\mathbf{1_4}$ and Nile Red, compared with the control samples containing only $\mathbf{1_4}$ or only Nile Red (Figure 5.4b).

The relative orientation of the aromatic rings of $\mathbf{1_4}$ was studied using UV-vis spectroscopy. When aromatic molecules aggregate, they are often arranged in a regular fashion. There are two common types of aggregates, H-aggregates (face-to-face arrangement) and J-aggregates (end-to-end arrangement) (Figure 5.5). Aggregate formation is accompanied by absorption spectrum changes, blue-shift for H-aggregates and red-shift for J-aggregates. A hypsochromic shift of UV absorbance, from 325 nm to 300 nm, was observed by increasing the concentration of $\mathbf{1_4}$, suggesting that the tetrameric macrocycles arranged themselves in an H-type aggregation[10] (Figure 5.6). The aggregate morphology was investigated by cryo-TEM. As shown in Figure 5.7a, membrane-like nanosheets were found. Their thickness is around 4.6 nm. The CPK model of $\mathbf{1_4}$ reveals that the distance between the two ends of the tetraethylene glycol chains is 4.8 nm. These results suggest that the nanosheets are formed by a single layer of $\mathbf{1_4}$ held together by hydrophobic effect interactions and π-π stacking of the phenyl rings (Figure 5.7b).

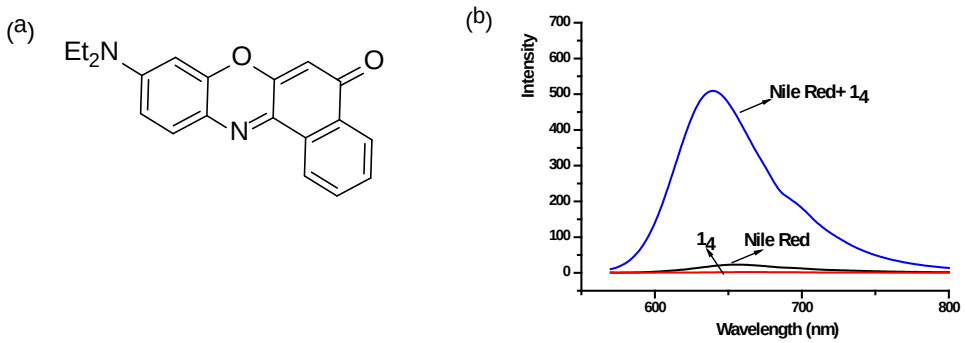

Figure 5.4. (a) Structure of Nile Red. (b) Fluorescent spectra of Nile Red (8.0×10^{-6} M; black line), the library prepared from building block **1** (1.0 mM; red line) and the mixture of Nile Red (8.0×10^{-6} M) and the library prepared from building block **1** (1.0 mM ; blue line) in aqueous borate buffer (50 mM, pH 8.3).

Figure 5.5. Illustration of (a) H-aggregates and (b) J-aggregates.

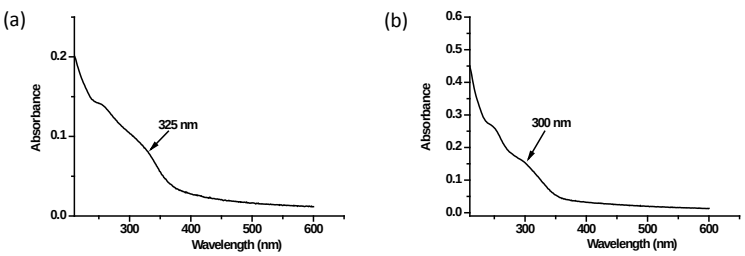

Figure 5.6. Uv-vis spectra of $\mathbf{1_4}$ at a concentration of (a) 8.0×10^{-5} M and (b) 1.6×10^{-4} M in an aqueous borate buffer (50 mM, pH 8.3).

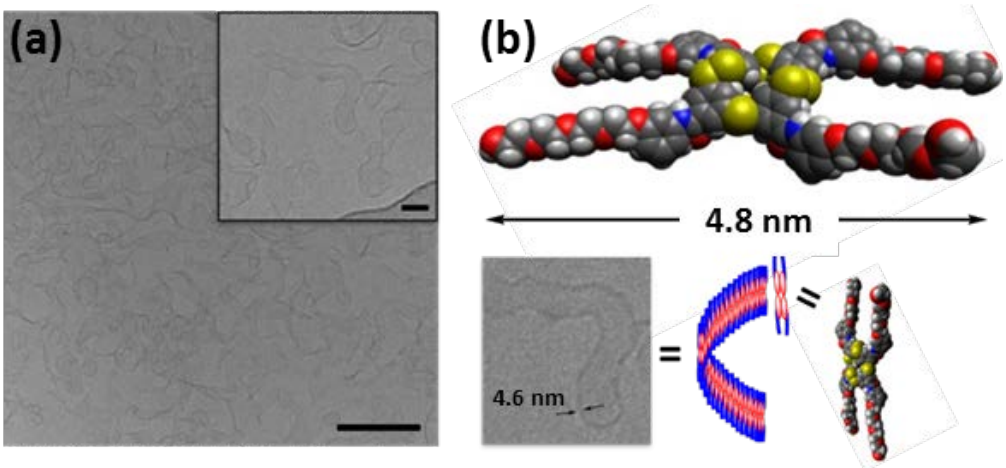

Figure 5.7. (a) Cryo-TEM image of a stirred DCL dominated by tetramer (**1_4**). Scale bar is 200 nm. The inset shows a magnified view with a scale bar of 50 nm; (b) molecular modeling of **1_4** and schematic representation of its proposed aggregation mode.

5.2.4 Membranes Growth Studied using Confocal Microscopy

Cryo-TEM is only suitable to visualize relatively small aggregates. Larger aggregates are unlikely to become trapped in the relatively thin film of water during sample preparation. Given the polydisperse nature of the aggregates we also studied the samples using confocal fluorescence microscopy. We set up a library by dissolving building block **1** in an aqueous solution (1.0 mM, pH 8.3). This sample was stirred during the oxidation process as in the previous experiments. There were no aggregates observed even after two days of oxidation (Figure 5.8). However, an exponential increase in fluorescence intensity (Figure 5.8f) was observed during the subsequent days, which corresponds well with the increase in the concentration of **1_4** monitored by HPLC. These results confirm that self-replication is accompanied by self-assembly. The aggregates of **1_4** (Figure 5.8b and 5.8c) were too small to characterize fully with confocal. Their shape is irregular, which agrees with observations by cryo-TEM. To check the stability of the aggregates, we stopped the stirring and analyzed the sample after one month. Much larger curved and more rigid membranes were observed (Figure 5.8e).

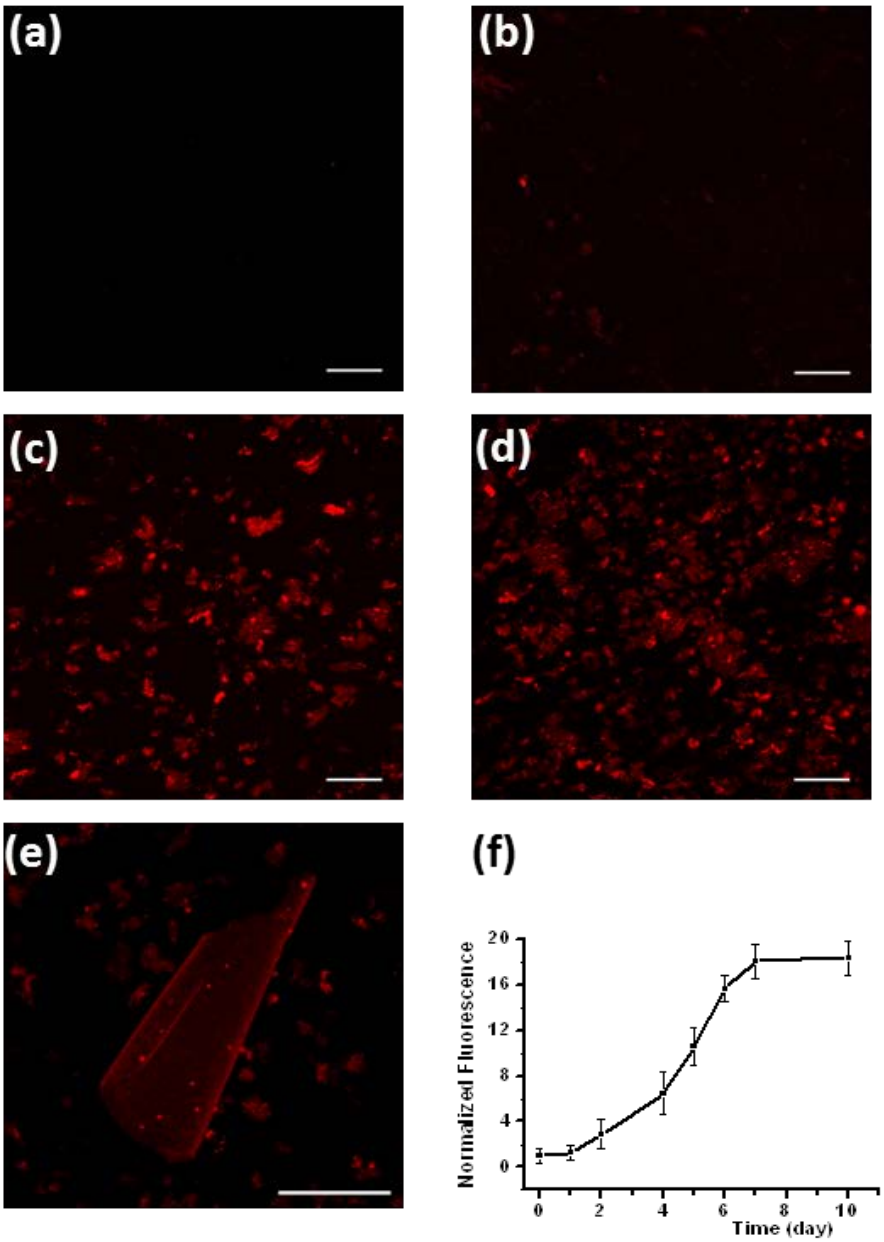

Figure 5.8. The library made from building block **1** monitored by confocal fluorescence microscopy after (a) 0, (b) 2, (c) 4, (d) 5 and (e) 30 day; (f) Normalized fluorescence intensity changes with time. All the scale bars correspond to 30 μm. Nile red (2.0×10^{-4} M) was added to the samples immediately prior to imaging.

5.2.4 Attempts to Prepare Vesicles

Cryo-TEM and confocal microscopy both showed formation of membrane-like sheets in the libraries. However, the shapes of these sheets are irregular. We attempted to prepare more regular aggregates. One way to achieve this is using the method of repetitive freeze-thaw cycles. We first prepared a library from building block **1** (1.0 mM) in a water solution (1.0 mL, pH 8.3). After 10 days oxidation, the dominant species is $\mathbf{1_4}$ as in previous libraries. We then removed the water by lyophilizing the sample. Once we obtained a dry sample, it was dissolved in 1.0 mL chloroform. The chloroform was slowly evaporated to obtain a lipid film under a flow of nitrogen in a test tube. The lipid film was left overnight in a desiccator under vacuum. Afterwards we hydrated the lipid film by the addition of 1.0 mL water to the test tube and vortexing the mixture for 5.0 minutes and followed by 5.0 minutes incubation. We then froze the mixture in liquid nitrogen and thawed it in a warm water bath. This freeze-thaw cycle was repeated ten times. We subsequently investigated the sample by cryo-TEM and found a similar morphology of the aggregates as for the previous sample (Figure 5.9), suggesting that this amphiphile shows only a limited tendency to form vesicles.

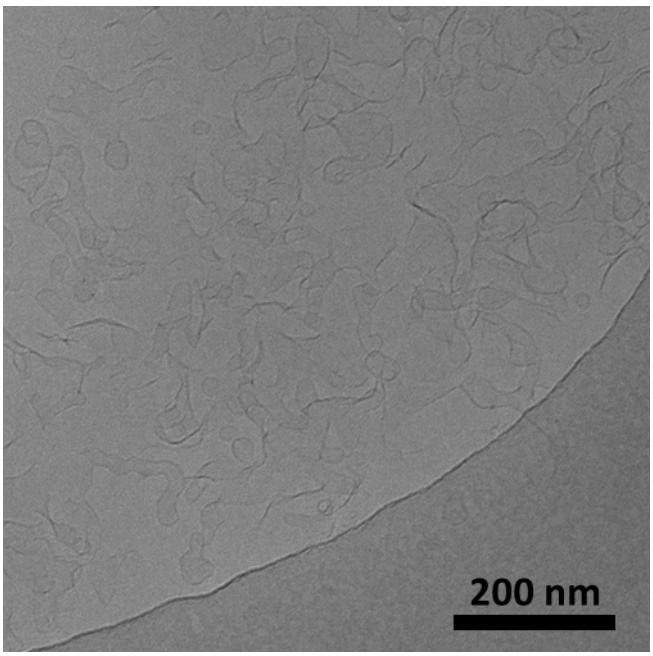

Figure 5.9. Cryo-TEM image of a tetramer ($\mathbf{1_4}$) sample after repetitive Freeze-Thaw cycles.

5.2.6 Influence of Mechanic Agitation on the Library Behavior

In Chapter 1, we have already discussed one example[6b] in which mechanic agitation was vital to the emergence of a self-replicator from a DCL. In this example, macrocycles stack on each other forming fibers. When the fibers grow long enough, they are broken by mechanic agitation, duplicating the number of catalytically active fiber ends. Besides this, the size of the macrocycles depended on the agitation method. Thus, it is of interest to investigate how mechanic agitation affects the behavior of the library studied in this chapter.

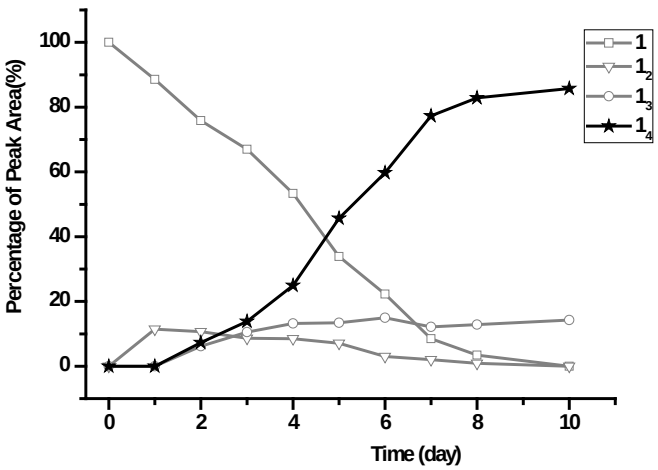

Figure 5.10 Kinetic study of a non-agitated library made from building block **1** (1.0 mM) in a 0.50 mL borate buffer (50 mM, pH 8.3).

We prepared another library from building block **1** (1.0 mM) in a 0.5 mL borate buffer (50 mM, pH 8.3). Unlike stirring the library as before, this sample was placed on the bench without any mechanic agitation. We then monitored the oxidation process by HPLC (Figure 5.10) and found similar behavior as observed for the stirred library. The monomer was oxidized at a comparable rate and the concentration of $\mathbf{1_4}$ also increased in a sigmoidal profile. These results show that the self-replication occurs even if the sample is not agitated. In the case of fiber-based self-replication systems, the fiber ends are probably active catalytic centres and their number remains the same even if the length of the fibers increased. However, in our sheet-based system, the edges of the sheets most likely promote the formation of $\mathbf{1_4}$. When the membrane-like sheets grow larger, the edge of the sheet also becomes larger, which makes self-replication possible even in the absence of agitation.

5.3 Conclusion

In conclusion, we have discovered the spontaneous emergence of self-replicating molecules from a complex mixture of continuously interconverting compounds driven by their self-assembly into membranes. While these membranes adopt irregular shapes, some fold and give rise to the formation of compartments. Our group previously reported[6b] self-replicators stacked on each other forming fibers where self-replication was critically dependent on mechanic agitation. Here we show the first example of compartments being formed from a self-replicator with self-replication taking place without mechanic agitation. This discovery may contribute to understanding of the origin of life, and opens up new possibilities creating life de-novo.

5.4 Experimental Section

5.4.1 Materials

All chemicals, unless otherwise stated, were the same as previous chapters. NMR spectra of building block **1** and synthetic intermediates were recorded using a Varian Mercury Plus (400 MHz) spectrometer. The synthesis of building block **1** is described in Scheme 5.2.

The compounds **a**[11], building block **2**[12] and **e**[6a] were prepared following literature procedures.

Synthesis of 2-(2-(2-(2-(3-nitrophenoxy)ethoxy)ethoxy)ethoxy)ethanol (b):

3-Nitrophenol (1.20 g, 8.61 mmol), K_2CO_3 (2.37 g, 17.22 mmol), **a** (3.00 g, 8.61 mmol), LiBr (9.00 mg, 0.10 mmol) and MeCN (70.0 mL) were added to a 250 mL three necked flask. The system was flushed with nitrogen and the mixture was refluxed for 2 days. The reaction mixture was filtered while hot and the solid residue was washed with MeCN. The filtrate was concentrated in vacuo. The residue was dissolved in 100 mL ethyl acetate and washed 3 times with 100 mL of a saturated K_2CO_3 solution in H_2O. Removing the solvent by reduced pressure yields **b** as a viscous dark orange oil (1.68 g, 5.33 mmol, 62%). ^{1}H NMR (400 MHz, CDCl3) δ 7.82 (d, J = 8.1, 1H), 7.75 (s, 1H), 7.41 (t, J = 10.2, 6.2, 1H), 7.25 (d, J = 1.9, 1H), 4.21 (t, J = 10.6, 2H), 3.93 – 3.84 (t, J=4.0, 2H), 3.77 – 3.64 (m, 10H), 3.63 – 3.57 (t, J=4.0, 2H). ^{13}C NMR (50 MHz, CDCl3) δ 129.89, 121.80, 115.91, 108.94, 72.48, 70.86, 70.64, 70.55, 70.29, 69.46, 68.11, 61.71. ESI-MS: calcd for $C_{14}H_{21}NO_7$: $[M^+$+H] 315.1318, Found: 315.1319.

Synthesis of 2-(2-(2-(2-(2-(3-nitrophenoxy)ethoxy)ethoxy)ethoxy)ethoxy)tetra hydro-2H-pyran (c):

Compound **b** (2.60 g, 8.20 mmol), 3,4-dihydro-2H-pyran (0.90 g, 10.7 mmol) and pyridinium p-toluenesulfonate (PPTS) (6.00 mg, 0.02 mmol) were added to DCM (25 mL) in a 50 mL round bottomed flask. The mixture was stirred under nitrogen overnight. Sodium bicarbonate (100 mg) and magnesium sulphate (1.00 g) were added and the mixture was stirred for 15 minutes. The mixture was filtered over a short pad of Celite/ silica gel (1 cm/ 4 cm) and was eluted with DCM. The solvent was removed under reduced pressure and purification by column chromatography yielded **c** as a yellow oil (1.08 g, 2.70 mmol, 33%). ^{1}H NMR (400 MHz, $CDCl_3$) δ 7.82 (d, J = 8.1, 1H), 7.75 (s, 1H), 7.41 (t, J = 10.2, 6.2, 1H), 7.25 (d, J = 1.9, 1H), 4.59 (t, J=2.8, 1H), 4.21 (t, J = 10.6, 2H), 3.93 – 3.84 (t, J=4.0, 2H), 3.77 – 3.64 (m, 12H), 3.63 – 3.57 (t, J=4.0, 2H). 1.84-1.62 (m, 2H), 1.60-1.42 (m, 4H). ^{13}C NMR (50 MHz, $CDCl_3$) δ 130.05, 121.97, 116.08, 109.15, 70.92, 70.90, 70.65, 70.62, 70.58, 70.55, 62.31, 30.70, 25.57, 19.59. ESI-MS: calcd for $C_{19}H_{29}NO_8$: [M^++H] 399.1893, Found: 399.1891.

Synthesis of 4-(2-(2-(2-(3-((tetrahydro-2H-pyran-2-yl) oxy) ethoxy) ethoxy) ethoxy) ethoxy) aniline (d):

Compound **c** (1.08 g, 2.70 mmol), Pd-C (60 mg) and MeOH (25 mL) were mixed. The mixture was stirred under an atmosphere of H_2 (hydrogen balloon) for 24 hours. The mixture was filtered over Celite and was washed with MeOH. Evaporation of the solvent yielded **d** as a viscous red oil (0.96 g, 2.6 mmol, 96%). ^{1}H NMR (400 MHz, $CDCl_3$) δ 7.04 (t, *J* = 7.9 Hz, 1H), 6.35 – 6.24 (m, 3H), 4.63 (t, J=4 Hz, 1H), 4.09 (t, J = 10.6, 1H), 3.85 (m, 3H), 3.77 – 3.64 (m, 12H), 3.63 – 3.57 (t, J=4.0, 2H). 1.84-1.62 (m, 2H), 1.60-1.42 (m, 4H). ^{13}C NMR (50 MHz, $CDCl_3$) δ 130.02, 108.05, 104.63, 101.85, 98.94, 70.80, 70.64, 70.61, 70.51, 30.55, 25.42, 19.47. ESI-MS: calcd for $C_{19}H_{31}NO_6$: [M^++H] 369.2151, Found: 369.2154.

Synthesis of N-(3-(2-(2-(2-(2-((tetrahydro-2H-pyran-2-yl)oxy)ethoxy)ethoxy) ethoxy)ethoxy) phenyl)-3,5-bis(tritylthio)benzamide (f):

3,5-Bis(tritylthio)benzoic acid (**e**) (0.50 g, 0.75 mmol) was dissolved in DMF (10.0 mL) was added to a 25 mL round bottomed flask. HOBt (0.107 g, 0.80 mmol) and DCC (0.165 g, 0.80 mmol) were added and the mixture was stirred for 15 minutes. Compound **d** (0.30 g, 0.80 mmol）in DMF (1.0 mL) was added to the mixture and it was stirred at room temperature for

12 hours. The precipitate was filtered off and the solvent was removed under reduced pressure. Purification by column chromatography (hexane: EtOAc= 5:1 → 3:1) yielded **f** as a viscous oil (0.38 g, 0.37 mmol, 49%). ^{1}H NMR (400 MHz, $CDCl_3$) δ 7.39 – 7.26 (m, 13H), 7.25 – 7.14 (m, 18H), 6.92 – 6.86 (m, 3H), 6.80 (s, 1H), 6.70 (dd, *J* = 8.1, 2.2 Hz, 1H), 6.34 – 6.28 (m, 1H), 4.63 (t, J=4 Hz, 1H), 4.09 (t, J = 10.6, 1H), 3.85 (m, 3H), 3.77 – 3.64 (m, 12H), 3.63 – 3.57 (m, 2H). 1.84 – 1.62 (m, 2H), 1.60 – 1.42 (m, 4H). ^{13}C NMR (50 MHz, $CDCl_3$) δ 144.04, 135.24, 132.30, 129.89, 127.80, 126.83, 71.42, 70.62, 70.27, 69.82, 67.64, 66.92, 34.10, 30.63, 25.78, 19.99. ESI-MS: calcd for $C_{64}H_{63}NO_7S_2$: [M^++H] 1021.4045, Found: 1021.4051.

Synthesis of N-(3-(2-(2-(2-(2-hydroxyethoxy)ethoxy)ethoxy)ethoxy)phenyl) -3,5-dimercaptobenzamide (1)

N-(3-(2-(2-(2-(2-((tetrahydro-2H-pyran-2-yl)oxy)ethoxy)ethoxy)ethoxy)ethoxy)phenyl)-3,5-bis(tritylthio)benzamide (**f**) (0.40 g, 0.40 mmol) was dissolved in trifluoroacetic acid (TFA) (3.20 mL, 39.2 mmol). The solution was stirred gently for 15 minutes. Triethyl silane (0.33 mL, 2.14 mmol) was added over a period of 15 minutes and the mixture was stirred for 15 minutes. The formed precipitate was filtered off, the TFA was removed with N_2 flow and other volatiles were removed under reduced pressure. The product was purified by automated silica column chromatography: (EtOAc with 0.1 % TFA and a gradient of MeOH 0 → 10%). The product was obtained as a yellow oil (30 mg, 0.066 mmol, 16%).^{1}H NMR (400 MHz, $CDCl_3$) δ 8.15 (s, 1H), 7.55 (s, 2H), 7.51 (s, 1H), 7.32 (s, 1H), 7.28 (s, 1H), 6.71 (d, *J* = 7.1, 2H), 3.86 (m, 2H), 3.70 (m, 12H), 3.58 (s, 2H). ^{13}C NMR (50 MHz, $CDCl_3$) δ 158.93, 139.01, 136.53, 133.27, 131.66, 129.84, 124.97, 113.34, 110.76, 107.49, 72.41, 69.62, 67.49, 61.57, 31.94, 29.71, 29.38, 14.14. ESI-MS: calcd for $C_{21}H_{27}NO_6S_2$: [M^++H] 454.1380, Found: 454.1358.

Dynamic combinatorial libraries

Dynamic combinatorial libraries were prepared by dissolving building block **1** and/or **2** and, in borate buffer (50 mM, pH 8.3) at the appropriate concentration. The final pH of the solution was adjusted to 8.3 by addition of 1.0 M KOH solution. Aliquots of 0.5 mL of the library solutions were places in capped HPLC vials in a dark environment for 10 days in the presence of oxygen from the air to allow oxidation of the thiols into disulfides.

5.4.2 General Methods

Analytical HPLC

Analytical HPLC was carried out on Hewlett Packard 1050 or 1100 systems coupled to UV detectors and the data were processed using HP Chemstation software. Separations were performed on a reversed phase Zorbax C8 column (4.6 x 150 mm, 5 µm particle size, Agilent). Except where otherwise stated, the chromatography was carried out at 45 °C using UV detection at 254 nm. The following LC analysis method was used: Solvent A: Water (0.1% v/v formic acid); Solvent B: Acetonitrile (0.1% v/v formic acid). Flow rate: 1.0 mL/min

Time (min)	B%
0	41
7	41
37	77

LC-MS analysis

An Accela High Speed LC system (ThermoFisher Scientifics, Courtaboeuf, France) was coupled to a LTQ-Fleet Ion Trap Mass Spectrometer. Water was obtained from a MilliQ Gradient system and LC-MS-grade acetonitrile was bought from BIOSOLVE.

Analysis of samples was performed using a reversed-phase HPLC column (Zorbax C8, 4.6 x 150 mm, 5 µm, Agilent) at 45 °C with an injection volume of 5 µL. All UV traces were obtained by monitoring at 254 nm. The LC method for LC-MS analysis method is the same as the HPLC method described above.

Mass spectra of all the library members were recorded in positive ion mode. The electrospray voltage was set to 4.3 kV, and the capillary voltage was set to 5.2 V; the sheath and auxiliary gas flows (both nitrogen) were 4 L/min and 2 L/min, respectively, and the drying gas temperature was 325 °C .

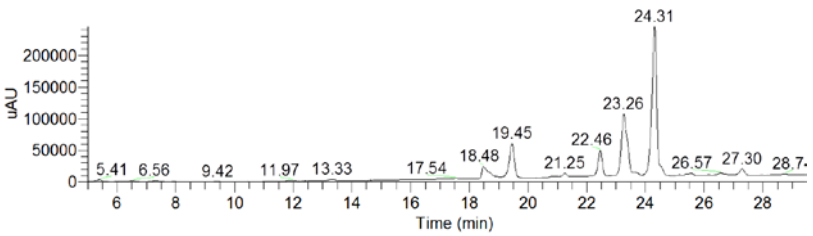

Figure 5.11 HPLC analysis of the fully oxidized library made from building blocks **1** (1.0 mM) and **2** (0.3 mM) in a 0.5 mL borate buffer (50 mM, pH 8.3) added 25 (mol) % of $\mathbf{1}_4$ after 4 days.

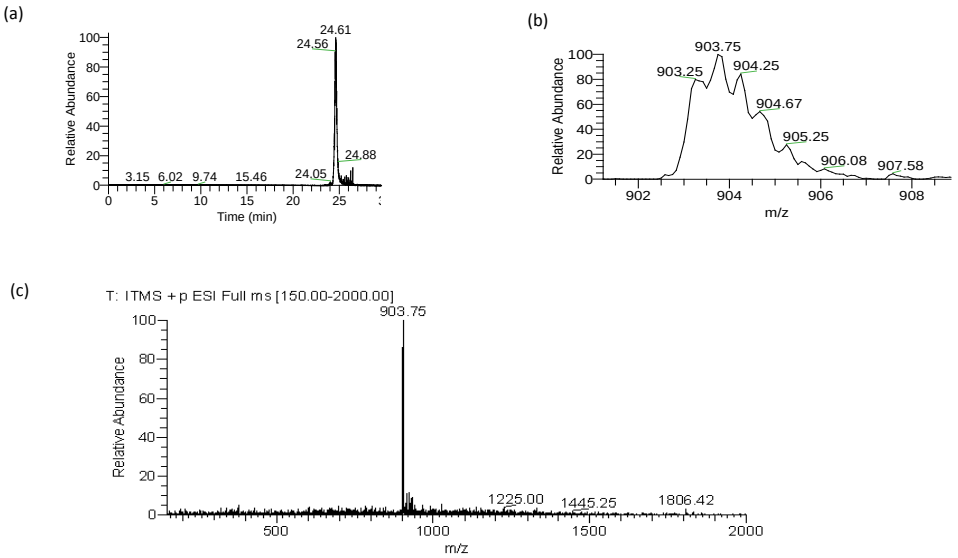

Figure 5.12 Asignment of $\mathbf{1_4}$ (a) Extracted ion chromatogram of mass between 903.50 and 904.50; (b) isotopic profile of the peak observed at 903.75; (c) ESI-MS spectrum of the HPLC peak at 24.31 min. Expected m/z for $[\mathbf{1_4}+2H]^{2+}$=903.69.

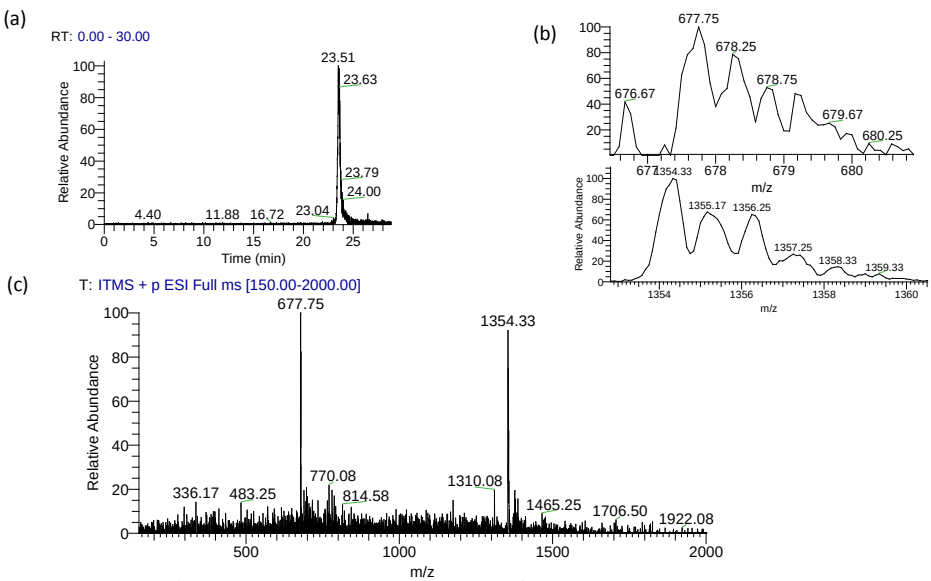

Figure 5.13 Asignment of $\mathbf{1_3}$ (a) Extracted ion chromatogram of mass between 677.50 and 678.00; (b) isotopic profile of the peak observed at at 677.75 and 1354.22; (c) ESI-MS spectrum of the HPLC peak at 23.26 min. Expected m/z for $[\mathbf{1_3}+H]^{1+}$=1354.12, $[\mathbf{1_3}+2H]^{2+}$=677.56.

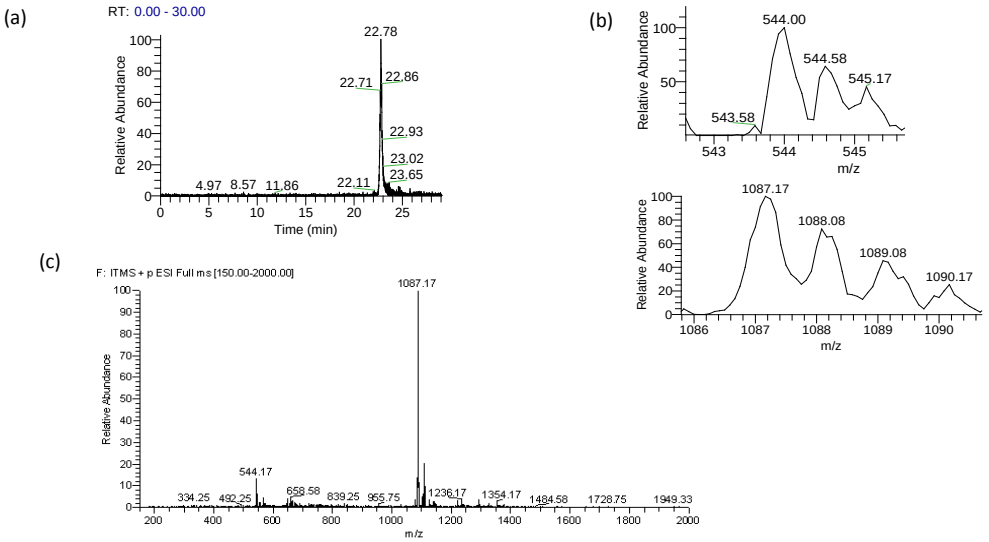

Figure 5.14 Asignment of $\mathbf{1_12_1}$ (a) Extracted ion chromatogram of mass between 543.50 and 544.50; (b) isotopic profile of the mass at 544.00 and 1087.17; (c) ESI-MS spectrum of the HPLC peak at 22.46 min. Expected m/z for $[\mathbf{1_22_1}+H]^{1+}$=1087.34, $[\mathbf{1_22_1}+2H]^{2+}$=544.17. The mass is corresponding to $\mathbf{1_22_1}$.

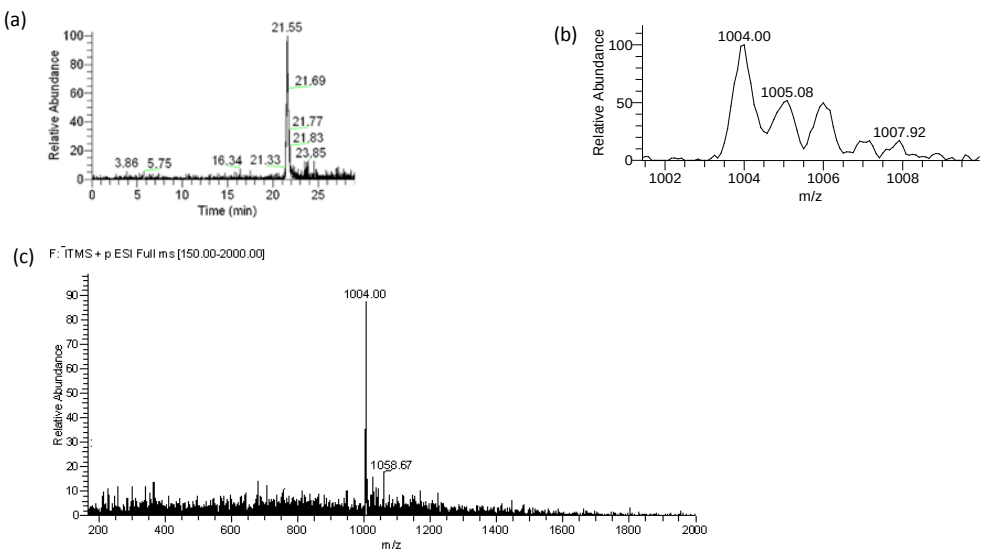

Figure 5.15 Asignment of $\mathbf{1_12_3}$ (a) Extracted ion chromatogram of mass between 1003.50 and 1004.50; (b) isotopic profile of the mass at 1004.00; (c) ESI-MS spectrum of the HPLC peak at 22.46 min. Expected m/z for $[\mathbf{1_12_3}+H]^{1+}$=1004.18.

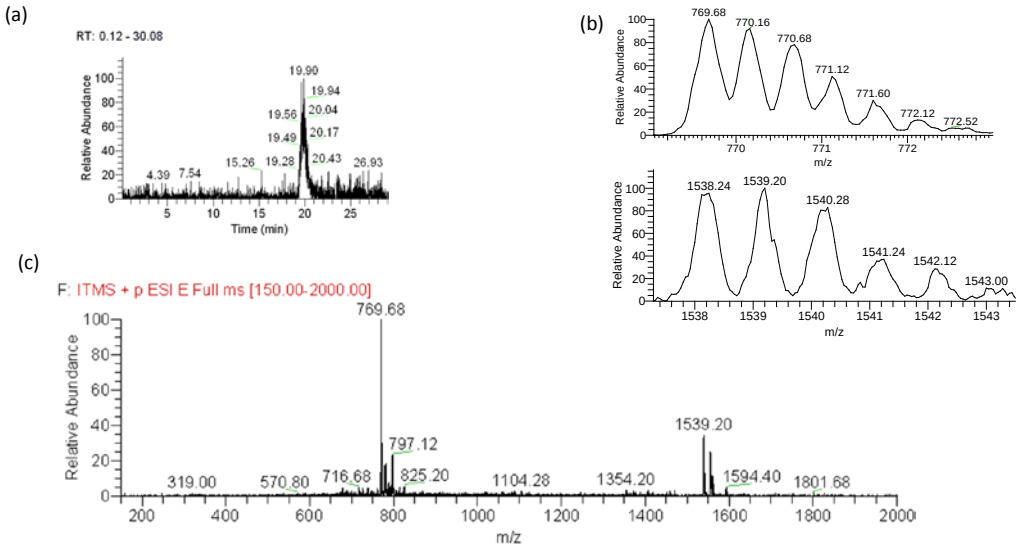

Figure 5.16 Asignment of $\mathbf{1_3 2_1}$ (a) Extracted ion chromatogram of mass between 769.00 and 770.00; (b) isotopic profile of the mass at 769.68 and 1539.20; (c) ESI-MS spectrum of the HPLC peak at 19.45 min. Expected m/z for $[\mathbf{1_1 2_3}+H]^{1+}$=1539.17 and $[\mathbf{1_3 2_1}+2H]^{2+}$=769.59. The mass is corresponding to $\mathbf{1_3 2_1}$.

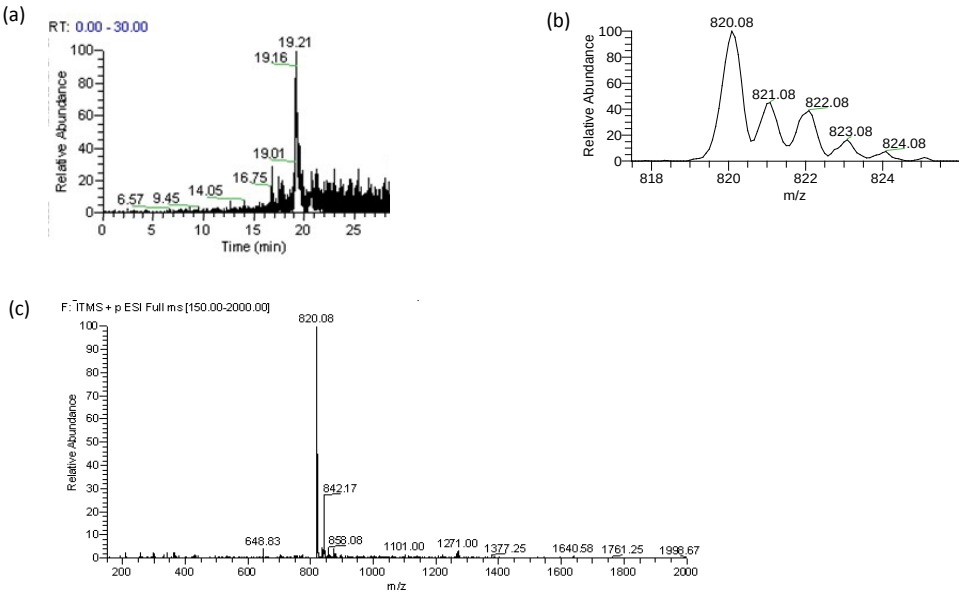

Figure 5.17 Asignment of $\mathbf{1_1 2_2}$ (a) Extracted ion chromatogram of mass between 819.50 and 820.50; (b) isotopic profile of the mass at 820.08; (c) ESI-MS spectrum of the HPLC peak at 18.48 min. Expected m/z for $[\mathbf{1_1 2_2}+H]^{1+}$=820.00.

Cryo-TEM analysis

A 10 μL drop of library sample was placed on a Quantifoil 3.5/1 holey carbon coated grid. Blotting and vitrification in ethane was done in a Vitrobot (FEI, Eindhoven, The Netherlands). The grids were observed in a Philips CM120 cryo-electron microscope operating at 120 kV with a Gatan model 626 cryo-stage. Images were recorded under low-dose conditions with a slow-scan CCD camera.

Fluorescent analysis

Fluorescence measurements were performed using a JASCO FP-6200 spectrophotometer. The fluorescence was measured by excitation at 550 nm (5 nm slit width) and recording the emission between 570 and 800 nm (5 nm slit width, 5 repeats averaged).

UV-vis analysis

UV-vis measurements were performed using a Varian Cary Bio UV-visible spectrophotometer. A quartz cuvette with 1 cm path length was used for measurements. The absorption spectra were recorded from 200 nm to 650 nm.

Fluorescence Microscopy

Sample preparation: Samples (**1_4**) made from building block **1** (1.00 mM) were labeled with Nile Red at a final concentration of 2.0×10^{-4} M prior to imaging.

Image acquisition: Imaging was performed on a commercial laser-scanning confocal microscope, LSM 710 (Carl Zeiss MicroImaging, Jena, Germany), using an objective C-Apochromat 40×/1.2NA, a solid state laser (488 nm) for excitation and ZEN2010B software. The pixel dwell times for laser-scanning ranged from 0.74 to 2.55 μs with a pixel step from 0.415 to 0.658 μm. Acquisition was performed with constant laser power at 20°C.

Movie acquisition: movies were rendered by rotating the 3D projection 360° along the x-axis at 4 frames per second. It was uploaded here: http://www.youtube.com/watch?v=pro-bYNbMvM

5.5 Acknowledgments

Wietse Smit is most gratefully acknowledged for synthesizing the dithiol building block as part of his bachelor research project. We thank Gemma M. Coll for performing the confocal microscopy and Mathieu Colomb-Delsuc for the measurement of cryo-TEM.

5.6 References

[1] Szostak, J. W.; Bartel, D. P.; Luisi, P. L. *Nature* **2001,** *409*, 387-390.

[2] Kauffman, S. A. *The origins of order;* Oxford University Press: Oxford, **1993**.

[3] Patzke, V.; von Kiedrowski, G. *Arkivoc* **2007,** *v*, 293-310.

[4] (a) Vidonne, A.; Philp, D. *Eur. J. Org. Chem.* **2009,** 593-610; (b) Huber, C.; Eisenreich, W.; Hecht, S.; Wachtershauser, G. *Science* **2003,** *301*, 938-940; (c) Walde, P.; Wick, R.; Fresta, M.; Mangone, A.; Luisi, P. L. *J. Am. Chem. Soc.* **1994,** *116*, 11649-11654.

[5] (a) Otto, S. *Acc. Chem. Res.* **2012**, *45*, 2200-2210; (b) Cougnon, F. B. L.; Sanders, J. K. M. *Acc. Chem. Res.* **2012**, *45*, 2211-2221; (c) Miller, B. L. *Dynamic Combinatorial Chemistry in Drug Discovery, Bioorganic Chemistry, and Materials Science*, Wiley, Hoboken, NJ, **2010**; (d) Reek, J. N. H.; Otto, S. *Dynamic Combinatorial Chemistry*, Wiley-VCH, Weinheim, **2010**. (e) Lehn, J.-M. *Chem. Soc. Rev.* **2007**, *36*, 151-160; (f) Corbett, P. T.; Leclaire, J.; Vial, L.; West, K. R.; Wietor, J.–L.; Sanders, J. K. M.; Otto, S. *Chem. Rev.* **2006**, *106*, 3652-3711.

[6] (a) Moulin, E.; Giuseppone, N. *Top. Curr. Chem.* **2012**, *322*, 87-105; (b) Carnall, J. M. A.; Waudby, C. A.; Belenguer, A. M.; Stuart, M. C. A.; Peyralans, J. J.-P.; Otto, S. *Science* **2010**, *327*, 1502-1506.

[7] Lang, B. *Curr. Opin. Colloid Interface Sci.* **2002**, *7*, 12-30.

[8] Zhang X.; Wang C. *Chem. Soc. Rev.* **2011**, *40*, 94-101.

[9] (a) Minkenberg, C. B.; Florusse, L.; Eelkema, R.; Koper, G. J. M.; Esch, J. H. V. *J. Am. Chem. Soc.* **2009**, *131*, 11274-11275; (b) Stuart, M. C. A.; van de Pas, J. C.; Engberts, J. B. F. N. *J. Phys. Org. Chem.* **2005**, *18*, 929-934.

[10] (a) Wang, J.; Kulago, A.; Browne, W. R.; Feringa, B. L. *J. Am. Chem. Soc.* **2010**, *132*, 4191-4196; (b) Cardolaccia, T.; Li, Y.; Schanze, K. S. *J. Am. Chem. Soc.* **2008**, *130*, 2535-2545; (c) Yao, S.; Beginn, U.; Gress, T.; Lysetska, M.; Wurthner, F. *J. Am. Chem. Soc.* **2004**, *126*, 8336-8348.

[11] Krishnamurty, R.; Brock, A. M.; Maly, D. J. *Bioorg. Med. Chem. Lett.* **2011**. *21*, 550-554.

[12] Corbett, P. T.; Sanders, J. K. M.; Otto, S. *Chem. Eur. J.* **2008**, *14*, 2153-2166.

Chapter 6

An "Ingredients" Approach to Functional Self-Synthesizing Materials: a Metal-Ion Selective Multi-Responsive Self-Assembled Hydrogel

In Chapter 4 and Chapter 5 we have seen that self-assembly provides the driving force for self-replication in DCLs. The outcome of the self-assembly process is a self-assembling material. Thus, DCC provides us a promising approach to the development of new materials. In this Chapter, by designing a building block to contain the right ingredients, a multi-responsive self-assembling hydrogel was obtained through a process of template-induced self-synthesis in a dynamic combinatorial library. The system can be switched between gel and solution by light, redox reactions, pH, temperature, mechanical energy and sequestration or addition of Mg(II) salt.

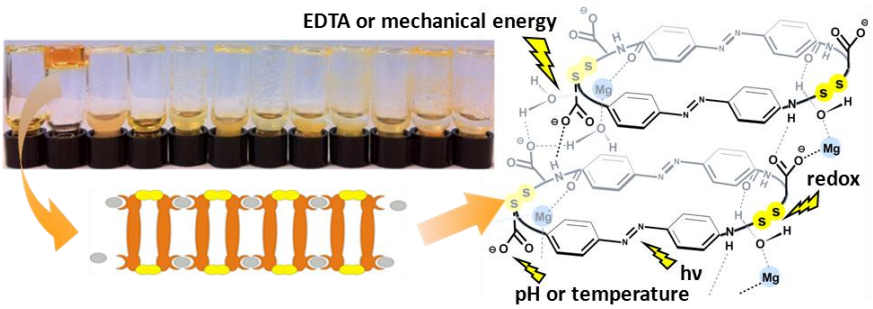

J. Li, I. Cvrtila, M. Colomb-Delsuc, E. Otten, S. Otto, *manuscript in preparation*

6.1 Introduction

Recent developments in dynamic combinatorial chemistry[1] have led to the new concept of self-synthesizing materials,[2] where a self-assembly process drives the synthesis of the very molecules that self-assemble. This intruiging concept exploits the reversibility of bond formation in dynamic combinatorial libraries (DCLs), which are mixtures of molecules capable of exchanging building blocks such that the composition tends to be governed by thermodynamics. Molecular recognition events will bias the product distribution of DCLs towards those library members that yield the largest overall binding energy for the system. Originaly, templates were used to bias the product distribution towards the formation of ligands for biomolecules[3] or synthetic receptors.[4] More recently it has been shown that, when no templates are added, self-selection in a dynamic combinatorial library, where library members bind to copies of themselves, may lead to the formation of materials that are not only self-assembling, but thereby also self-synthesising.[2a-2d] We now report the first example where an externally added template drives self-assembly. While the template does not participate in dynamic covalent bond formation, it alters the library distribution in a small DCL based on a new photoswitchable building block. We also demonstrate the potential of an "ingredients" approach to functional materials, where it is sufficient to provide the ingredients for specific properties in the form of building blocks, and allow the material to build itself from these. The result is a self-assembling and self-synthesizing hydrogel. Hydrogels are playing an increasingly important role in a diverse range of applications, such as drug delivery, sensing, tissue engineering and wound healing.[5] Desirable properties include stimuli-responsiveness and self-healing ability. While conventional gel chemistry is dominated by polymers, more recently interest in gelators has extended to small organic molecules[6] and their metal-ion complexes.[7] We now describe the dynamic combinatorial development of a highly metal-ion selective self-assembled hydrogel that is uniquely multi-responisve: it may be switched between gel and solution states by light, mechanical energy, redox chemistry, temperature changes, pH changes and metal ion chelation and is self-healing.

Since our understanding of self-assembly processes in water is still incomplete, the reliable design of self-assembled hydrogelators remains a challenge. In the dynamic combinatorial approach to such materials it is not necessary to design every step of the assembly process or even to design the self-assembling molecule. It is sufficient to only

provide the system with the right building blocks. The self-assembly process itself then instructs the system to synthesize the appropriate molecules from these building blocks. We decided to use this "ingredients" approach to develop a hydrogel that is responsive to light, redox chemistry, metal-ion chelation and ideally also mechanical energy. The necessary ingredients for achieving this many functions had to be contained in the design of the building blocks.

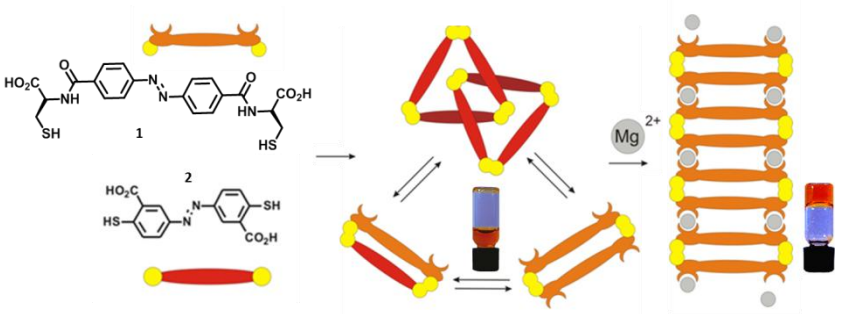

Scheme 6.1. DCLs of building block 1 and 2 with or without MgCl2.

We envisaged that light-responsiveness could be achieved by incorporating an azobenzene photoswitch.[8] Redox responsiveness may be realized by the use of disulfide bonds, that function as reversible covalent linkages at the same time.[9] Metal-ion affinity may be provided by incorporating carboxylate and carbonyl groups.[7a,7b] Metal-ligand coordination may also be sensitive to pH. Finally, mechanical and temperature sensitivity may realized by ensuring that the hydrogel self-assembles from small molecular constituents through relatively weak interactions. Potential ingredients for driving the self-assembly process are already contained in the design elements described above and include hydrophobic and π-π interactions between the azobenzene units[10] and metal ions that may potentially bridge between carboxylate groups. These considerations led us to design and synthesize building blocks **1** and **2** (Scheme 6.1, for synthesis, see Experimental Section).

6.2 Results and Discussion

6.2.1 DCL Preparation and Component Analysis

A small DCL was prepared by dissolving building blocks **1** (5.0 mM) and **2** (2.0 mM) in aqueous borate buffer (50 mM, pH 8.1). The DCL was placed in a capped vial in a dark environment for 7 days in the presence of oxygen from the air to allow oxidation of the thiols

into disulfides. Residual thiolate mediates the disulfide exchange reaction that enables equilibration of the DCL.[9] The resulting free-flowing solution was analysed by HPLC-MS (Figure 6.1a), which revealed that the main species in the library were dimer $\mathbf{1}_2$, hybrid dimer $\mathbf{1}_1\mathbf{2}_1$, tetramer $\mathbf{1}_2\mathbf{2}_2$ and a [2]catenane $\mathbf{2}_3\mathbf{2}_3$ built from two mechanically interlocked trimers of building block **2**.[11]

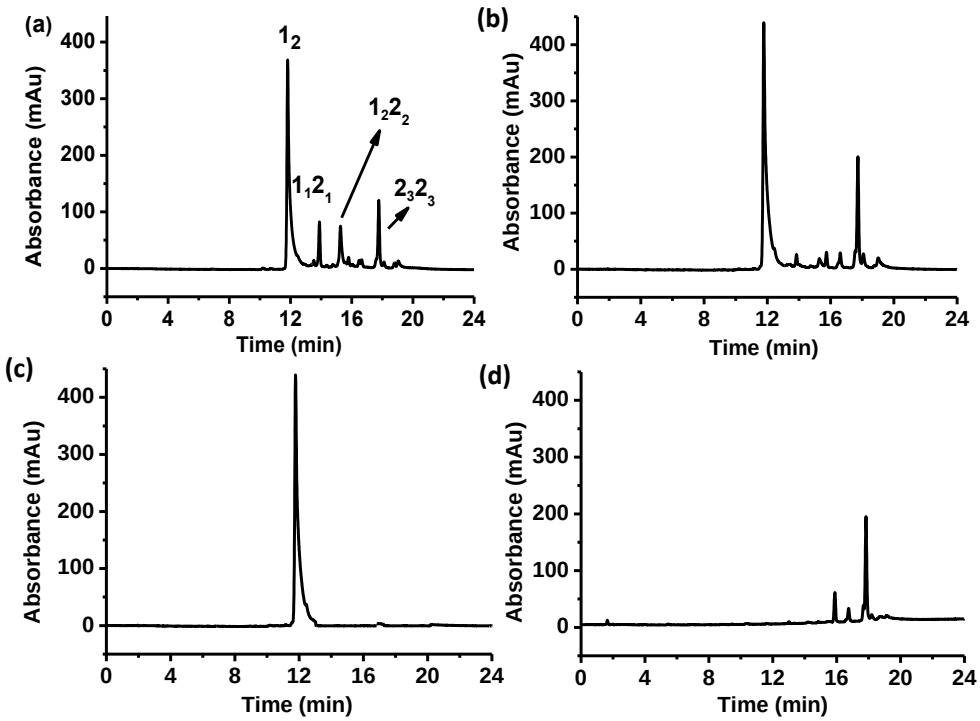

Figure 6.1. HPLC-MS analysis of a DCL made from building block **1** (5.0 mM) and **2** (2.0 mM) (a) with; (b) without MgCl2 (20 mM); DCL made from only (c) building block **1** (5.0 mM); and (d) building block **2** (2.0 mM) with MgCl2 (20 mM) in an aqueous borate buffer (50 mM, pH 8.1).

We then investigated the response of the DCL to the introduction of metal-ions. Most of the metal salts we introduced ($CaCl_2$; $SrCl_2$; $BaCl_2$; $AlCl_3$; $ZnCl_2$; $CdCl_2$; $HgCl_2$; $CuCl_2$; $NiCl_2$; $FeCl_2$) failed to induce gelation, with one notable exception: a transparent hydrogel was obtained in the presence of $MgCl_2$ (Figure 6.2). Analysis by HPLC-MS shows that in the presence of this template the concentrations of $\mathbf{1}_2$ and $\mathbf{2}_3\mathbf{2}_3$ increased at the expense of $\mathbf{1}_1\mathbf{2}_1$ and $\mathbf{1}_2\mathbf{2}_2$ (Figure 6.1b). The disappearance of the mixed dimer and tetramer indicates that $MgCl_2$ induces the sorting of the DCL.

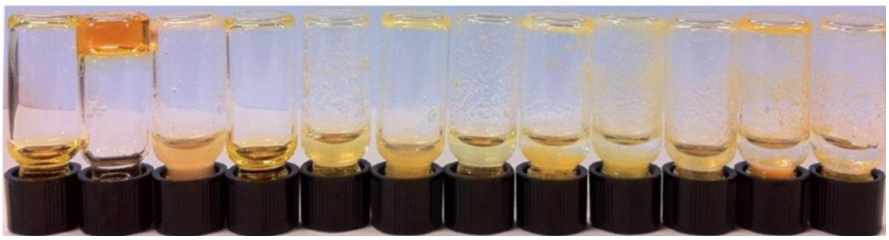

Figure 6.2. Appearance of DCLs made from (a) only building block **1** (5.0 mM) in borate buffer (50 mM, pH 8.1) and with 20 mM metal salts; (b) MgCl2; (c) CaCl2; (d) SrCl2; (e) BaCl2; (f) AlCl3; (g) ZnCl2; (h) CdCl2; (i) HgCl2; (j) CuCl2; (k) NiCl2; (l) FeCl2.

In order to clarify which component was responsible for gelation, two DCLs were made by dissolving building block **1** (5.0 mM) or **2** (2.0 mM) with $MgCl_2$ (20 mM) in borate buffer (50 mM, pH 8.1). Only the DCL prepared from **1** turned into a hydrogel, whereas the one made from **2** and $MgCl_2$ remained a free-flowing solution. HPLC-MS analysis (Figure 6.1c) of the hydrogel only showed one peak whose mass corresponds to $\mathbf{1}_2$, suggesting that gelation is the consequence of the formation of coordinative bonds between $\mathbf{1}_2$ and Mg^{2+}. Further evidence for this mode of assembly was obtained by adding a well-known strong chelator, ethylene diamine tetraacetic acid (EDTA; 5.0 mM), to the hydrogel, which resulted in the immediate conversion of the gel into a non-viscous solution. When another portion of $MgCl_2$ (20 mM) was added, the solution reverted back to the hydrogel after 2 days.

6.2.2 Gelation by Self-Assembly of 1_2 and Mg(II)

In order to provide more detailed structural insights we attempted to obtain crystals of the $\mathbf{1}_2$-Mg^{2+} assembly that were suitable for X-ray diffraction studies. While all attempts using Mg^{2+} as a template failed, similar experiments with Ca^{2+} were successful. The Ca^{2+} complex crystallizes in space group $P2_1$ as $(\mathbf{1}_2)Ca_2(H_2O)_{15}$, $Z = 2$. In its crystal structure two distinct organizational motifs can be recognized. Firstly, linear stacks of azobenzene moieties are formed (Figure 6.3a). The stacks show a spacing between the aromatic rings that alternates between 3.3 Å for the azobenzene units within a macrocycle and 3.6 Å for the corresponding distance between two adjacent macrocycles. Secondly, the crystal structure reveals a chain comprising calcium ions coordinated by the amide carbonyl oxygen and the carboxylate oxygens of macrocycle $\mathbf{1}_2$ (Figure 6.3b and Figure 6.3c). Water molecules are involved as bridging ligands, mediating the interactions between every second amide carbonyl or

carboxylate group and the calcium ion. Similar bridging water molecules are also frequently encountered in protein-ligand binding.[12] In addition neighbouring molecules of $\mathbf{1}_2$ are also interacting directly by hydrogen bonding between amide NH and carboxylate groups.

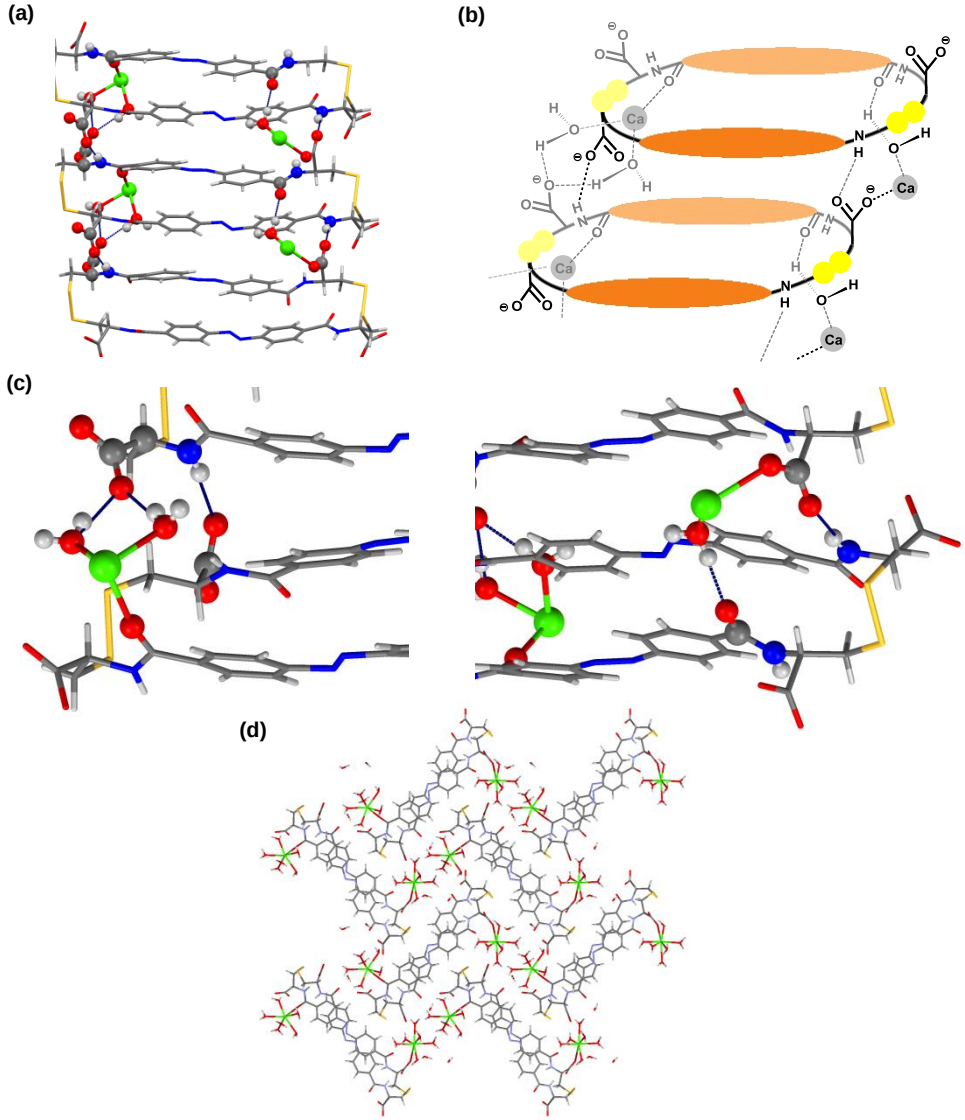

Figure 6.3. X-ray crystal structure of $(\mathbf{1}_2)Ca_2(H_2O)_{15}$ (a) Stacking of the azobenzene moieties and (b) and (c) interactions between neighbouring $\mathbf{1}_2$ moieties are mediated by calcium ions and water; (d) Packing of the $\mathbf{1}_2$ moieties (blue-gray) and the hydrated calcium cations (green and red) (view along the a axis).

The fact that we could obtain crystals for the Ca-**1**$_2$ complex, but not for the Mg^{2+} complex may hold a clue as to why gelation occurs only with Mg^{2+}, but not with the closely similar Mg^{2+}. The Ca-**1**$_2$ complex appears to be capable of assembling into fibre like structures similar to those formed by the Mg-**1**$_2$ complex (vide infra). However, for Ca^{2+} the assembly process does not stop at the fibre stage, and the fibres assemble laterally into the three-dimensional arrangement shown in Figure 6.3d. In this assembly the Ca^{2+} ion is coordinated by seven ligands. Mg(II) has more rigid coordination preferences than Ca(II) and is usually six-coordinate,[13] and we speculate that this difference is at the heart of the difference in gelation behaviour between the two complexes.

Closer inspection of the packing in Figure 6.3d suggests that the water molecules play a crucial role in the lateral association of the stacks of **1**$_2$ by bridging adjacent Ca^{2+} ions. We reasoned that if we could replace some of these water ligands by charged ligands we may be able to introduce electrostatic repulsion between the stacks and prevent their lateral association which should promote gelation. Indeed, oxidizing building block **1** (5.0 mM) in the presence of 500 mM of glycine and 20 mM $CaCl_2$ led to a turbid hydrogel. However, the stability of this gel was inferior to that made with $MgCl_2$ in the absence of glycine and after standing for 3 days we obtained a free-flowing suspension. Given the metastable nature of the calcium gel we did not further characterize this material but focussed our efforts on the magnesium hydrogel and assessed to what extent its structure resembles that of the stacks of **1**$_2$ observed in the crystal structure of the calcium complex of **1**$_2$.

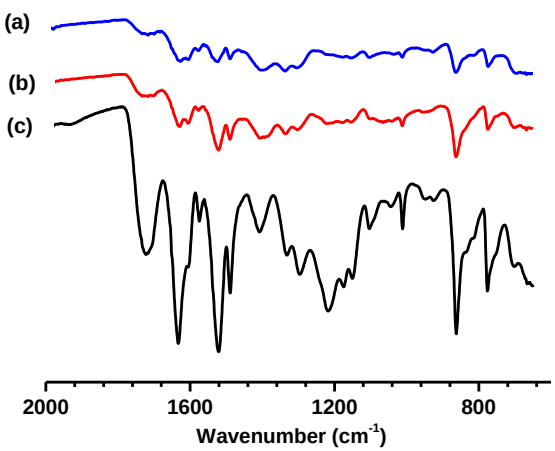

Figure 6.4. IR spectra of (a) Ca-**1**$_2$ complex, (b) the hydrogel made from **1**$_2$ and Mg^{2+} and (c) **1**$_2$.

Infrared spectra (see Figure 6.4) were recorded for $\mathbf{1}_2$, the Ca-$\mathbf{1}_2$ complex and the hydrogel made from $\mathbf{1}_2$ and Mg^{2+}.[14] In the IR spectrum of $\mathbf{1}_2$, the C=O and C-O stretching vibrations of the carboxylate groups are observed at 1721 cm^{-1} and 1218 cm^{-1} respectively. In the spectrum of the Ca-$\mathbf{1}_2$ complex these bands are shifted and have a much reduced intensity. The spectrum of the Mg-$\mathbf{1}_2$ xerogel is very similar to that of the Ca-$\mathbf{1}_2$ complex, suggesting similar assembly modes in the Ca^{2+} and Mg^{2+} complexes of $\mathbf{1}_2$.

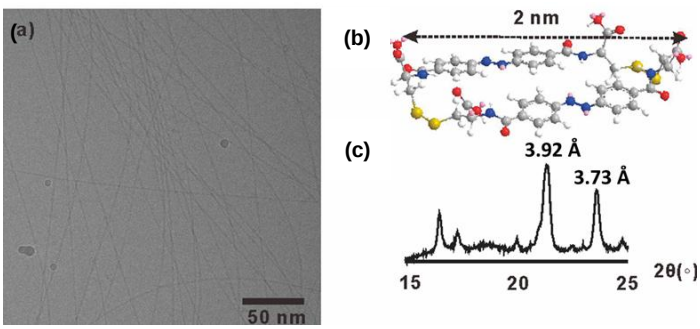

Figure 6.5. (a) Cryo-TEM micrograph of the hydrogel; (b) molecular modelling of $\mathbf{1_2}$ by Chem 3D; (c) Powder XRD of the dry sample of hydrogel made from $\mathbf{1_2}$ (2.5 mM) and $MgCl_2$ (20 mM).

The magnesium hydrogel was studied using cryo-TEM (Figure 6.5a), which revealed the presence of thin fibres with a diameter of approximately 2 nm, which matches the diameter of the calculated minimum energy conformation of macrocycle $\mathbf{1}_2$ in the gas phase and the diameter of the $\mathbf{1_2}$ in the Ca^{2+} complex. The analysis of powder XRD data of the xerogel (Figure 5c) revealed the typical distance of 3.73 Å and 3.92 Å which may be attributed to two different kinds of π-π stacking arrangements, reminiscent of those in the crystal structural of Ca-$\mathbf{1}_2$ complex (Figure 3a). Taken together, these observations suggest an assembly mode for the Mg^{2+} gel that is similar to the stacks of $\mathbf{1_2}$ that are encountered in the crystal structure of the Ca^{2+}-$\mathbf{1_2}$ complex, as depicted in Figure 6.3a and 6.3b.

6.2.3 Responsiveness and Self-healing of the Hydrogel

We investigated the responsiveness of the hydrogel to different stimuli. We have already discussed the responsiveness to Mg(II) chelation above. Since the $\mathbf{1}_2$ macrocycles that form the hydrogel are linked by disulfide bonds, the hydrogel should also be redox-responsive. Indeed, adding two equivalents of dithiothreitol reducing agent to the hydrogel, converted it into a solution containing monomer **1** (Figure 6.6). A hydrogel could be re-formed by oxidation through exposing the solution to oxygen from the air for 7 days.

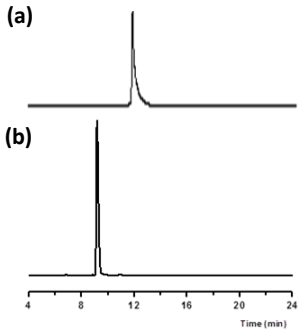

Figure 6.6. HPLC analysis of the hydrogel made by **1** (5.0 mM) and $MgCl_2$ (20 mM) in borate buffer (50 mM, pH 8.1) (a) before and (b) 10 mins after addition of 10 mM DTT. The peak at 9.3 min corresponds to monomer **1** as verified by independent injection of **1**.

We could also switch between solution and gel states by light. After 30 minutes of UV irradiation at 375 nm, the *trans* form of the azobenzene unit was converted to *cis* form, destroying the hydrogel, presumably by disrupting π-π stacking and fibre organization. The hydrogel is re-formed by letting the sample rest in a dark environment for 5 days. Recovery of the hydrogel can be accelerated by irradiating the sample at 420 nm; recovery of the gel now took 3 days. The switching process was monitored by UV-vis spectroscopy (Figure 6.7a).

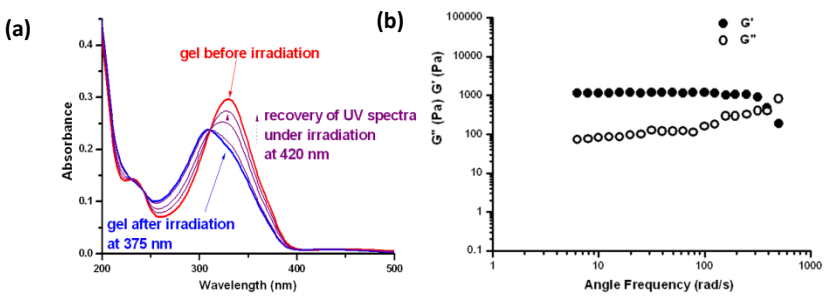

Figure 6.7. a) Change in the UV-vis spectrum of $\mathbf{1}_2$ (1.0×10^{-5} M) hydrogel made by **1** (5 mM) and $MgCl_2$ (20 mM) in 50 mM borate buffer pH 8.1 upon irradiation at 375 nm and recovery of the spectrum upon irradiation at 420 nm; b) Frequency sweep rheology data for the hydrogel made from $\mathbf{1}_2$ and $MgCl_2$.

We found that the hydrogel is also temperature responsive. Upon heating the gel to 40 ℃ for 30 minutes, it turned into a clear solution. When the temperature was reduced back to

20 ℃, the sample gelled again after 2 days. Similarly, changing the pH to 5.0, the hydrogel was destroyed. When switching the pH back to 8.1, the hydrogel was re-formed after 2 days.

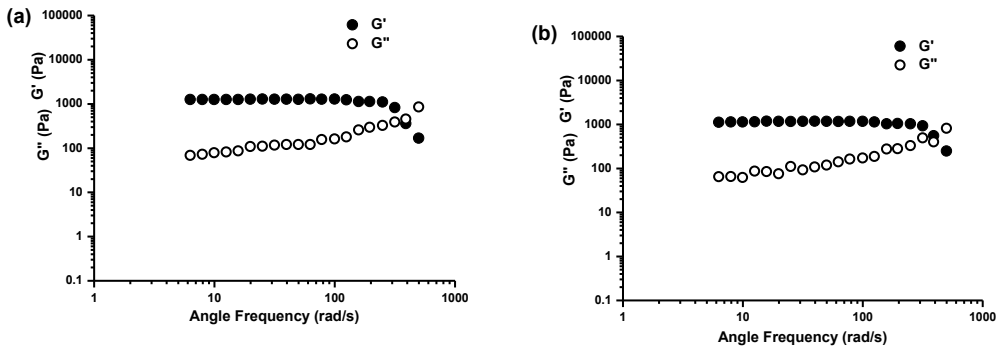

Figure 6.8. Frequency sweep rheological measurements for (a) the self-healed hydrogel that was obtained after resting the sample of Figure 6.7b for 2 days and (b) the same self-healed hydrogel, after it had been disrupted by high-frequency oscillations a second time.

Finally, we tested the responsiveness of the hydrogel to mechanical energy and potential for self-healing. The hydrogel could be disrupted by vigorous shaking and self-heals when rested for 2 days. We further investigated this behaviour by using oscillatory rheology measurements. At low oscillatory frequencies, the storage modulus (G') is one order of magnitude larger than the loss modulus (G"). When angle frequency was increased beyond 390 rad s^{-1} the hydrogel was disrupted (Figure 6.7b). After resting the disrupted hydrogel for 2 days, the rheology experiment was repeated and gave identical results (Figure 6.8). Repeating disruption-healing sequence a second time gave, again, identical results, suggesting that the processes of rupture and healing are fully reversible.

6.3 Conclusion

In conclusion, we have shown that providing the appropriate ingredients to a dynamic combinatorial library may lead to the self-synthesis of a new self-assembled material that combines within it all the functional elements that were included in the building block design. In this case the result was a Mg^{2+}-selective self-healing hydrogel that may be switched between gel and solution state by light, sequestration or addition of Mg^{2+}, reduction or oxidation, pH or temperature changes and mechanical energy. These results demonstrate the power of an "ingredients" approach for the development of new self-synthesizing materials with properties that may be specifically targeted.

6.4 Experimental Section

6.4.1 Materials

All chemicals, unless otherwise stated, were purchased from Sigma-Aldrich and used as received. HPLC or LC-MS grade solvents were from BIOSOLVE. All solvents used in synthesis were distilled prior to use and anhydrous solvents were distilled from a drying agent under a nitrogen atmosphere. NMR spectra of building block **1** and synthetic intermediates were recorded using a Varian Mercury Plus (400 MHz) spectrometer. The synthesis procedure of building block **1** is described below (Scheme 6.3). Building block **2** was prepared as described in Chapter 2.

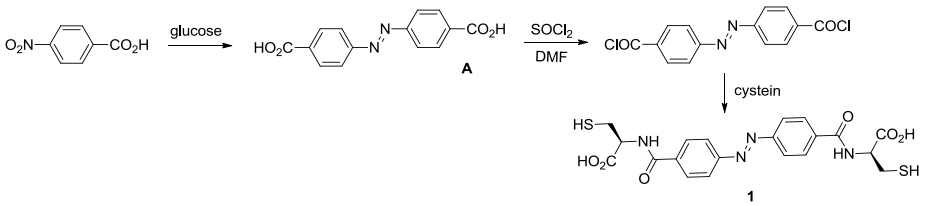

Scheme 6.3. Synthetic rout to building block **1**

Synthesis of 4,4'-(diazene-1,2-diyl)dibenzoic acid (A)[15]

4-Nitrobenzoic acid (5.00 g, 30.0 mmol) and sodium hydroxide (17 g) were mixed in water (75 mL) and heated until the solid had dissolved. A hot aqueous solution of glucose (30 g in 50 mL water) was added dropwise into the above solution at 50 ℃. The solution was left to react at room temperature for 8 hours and the brown precipitates were filtered and washed with a saturated NaCl solution. The precipitates were then dissolved in water and carefully acidified by acetic acid (20 mL) to produce pink precipitates while bubbling air through the mixture. The final product was filtered, washed with water and dried in vacuum to yield **A** (3.2 g, 80 %). ^{1}H NMR (400 MHz, DMSO-d6): δ ppm) = 8.01-8.03 (d, 4H), 8.16-8.18 (d, 4H), 13.21 (broad, 2H). ^{13}C NMR (100 MHz, DMSO-d6): ppm) = 123.29, 131.15, 133.87, 154.67, 167.07. ESI-MS: calcd for C14H10N2O4: *m/z* 269.0641 [M^{+}-H], found 269.0538 [M^{+}-H].

Synthesis of (2S,2'S)-2,2'-((4,4'-((E)-diazene-1,2-diyl)bis(benzoyl))bis(azanediyl)) bis(3-mercaptopropanoic acid) (1):

4,4'-(Diazene-1,2-diyl)dibenzoic acid (**A**) (0.27 g, 0.99 mmol) and thionyl chloride (6 mL)

were refluxed overnight at 85 ℃. The solution was evaporated several times from toluene and the solid azobenzene-4,4'-dicarboxylic acid chloride (0.30 g, 99 %) was dissolved in DMF (11 mL) and combined with a solution of cysteine (240 mg, 2.00 mmol) and DIPEA (0.500 mL, 2.21 mmol) in water (4 mL). The mixture was stirred overnight at RT. The product was precipitated from DMF/water to yield 0.36 g (82 %) of an orange powder. ^{1}H NMR (400 MHz, D_2O): δ ppm) = 7.89-7.91 (d, 4H), 7.96-7.98 (d, 4H), 4.13 (dd, J = 6.1 Hz, 7.3 Hz, 2 H, α-H), 3.51-3.53 (m, 2 H, β-H), 3.05- 3.14 (m, 2 H, β-H). ^{13}C NMR (400 MHz, D_2O): δ ppm) = 28.52, 61.03, 122.74, 126.75, 128.58, 133.87, 144.53, 173.21. ESI-MS: calcd for $C_{20}H_{20}N_4O_6S_2$: *m/z* 475.0824 [M^--H], found 475.0912 [M^--H].

Dynamic combinatorial libraries

Dynamic combinatorial libraries were prepared by dissolving building block **1** and/or **2** and, where needed, metal salt (20 mM) in borate buffer (50 mM, pH 8.2) at the appropriate concentration. The final pH of the solution was adjusted to 8.2 by addition of 1.0 M KOH solution. Aliquots of 0.5 mL of the library solutions were placed in capped HPLC vials in a dark environment for 7 days in the presence of oxygen from the air to allow oxidation of the thiols into disulfides. The hydrogel was made using a similar procedure but with a concentration of $MgCl_2$ (20 mM).

6.4.2 General Methods

Analytical HPLC

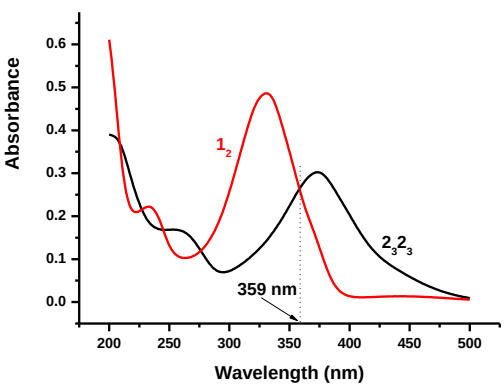

Figure 6.9. UV spectra of $\mathbf{1}_2$ (in red) and $\mathbf{2}_3\mathbf{2}_3$ (in black) at identical concentrations (2.0×10^{-5} M).

Analytical HPLC was carried out on Hewlett Packard 1050 or 1100 systems coupled to UV detectors and the data were processed using HP Chemstation software. Separations were performed on a reversed phase Zorbax C8 column (4.6 × 150 mm, 5 μm particle size,

Agilent). Except where otherwise stated, the chromatography was carried out at 45 ℃ using UV detection at 359 nm, which corresponds to the wavelength where $\mathbf{1}_2$ and $\mathbf{2}_3$-$\mathbf{2}_3$ have the same molar absorbtivity (see Figure 6.9). The HPLC method is the one used for LC-MS, described below.

UPLC/LC-MS analysis

An Accela High Speed LC system (ThermoFisher Scientifics, Courtaboeuf, France) was coupled to a LTQ-Fleet Ion-Trap Mass Spectrometer. Water was obtained from a MilliQ Gradient system and LC-MS-grade acetonitrile was bought from BIOSOLVE.

Analysis of samples was performed using a reversed-phase HPLC column (Zorbax C8, 4.6 x 150 mm, 5 μm, Agilent) at 45 °C with an injection volume of 3.0 μL. All UV traces were obtained by monitoring at 359 nm, which corresponds to the wavelength where 12 and 23-23 have the same molar absorbtivity (see Figure 6.9). The following LC method was used:

Solvent A: water (0.1% v/v formic acid); Solvent B: acetonitrile (0.1% v/v formic acid)

Flow rate: 1.0 mL/min

Time (min)	%B
0	5
30	95

Mass spectra of the [2] catenane were recorded in positive ion mode. The electrospray voltage was set to 3.4 kV, and the capillary voltage was set to 5.0 V; the sheath and auxiliary gas flows (both nitrogen) were 2.0 L/min and 2.0 L/min, respectively, and the drying gas temperature was 320 ℃. The MS-MS experiment was performed on the parent mass at 1994.3 (m/z) with a normalized collision energy at 35 eV and the act time is 30.00 ms.

The mass spectra of $\mathbf{1}_2$, $\mathbf{1}_1\mathbf{2}_1$ and $\mathbf{1}_2\mathbf{2}_2$ were obtained by UPLC-TOF (Waters Xevo G2 Tof ACQUITY UPLC H-class System). Chromatographic separation was performed at 45 ℃. Except for changing the flow rate to 0.5 mL/min, the same column and eluent gradient were used for the HPLC analysis. The mass scan range was from 600 to 2000 m/z in positive electrospray mode. The capillary and cone voltage were set at 3.0 KV and 30 V, respectively. The desolvation gas flow was 800 L/h at 500 ℃; the cone gas flow was 25 L/h at 120 ℃. All analyses were performed using the lockspray and Leucine-enkephalin was used as a lockmass. For MS-MS experiment, collision gas was argon 99.995% with a performance at the T-Wave collision cell. The collision energy at 25 eV was applied to the collision cell.

UPLC-MS Analysis of the DCLs

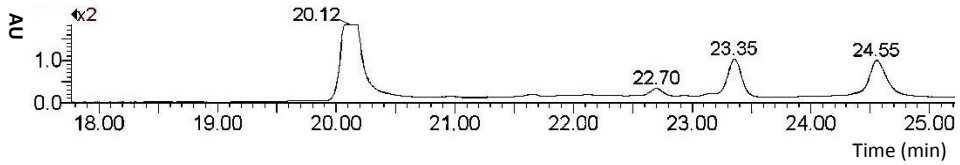

Figure 6.10 UPLC analysis of the fully oxidized library made from building blocks **1** (5.0 mM) and **2** (2.0 mM) in a 0.5 mL borate buffer (50 mM, pH 8.1).

(a)

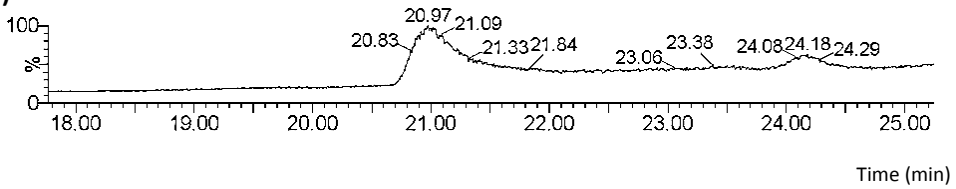

(b)

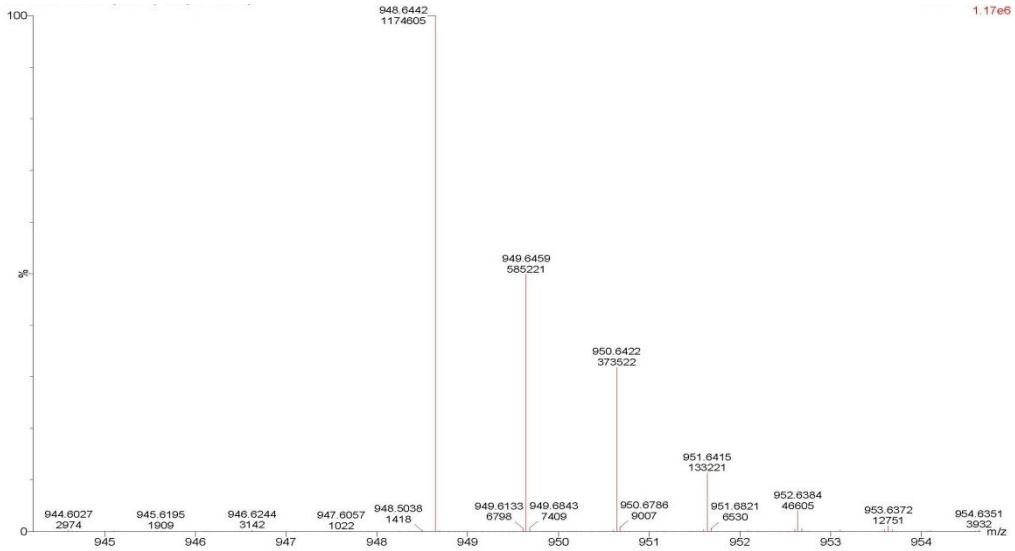

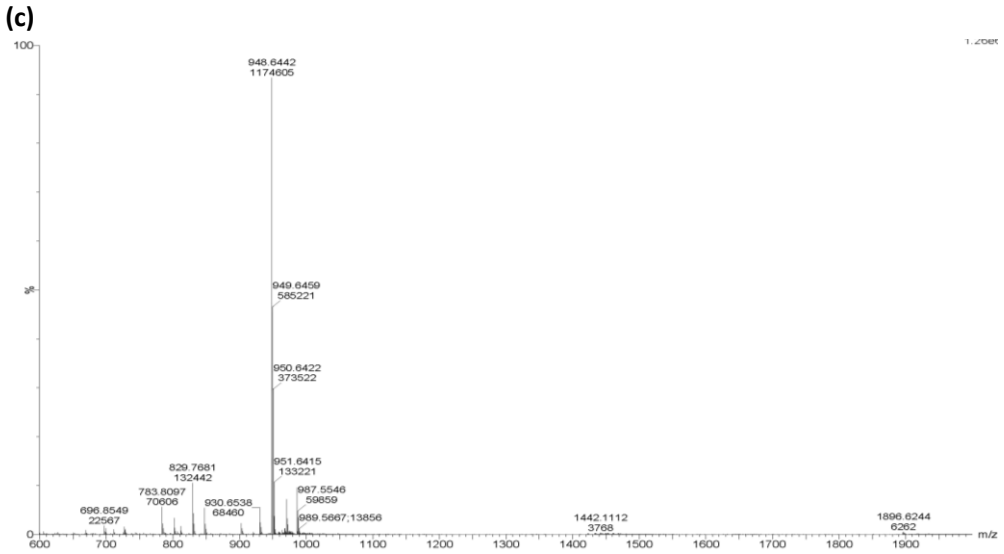

Figure 6.11 Asignment of $\mathbf{1}_2$ (a) Extracted ion chromatogram of m/z 948.00 - 949.00; (b) isotopic profile of the peak observed at 948.6442; (c) ESI-MS spectrum of the HPLC peak at 20.12 min. Expected m/z for $[\mathbf{1}_2+H]^+$ = 948.6438..

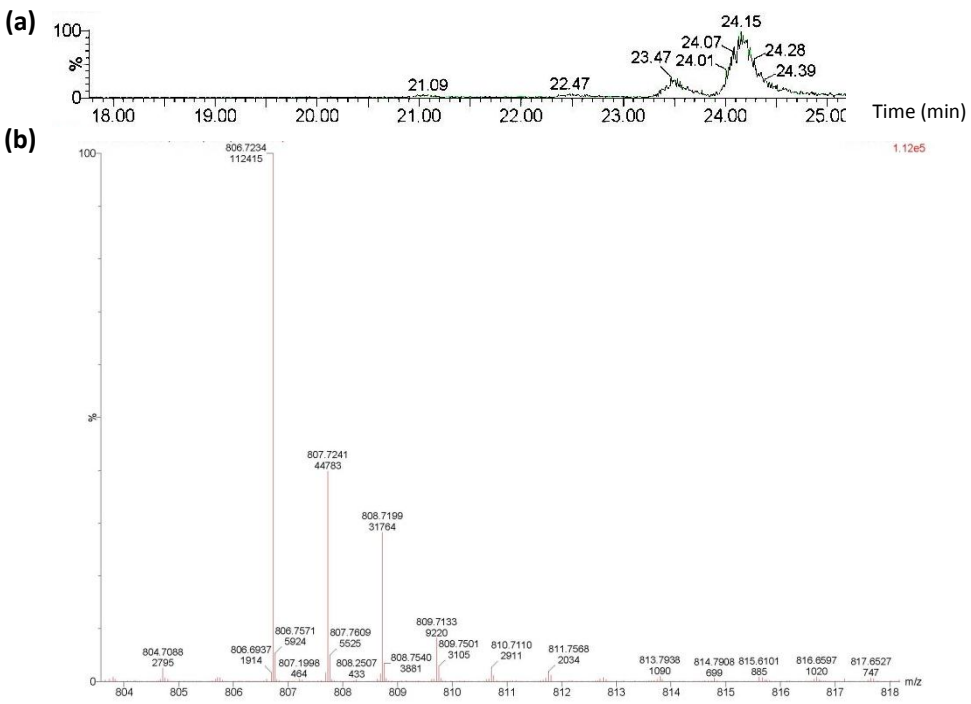

(c)

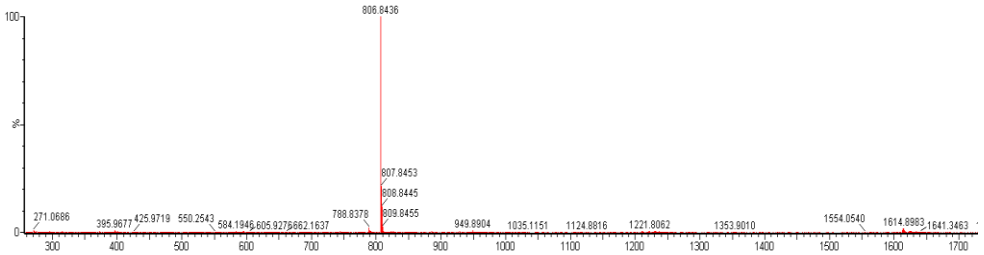
806.8436
807.8453
808.8445
809.8455
271.0686
395.9677
425.9719
550.2543
584.1946
605.9279
662.1637
788.8378
949.8904
1035.1151
1124.8816
1221.8062
1353.9010
1554.0540
1614.8983
1641.3463

(d)

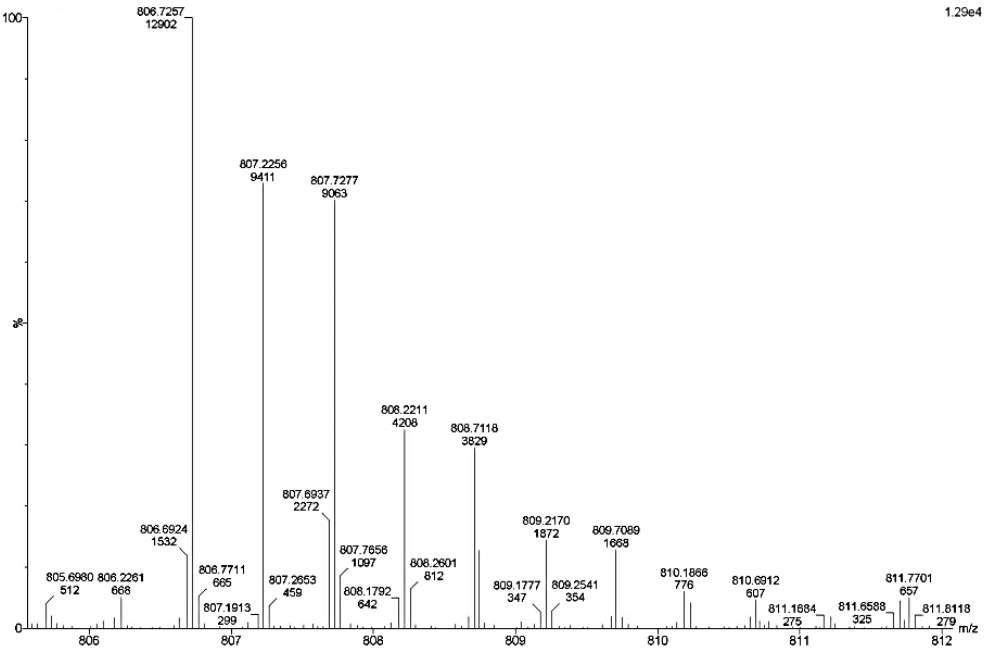
1.29e4
806.7257
12902
807.2256
9411
807.7277
9063
808.2211
4208
808.7118
3829
807.6937
2272
809.2170
1872
809.7089
1668
806.6924
1532
807.7656
1097
808.2601
812
805.6980
512
806.2261
668
806.7711
665
807.2653
459
807.1913
299
808.1792
642
809.1777
347
809.2541
354
810.1866
776
810.6912
607
811.7701
657
811.1684
275
811.6588
325
811.8118
279
%
m/z

(e)

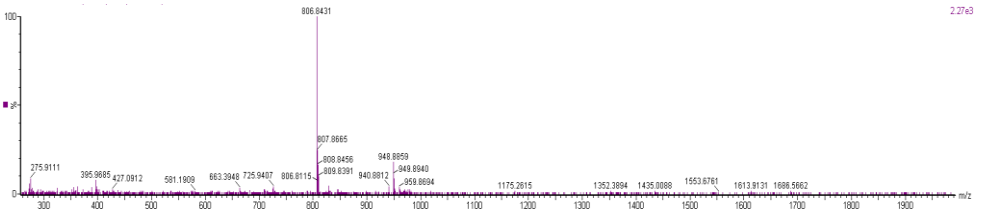
2.27e3
806.8431
807.8665
809.8456
809.8391
948.8859
949.8940
959.8694
940.8812
275.9111
395.9685
427.0912
581.1909
663.3948
725.9497
806.8115
1175.2615
1352.3894
1435.0088
1553.6761
1613.8131
1686.5662
%
m/z

(f)

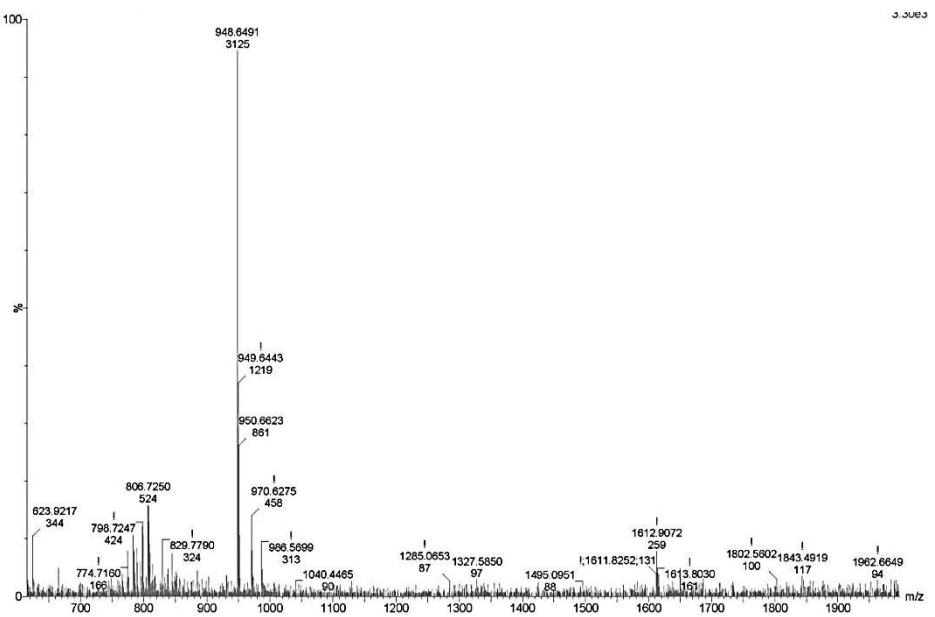

Figure 6.12 Asignment of $\mathbf{1_1 2_1}$ (a) Extracted ion chromatogram of m/z 806.00 - 807.00; (b) isotopic profile of the peak observed at 806.7434; (c) ESI-MS spectrum of the HPLC peak at 22.70 min. Expected m/z for $[\mathbf{1_1 2_1}+H]^+$ = 806.7381 and asignment of $\mathbf{1_2 2_2}$ (d) isotopic profile of the peak observed at 806.7275; (e) ESI-MS spectrum of the HPLC peak at 23.35 min. Expected m/z for $[\mathbf{1_2 2_2}+2H]^{2+}$ = 806.7581; (f) An MS-MS experiment on the 1612.9072 ion gives a singly charged ion with mass 948.6491 as the main peak, which corresponds to a dimer of **1**, suggesting that the sequence of $\mathbf{1_2 2_2}$ corresponds to **1-1-2-2**.

Infrared spectroscopy

Infrared spectroscopy were obtained from powders made by lyophilizing a solution of dimer $\mathbf{1}_2$ or a hydrogel made from $\mathbf{1_2}$ and $MgCl_2$, respectively. The spectra were recorded on a JASCO V-630 ATR IR spectrophotometer.

Cryo-TEM analysis

A 10 μL drop of hydrogel sample was placed on a Quantifoil 3.5/1 holey carbon coated grid. Blotting and vitrification in ethane was done in a Vitrobot (FEI, Eindhoven, The Netherlands). The grids were observed in a Philips CM120 cryo-electron microscope operating at 120 kV with a Gatan model 626 cryo-stage. Images were recorded under low-dose conditions with a slow-scan CCD camera.

Calculation of minimum-energy conformation of $\mathbf{1_2}$ in the gas phase

The minimum-energy conformation of $\mathbf{1_2}$ in the gas phase was determined by Chem 3D using the MM2 force field.

Powder XRD analysis

The powder XRD data for the hydrogel was recorded on a Bruker D8 instrument using Ge-monochromated CuKα_1 radiation. The sample was made by lyophilizing a sample of hydrogel. It was fixed on a disc sample holder and the powder XRD data were recorded in transmission mode (2θ range, 10–30 °; total time, 24 h).

Single crystal preparation and X-ray diffraction analysis

Small orange needles of $(\mathbf{1_2})Ca_2(H_2O)_{15}$ appeared as a precipitate after mixing equal amounts of a 5.0 mM solution of $\mathbf{1_2}$ in 50 mM borate buffer, pH=8.1, and a 20 mM solution of $CaCl_2$, the Ca : $\mathbf{1_2}$ ratio thus being 4:1. In order to obtain larger crystals, sufficient for diffraction analysis, the mixture was left standing for several weeks, thereby allowing for Ostwald ripening to occur.

Diffraction measurement was made on a Bruker D8 Venture instrument with PHOTON 100 detector, using graphite monochromated CuKα_1 radiation (λ = 1.54178 Å). The data set was collected using the ω scan mode over the 2θ range up to 149.54 °. The measurement was performed at 100 K. The structure was solved by direct methods using SHELXS and refined using SHELXL[16] and WinGX crystallographic suite of programs.[17] The structural refinement was performed on F^2 using all data. The stereochemistry of the compound was known from the synthesis, since L-cysteine was used, and it was also confirmed from the Flack parameter. Oxygen atom O22 was found to be in a slight structural disorder, its thermal elipsoid being elongated. Since it was not possible to resolve this by splitting the oxygen peak into two partitions, the ISOR restraint was used. The hydrogen atoms connected to carbon atoms were placed in calculated positions using the riding model, while those on the nitrogen and oxygen atoms were located from the differential electron density map and refined using bond and angle restraints when needed. The crystallographic information file (cif) is available from the Cambridge Crystallographic Centre with quotation number 946762.

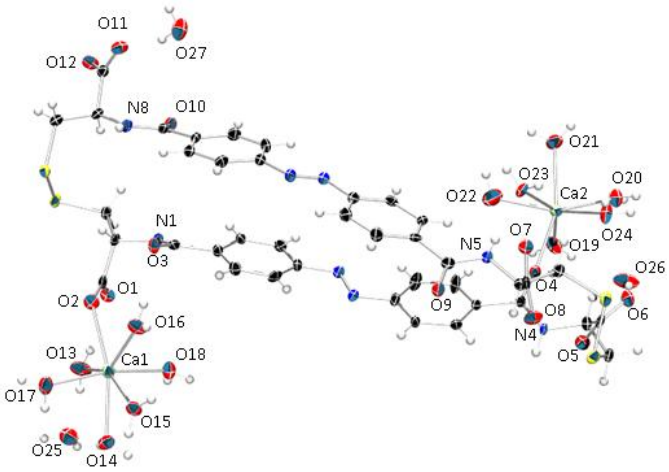

Figure 6.13 ORTEP plot of the asymmetric unit in the crystal structure of (**1₂**)$Ca_2(H_2O)_{15}$. The thermal elipsoids are drawn at 50% probability level and the hydrogen atoms are shown as spheres of arbitrary radius.

Table 6.1. Crystallographic data for (**1₂**)$Ca_2(H_2O)_{15}$

Chemical formula	$C_{40}H_{32}N_8O_{12}S_4Ca_2(H_2O)_{15}$
M_r	1295.38
Crystal system	Monoclinic
Space group	$P2_1$
a/Å	7.1287(2)
b/Å	19.9193(5)
c/Å	19.8284(5)
α/ °	90
β/ °	99.2020(10)
γ/ °	90
V/Å^3	2779.37(13)
Z	2
Z'	1
ρ_{calc}/(g cm^{-3})	1.548
μ/mm^{-1}	4.009
F[000]	1356
Crystal size/mm^3	0.20×0.01×0.01

Reflections collected	36789
Unique reflections	9978
Observed reflections	7899
Parameters	842
$R1$(obs)	0.0533
wR_2(all)	0.1236
S	1.027
Max./min $\Delta\rho$/(e/Å^3)	0.717/−0.691

Table 6.2. List of the most important hydrogen bonds (those involved in forming stacks of $\mathbf{1_2}$ moieties are shaded).

Hydrogen bond	d(D,H)/Å*	d(D,A)/Å*	d(A,H)/Å	ϕ(D,H,A)/ °*
O13—H45···O25	0.86(2)	2.658(6)	1.81(2)	169(2)
O13—H46···O1	0.86(2)	2.806(5)	2.07(3)	144(2)
O14—H47···O25	0.86(4)	2.877(6)	2.07(4)	156(4)
O16—H51···O3	0.86(4)	2.819(5)	1.99(5)	161(4)
O19—H57···O26	0.86(4)	2.883(6)	2.09(5)	153(4)
O26—H72···O6	0.86(4)	2.680(6)	1.83(4)	173(4)
O27—H73···O11	0.86(4)	2.889(6)	2.05(4)	165(3)
N4—H42···O8^a	0.87(3)	2.922(5)	2.06(3)	171(2)
O18—H55···O3^a	0.86(4)	2.752(6)	1.90(4)	169(4)
O25—H70···O2^a	0.86(4)	2.734(6)	1.93(4)	156(4)
O14—H48···O7^b	0.86(4)	2.862(5)	2.02(4)	165(4)
O17—H54···O19^c	0.86(3)	2.837(6)	2.02(4)	159(3)
O15—H49···O26^c	0.86(3)	2.711(6)	1.86(3)	169(3)
O15—H50···O8^d	0.86(3)	2.822(5)	1.97(3)	170(3)
O16—H52···O7^d	0.86(4)	2.662(5)	1.81(4)	170(3)
O17—H53···O10^e	0.86(4)	2.761(5)	1.92(4)	165(3)
O25—H69···O27^e	0.86(2)	2.931(6)	2.08(2)	169(1)
O20—H59···O15^f	0.86(5)	2.948(6)	2.14(5)	157(4)
O19—H58···O12^g	0.86(5)	2.869(6)	2.03(5)	164(4)
O20—H60···O9^h	0.86(5)	2.844(6)	2.00(5)	166(4)
O24—H68···O9^h	0.86(3)	2.753(6)	1.91(2)	168(2)
O21—H61···O14^i	0.86(2)	2.894(6)	2.04(2)	171(1)

O21—H62···O11^{j}	0.86(4)	2.927(5)	2.09(4)	165(3)
O23—H65···O12^{j}	0.86(3)	2.781(5)	1.92(2)	175(3)
O22—H63···O11^{j}	0.86(1)	2.693(5)	1.84(1)	168(1)
N8—H44···O1^{k}	0.87(3)	2.950(6)	2.11(3)	164(2)
O23—H66···O5^{k}	0.86(3)	2.785(5)	1.94(3)	167(3)
O27—H74···O10^{k}	0.86(2)	2.905(5)	2.05(2)	173(2)
O24—H67···O5^{k}	0.86(4)	2.632(6)	1.81(4)	160(4)

a) *x*−1, *y*, *z*; b) −*x*, *y*−1/2, −*z*+1; c) *x*, *y*−1, *z*; d) –*x*+1, *y*−1/2, −*z*+1; e) –*x*+1, *y*−1/2, −*z*+2; f) *x*, *y*+1, *z*; g) –*x*+1, *y*+1/2, −*z*+2; h) –*x*+1, *y*+1/2, −*z*+1; i) *x*+1, *y*+1, *z*; j) –*x*+2, *y*+1/2, −*z*+2; k) *x*+1, *y*, *z*; *Due to poor resolution (0.93 Å) and restraints used, the only data to be used for H-bonding analysis were D—A distances.

Table 6.3. Ca—O bond lengths (distances to the atoms belonging to $\mathbf{1_2}$ molecules are shaded)

Bond	*d*(Ca—O)/Å
Ca1—O2	2.517(3)
Ca1—O13	2.343(4)
Ca1—O14	2.533(4)
Ca1—O15	2.467(4)
Ca1—O16	2.325(4)
Ca1—O17	2.343(4)
Ca1—O18	2.372(4)
Ca2—O4	2.291(4)
Ca2—O19	2.482(4)
Ca2—O20	2.384(4)
Ca2—O21	2.387(4)
Ca2—O22	2.417(5)
Ca2—O23	2.521(4)
Ca2—O24	2.351(4)

Photo Responsiveness of the Hydrogel

The hydrogel was made by mixing $\mathbf{1_2}$ (2.5 mM) and $MgCl_2$ (20 mM) in 0.5 mL borate buffer (50 mM, pH 8.1) in a 1.5 mL HPLC vial . It turned into solution upon 30 minutes UV irradiation at 375 nm (LED UV light, 500 mW). The distance between the sample and light source was about 2 cm.

After 30 minutes irradiation at 420 nm (visible light, 60 W), the *cis* form of azobenzene moiety converted into the *trans* form. This free-flowing sample turned into gel again after resting for 3 days.

Redox Responsiveness of the Hydrogel

A hydrogel was produced oxidizing a solution of building block **1** (5.0 mM) and $MgCl_2$ (20 mM) in borate buffer (50 mM, pH 8.1) for 7 days fully oxidation in the air. The addition of DTT (10 mM) to the gel, resulted into the rapid conversion back into a free-flowing solution.

Rheology

Rheological measurements were carried out on a TA instruments AR-G2 rheometer, using a cone-and-plate geometry (truncated 4/40 cone, 4 ° cone angle, 40 mm diameter). The gap distance was fixed at 99 μm and covered with a solvent trap in order to prevent sample evaporation. Hydrogels (building block **1** (5.0 mM) and $MgCl_2$ (20 mM), 0.80 mL total volume) were made on the plate. A dynamic frequency sweep was performed over a range of frequencies from 1-390 rad s^{-1} at 0.1% constant strain at 298 K. G' and G'' values are an average of three repeats.

6.5 Acknowledgements

Ivica Cvrtila and Edwin Otten are greatly acknowledged for the help with the crystal structure determination. We thank Mathieu Colomb-Delsuc for cryo-TEM measurements.

6.6 References

[1](a) Otto, S. *Acc. Chem. Res.* **2012**, *45*, 2200-2210. (b) Moulin, E.; Cormosw, G.; Giuseppone, N. *Chem. Soc. Rev.* **2012**, *41*, 1031-1049. (c) Cougnon, F. B. L.; Sanders, J. K. M. *Acc. Chem. Res.* **2012**, *45*, 2211-2221. (d) Lehn, J. M. *Chem. Soc. Rev.* **2007**, *36*, 151-160. (e) Corbett, P. T.; Leclaire, J.; Vial, L.; West, K. R.; Wietor, J.-L.; Sanders, J. K. M.; Otto, S. *Chem. Rev.* **2006**, *106*, 3652-3711. (f) Miller, B. L. *Dynamic Combinatorial Chemistry in Drug Discovery, Bioorganic Chemistry, and Materials Science*, Wiley, Hoboken, NJ **2010**. (g) Reek, J. N. H.; Otto, S. *Dynamic Combinatorial Chemistry*, Wiley-VCH, Weinheim **2010**.

[2] (a) Carnall, J. M. A.; Waudby, C. A.; Belenguer, A. M.; Stuart, M. C. A.; Peyralans, J. J. P.; Otto, S. *Science* **2010**,

327, 1502-1506. (b) Li, J.; Carnall, J. M. A.; Stuart, M. C. A.; Otto, S. *Angew. Chem. Int. Ed.* **2011**, *50*, 8384-8386; (c) Nguyen, R.; Allouche, L.; Buhler, E.; Giuseppone, N. *Angew. Chem. Int. Ed.* **2009**, *48*, 1093-1096. (d) Williams, R. J.; Smith, A. M.; Collins, R.; Hodson, N.; Das, A. K.; Ulijn, R. V. *Nature Nanotech.* **2009**, *4*, 19-24. (e) Rubinov, B.; Wagner, N.; Matmor, M.; Regev, O.; Ashkenasy, N.; Ashkenasy, G. *ACS Nano* **2012**, *6*, 7893-7901. (f) Rubinov, B.; Wagner, N.; Rapaport, H.; Ashkenasy, G. *Angew. Chem. Int. Ed.* **2009**, *48*, 6683-6686. (g) Giuseppone, N. *Acc. Chem. Res.* **2012**, *45*, 2178-2188; h) Sadownik, J. W.; Ulijn, R. V. *Curr. Opin. Biotechnol.* **2010**, *21*, 401-411.

[3] (a) Clipson, A. J.; Bhat, V. T.; Mcnae, I.; Caniard, A. M.; Campopiano, D. J.; Greaney, M. F. *Chem. Eur. J.* **2012**, *18*, 10562-10570. (b) Demetriades, M.; Leung, I. K. H.; Chowdhury, R.; Chan, M. C.; McDonough, M. A.; Yeoh, K. K.; Tian, Y. M.; Claridge, T. D. W.; Ratcliffe, P. J.; Woon, E. C. Y.; Schofield, C. J. *Angew. Chem. Int. Ed.* **2012**, *51*, 6672-6675. (c) Cappelletti, G.; Cartelli, D.; Peretto, B.; Ventura, M.; Riccioli, M.; Colombo, F.; Snaith, J. S.; Borrelli, S.; Passarella, D. *Tetrahedron* **2011**, *67*, 7354-7357. (d) Durai, C. R. S.; Harding, M. M. *Aust. J. Chem.* **2011**, *64*, 671-680. (e) Lopez-Senin, P.; Gomez-Pinto, I.; Grandas, A.; Marchan, V. *Chem. Eur. J.* **2011**, *17*, 1946-1953.

[4] (a) Hamieh, S.; Ludlow, R. F.; Perraud, O.; West, K. R.; Mattia, E.; Otto, S. *Org. Lett.* **2012**, *14*, 5404-5407. (b) Klein, J. M.; Saggiomo, V.; Reck, L.; Luning, U.; Sanders, J. K. M. *Org. Biomol. Chem.* **2012**, *10*, 60-66. (c) Beeren, S. R.; Sanders, J. K. M. *J. Am. Chem. Soc.* **2011**, *133*, 3804-3807. (d) Bru, M.; Alfonso, I.; Bolte, M.; Burguete, M. I.; Luis, S. V. *Chem. Commun. 2011*, **47**, 283-285. (e) Rodriguez-Docampo, Z.; Eugenieva-Ilieva, E.; Reyheller, C.; Belenguer, A. M.; Kubik, S.; Otto, S. *Chem. Commun.* **2011**, *47*, 9798-9800.

[5] (a) Zhang, M.; Xu, D.; Yan, X.; Chen, J.; Dong, S.; Zheng, B.; Huang, F. *Angew. Chem. Int. Ed.* **2012**, *51*, 7011-7015. (b) Appel, E. A.; Loh, X. J.; Jones, S. T.; Biedermann, F.; Dreiss, C. A.; Scherman, O. A. *J. Am. Chem. Soc.* **2012**, *134*, 11767-11773. (c) Wang, Q.; Mynar, J. L.; Yoshida, M.; Lee, E.; Lee, M.; Okuro, K.; Kinbara, K.; Aida, T. *Nature* **2010**, *463*, 339-343. (d) Dastidar, P. *Chem. Soc. Rev.* **2008**, *37*, 2699-2715. (e) Yang, Z.; Ho, P. L.; Liang, G. L.; Chow, K. H.; Wang, Q. G.; Cao, Y.; Guo, Z. H.; Xu, B. *J. Am. Chem. Soc.* **2007**, *129*, 266-267. (f) Smith, D. K. *Adv. Mater.* **2006**, *18*, 2773-2778. (g) Sone, E. D.; Zubarev, E. R.; Stupp, S. I. *Angew. Chem. Int. Ed.* **2002**, *41*, 1705-1709.

[6] (a) Segarra-Maset, M. D.; Nebot, V. J.; Miravet, J. F.; Escuder, B. *Chem. Soc. Rev.* **2013**, 42, 7086-7098. (b) Lloyd, G. O.; Steed, J. W. *Nature Chem.* **2009**, *1*, 437-442. (c) Sangeetha, N. M.; Maitra, U. *Chem. Soc. Rev.* **2005**, *34*, 821-836. (d) Estroff, A.; Hamilton, A. D. *Chem. Rev.* **2004**, *104*, 1201-1217. (e) Esch, J. H. V.; Feringa, B. L. *Angew. Chem. Int. Ed.* **2000**, *39*, 2263-2266.

[7] (a) Hui, J. K. H.; MacLachlan, M. J. *Coord. Chem. Rev.* **2010**, *254*, 2363-2390. (b) Piepenbrock, M. M.; Lloyd, G. O.; Clarke, N.; Steed, J. W. *Chem. Rev.* **2010**, *110*, 1960-2004. (c) Lee, C. C.; Grenier, C.; Meijer, E. W.; Schenning, A. P. H. J. *Chem. Soc. Rev.* **2009**, *38*, 671-683. (d) Fages, F. *Angew. Chem. Int. Ed.* **2006**, *45*, 1680-1682.

[8] (a) Banbara, H. M. D.; Buidette, S. C. *Chem. Soc. Rev.* **2012**, *41*, 1809-1825. (b) Beharry, A. A.; Woolley, G. A. *Chem. Soc. Rev.* **2011**, *40*, 4422-4437. (c) Takashima, Y.; Hatanaka, S.; Otsubo, M.; Nakahata, M.; Kakuta, T.; Hashidzume, A.; Yamaguchi, H.; Harada, A. *Nat. Commun.* **2012**, *3*, 1270. (d) Rajaganesh, R.; Gopal, A.; Das, T. M.; Ajayaghosh, A. *Org. Lett.* **2012**, *14*, 748-751; e) Suzuki, T.; Shinkai, S.; Sada, K. *Adv. Mater.* **2006**, *18*, 1043-1046.

[9] Otto, S.; Furlan, R. L. E.; Sanders, J. K. M. *J. Am. Chem. Soc.* **2000**, *122*, 12063-12064.

[10] (a) Reuter, R.; Wegner, H. A. *Chem. Commun.* **2013**, *49*, 146-148. (b) Burattini, S.; Greenland, B. W.; Merino, D. H.; Weng, W.; Seppala, J.; Colquhoun, H. M.; Hayes, W.; Mackay, M. E.; Hamley, I. W. Rowan, S. J. *J. Am. Chem. Soc.* **2010**, *132*, 12051-12058. (c) Kuiper, J. M.; Engberts, J. B. F. N. *Langmuir* **2004**, *20*, 1152-1160.

[11] See Chapter 2 in this Thesis.

[12] (a) Ball, P. *Chem. Rev.* **2008**, *108*, 74-108. (b) Karplus, M.; Faerman, C. *Curr. Opin. Struct. Biol.* **1994**, *4*, 770-776.

[13] Bock, C. W.; Kaufman, A.; Glusker, J. P. *Inorg. Chem.* **1994**, *33*, 419-427.

[14] The samples for IR analysis were obtained by lyophilizing DCL samples of $\mathbf{1_2}$ in the presence and absence of $MgCl_2$.

[15] Ghosh, S.; Banthia, A. K.; Chen, Z. *Tetrahedron* **2005**, *61*, 2889-2896.

[16] Sheldrick, G. M. *Acta Cryst.* **2008**, *A64*, 112–122.

[17] Farrugia, L. J. J. *Appl. Cryst.* **1999**, *32*, 837-838.

Chapter 7

Hydrogel Formation upon Photo-Induced Covalent Capture of Stacks of Self-Assembling Dynamic Combinatorial Macrocycles

In Chapter 6 we have developed an "ingredients" approach for developing a new self-synthesizing hydrogel. From previous work by our group, we known that hexameric disulfide macrocycles emerge upon shaking a DCL made from a peptide derived dithiol building block, forming nanofibers. Can such nanofibers be further stabilized into hydrogels? In this Chapter, we show how photo-initiated disulfide exchange converts fibrous stacks of macrocycles into polymeric products, enhancing the stability of the fibers and causing gelation of the aqueous solution.

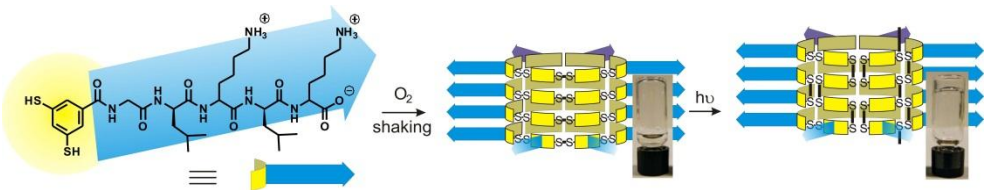

Part of this chapter has been published:

J. Li, J. M. A. Carnall, M. C. A. Stuart, S. Otto, *Angew. Chem. Int. Ed.* **2011**, *50*, 8384-8386.

7.1 Introduction

Our group recently reported how hexameric disulfide macrocycles emerge upon shaking a DCL made from dithiol **1** (Scheme 1).[1] This building block is equipped with a short peptide sequence, predisposed to β-sheet formation by alternating hydrophobic and hydrophilic amino-acid residues. While the peptide is too short to self-assemble on its own, the DCL made upon oxidizing dithiol **1** in aqueous solution contains a number of macrocycles of different ring size that display a different number of peptides. We reasoned that self-assembly becomes feasible for a critical macrocycle size that displays a sufficient number of peptides. Indeed, for a DCL made from **1** that is agitated by shaking, self-assembly of the hexameric macrocycles ($\mathbf{1}_6$) occurs, resulting in the formation of fibers and shifting the product distribution in favor of cyclic hexamer. The solution remains free flowing as the fibers are fragile and break when subjected to moderate shear forces.[1]

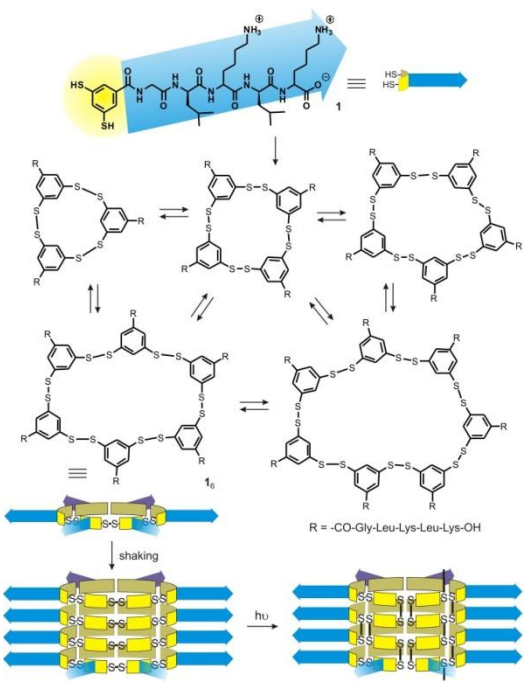

Scheme 7.1. Shaking a dynamic combinatorial library made from dithiol building block **1** in aqueous borate buffer (50 mM, pH 8.1) gives rise to stacks of disulfide macrocycles, which are covalently captured upon photo-irradiation (365 nm) to produce polymers/oligomers of **1**.

Hydrogels are often a much more stable state than isolated fibers in solution.[2] In Chapter 6, we have developed an "ingredients" approach for developing a new self-synthesizing hydrogel. As the hexameric macrocycles ($\mathbf{1}_6$) formed by the linkage of disulfide bonds, photo-initiated disulfide exchange may convert fibrous stacks of macrocycles into polymeric products, enhancing the stability of the fibers and causing gelation of the aqueous solution.

7.2 Results and Discussion

7.2.1 Hydrogel Formation and Component Analysis

We have since discovered that photo-irradiation (3 days, using an 8 W UV lamp, 365 nm) of a non-agitated solution containing hexamer fibers ([$\mathbf{1}_6$] ≈ 0.6 mM) results in the formation of a hydrogel[3] (Figure 7.1a). Oscillatory rheology[4] experiments showed that a relatively rigid gel is formed with a ratio between storage (G') and loss (G") moduli of 12 at low oscillatory frequencies (Figure 7.2).

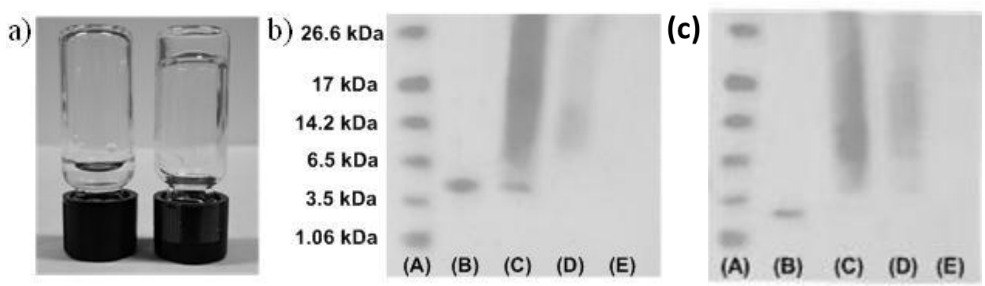

Figure 7.1. (a) Photograph of samples containing predominantly 16 prior to (left) and after (right) three days of photo-irradiation using an 8 W UV lamp. SDS-PAGE analysis of a sample (b) of $\mathbf{1}_6$ and a sample (c) of $\mathbf{1}_3$ and $\mathbf{1}_4$ prior to photo-irradiation (lane B) and after 1 day (lane C), 2 days (lane D) and 3 days (lane E) of irradiation. Lane A shows the standard molecular weight ladder.

It has been reported that photo-irradiation of disulfides can induce their homolytic cleavage[5] giving thiol radicals that can attack nearby disulfide bonds, resulting in disulfide exchange.[6] This underutilized radical mediated exchange mechanism is different from the ionic (thiolate-anion mediated) mechanism[7] that is typically used in dynamic covalent disulfide chemistry. We believe that this photo-induced disulfide exchange causes a

rearrangement of the disulfide bonds within the fibers, as shown in Scheme 1, without altering the global architecture of the fibers.[8]

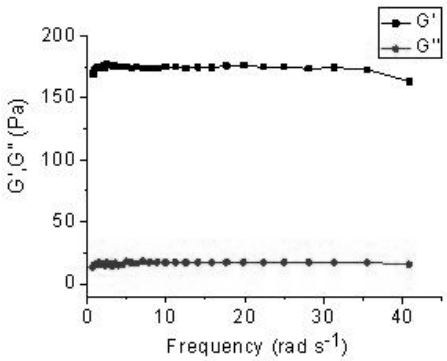

Figure 7.2. Rheological characterization of the hydrogel formed by photo-irradiating a solution of $\mathbf{1_6}$ (3.8 mM in **1**) for three days.

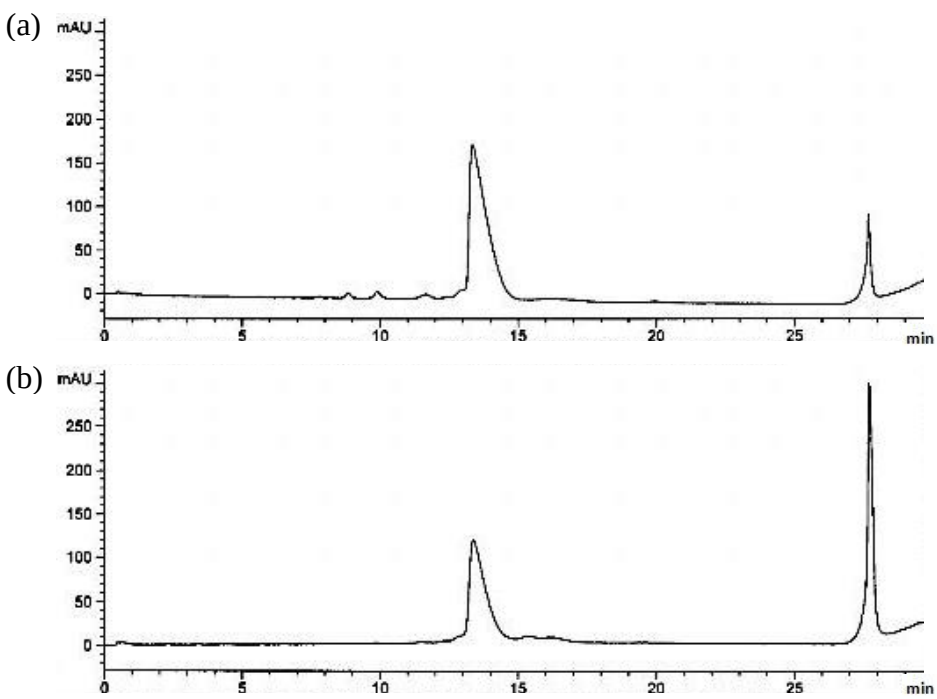

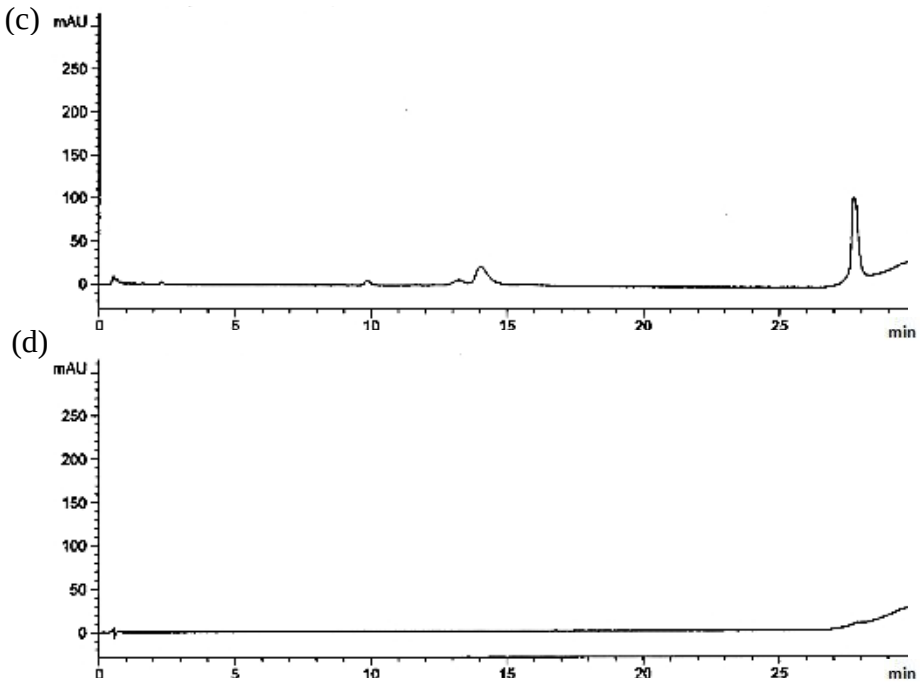

Figure 7.3. HPLC analysis of a sample containing $\mathbf{1}_6$ (3.8 mM in **1**) (a) prior to photo-irradiation and after (b) 1 day; (c) 2 days and (d) 3 days of irradiation. Absorbance was monitored at 254 nm.

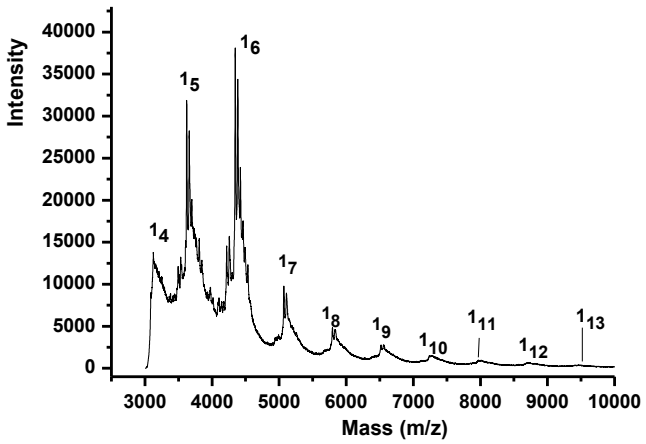

Figure 7.4. MALDI-TOF spectrum of a hydrogel sample made from $\mathbf{1}_6$ (3.8 mM in **1**) after 3 days of irradiation.

We analyzed the composition of the solution of fibrous $\mathbf{1}_6$ by HPLC/MS (Figure 7.3) during photo-irradiation and observed that the peak associated with $\mathbf{1}_6$ decreased gradually until, after three days, it was no longer detectable. As we were unable to detect by HPLC most of the compounds that were produced upon irradiation, we switched to SDS-PAGE analysis. Figure 7.1b shows that, in the course of the irradiation, larger molecular weight species are produced which subsequently also decrease in concentration (lane C-E). After three days of irradiation we fail to detect any peptide material by SDS-PAGE (lane E), suggesting that compounds of molecular weight (MW) in excess of 30,000 (42 units of **1**) are present. These results suggest that photo-irradiation induces the conversion of $\mathbf{1}_6$ (MW 4343.68) into polymers of **1** (Scheme 1). Attempts to analyze the length distribution of these polymers by gel permeation chromatography failed, due to the gelatinous nature of the samples. Analysis by MALDI-TOF mass spectrometry was hampered by extensive fragmentation of the disulfide linkages (Figure 7.4).

7.2.2 Hydrogel Organization Analysis

While the internal molecular structure of the fibers changed dramatically, their global appearance and organization into β-sheets were unaffected. Figure 7.5 shows cryo-TEM micrographs of the fibers of $\mathbf{1}_6$ prior to photo-irradiation and the same sample after three days of irradiation. The appearances of the two samples are remarkably similar, despite one being a gel and the other a free-flowing solution.

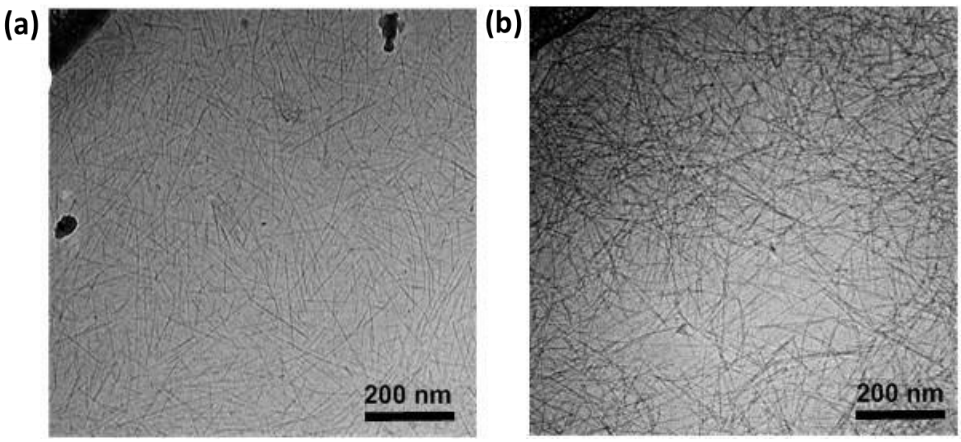

Figure 7.5. Cryo-TEM images of a sample containing predominantly $\mathbf{1}_6$ a) prior to photo-irradiation and b) after three days of photo-irradiation using a 8 W UV lamp.

We analyzed the effect of photo-irradiation on a dilute sample of $\mathbf{1}_6$ by circular dichroism, but could not detect any change in the CD spectrum. Both samples showed the typical signature of β-sheet assembly (Figure 7.6). We also performed thioflavin T fluorescence assays,[9] which indicated that the amyloid-like β-sheet structure that was present prior to photo-irradiation persists (Figure 7.7).

In order to confirm that photo-irradiation acted only on the disulfide bonds we have reduced the gel sample obtained after three days of photo-irradiation by adding 10 equivalents of dithiothreitol, resulting in the quantitative recovery of building block **1** (Figure 7.8 shows the HPLC analysis). This experiment also demonstrates that the peptide-derived hydrogels are not only photo-responsive but also redox-responsive.[10,11]

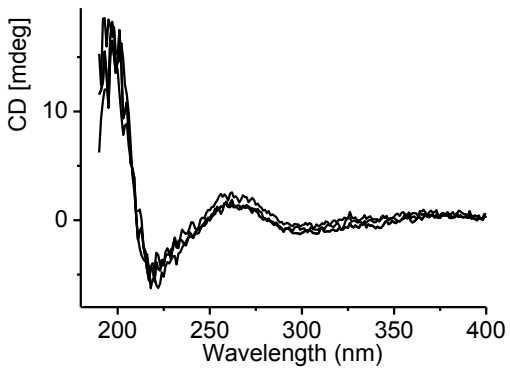

Figure 7.6. CD spectra of a sample containing $\mathbf{1}_6$ ($[\mathbf{1}]_{total}$=0.0126 mM) prior to photo-irradiation and after 1 day; 2 days and 3 days of irradiation.

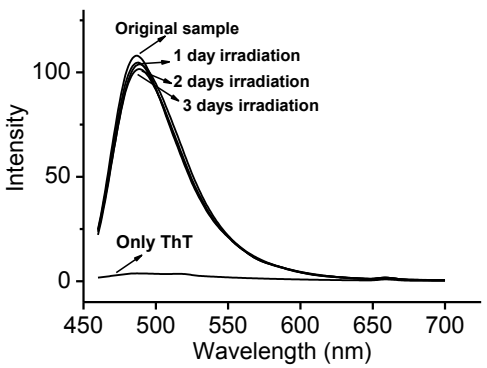

Figure 7.7. Fluorescent spectra of thioflavin T, thioflavin T + $\mathbf{1}_6$ prior to photo-irradiation and after 1 day; 2 days and 3 days of irradiation.

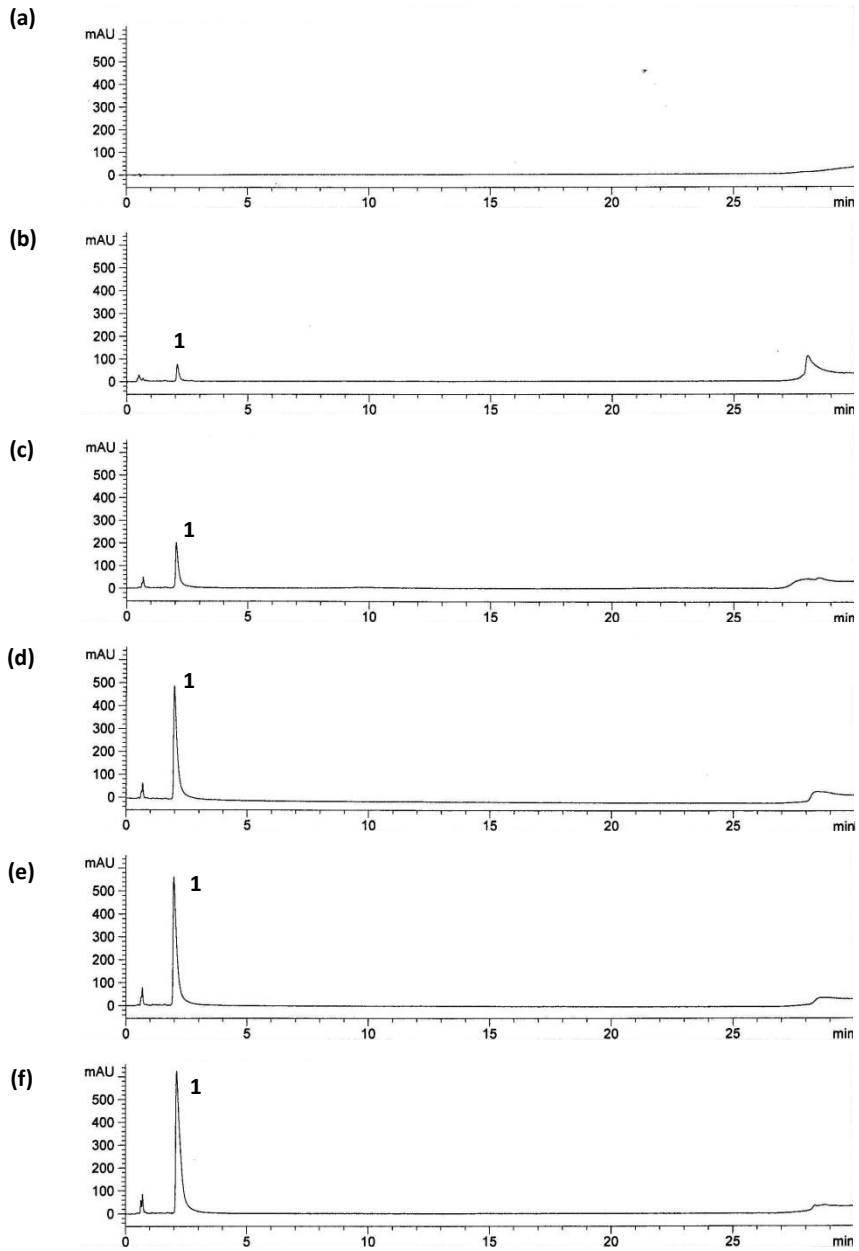

Figure 7.8. HPLC analysis of the reduction of the hydrogel made by irradiating a solution of $\mathbf{1}_6$ (3.8 mM in **1**) (a) prior to the addition of reducing agent and (b) upon addition of 2 equiv. (with respect to 1); (c) 4 equiv.; (d) 6 equiv.; (e) 8 equiv. and (f) 10 equiv. of dithiothreitol.

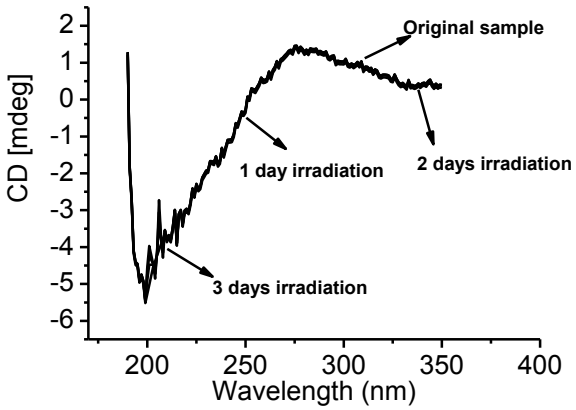

Figure 7.9. CD spectra of a sample containing $\mathbf{1}_3$ and $\mathbf{1}_4$ ($[\mathbf{1}]_{total}$=0.0126 mM) prior to photo-irradiation and after 1 day; 2 days and 3 days of irradiation.

The organization of the peptides into β-sheets prior to photo-irradiation is essential for gel formation as apparent from the following control experiment: We irradiated a sample consisting of mainly trimer and tetramer macrocycles, that do not self-assemble,[2e] and did not observe any gelation, nor any evidence for fibres in the cryo-TEM analyses, nor any evidence for β-sheet formation in the CD analysis (Figure 7.9). Yet disulfide polymerization did occur as evident from SDS-PAGE analyses (Figure 7.1c).

7.3 Conclusion

In conclusion, our results indicate that dynamic covalent disulfide linkages are not only instrumental in dynamic combinatorial discovery of self-assembling materials, but can also be used for the further stabilization of the resulting self-assembled structures in a process akin to covalent capture.[12] This strategy adds an element of kinetic control to the assembly process, thereby expanding the variety of structures that can be accessed using reversible covalent chemistry beyond those that represent directly accessible thermodynamic minima. The macrocyclization-self-assembly followed by ring-opening polymerization route provides access to polymers with a well-defined folded structure.

7.4 Experimental Section

7.4.1 Materials

All chemicals, unless otherwise stated, were purchased from Sigma-Aldrich and used as received. HPLC or LC-MS grade solvents were from BIOSOLVE. All solvents used in synthesis were distilled prior to use and anhydrous solvents were distilled from a drying agent under a nitrogen atmosphere. Building block **1** was obtained from Cambridge Peptides. The libraries were prepared by dissolving building block **1** in borate buffer (50 mM, pH 8.1) to obtain a 3.8 mM solution. The pH of the solution was adjusted to 8.1 by addition of 1.0 M KOH solution. The final volume of each library was 500 μL. Shaken samples were placed in an Eppendorf Thermomixer Comfort (orbital shaker) and shaken at 1200 rpm with an orbital radius of 1.5 mm. Standing samples were placed in a dark environment giving a mixture of $\mathbf{1}_3$ and $\mathbf{1}_4$. All library experiments were carried out at ambient temperature. The samples were irradiated using a TLC desk lamp (8 W, 365 nm, 220 V) at a distance of 3 cm.

7.4.2 General Methods

Rheology

Rheological measurements were carried out on a TA instruments AR-G2 rheometer, using a cone-and-plate geometry (truncated 4/40 cone, 4 ° cone angle, 40 mm diameter). The gap distance was fixed at 99 μm and covered with a solvent trap in order to prevent sample evaporation. Hydrogels (1.25 mL total volume) were transferred to the plate. A dynamic frequency sweep was performed over a range of frequencies from 0.1-45 rad s^{-1} at 0.1 % constant strain at 298 K. G' and G" values are an average of three repeats.

Cryo-TEM

A small drop of suspension was placed on a Quantifoil 3.5/1 holey carbon coated grid. Blotting and vitrification in ethane was done in a Vitrobot (FEI, Eindhoven, The Netherlands). The grids were observed in a Philips CM120 cryo-electron microscope operating at 120 kV with a Gatan model 626 cryo-stage. Images were recorded under low-dose conditions with a slow-scan CCD camera.

Circular dichroism (CD)

CD spectra were obtained at 298 K on JASCO CD spectropolarimeter J-715, with a data

pitch of 1 nm, a response time of 2 seconds and a scanning speed 100 nm/min. All reported spectra are an average of 10 repeats.

Fluorescent analysis

Fluorescence measurements were performed on a JASCO FP-6200 spectrophotometer. Thioflavin T (ThT) was dissolved to a concentration of 22 μM in sodium phosphate buffer (50 mM, pH=8.2). To 920 μL ThT solution, 80 μL diluted sample (0.127 mM in **1**) was added. The mixture was incubated for 2 min. and the fluorescence measured by excitation at 440 nm (5 nm slit width) and recording the emission between 460 and 700 nm (5 nm slit width, 5 repeats averaged).

LC-MS analysis

An Accela High Speed LC system (ThermoFisher Scientifics, Courtaboeuf, France) was coupled to a LTQ-Fleet Ion Trap Mass Spectrometer. Water was obtained from a MilliQ Gradient system and LC-MS-grade acetonitrile was bought from BIOSOLVE. Heptafluorobutyric acid (HFBA) was provided by Fluka.

Analysis of samples was performed using a reversed-phase HPLC column (Prodigy C18, 2 x 150 mm, 5 μm, Phenomenex) at 45 °C with an injection volume of 2 μL. All UV traces were obtained by monitoring at 254 nm. The following LC analysis method was used:

Solvent A: Water (0.2% v/v HFBA); Solvent B: Acetonitrile (0.2% v/v HFBA)

Flow rate: 0.8 mL/min

Time (min)	B%
0	35
7	38.5
25	38.5
30	90

Mass spectra were recorded in positive ion mode. The electrospray voltage was set to 5.0 kV, and the capillary voltage was set to 36 V; the sheath and auxiliary gas flows (both nitrogen) were 10 L/min and 3 L/min, respectively, and the drying gas temperature was 320 ℃.

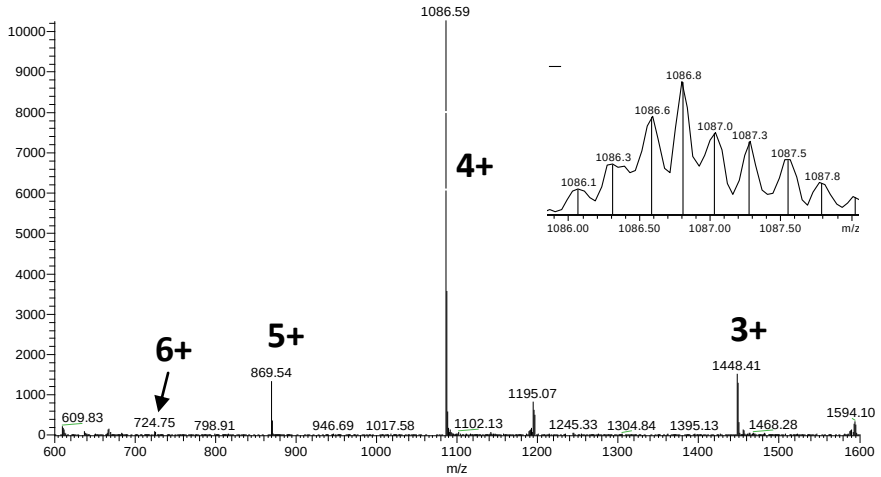

Figure 7.10. ESI-MS spectra of $\mathbf{1_6}$. Expansion of the molecular ion is shown as inset. Calculated isotopic profile (species, relative abundance): 4340.069 (M, 44); 4341.07 (M+1, 94); 4342.08 (M+3, 71); 4344.07 (M+4, 54). Calculated m/z: 1448.36 $[M+3H]^{3+}$; 1086.52 $[M+4H]^{4+}$; 869.42 $[M+5H]^{5+}$; 742.68 $[M+6H]^{6+}$; observed m/z: 1448.41 $[M+3H]^{3+}$; 1086.59 $[M+4H]^{4+}$; 869.54 $[M+5H]^{5+}$; 742.75 $[M+6H]^{6+}$.

Analytical HPLC analysis

Analytic HPLC was carried out on Hewlett Packard 1050 or 1100 systems coupled to UV detectors and the data were processed using HP Chemstation software. Separations were performed on a reversed phase Prodigy C18 column (2.1 x 150 mm, 5 μm particle size, Phenomenex). Except where otherwise stated, the chromatography was carried out at 45 ℃ and using UV detection at 254 nm. The HPLC analysis method is the same as LC method used for LC-MS, described above.

MALDI-TOF analysis

The MALDI-TOF mass spectra were measured on a PerSeptive Biosystems Voyager-DE Pro instrument. Samples were prepared by mixing 5 mg of the hydrogel and matrix solution (20 mg 2,5-dihydroxybenzoic acid in 1 mL 50% acetonitrile solution containing 0.1% TFA) and sonicating the mixture for 10 minutes.

SDS-PAGE analysis

SDS-PAGE was performed using a stacking polyacrylamide gel (4 % cross-linking), a resolving polyacrylamide gel (16 % cross-linking) and a loading buffer consisting of 150

mM of Tris-HCl, 30% glycine, 0.05% Coomassie Blue G-250 and 12 % of SDS at pH 7.00. The standard ladder (M3546-1VL Molecular Weight Marker Ultra-Low Range) was obtained from Sigma Aldrich. The solutions for analysis were prepared by mixing 2.0 μL sample and 2.0 μL loading buffer and sonicating this mixture for 5 minutes. Aliquots of 2.0μL of the resulting solution were injected into the gel wells.

7.5 Acknowledgements

Dr. Jacqui M. A. Carnall is most gratefully acknowledged for discovering the hydrogel. We thank Dr. Marc C. A. Stuart for cryo-TEM measurements.

7.6 References

[1] Carnall, J. M. A.; Waudby, C. A.; Belenguer, A. M.; Stuart, M. C. A.; Peyralans, J. J. P.; Otto, S. *Science* **2010**, *327*, 1502-1506.

[2] (a) Vlierberghe, S. V.; Dubruel, P.; Schacht, E. *Biomacromolecules* **2011**, *12*, 1387-1408; (b) Peppas, N. A.; Hilt, J. Z.; Khademhosseini, A.; Langer, R. *Adv. Mater.* **2006**, *18*, 1345-1360; (c) Fisher, O. Z.; Khademhosseini, A.; Langer, R.; Peppas, N. A. *Acc. Chem. Res.* **2010**, *43*, 419-428; (d) Hirano, Y.; Mooney, D. J. *Adv. Mater.* **2004**, *16*, 17-25.

[3] Estroff, L. A.; Hamilton, A. D. *Chem. Rev.* **2004**, *104*, 1201-1217.

[4] Yan, C. Q.; Pochan, D. J. *Chem. Soc. Rev.* **2010**, *39*, 3528-3540.

[5] Lee, Y. R.; Chiu, C. L.; Lin, S. M. *J. Chem. Phys.* **1994**, *100*, 7376-7384.

[6] (a) Gupta, D.; Knight, A. R. *Can. J. Chem.* **1980**, *58*, 1350-1354. (b) Banchereau, E.; Lacombe, S.; Ollivier, J. *Tetrahedron Lett.* **1995**, *36*, 8197-8200. (c) Otsuka, H.; Nagano, S.; Kobashi, Y.; Maeda, T.; Takahara, A. *Chem. Commun.* **2010**, *46*, 1150-1152.

[7] (a) Fava, A.; Iliceto, A.; Camera, E. *J. Am. Chem. Soc.* **1957**, *79*, 833-838. (b) Otto, S.; Furlan, R. L. E.; Sanders, J. K. M. *J. Am. Chem. Soc.* **2000**, *122*, 12063-12064. (c) Fernandes, P. A.; Ramos, M. J. *Chem. Eur. J.* **2004**, *10*, 257-266.

[8] While we cannot completely exclude inter-fiber crosslinking, the fact that we obtain a gel upon concentrating a fiber solution that was irradiated after 100-fold dilution ([$\mathbf{1_6}$] = 0.006 mM) suggests that disulfide exchange takes place predominantly within fibers.

[9] Levine, H. *Protein Sci.* **1993**, *2*, 404-410.

[10] For reviews on stimuli-responsive peptide materials, see: a) Mart, R. J.; Osborne, R. D.; Stevens, M. M.; Ulijn,

R. V. *Soft Matter* **2006**, *2*, 822-835; b) Lowik, D. W. P. M.; Leunissen, E. H. P.; van den Heuvel, M.; Hansen,M. B.; van Hest, J. C. M. *Chem. Soc. Rev.* **2010**, *39*, 3394-3412.

[11] Gels that respond to multiple stimuli are still rare. For examples, see: (a) Murata, K.; Aoki, M.; Suzuki, T.; Harada, T.; Kawabata, H.; Komori, T.; Ohseto, F.; Ueda, K.; Shinkai, S. *J. Am. Chem. Soc.* **1994**, *116*, 6664-6676. (b) Ahmed, S. A.; Sallenave, X.; Fages, F.; Mieden-Gundert, G.; Muller, W. M.; Muller, U.; Vogtle, F.; Pozzo, J. L. *Langmuir* **2002**, *18*, 7096-7101. (c) Ayabe, M.; Kishida, T.; Fujita, N.; Sada, K.; Shinkai, S. *Org. Biomol. Chem.* **2003**, *1*, 2744-2747. (d) Qiu, Z. J.; Yu, H. T.; Li, J. B.; Wang, Y.; Zhang, Y. *Chem. Commun.* **2009**, 3342-3344. (e) Komatsu, H.; Matsumoto, S.; Tamaru, S.; Kaneko, K.; Ikeda, M.; Hamachi, I. *J. Am. Chem. Soc.* **2009**, *131*, 5580-5585. (f) Wang, C.; Chen, Q.; Sun, F.; Zhang, D. Q.; Zhang, G. X.; Huang, Y. Y.; Zhao, R.; Zhu, D. B. *J. Am. Chem. Soc.* **2010**, *132*, 3092-3096.

[12] (a) Hartgerink, J. D. *Curr. Opin. Chem. Biol.* **2004**, *8*, 604-609. (b) Prins, L. J.; Scrimin, P. *Angew. Chem. Int. Ed.* **2009**, *48*, 2288-2306.

Chapter 8

Epilogue: Contributions and Outlooks

Now that all the experimental work has been described in the previous chapters, it is the time to evaluate what has been accomplished in the final chapter of this thesis. The six experimental chapters mainly concern three topics: supramolecular complexation, self-replication and self-synthesizing materials. The contribution of each of these topics is put into perspective. Finally, the prospects for self-organization in complex chemical systems are discussed.

8.1 Goal and Achievements

The goal of this thesis is investigating self-organization in complex chemical systems and uncovering some of the fundamental principles behind the subject of systems chemistry. To achieve this goal, the first thing that should be considered is fabrication of complex chemical systems. In Chapter 1, we reviewed the current frontiers of dynamic combinatorial chemistry (DCC), suggesting that it should provide a powerful framework for the study of complex chemical systems.

In chapter 2, self-assembled [2] and [3] catenanes were produced from a simple DCL. Although the molecular recognition driven synthesis of such dynamic combinatorial catenanes is quite common using DCC, we showed the first example of methodology for extracting the equilibrium constants for the formation of these catenanes. This new method provides useful insights into the binding interactions underlying the catenation process, which are not accessible by traditional titration measurements. The results of the quantitative assessment showed that the [3] catenanes self-assembled with positive or negative cooperativity.

These results inspired us to design and synthesize a new building block for the research in Chapter 3. Inspired by the cooperativity discovered in Chapter 2, we inferred that the simultaneous use of two templates in one library may also result in positive or negative cooperativity. Thus, in Chapter 3, two templates were introduced together in a single library. They quantitatively amplified a macrocycle through cooperative self-assembly into a "Russian Doll" type ternary molecular complex, which is the first example of simultaneous casting and molding of a library member. These results indicate that using more than one template molecule in a library may increase the possibility of the occurrence of cooperativity and enables access to increasingly complex supramolecular assemblies.

The two examples in Chapter 2 and Chapter 3 both revealed that cooperativity played a significant role in self-assembly of supramolecular complexes between library members and template molecules. The cooperative self-assembly may help the emergence of an unexpected receptor from a complex chemical system. Self-assembly can also occur by the aggregation of identical molecules. Our group recently found that self-assembly of a library member results in self-templating; i.e. the library member promotes its own formation. In Chapter 4 we described a system in which a template is crucial for allowing the self-assembling library member to reach the critical aggregation concentration. Once this

concentration has been exceeded, the library member catalyzed its own formation. This is the first example of the emergence of a self-replicator assisted by a template molecule. This example enriches the knowledge of self-replication in complex chemical mixtures. Since features of self-organization and self-replication are often considered the hallmark of living systems, the research in Chapter 4 is relevant to the question of the origin of life.

While defining life is surprisingly difficult, it is generally accepted that life requires the following key ingredients: compartmentalization, metabolism and reproduction. Combining two or more of these components in one system may help us gain a better understanding of the origin of life. In Chapter 5, we show the first example of compartments being formed from a self-replicator with self-replication taking place without mechanic agitation.

Chapters 4 and 5 showed that self-assembly in complex chemical systems may drive the occurrence of self-replication. The outcome of such self-assembly is a self-synthesizing material. In Chapter 6 we integrated the ingredients for specific properties that we wanted the material to exhibit in the structure of the building blocks and allowed the material to build itself from these building blocks. The result was a self-synthesizing hydrogel. This example demonstrated that it is not necessary to design the self-assembling molecules. If the right building blocks are provided, the self-assembly process will instruct the system to selectively synthesize the appropriate molecules from these building blocks.

For the further development of hydrogel materials, in Chapter 7, we show that photo-initiated disulfide exchange stabilized self-synthesizing fibers into a hydrogel form. This strategy adds an element of kinetic control to the self-assembly process.

8.2 Prospects and Outlooks

This thesis extensively focused on the self-assembly in complex chemical systems fabricated by using dynamic combinatorial chemistry. From self-assembly of library members with added template molecules to self-assembly by only library members, all these working examples show that the self-assembly can help the complex systems selectively amplify those right library species that give rise to intriguing structures. Nevertheless, we are just at the starting point of studying complex chemical systems. Hopefully, the suggestions I list below will contribute to the further development of this new subject.

First of all, most of the libraries that were prepared in this thesis were formed from only a single building block. To obtain more interesting results, more building blocks being present

in one DCL can enrich the library diversity, which would provide more opportunities for the emergence of unexpected structures when two template molecules are introduced as in Chapter 3. I suggest that more template molecules should be considered in future libraries.

Furthermore, it is interesting to investigate competition of two or more self-replicating systems in a single library. Will these two self-replicators coexist, or will one be driven to extinction, or will the system evolve to give new self-replicators? The answer to such questions may shed some light on possible mechanisms of molecular evolution. It is also interesting to investigate self-replicating systems starting from a pair of enantiomorphs. Will the symmetry of the system be broken by seeding the achiral library using one enantiomer? The answer to this question may give us more insights into explaining why, for example, most amino acids are L in nature.

Finally, all the systems investigated in this thesis are closed. There are no substance exchanges with the environment. It is interesting to extend our work into dissipative dynamic combinatorial libraries. The study of such far-from-equilibrium systems may allow us to discover phenomena that do not occur in equilibrium systems such as bistability, bifurcations, oscillations, evolution and, ultimately, life.

Summary

Life is a highly dynamic and complex system containing components such as membranes, nucleic acids and proteins. Many of the processes of self-organization that give rise to life are still a mystery for scientists. Learning how to understand much simpler synthetic systems may shed some light on this intriguing issue. Our group has been investigating the subject of dynamic combinatorial chemistry for more than ten years and gradually realized that it is a promising tool to fabricate complex synthetic systems. In Chapter 1, we introduced the fundamental principles behind this subject and reviewed the current state of art in dynamic combinatorial chemistry. We concluded that there is still plenty of room for further development. For instance, while there are many reports of templating in dynamic combinatorial chemistry, in nearly all cases only one template molecule is introduced into the systems. Simultaneous use of two or more templates may yield complex systems in which self-organization may give rise to unexpected outcomes. Furthermore, there are only limited examples of self-replication in dynamic combinatorial libraries. The mechanism behind the emergence of self-replicators from dynamic combinatorial libraries is still poorly understood. Finally, the application of dynamic combinatorial chemistry, for developing self-synthesizing materials is still at an early stage. In this thesis six different projects are described that address some of these topics.

In Chapter 2, we designed and synthesized an azobenzene derived dithiol building block. In the library prepared from only this building block, the dominant species was a [2]catenane consisting of two interlocked trimeric macrocycles. When the same library was made from this building block, but now in the presence of cyclodextrin homologues (α, β or γ-CD) as templates, the original [2]catenane was converted into a family of [2] and [3] catenanes comprised of macrocycles of our azobenzene building block interlocked with some of the cyclodextrins. The library member distribution depended on the concentration of the cyclodextrins added, which inspired us to develop a quantitative method for extracting the equilibrium constants for the individual catenation steps. The results reveal that the self-organized [3]catenanes form by positive (for β-CD) or negative (for γ-CD) cooperativity.

This method for quantitative assessment of equilibrium constants for catenation is potentially applicable to any catenanes containing dynamic covalent bonds.

Considering that γ-cyclodextrin (γ-CD) can include two naphthalene moieties into its hydrophobic cavity, we introduced it as a template molecule to investigate libraries prepared from a naphthalene derived unsymmetrical dithiol building block in Chapter 3. From previous work in our group we know that this building block forms a mixture of four tetramer isomers (**T1** to **T4**) which can interlock to give rise to a series of isomeric [2]catenanes. These [2]catenane isomers are the dominant species in the DCL prepared from only this building block. We first prepared a library from the building block and γ-CD. Tetramers **T1** and **T2** were amplified approximately equally. We then developed another template molecule, a benzene-derived ammonium salt, which was also introduced into the library. After full oxidation, we found that the tetramer **T4** was strongly amplified. When the benzene-derived ammonium salt and γ-CD were introduced together as templates, tetramer **T3** was amplified in almost quantitative yield. Interestingly, individually neither the ammonium salt template nor γ-CD was able to amplify **T3**. These results revealed that the four tetramer isomers could be amplified selectively, which allowed us to purify them and elucidate their structures by partially reducing the disulfide macrocycles and analyzing the distribution of the resulting fragments. By measuring the binding constants of each binding step in the formation of the ternary complex consisting of the two templates and tetramer **T3**, we concluded that the unusual amplification of this compound is due to the positive cooperative self-assembly of the three components together. This system represents the first example of simultaneous casting and molding of a library member.

From the previous work in our group we know that the [2]catenanes described in Chapter 3 can be converted into tetramer isomers by introducing as adamantine derived ammonium salt as a template. Inspired by his work, in Chapter 4 we prepared DCLs using the same building block and the same template, but this time we gradually increased the concentration of the template. A distinctly nonlinear increase in amplification factor of one of the tetramer isomers was observed, which we could attribute to the autocatalytic formation of this tetramer. Autocatalysis was driven by self-assembly of the tetramer **T4** into nanosheets. Self-assembly required **T4** to be present at a concentration above the critical aggregation concentration. The role of the template was to raise the amount of the tetramer above this critical concentration. These results represent the first example of a self-replicating molecule that requires a template for its formation even though it can replicate autonomously once it is present at a sufficient concentration.

In Chapter 5, we also focused on self-replication in DCLs. We first prepared a DCL using an amphiphilic dithiol building block. By monitoring the distribution of all the library species we found that the tetramer of this amphiphilic building block can self-replicate. We then mixed this building block with another dithiol building block to produce a more complex library. Seeding this library by the tetramer promoted its own formation. Self-replication was driven by the self-assembly of the tetramer into membranes, some of which folded and gave rise to the formation of compartments. In previous work by our group, mechanic agitation played a crucial role in the self-replication process, whereas in the present study we did not find a significant difference between the library with and without applying agitation. This may be the result of the different shape of the aggregates. In the case of sheet-based systems, when the membranes grow larger, the growing edge becomes larger as well, benefitting self-replication. In contrast, in the mechanosensitive replicators, aggregation takes place in the shape of fibres that grow from their ends. Increasing the numbers of ends requires mechanically induced fibre fragmentation.

In Chapter 6, we further developed the newly emerged concept of self-synthesizing materials. We used an “ingredients” approach to obtain a functional self-synthesizing hydrogel. Using DCC, it is not necessary to design the self-assembling molecule. If the right building blocks are provided, the self-assembly process itself assists the systems to synthesize the appropriate molecules from these building blocks. By coupling cysteine and an azobenzene-derived dicarboxylic acid, we produced an analogue to the azobenzene building block introduced in Chapter 2. Mixing these two building blocks together with different metal ion templates, we found that only Mg^{2+} induced the formation of a hydrogel. We found that the dimer of the new cysteine-azobenzene conjugate was responsible for gelation. However, when this gelator was mixed with a very similar cation, Ca^{2+}, we did not obtain a gel but crystalline solid of which we were able to obtain a crystal structure. The Mg hydrogel was self-healing and switchable between gel and solution by light, sequestration or addition of Mg^{2+}, reduction or oxidation, pH or temperature changes and mechanical energy. These results demonstrate the power of an "ingredients" approach for the development of new self-synthesizing materials with properties that may be specifically targeted.

Our group has previously discovered the efficient production of nanofibers by oxidizing an aqueous solution of a dithiol building block functionalized with a short peptide chain. Initially, the oxidation of the thiol groups gives rise to an equilibrium mixture of macrocycles carrying different numbers of peptide chains. Only the larger of these macrocycles are able to stack into fibers. In Chapter 7, we found that irradiating these fibers causes the exchange of

disulfide bonds, resulting in the conversion of the discrete macrocycles into oligomeric products. This photo-induced ring-opening polymerization increases the stability of the fibers, making these strong enough to enable gelation of the aqueous solvent. However, when the library containing only smaller macrocycles (trimers and tetramers) was irradiated under the same conditions, no gel was obtained, even though polymerization still occurred. Thus, the organization of the peptides into β-sheets prior to photo-irradiation appears to be essential for gel formation. This hydrogel was observed to be redox-responsive.

Samenvatting

Het leven is een zeer dynamisch en complex systeem, bestaande uit componenten zoals membranen, aminozuren en eiwitten. De zelforganisatie van deze structuren is nog steeds een mysterie voor vele wetenschappers. Begrijpen hoe simpele synthetische systemen zich gedragen kan inzicht bieden met betrekking tot de organisatie van de moleculaire componenten van levende systemen. Onze groep heeft meer dan tien jaar onderzoek gedaan op het gebied van dynamische combinatoriële chemie (DCC) en is tot het inzicht gekomen dat dit een nuttige manier is om complexe synthetische systemen te genereren. In hoofdstuk 1 introduceren we het fundamentele principe van dit onderwerp en geven we een overzicht van de recente ontwikkelingen in dit onderzoeksveld. We constateren dat er nog genoeg ruimte is voor verdere ontwikkelingen. De meeste gepubliceerde voorbeelden gebruiken bijvoorbeeld maar één molecuul als mal (*template*) in het systeem. Meerdere moleculen tegelijkertijd gebruiken, die fungeren als mal, kan beschouwd worden als een optie om meer complexe systemen te construeren, waarin zelforganisatie wellicht onverwachte resultaten zal opleveren. Er zijn maar weinig voorbeelden van dynamische combinatoriële bibliotheken (DCBen) waarin zelfreplicatie voorkomt. Het mechanisme van het ontstaan van een replicator vanuit een dynamische combinatoriële bibliotheek is nog steeds niet volledig opgehelderd. Het onderzoek naar zelf replicerende systemen staat nog in de kinderschoenen en biedt dus de mogelijkheid voor het ontdekken van meer toepassingen van de dynamische combinatoriële chemie. De resultaten van zes projecten op het gebied van dynamische combinatoriële chemie worden hieronder samengevat.

In hoofdstuk 2 wordt de ontwikkeling van een azobenzeen dithiol beschreven. De DCB gevormd uit alleen deze bouwsteen werd gedomineerd door een [2]catenaan bestaande uit twee in elkaar verstrengelde cyclische trimeren. Wanneer vergelijkbare DCBen werden gemaakt in aanwezigheid van cyclodextrine homologen als moleculaire mal werd de [2]catenaan bestaande uit zes eenheden van de bouwsteen omgezet naar een verzameling van [2] en [3]catenanen bestaande uit cyclische oligomeren van de bouwsteen, verstrengeld met een cyclodextrine. De concentratie van de verbindingen in de DCB was afhankelijk van de

concentratie van de toegevoegde cyclodextrines, wat ons inspireerde tot het ontwikkelen van een kwantitatieve methode voor het bepalen van de evenwichtsconstantes voor elke individuele stap in de vorming van de catenaan. De resultaten laten zien dat de zelforganisatie van de [3]catenanen gepaard gaat met positieve (voor β-CD) en negatieve (voor γ-CD) coöperativiteit. Deze kwantitatieve methode voor het bepalen van de evenwichtsconstantes is wellicht algemeen toepasbaar voor systemen waarin catenanen worden gevormd via dynamische covalente bindingen.

Gezien het feit dat **γ-**cyclodextrine twee naftaleen moleculen kan binden in zijn hydrofobe holte, hebben we dit molecuul als een moleculaire mal geïntroduceerd om het gedrag van een DCB bestaande uit niet-symmetrische naftaleen bouwstenen te bestuderen. Dit werk is beschreven in hoofdstuk 3. Door voorgaand werk van Kevin West in onze groep weten we dat deze bouwsteen vier tetramere isomeren vormt die kunnen verstrengelen tot [2]catenaan isomeren. Deze [2]catenaan isomeren zijn de belangrijkste producten in de DCB gemaakt van deze bouwsteen. Toen we daarna een bibliotheek maakten van deze bouwsteen in aanwezigheid van γ-CD zagen we dat twee isomere tetrameren in gelijke mate toenamen in concentratie. Daarnaast werd nog een moleculaire mal ontwikkeld, een ammonium zout van een benzeen derivaat, welke ook werd toegevoegd aan de bibliotheek gemaakt van de naftaleen bouwsteen. Na volledige oxidatie zagen we dat een derde tetrameer sterk was geamplificeerd. Wanneer het ammonium zout van het benzeen derivaat en γ-CD samen werden toegevoegd als moleculaire mal voor de DCB, resulteerde dit in de selectieve vorming van een vierde isomeer van de naftaleen tetrameer.

Deze resultaten geven aan dat de vier isomeren van de tetrameer selectief geamplificeerd worden, wat ons de mogelijkheid gaf om deze te isoleren en hun structuur te bepalen door middel van partiële reductie van de disulfide bindingen en ^{13}C NMR. Door middel van het meten van de bindingsconstantes voor elke bindingsstap in de vorming van een complex bestaande uit drie eenheden, waarvan twee moleculaire mallen en de specifiek geamplificeerde tetrameer, konden we concluderen dat deze onverwachte amplificatie het resultaat is van de positieve coöperatie in de zelfassemblage van de drie componenten. Dit is het eerste voorbeeld van het gelijktijdige “casting” en “molding” van een verbinding in een DCB. Echter is het nog steeds onduidelijk waarom juist deze ene isomeer wordt geamplificeerd door de twee moleculaire mallen. Het antwoord hiervoor zal mogelijkerwijs kunnen blijken uit de kristalstructuren van de complexen van de isomeren en de gast moleculen welke in de toekomst verkregen zal moeten worden.

Door voorafgaand werk van Kevin West weten we dat [2]catenanen, welke werden beschreven in het vorige hoofdstuk, omgezet kunnen worden in isomeren van tetrameren door middel van een adamantaan ammonium zout als moleculaire mal. In hoofdstuk 4 hebben we, geïnspireerd op dit werk, DCBen opgezet door middel van het gebruiken van dezelfde bouwsteen en moleculaire mal. Echter werd in dit geval de concentratie van de moleculaire mal langzaam vergroot in de DCBen. Dit resulteerde in een niet-lineaire verhoging in de amplificatie factor voor één van de tetrameer isomeren, wat veroorzaakt wordt door autokatalyse van deze tetrameer. Autokatalyse trad alleen maar op wanneer de tetrameer een concentratie hoger dan de kritische aggregatie concentratie had, zodat deze kon assembleren in nanosheets. Deze ontdekking geeft inzicht in het mechanisme van zelf-replicerende processen.

In hoofdstuk 5 ligt de nadruk op de zelf-replicatie in DCBen. Een DCB werd gemaakt van een amfifiele dithiol bouwsteen. Door middel van het bestuderen van de concentraties van de verschillende verbindingen in de DCB zagen we dat de tetrameer bestaande uit de amfifiele bouwstenen in staat was zichzelf te repliceren. Wanneer deze bouwsteen gemengd werd met een andere dithiol bouwsteen werd er een veel complexere DCB verkregen. Autokatalyse werd aangetoond door een kleine hoeveelheid tetrameer als “zaad” toe te voegen aan deze DCB. De zelfreplicatie van de tetrameer werd gedreven door de zelfassemblage naar membraanachtige structuren, welke ten dele konden vouwen en hiermee compartimentalisatie verwezenlijkten. In voorafgaand onderzoek was aangetoond dat mechanische agitatie van een DCB van grote invloed kan zijn op het zelfreplicatie proces. Zelfreplicatie vond alleen plaats in de gevallen waar de DCBen werden onderworpen aan een vorm van agitatie. In deze systemen konden de zelfreplicerende moleculen assembleren in fibers waarvan de uiteinden fungeerden als katalytische centra. Met behulp van mechanische energie werden de fibers gebroken, wat leidde tot meer katalytische uiteinden en zorgde voor zelfreplicatie. Het gedrag van de DCBen beschreven in dit hoofdstuk was echter anders: de samenstelling van de DCB was niet afhankelijk van mechanisch energie. Dit is waarschijnlijk het resultaat van een verschillende manier van zelfassemblage. In het geval van aggregatie in membraanachtige structuren zorgde het groeien van de membranen ervoor dat ook het katalytische oppervlak wordt vergroot, wat een voordelige uitwerking had op de zelfreplicatie, zonder dat daar mechanische energie voor nodig was.

Om de toepassingen van zelf-assemblage in DCBen uit te breiden hebben we het concept van zelf-synthetiserende materialen verder ontwikkeld. In hoofdstuk 6 maken we gebruik van een “ingrediënten” methode waarmee we een functionele zelf-synthetiserende hydrogel hebben ontwikkeld. Met behulp van DCC is het niet nodig om het zelf assemblerende

molecuul in zijn geheel te ontwerpen. Wanneer de juiste bouwstenen worden gebruikt dan wordt in een DCB door middel van zelfassemblage in deze systemen de juiste moleculen gevormd vanuit deze bouwstenen. Door de koppeling van cysteïne met een azobenzeen dicarbonzuur werd een vergelijkbare azobenzeen dithiol bouwsteen gevormd als de in hoofdstuk 2 beschreven bouwsteen. Door middel van het mengen van deze twee bouwstenen met verschillende metaalionen als moleculaire mallen werd duidelijk dat Mg^{2+} de vorming van een gel induceerde in de DCB. Daarnaast werd duidelijk dat het dimeer van de bouwsteen betrokken was bij de vorming van de gel. Wanneer dit dimeer werd gemengd met een vergelijkbaar cation (Ca^{2+}) werd geen gel gevormd maar een kristallijne structuur. De Mg-dimeer hydrogel toonde zelf-heling en kon worden geschakeld tussen gel en oplossing door middel van licht, wegvangen of toevoeging van Mg^{2+}, reductie of oxidatie, pH verandering, of veranderingen in temperatuur of mechanische energie. Deze resultaten demonstreren de kracht van deze "ingrediënten" benadering voor de ontwikkeling van nieuwe zelf-synthetiserende materialen met eigenschappen die specifiek kunnen worden beïnvloed.

Eerder heeft onze groep ontdekt dat nanofibers efficiënt geproduceerd konden worden door middel van oxidatie van een waterige oplossing van een dithiol bouwsteen welke een korte peptideketen bevat. Aanvankelijk werd door de oxidatie van de dithiol bouwsteen een DCB gevormd bestaande uit macrocyclische oligomeren met verschillende ringgroottes. Alleen de grotere oligomeren bleken in staat om te stapelen en fibers te vormen. In hoofdstuk 7 wordt beschreven hoe het bestralen van deze fibers leidde tot de uitwisseling van de disulfide bindingen wat resulteerde in de vorming van een polymere keten. Deze foto-geïnduceerde ringopeningpolymerisatie verhoogt de stabiliteit van de fibers, wat deze sterk genoeg maakt om in waterige oplossingen een gel te vormen. Wanneer een DCB met kleinere cyclische oligomeren werd bestraald, werd er geen gel gevormd, ook al was er wel polymerisatie. Deze resultaten geven aan dat de organisatie van de peptiden in β-sheets, voordat de bestraling met licht plaats vind, essentieel is voor de vorming van een gel. Deze hydrogel was redox-responsief.

Acknowledgments

Everything comes to an end. Recalling the past four years in Groningen, I will never regret that I obtained my doctoral degree here. I really enjoy living and doing research in Groningen during the past four years. I believe that I have made great progress in this period. Of course, I would not have had this precious time without the help and support from my colleagues, friends and family. Here I would like to express my sincere acknowledgment to all of them.

First of all, I would like to gratefully and sincerely thank Prof. Sijbren Otto for giving me the opportunity to complete my PhD thesis in his research group. Before I came to the Netherlands, I never talked with people in English. Sijbren showed great patience to understand my poor spoken English during the interview for the PhD position. After I joined the group, he always encouraged me to explore and develop my own ideas. I could always knock on his door when I had difficulties in the course of my research. His ability of converting serendipitous observations into new possibilities, coming up with ideas and understanding the obvious has impressed me a lot and will always guide me in my future career.

Then, of course, I would like to thank all my lab mates in the Otto group, past and present, for all the help. Mathieu is the person who picked me up at the reception desk in building Nijenborgh 4. Also afterwards he helped me a lot by measuring TEM samples. We also enjoyed the French and Chinese food together. Music and films are also our shared topics. Thank you for everything, my friend Mathieu and good luck for your future! Jerome is the first person who I worked with. He taught me how to operate all the instruments in the institute, which helped me work independently later. Jerome, I am really grateful for your kind guidance. Hugo provided me lists of housing agencies to find accommodation when I firstly arrived in Groningen. He also supplied me with a building block to finish my projects. Hugo, thank you! Enjoy your life in your hometown! Thanks also to Piotr for discussing our research projects and science together. I appreciate your generous help on the molecular dynamics simulations. I also enjoy the time we spend together in the lab. Thank you for your

company! I wish you all the best for your PhD. I would like to thank Shuo for his help not only with work but also life. Even after I left Groningen, you still helped me mailing things to Oxford. Thanks a lot, Shuo! All the best!

My acknowledgement will not be complete without the mention of the other lab mates, Andras, Asish, Boris, David, Elio, Gael, Giulia, Ivica, Jan, Manuel, Meniz, Morteza, Saleh, Vittorio, Yang and Yigit. Thank you guys for your delightful company and nice food at tea time. And I am also grateful to Agostino, Andrew and Wietse for choosing my proposals and working together with me. Your hard work is paid off by exciting research results. I hope you guys have a bright future!

A lot of people from outside our group have been helpful as well. I would like to thank Wesley for his assistance with the various spectrometers. He also helped me with setting up UV irradiation equipment. Without his help, the photo-induced gelation project would not have been completed so effectively. This project also received help from Jeffrey Bos. He gave me useful advice when I performed SDS-PAGE experiments. Thank you, Jeffrey! Good luck for your future. Next I would like to express my thanks to Theodora and Monique for their assistance of HPLC and HPLC-MS analyses. Jiawen and Jens taught me how to use the auto flash column machine, which helped me a lot in the synthesis of the building block described in Chapter 5. I also would like to thank Francesca for her assistance with NMR experiments. Thank you guys very much and all the best for your PhDs.

I would like to acknowledge other friends. Life never became lonely with your nice company. Lifei, Kai, Depeng, Bin, Qian, Jiajia, Jiaobing, Zongtao, Yange, Jiawei, Nopporn, Martin, Xiaoyan, Lili, Celine, Pattama, Massimo, Hella, Valentin, Arjen, Jochem, Jos, Robby, Kuangyan…the list is endless…thanks to you all.

Finally, I would like to thank my family. I cannot imagine my life without the love and blessings from my parents and my sister. Thank you mom and dad for moral and material support and giving me the liberty to choose what I desire. I also want to express my best acknowledgement to my wife, Zhao. We met in Groningen and started our life here. We also supported each other for completing our PhD. Thank you for your support, love and understanding.